

Engineering polymers with uniform crystallisable units

Josien Krijgsman

2002

Ph.D. thesis
University of Twente



Twente University Press

Also available in print:

<http://www.tup.utwente.nl/catalogue/book/index.jsp?isbn=9036518121>

Engineering polymers with uniform crystallisable units



The research described in this thesis was financially supported by the Dutch Polymer Institute (DPI), the Netherlands.



Twente University Press

Publisher:

Twente University Press

P.O. Box 217, 7500 AE Enschede, the Netherlands

www.tup.utwente.nl

Print: Océ Facility Services, Enschede

© J. Krijgsman, Enschede, October 2002

No part of this work may be reproduced by print, photocopy, or any other means without the permission in writing from the publisher.

ISBN 90 365 18121

ENGINEERING POLYMERS WITH UNIFORM CRYSTALLISABLE UNITS

SEGMENTED COPOLYMERS BASED ON
POLY(2,6-DIMETHYL-1,4-PHENYLENE ETHER)

PROEFSCHRIFT

ter verkrijging van
de graad van doctor aan de Universiteit Twente,
op gezag van de rector magnificus,
prof. dr. F.A. van Vught,
volgens besluit van het College voor Promoties
in het openbaar te verdedigen
op vrijdag 1 november 2002 om 15.00 uur

door

Josien Krijgsman

geboren op 18 mei 1975
te Den Helder

Dit proefschrift is goedgekeurd door:

Promotor: prof. dr. J. Feijen

Assistent-promotor: dr. R.J. Gaymans

Wetenschap is wat ik doe als ik niet weet wat ik aan het doen ben.

Werner von Braun

Voorwoord

In het proefschrift dat nu voor u ligt staan de resultaten van het werk beschreven dat ik de afgelopen vier jaar heb uitgevoerd in de groep “Synthese en Technologie van Engineering Plastics”, kortweg STEP. Vier jaar, dat lijkt heel lang als je er mee begint, maar zoals iedereen me toen al toevertrouwde vliegen die jaren voorbij. Dat is natuurlijk mede het gevolg van het leuke onderzoek en de gezelligheid in de vakgroep. Een aantal mensen wil ik daarom in dit stukje in het bijzonder bedanken.

In de eerste plaats wil ik Reinoud Gaymans bedanken, omdat hij mij de mogelijkheid heeft gegeven om binnen zijn STEP-groep mijn promotieonderzoek uit te voeren. Vooral je enthousiaste begeleiding, betrokkenheid en het feit dat de deur altijd open stond zal me bijblijven. Daarnaast hebben we met de groep verschillende congressen in Amerika en dichterbij huis bezocht, wat zeer leerzaam en leuk was. Ook wil ik jou en Mieke bedanken voor de gastvrijheid en het heerlijke eten bij de jaarlijkse BBQ's en diners.

Ik wil ook mijn promotor Prof. Feijen bedanken voor zijn interesse in mijn onderzoek en de correctie van mijn proefschrift. Bedankt voor de snelle correctie en de (bijna) rookvrije besprekingen.

Mijn afstudeerders Edwin Biemond en Debby Husken wil ik bedanken voor hun bijdrage aan mijn werk. Het was leuk en leerzaam om met jullie samen te werken! En ik ben blij dat jullie allebei ook AIO in onze groep zijn geworden.

Een aantal experimenten was niet mogelijk geweest zonder de hulp van de volgende personen. Voor het uitvoeren van de eindgroep concentratie metingen wil ik Wim Lengton bedanken. Clemens Padberg, bedankt voor het uitvoeren van de AFM en GPC metingen en je hulp bij alle technische probleempjes bij de DSC apparatuur. Dhr. Koster wil ik bedanken voor het uitvoeren van de WAXD metingen. Voor alle technische en praktische zaken op het lab wil ik Zlata Rekenji en John Kooiker bedanken. En Karin Hendriks, bedankt voor je inzet bij alle administratieve zaken.

De huidige STEPPers Wilco, Martijn, Edwin en Debby wil ik bij deze bedanken voor het kritisch doorlezen van mijn concept proefschrift. Gelukkig hebben jullie er nog heel wat vervelende fouten uit kunnen halen die ik zelf op een gegeven moment echt niet meer zag na het typen en herlezen van de ruim 400.000 tekens. En Martijn en Edwin, alvast bedankt voor het paraniften of 1 november.

Tot zover het serieuze deel, want werktijd is natuurlijk maar een kwart van de tijd in een week en er is dus meer voor nodig om de tijd te laten vliegen. Naast een gezellige werksfeer met mijn collega's van de STEP-groep waren er buiten werktijd regelmatig borrels, etentjes, verjaardagen, uitjes, de jaarlijkse triatlon, zeilweekenden en zelfs een snowboard-weekend en weekendje Rome! Naast de STEPPers wil ik daarvoor ook alle andere polymeer-AIO's en afstudeerders van PBM, RBT en MTP bedanken. Na mijn verhuizing naar Deventer kon ik helaas iets minder impulsief en vaak meedoen met alle activiteiten. Gelukkig stond een logerbed altijd klaar bij Martijn, Wilco of Edwin indien nodig.

De 3-wekelijkse vakgroepvolleybalcompetitie waar we altijd fanatiek aan meededen zal ik zeker ook missen. Ype, Joost, Annemieke, Priscilla en Debby, hopelijk worden jullie ooit nog een keer kampioen en verslaan jullie de altijd overmachtige technische dienst.

Naast alle collega's wil ik ook mijn studie-, volleybal- en zeilvrienden bedanken voor alle gezellige avonden en weekenden in Enschede en door het hele land. Door jullie ben ik niet zo'n AIO geworden die veel avonden en weekenden kon doorwerken en daar ben ik blij om. En ondanks alle afleiding heb ik het toch in vier jaar kunnen afronden.

Ook mijn ouders wil ik bedanken voor hun steun en interesse in mijn onderzoek. Hoewel mijn verhalen waarschijnlijk moeilijk te volgen waren deden jullie toch altijd je best om te snappen waar ik mee bezig was. En jullie wisten me altijd wel weer op te peppen als ik het even niet meer zag zitten. Gelukkig is het ondanks mijn getwijfel of ik wel de juiste keuze maakte toch weer goed gekomen. Misschien dat ik er nog een keer van leer...

Maarten, tot slot ben jij aan de beurt voor een bedankje. Je was altijd geïnteresseerd in en verrassend kritisch over mijn onderzoek en dat heeft me zeer geholpen. Hoewel het op-en-neer reizen vanaf Deventer me af en toe tegenstond ben ik erg blij dat we zijn gaan samenwonen. En gelukkig hadden we tussen alle lange werkdagen, (volleybal)avonden en drukke weekenden ook nog wel tijd ('holy Thursday') voor elkaar. Gelukkig kunnen we binnenkort de schade inhalen. Nog even en we zitten op het eerste het beste terras in Christchurch aan een welverdiend biertje (en een kiwi)!

Josien

Contents

Chapter 1	Introduction	1
Chapter 2	Synthesis of telechelic poly(2,6-dimethyl-1,4-phenylene ether)	5
Chapter 3	Copolymers of poly(2,6-dimethyl-1,4-phenylene ether) and ester units	37
Chapter 4	Copolymers of poly(2,6-dimethyl-1,4-phenylene ether) and poly(dodecane terephthalate)	61
Chapter 5	Synthesis and characterisation of uniform bisester tetra-amide segments	75
Chapter 6	Synthesis and properties of copolymers of PPE, dodecanediol and uniform tetra-amide units.	95
Chapter 7	Thermal-mechanical properties of copolymers of PPE, dodecanediol and tetra-amide units	127
Chapter 8	Thermal-mechanical properties of copolymers of PPE, different extenders and uniform tetra-amide units	147
Chapter 9	Synthesis and properties of thermoplastic elastomers based on PTMO and tetra-amide units	171
Chapter 10	Tensile and elastic properties of thermoplastic elastomers based on PTMO and tetra-amide units	201
Summary		225
Levensloop		229

Chapter 1

General introduction

The importance of polymer materials as construction materials is continually growing. Polymers are a cheap and light alternative to conventional materials used for construction. Recently, in particular the market for high temperature polymers is growing^{1,2}. Such polymers should have high mechanical strength and modulus, stability to various environments (chemical, solvent, UV, oxygen) and good dimensional stability at elevated temperatures. Other attractive properties can include resistance to corrosion, wear and moisture, low flammability, insulating properties and processability. The demand for this type of materials comes from technological areas such as advanced air- and spacecraft, electronics, automotive industry and several consumer applications. In the automotive industry there is a specific need for materials with excellent chemical resistance to automotive fluids such as engine oil, transmission fluid, anti-freeze and road salt. For some applications it may also be important that the modulus is high up to temperatures of 180-200°C. For example, several parts for construction of cars (such as bumpers) must withstand the high temperatures of the e-coating process (up to 200°C). New applications include exterior, interior and 'under the hood' parts. The major advantages of heat-resistant polymers over metals are the weight savings and the ease of processing into a wide range of shapes and forms¹⁻³.

Amorphous polymers usually have a long-term service capability up to 30°C below their glass transition temperature (T_g). Thus in order to allow the use of polymers in situations where high dimensional stability up to high temperatures is needed, the material should have a high T_g . For example polycarbonate (PC) and poly(phenylene ether) (PPE) are known to have a high dimensional stability up to their T_g (respectively at 150°C and 215°C).

A major disadvantage of amorphous polymers is their low solvent resistance. This is in particular important in automotive applications. Alternatively semi-crystalline polymers may be used, which generally possess a better solvent resistance. However with a melting temperature of about 300°C, their T_g 's are generally not so high. Most semi-crystalline materials follow 'the 2/3 rule' for T_g/T_m ratio, which rule indicates that the ratio between glass transition and melting temperature (T_m) (in K) is about 2/3. For example, with a maximum practical melting temperature of 300°C, the T_g would only be 110°C. A high T_g (>110°C) means automatically a very high T_m with the possibility of thermal degradation during melt processing. Thus a polymer system with a high T_g and a not too high T_m (and thus with a higher T_g/T_m ratio) is highly interesting. Some (co)polymers have a high T_g/T_m ratio, however, these (co)polymers generally have a poor crystalline order. Such polymers crystallise slowly and only to a low extent. On melt processing, a slow crystallising polymer will result in a very low crystalline material with a poor solvent resistance.

The high T_g polymers like polycarbonates and poly(phenylene ether) do not crystallise from the melt during melt processing. A way to obtain a material with a high T_g and a good solvent resistance is to blend these materials with a semi-crystalline polymer. For example PC is often blended with poly(butylene terephthalate) (Xenoy[®]) and PPE with polyamide-6,6 (Noryl-GTX[®]). Both contain a small amount of rubber as well, to improve the impact properties. In Figure 1.1 the storage and loss modulus of these two high temperature blends are given as a function of temperature⁴. A disadvantage of such blends is that they will easily undergo phase separation on macroscale, with usually delamination and low impact strength as a result. The morphology is complex and the modulus below the T_g of the amorphous polymer is lower due to the presence of the semi-crystalline polymer phase. The semi-crystalline polymer shows a second, lower T_g of the amorphous part next to the melting temperature of the crystalline part. The dimensional stability of such a blend is very high only up to the lowest T_g . Another disadvantage of such a blend material is that a high semi-crystalline polymer content (about 40%) is needed in order to obtain enough crystallinity and the right morphology for a good solvent resistance. A co-continuous crystalline morphology is necessary for good solvent resistance and therefore a high crystalline content is needed.

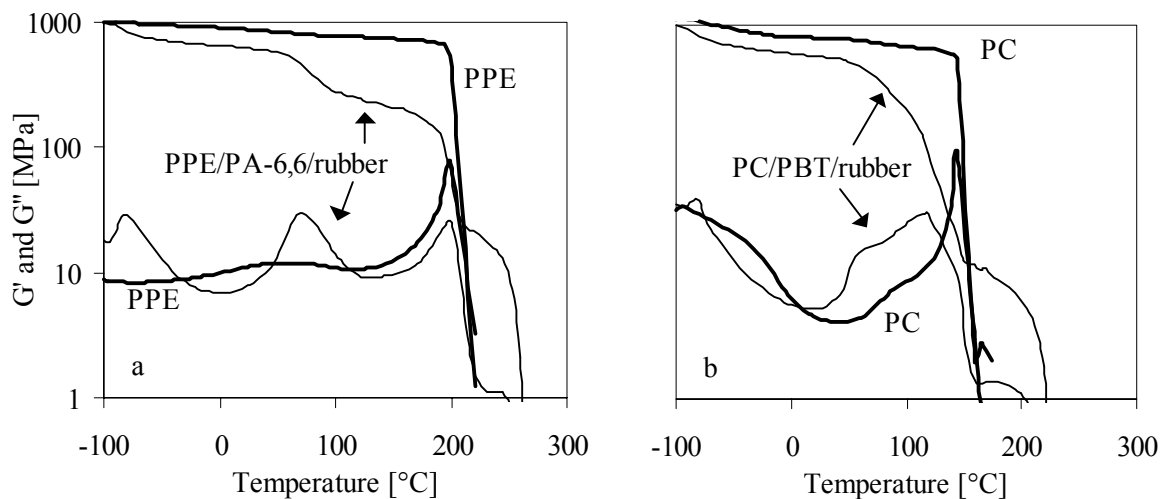


Figure 1.1a and b: Storage and loss modulus of two high temperature materials a) PPE/PA-6,6 blend (Noryl-GTX[®]) and b) PC/PBT blend (Xenoy[®]) compared to the corresponding amorphous homopolymers; both contain some rubber to improve the impact properties⁴.

Another strategy to obtain a material with a high T_g and T_m is to blend a semi-crystalline material and an amorphous high T_g material that are miscible. The T_g of the mixed amorphous phase will then be in between of the T_g 's of the two polymers that form the mixed phase. The T_g of the mixed phase will change proportional to the amount of both polymers. These blends will have one T_g and one T_m and have high dimensional stability up to the T_g of the mixed amorphous phase. However only few of such blends are known.

An example of such a combination is a blend of syndiotactic polystyrene (sPS) and PPE⁵. Pure sPS is able to crystallise, with a maximum degree of crystallinity of 60% and a melting temperature of 270 °C. It has a T_g of 100 °C and a T_g/T_m ratio of 0.68. By blending sPS and PPE the T_g of the amorphous phase (sPS/PPE) increases with increasing PPE content.

However, at the same time the crystallinity of sPS decreases with increasing PPE content and crystallisation during melt processing is difficult at higher PPE levels. So for most applications this blend does not result in a polymer system which has a sufficiently high T_g and a good solvent resistance.

Besides the low crystallisability on melt processing of these blends of an amorphous and a semi-crystalline polymer, another disadvantage is that they are not transparent because of phase separation and crystallisation into spherulites. It would be very interesting to have transparent polymer systems that have a high T_g , a high T_g/T_m ratio and a fast crystallisation on cooling from the melt. It is expected that this combination of properties can be obtained in a segmented copolymer consisting of amorphous segments with a high glass transition temperature and fast crystallising, uniform crystallisable segments. Thus far only segmented copolymers based on amorphous segments with a low T_g are known. Especially segmented copolymers consisting of poly(tetramethylene oxide) and uniform di-amide units were found to crystallise very fast and complete upon cooling from the melt⁶. These materials had a good solvent resistance and were transparent. It will be interesting to study the crystallisability of segmented copolymers with uniform crystallisable units that have a high glass transition temperature, and thus a high T_g/T_m ratio, which is the subject of this thesis. Uniform tetra-amide units will be used instead of di-amide units, because high melting temperatures are needed when amorphous segments with a high T_g are used.

Research aim

The aim of the work described in this thesis is to study the synthesis and structure-property relationships of semi-crystalline segmented copolymers with a high T_g . Therefore a new type of segmented copolymers based on an amorphous segment with a high glass transition temperature ($>100^\circ\text{C}$) will be developed. These segmented copolymers will have a much higher T_g/T_m ratio than the segmented copolymers that are currently known. In particular segmented copolymers based on poly(2,6-dimethyl-1,4-phenylene ether) (PPE) as amorphous segment will be studied. As crystallisable segment a uniform tetra-amide unit will be used. An important issue is to study the effect of the high T_g/T_m ratio on the crystallisation behaviour. It would be very interesting if the research would lead to a novel high T_g polymer with a T_g of at least 150°C , that crystallises fast from the melt, has a good solvent resistance and is transparent. Such a material may serve as an alternative to known high temperature polymers e.g. for use as or in construction materials in high temperature applications.

Structure of this thesis

In *Chapter 2* the synthesis and characterisation of short, bifunctional PPE segments (PPE-2OH and PPE-2T telechelics) is described. PPE-2OH is prepared by redistribution of high molecular weight commercial PPE and PPE-2T by endgroup modification of PPE-2OH. PPE-2T has terephthalic methyl ester endgroups. In *Chapter 3* amorphous polyether-ester copolymers based on these PPE-2T telechelics and different diols that have reduced glass

transition temperatures and improved processability compared to pure PPE are presented. *Chapter 4* relates to the thermal-mechanical properties of copolymers of PPE-2T and poly(dodecane terephthalate) segments of different lengths. Copolymers with high PPE content and high PDDT content are described successively. In *Chapter 5* the synthesis and characterisation of the uniform bisester tetra-amide segments that are used as crystallisable units in the copolymers in this project are described. *Chapter 6* describes the synthesis and characterisation of copolymers of PPE-2T and different uniform tetra-amide segments, linked by dodecanediol (C12). Next to the thermal-mechanical properties, this chapter relates to the results obtained by DSC, WAXD, water absorption and melt rheology experiments. *Chapter 7* is directed to the thermal-mechanical properties of copolymers of PPE-2T and tetra-amide segments, linked by dodecanediol. Different series of copolymers are presented, in which the tetra-amide content, PPE-2T length and type, and uniformity of the tetra-amide segments were varied. In *Chapter 8* the thermal-mechanical properties of copolymers based on PPE-2T or PPE-2OH telechelics and tetra-amide units with different extenders than dodecanediol are discussed. The tetra-amide content was varied and the influence of the length and flexibility of the extender on the crystallisation behaviour was studied. *Chapter 9* relates to the use of the crystallisable tetra-amide segments in thermoplastic elastomers based on poly(tetra-methylene oxide) as an amorphous segment. The synthesis and characterisation of these copolymers that have a low T_g below room temperature is described. In *Chapter 10* the elastic properties of meltspun fibres of these thermoplastic elastomers are discussed.

Literature

1. G. Odian, 'Principles of Polymerization', Third Edition, John Wiley & Sons, New York, Chapter 2, 40 (1991).
2. C. Eckert, Chemistry & Industry, 14, 556 (1995).
3. Automotive Engineering, 102, 35 (1994).
4. Xenoy[®] (C101) and Noryl-GTX[®] (914) were provided by GE Plastics (Bergen op Zoom, the Netherlands).
5. S. Duff, S. Tsuyama, T. Iwando, F. Fujibayashi, C. Birkinshaw, Polymer, 42, 991 (2001).
6. M.C.E.J. Niesten, J. Feijen, R.J. Gaymans, Polymer, 41, 8487 (2000).

Chapter 2

Synthesis of telechelic poly(2,6-dimethyl-1,4-phenylene ether)

Abstract

Telechelic poly(2,6-dimethyl-1,4-phenylene ether) (PPE) segments are interesting starting materials for example for copolymerisation. A good method to make partly bifunctional PPE-2OH is by redistribution or depolymerisation of high molecular weight commercial PPE with tetramethyl bisphenolA. The product has a bimodal molecular weight distribution because only ~70-80% of high molecular weight starting material is depolymerised. The phenolic endgroups can be modified easily by a fast and complete reaction with methyl chlorocarbonyl benzoate. The product after endgroup modification is called PPE-2T and has terephthalic methyl ester endgroups and a molecular weight of 2000-4000 g/mol. The functionality of these PPE-2T segments is around 1.8. The bimodal PPE-2OH and PPE-2T products can be separated in a high and low molecular weight fraction by selective precipitation of the high molecular weight fraction. The low molecular weight fraction has a narrow molecular weight distribution with a polydispersity between 1.2 and 1.5.

Introduction

Poly(2,6-dimethyl-1,4-phenylene ether)¹⁻³ (PPE) or poly(2,6-dimethyl-1,4-phenylene oxide) (PPO) is a linear amorphous polymer with a very high glass transition temperature of approximately 215°C⁴. PPE has excellent properties such as high toughness, high dimensional stability, good flame retardation and low moisture uptake. PPE can be made by several methods. The main route to high molecular weight PPE is by oxidative polymerisation of 2,6-dimethylphenol (DMP) (Figure 2.1)^{1-3,5-7}. Alternative methods are synthesis by halogen displacement polymerisation^{1-3,8-11} or phase transfer catalysed polymerisation^{1-3,12} of 4-bromo-2,6-dimethylphenol (BDMP). Only the first method is performed on a commercial scale.

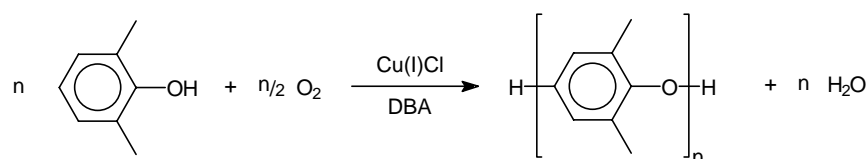


Figure 2.1: Oxidative polymerisation of 2,6-dimethylphenol.

The process for oxidative polymerisation of DMP to high molecular weight PPE (Figure 2.1) was first described by Hay in 1959⁵⁻⁷. The reaction is catalysed by a Cu(I)Cl/amine (preferably dibutylamine) catalyst system. In theory PPE has one 3,5-dimethyl-4-hydroxyphenyl ‘head’ endgroup and one 2,6-dimethylphenoxy ‘tail’ endgroup per chain. However, the oxidative polymerisation can give rise to side reactions, especially when the molecular weight increases². The first side reaction results in the presence of Mannich base type endgroups (Figure 2.2a) as a result of incorporation of the secondary amines that are used as a ligand for copper¹³. These endgroups are less reactive than the normal phenolic endgroups.

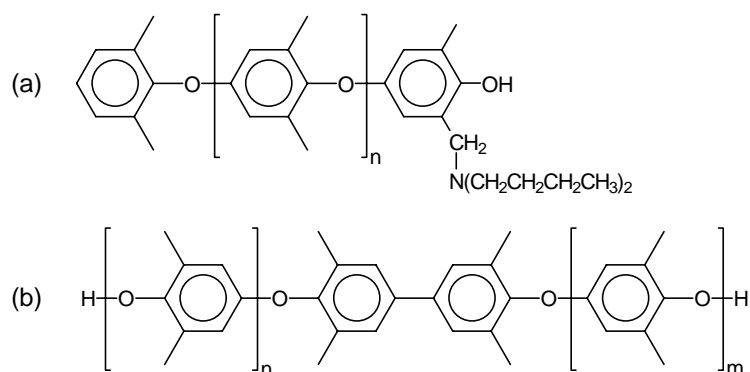


Figure 2.2: Impurities in PPE: (a) Mannich base endgroup, (b) TMDPQ incorporation.

The second side reaction yields the coloured TMDPQ (3,3',5,5'-tetramethyl-4,4'-diphenyl-quinone). TMDPQ can be incorporated in the polymer chain by the quinone coupling reaction between PPE and TMDPQ. This reaction leads to a bifunctional polymer with two OH-functionalities (Figure 2.2b). In linear polymers each polymer chain may contain at most one tetramethylbiphenyl unit derived from TMDPQ. In theory the biphenyl unit can be found,

either at the end of the chain¹⁴ ($m = 0$) or internally¹⁵, but usually the biphenyl unit will be incorporated somewhere inside the polymer chain¹⁶. In commercial high molecular weight PPE grades over 80% of the polymer chains contain a tetramethylbiphenyl unit derived from TMDPQ or a Mannich base type endgroup^{14,17}.

Although the commercial high molecular weight PPE's contain an appreciable amount of chains with a tetramethylbiphenyl unit that are bifunctional (Figure 2.2b), the phenolic functionality (concentration of 3,5-dimethyl-4-hydroxyphenyl 'head' endgroups) is in general lower than one, especially when high molecular weight polymers are made^{2,14,17}. Bifunctional poly(2,6-dimethyl-1,4-phenylene ether) segments or α,ω -bishydroxy functional PPE telechelics (PPE-2OH) of 500-5000 g/mol are interesting for use in copolymerisation to segmented copolymers or multiblock copolymers. There are different methods to make these low molecular weight PPE-2OH segments.

Synthesis of PPE-2OH

PPE telechelics (PPE-2OH) can be synthesised in different ways, which can be divided into three groups: from monomers (copolymerisation), from low molecular weight PPE-OH (coupling) and from high molecular weight PPE-OH (depolymerisation).

PPE-2OH from monomers

PPE-2OH can be prepared from monomers by copolymerisation. For example PPE-2OH (Figure 2.3) can be obtained by co-oxidation of 2,6-dimethylphenol (DMP) and 2,2'-di(4-hydroxy-3,5-dimethylphenyl)propane (tetramethyl bisphenol A, TMBPA) as was described by Heitz et al¹⁸⁻²⁰.

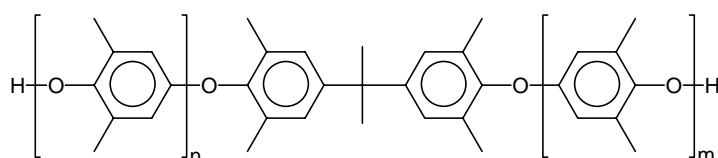


Figure 2.3: PPE-2OH (n or m can be 0) by copolymerisation of DMP and TMBPA.

The molecular weight depends on the molar ratio of both monomers. For PPE-2OH with a number average molecular weight below 1000 g/mol the phenolic OH functionality can reach values of 1.6-2.0 after 5-7 hours. With increasing reaction time the mono-functional product is converted into bifunctional ones, and the bisphenol is transferred from the chain ends into the chain. With decreasing TMBPA concentration PPE-2OH of higher molecular weight can be made. However, then redistribution (depolymerisation) is also taking place. Due to the redistribution reaction it is difficult to control the degree of polymerisation and the polymer chain ends functionality^{21,22}.

The formation of high molecular weight species can largely be prevented by using a solvent-nonsolvent mixture whereby PPE-2OH above a certain molecular weight precipitates out of the reaction mixture^{21,22}. In this way well-defined PPE-2OH with number average molecular

weights ranging from 1000 to 5000 g/mol can be prepared. PPE-OH as well as PPE-2OH prepared by this method contains no TMDPQ or Mannich base type endgroups²¹⁻²³.

Next to oxidative copolymerisation of DMP, PPE-2OH can also be synthesised by copolymerisation of 4-bromo-2,6-dimethylphenol (BDMP) and TMBPA. The halogen displacement polymerisation of BDMP⁸⁻¹¹ can be performed using an oxidant such as a cupric amine catalyst. By the halogen displacement copolymerisation of DMP and TMBPA, PPE-2OH with a functionality of 1.7-1.9 can be made. The number average molecular weight of the product is 900-3600 g/mol, depending on the molar ratio of the two monomers¹⁸. Alternatively BDMP can be polymerised by phase transfer catalysed polymerisation¹². This reaction proceeds via a radical-anion mechanism. By phase transfer catalysed copolymerisation of BDMP in the presence of TMBPA, PPE-2OH with a functionality of 2.0 and $M_n = 2700$ g/mol can be made²⁴. However the reaction time is very long.

PPE-2OH from low molecular weight PPE-OH

Another method to obtain bifunctional PPE is coupling of two monofunctional PPE chains of low molecular weight. This can be done for example by condensation with formaldehyde¹⁸. Coupling can also be performed with TMDPQ¹⁵. Products with two phenolic endgroups can only be obtained with a well-defined monofunctional PPE-OH. The molecular weight of the products is doubled. In general, the functionality of the coupling product is lower than two.

PPE-2OH from high molecular weight PPE-OH

Recently a good and simple method to produce short bifunctional PPE-2OH segments was described^{17,26}. Bifunctional PPE telechelics with two phenolic endgroups can be prepared by redistribution (depolymerisation) of high molecular weight PPE with bisphenols. Tetramethyl substituted bisphenols will be incorporated in the middle of the chains as well as at the chain ends. Unsubstituted bisphenols are only incorporated at the chain ends. The reaction can be performed without a catalyst. However the rate of redistribution is increased by adding a catalyst, for example CuCl/DMAP, Cu(NO₃)₂·2H₂O/N-methylimidazole, tetramethyl-diphenoquinone (TMDPQ) or benzoyl peroxide^{17,27,28}.

Pure telechelic PPE-2OH with a narrow molecular weight distribution can be prepared by redistribution of a well-defined monofunctional PPE-OH with a bisphenol using CuCl/DMAP or Cu(NO₃)₂·3H₂O/N-methylimidazole as a catalyst. However these reactions are very slow with reaction times up to two weeks. Only TMDPQ and benzoyl peroxide show fast redistribution reactions, but with side reactions. The redistribution with TMDPQ is most widely studied. TMDPQ is incorporated in the polymer chain during the reaction (Figure 2.2b), which is not a problem when the objective is to obtain PPE-2OH. TMDPQ can also lead to oxidative coupling, but only when a base is present. Although TMDPQ is partially incorporated and partially reacted to tetramethylbiphenol it is generally called a catalyst.

The mechanism of the redistribution reaction catalysed by TMDPQ is shown in Figure 2.4^{15,17,27}. Reaction of TMDPQ with the 3,5-dimethyl-4-hydroxyphenyl 'head' endgroup of PPE or TMPBA will initially generate a phenoxy radical endgroup of PPE (A) or TMBPA (B)

and the dipheno-semiquinone (C). The resulting phenoxy radical of TMBPA (B) can join in the redistribution reaction and couple with a polymer radical (A) via a quinone ketal intermediate (D). This quinone ketal can dissociate back to A and B or split into two new radicals; a shorter polymer radical (E) and a new chain in which TMBPA is coupled to a monomer unit of the PPE chain (F). This reaction sequence continues throughout the reaction, thereby gradually depolymerising or unzipping the PPE chain.

The semiquinone (C) can couple with a polymer radical (A) as well to form a quinone ketal intermediate (G) which reacts in the same way as intermediate D. The semiquinone can also abstract a hydrogen from a phenol (PPE chain or TMBPA) to form the biphenol 3,3',5,5'-tetramethyl-4,4'-biphenol.

The chains that contain a bisphenol unit derived from TMBPA can be re-initiated at the hydroxyl group of the bisphenol unit. In this way TMBPA can be incorporated in the middle of the chain as well. In the same way biphenols derived from TMDPQ can be incorporated in the middle of the chain.

Next to these redistribution reactions, also intermolecular rearrangements take place via the ketal intermediates. For example the intermediate G can rearrange via G' to G'' which is an enolisable keton that will be tautomerised to a polymer chain with a phenolic 'head' endgroup instead of a 'tail' endgroup (J)²⁹. As a result of these rearrangement reactions the product hardly contains 2,6-dimethylphenoxy 'tail' endgroups.

A requirement for the redistribution reaction is that both of the reacting species have at least one phenolic endgroup^{15,28,30-32}. This is confirmed by the observation that no depolymerisation of PPE occurred after complete acetylation of the phenolic endgroups^{27,31}. Therefore starting with well-defined monofunctional PPE-OH is preferred.

A disadvantage of commercial high molecular weight PPE as a starting material for redistribution is that it has a phenolic functionality below one, due to side reactions during the polymerisation reaction^{14,17}. It was found that endgroups such as the 2,6-dimethylphenoxy 'tail' endgroups, Mannich type endgroups and tetramethylbiphenyl endgroups derived from TMDPQ are degradation resistant and do not react in the redistribution reaction²⁸. Only chains with at least one phenolic 'head' endgroup can be initiated in the redistribution reaction and will be depolymerised. As a result the redistribution product of commercial PPE will consist of two fractions, a low molecular weight depolymerised fraction and a high molecular weight fraction that has not reacted.

About half of the chains in commercial high molecular weight PPE contain a tetramethylbiphenyl unit. When such a chain has only one phenolic endgroup, unzipping can continue only up to the position of the tetramethylbiphenyl unit in the chain. Then a chain with a non-reactive endgroup for further redistribution remains. Thus, some chains will be depolymerised only partially.

Another disadvantage of working with high molecular weight PPE as a starting material for redistribution is that the rate of the redistribution reaction decreases with increasing molecular weight of the starting material. This is caused by the decreasing phenolic endgroup concentration in solution with increasing molecular weight²⁷.

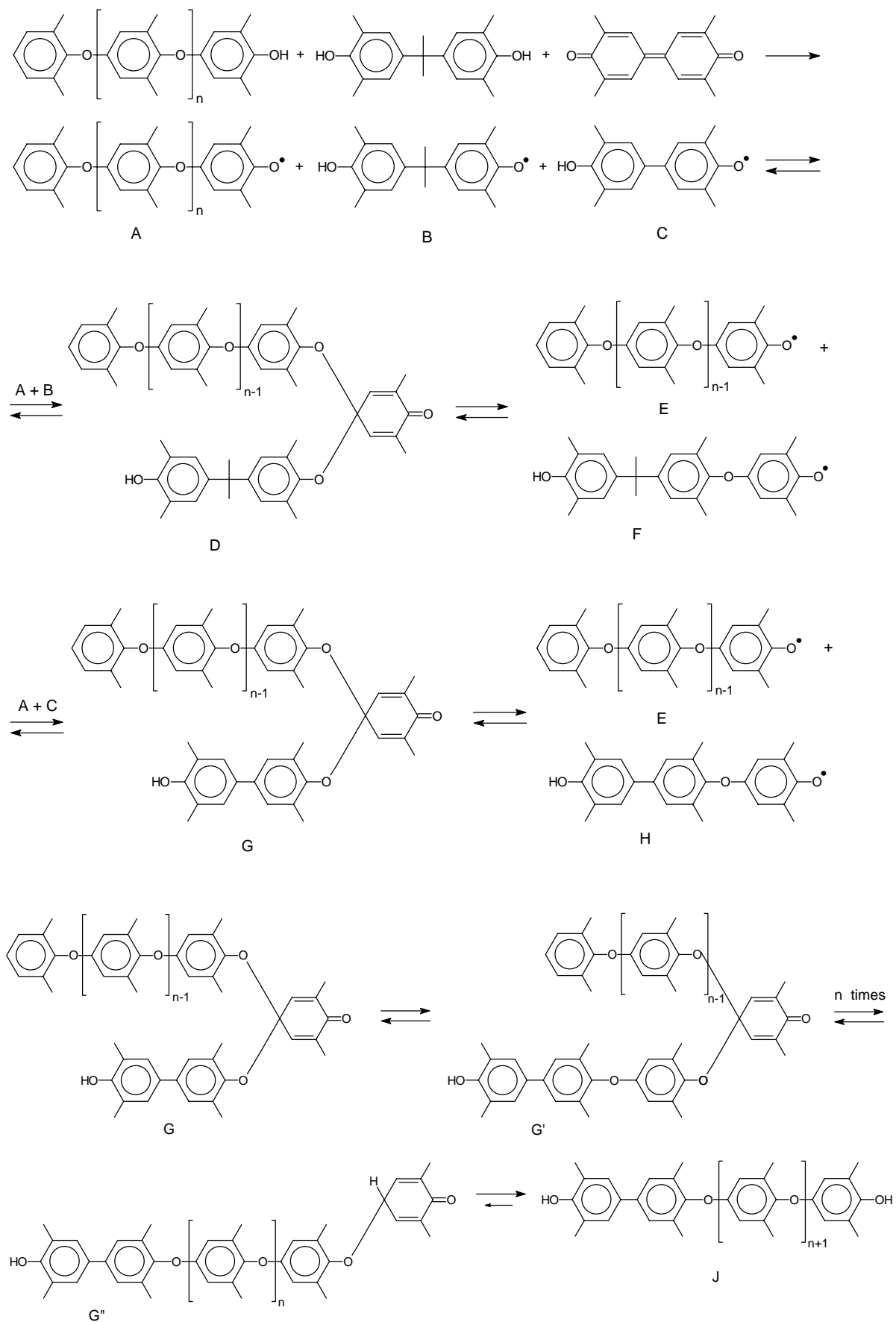


Figure 2.4: Mechanism of the redistribution reaction^{15,17,27}.

Percec et al^{32,33} studied an alternative method to perform redistribution by phase transfer catalysed depolymerisation of PPE. Depolymerisation of commercial PPE and well-defined PPE-OH in the presence of 2,4,6-trimethylphenol or 4-tert-butyl-2,6-dimethylphenol are compared. Polymers obtained by depolymerisation of a commercial PPE show a bimodal molecular weight distribution and are depolymerised for only 64%. Starting with a well-defined PPE-OH prepared by phase transfer catalysed polymerisation¹² yields depolymerised PPE chains that are functionalised for 92%. This redistribution product shows a bimodal molecular weight distribution as well, however the high molecular weight fraction is much smaller in this case.

Endgroup modification

A disadvantage of the telechelic PPE-2OH segments in a reaction is the low reactivity of the phenolic endgroup. Therefore direct use of PPE-2OH in for example a (poly)condensation type reaction is not well possible and endgroup modification is preferred.

The terminal hydroxyl groups of PPE are less acidic than the phenolic ones, due to electron-donating effects of the methyl groups in the ortho-positions and the ether oxygen in para-position. Similarly, the steric influence of two methyl groups is significant in reactions with bulky electrophiles. Also, the conformational behaviour of PPE in solution influences the conversion. In non-polar solutions the terminal hydroxyl groups are barely accessible. On the other hand, PPE is insoluble in strongly polar solvents³⁴.

Possible modification routes are based on etherification or esterification reactions³⁴⁻³⁶. Modification by ether linkage is preferred, because the phenolic esters are less stable under acidic or basic hydrolytic conditions²². This is caused by the good leaving group character of phenolates, which are formed during decomposition or hydrolysis of the phenolic esters³⁷. However, with shielded aromatic esters like these PPE-esters with 2,6-dimethyl substitution this effect might not be so strong.

Etherification

The 2,6-disubstituted phenols cannot be etherified to high conversions under normal Williamson etherification reaction conditions. However these phenols can be quantitatively etherified in the presence of phase-transfer catalysts²². These reactions can lead to several functional endgroups such as cyano, amino, allyl, methoxy, nitro and carboxylic acid^{37,38}. For example etherification using chloro-ethylamine leads to a product with amino endgroups. Synthesis of aliphatic hydroxyl terminated PPE can only be performed in a two step reaction using the allyl-terminated PPE. These reactions are almost quantitative (>95% modification). However, these etherification reactions seem less interesting from a commercial point of view.

Esterification

In theory esterification of phenolic endgroups can be performed using acid chlorides, acid anhydrides, phenyl esters and methyl esters. However the reactivity decreases strongly in this order. In practice only reactions where functionalisation is obtained with reactants like acid

chlorides^{14,39} or anhydrides^{40,41} are fast and complete. And as the resulting ester group must be hydrolytically stable, aromatic acids are preferred.

The acid chloride modification reaction seems particularly interesting for modification of the phenolic endgroups of PPE-2OH with terephthalic acid chlorides. It was found for example that it is possible to react the phenolic endgroups of PPE-OH or PPE-2OH completely with a stoichiometric amount of terephthaloyl chloride as a coupling agent³⁹. Modification of the phenolic endgroups of PPE by reacting PPE-OH with an excess of terephthaloyl chloride, followed by reaction with an aliphatic diol yields PPE with aliphatic hydroxyl endgroups^{14,42}.

PPE with reactive terephthalic ester endgroups can be obtained by reacting the phenolic endgroups with terephthaloyl chloride and an alcohol (methanol or phenol) or by a direct reaction with the half ester half acid chloride methyl chlorocarbonyl benzoate (MCCB) (Figure 2.5). When PPE-2OH is used as a starting material, this reaction results in PPE with terephthalic methyl ester groups on both ends of the chain. This PPE segment with two methyl ester functionalities is called PPE-2T (in which T stands for the terephthalic endgroup). It is expected that next to the phenolic 'head' units also tetramethyl bisphenolA and tetramethylbiphenyl endgroups will be functionalised by the acid chloride. The Mannich base type endgroups have a lower reactivity and will react only partially with the acid chloride.

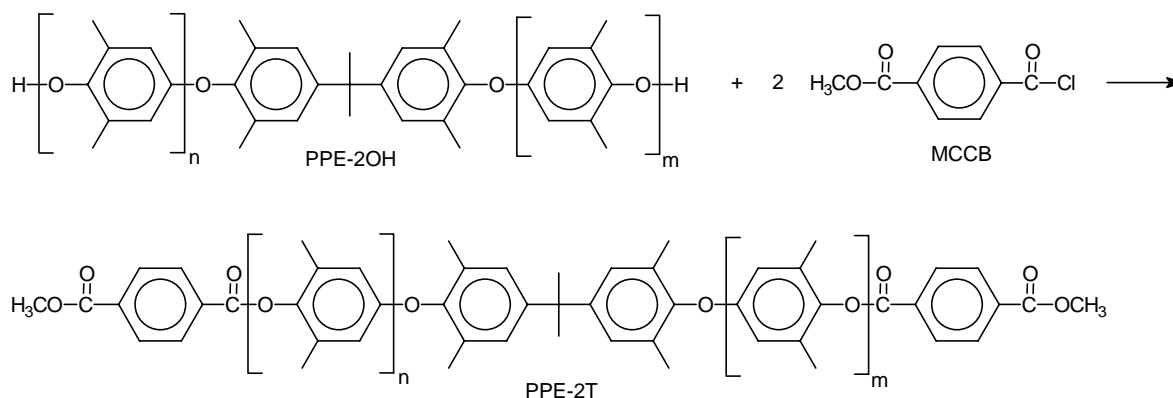


Figure 2.5: Molecular structure of PPE-2T that is obtained after reacting PPE-2OH with methyl chlorocarbonyl benzoate (MCCB).

Aim

In this chapter, the synthesis and characterisation of PPE-2OH and PPE-2T will be discussed. PPE-2OH was made by redistribution of high molecular weight commercial PPE with tetramethyl bisphenol A and tetramethyl diphenoquinone as a catalyst. PPE-2T was obtained after endgroup modification of PPE-2OH with MCCB. Also a method to separate the bimodal redistribution product into two monomodal fractions will be presented. For all products different methods to determine the average molecular weight of the products will be discussed. The products were analysed using titration, ¹H-NMR, GPC, viscometry and DSC.

Experimental

Materials. Dimethyl terephthalate (DMT), triethylamine, toluene and methanol were purchased from Merck. 4,4'-Isopropylidenebis(2,6-dimethylphenol) (tetramethyl bisphenol A, TMBPA) was purchased from Aldrich. Methyl-(4-chlorocarbonyl) benzoate (MCCB) was obtained from Dalian (No.2 Organic Chemical Works, P.R.C.O.). Poly(2,6-dimethyl-1,4-phenylene ether) (PPO-803[®]) used in the redistribution reaction and 3,3',5,5'-tetramethyl-1,4-diphenoquinone (tetramethyl diphenoquinone, TMDPQ) were obtained from GE Plastics (Bergen op Zoom, The Netherlands). PPO-803[®] has a number average molecular weight of 11.000 g/mol. All chemicals were used as received.

PPE-2OH. 40 Gram PPO-803[®] was dissolved in 400 ml toluene at 60°C in air. Subsequently tetramethyl bisphenolA (TMBPA) (4.0 g, 14 mmol) dissolved in 20 ml methanol was added. The reaction was started by the addition of tetramethyl diphenoquinone (TMDPQ) (0.40 g, 1.7 mmol). After 3 hours the reaction mixture was added to a 10-fold excess of methanol to precipitate the product. The precipitated polymer was collected by filtration, washed with methanol and dried in a vacuum oven at 50°C.

PPE-2T (two-step). 10 Gram redistributed PPE-2OH (5.1 mmol OH) was dissolved in 100 ml toluene at 70°C under nitrogen flow. Then a 1.5 excess of methyl chlorocarbonyl benzoate (MCCB) (1.5 gram, 7.6 mmol) was added. After 30 minutes a 1.5 excess (to MCCB) of triethylamine (1.2 g, 11 mmol) was slowly added dropwise. After 3 hours the reaction mixture was added to a 10-fold excess of methanol to precipitate the product. The precipitated polymer was collected by filtration, washed with methanol and dried in a vacuum oven at 50°C.

PPE-2T (one-pot). The synthesis of PPE-2T was simplified by performing the redistribution reaction with TMBPA and the endgroup modification reaction with MCCB in one pot without precipitation between both steps. 40 Gram PPO-803[®] was dissolved in 400 ml toluene at 60°C in air. Subsequently TMBPA (4.0 g, 14 mmol) was added. The reaction was started by the addition of TMDPQ (0.40 g, 1.7 mmol). After 2 hours reaction time, the temperature was raised to 70°C and set under nitrogen flow. Then a 1.5 excess to the total OH concentration of PPE, TMBPA and TMDPQ (10 g, 50 mmol) of MCCB was added. After 30 minutes a 1.5 excess (to MCCB) of triethylamine (7.6 g, 75 mmol) was slowly added dropwise. After 3 hours the reaction mixture was added to a 10-fold excess of methanol to precipitate the product. The precipitated polymer was collected by filtration, washed with methanol and dried in a vacuum oven at 50°C.

Fractionated PPE-2OH. The PPE-2OH that is obtained as described above has a broad (bimodal) molecular weight distribution. This product could be separated in two fractions by partial precipitation. The redistribution method was the same as for the synthesis of PPE-2OH, except for the precipitation step. After 3 hours reaction, 200 ml of methanol was added to the reaction mixture to precipitate the high molecular weight fraction selectively. The high

molecular weight product was collected by filtration, washed with methanol and dried in a vacuum oven at 50°C. The filtrate was then added to a 10-fold excess of methanol to precipitate the low molecular weight fraction. The low molecular weight product was collected by filtration, washed with methanol and dried in a vacuum oven at 50°C.

Fractionated PPE-2T (one-pot). The PPE-2T that is obtained in the one-pot reaction as described above has a broad (bimodal) molecular weight distribution. This product could be separated in two fractions by partial precipitation in the same way as the fractionated PPE-2OH, except that now 175 ml of methanol was added to the reaction mixture to precipitate the high molecular weight fraction.

NMR. ¹H-NMR spectra were recorded on a Bruker spectrometer at 300 MHz. CDCl₃ was used as a solvent.

Viscometry. The inherent viscosity of the polymers was determined with a capillary Ubbelohde type 0C at 25°C, using a polymer solution with a concentration of 0.1 g/dl in chloroform.

GPC. GPC measurements were carried out with polymer solutions in chloroform (5 mg/ml), filtrated via 0.45 μm Schleicher&Schuell filters. The molecular weight was determined using GPC with a Waters model 510 pump, a differential refractometer model 411, a viscotek H502 viscometer and Waters columns HR4 + HR2 + HR0.5 and a 500Å guard column in series. A flow rate of 1.5 ml/min was used with chloroform as a solvent at 25°C. Calibration was performed with 9 monodisperse polystyrene standards (range 827-1450 g/mol).

OH concentration. The concentration of phenolic endgroups (3,5-dimethyl-4-hydroxyphenyl 'head' endgroups, tetramethyl bisphenolA endgroups and tetramethylbiphenyl endgroups) was determined by titration using a Metrohm titroprocessor type EA636 with Ross glass electrodes. PPE samples (400 mg) were dissolved in pyridine and tetrabutyl ammonium hydroxide in isopropanol/methanol (0.1 M) was used as a titrant.

DSC. DSC spectra were recorded on a Perkin Elmer DSC7 apparatus, equipped with a PE7700 computer and TAS-7 software. Dried samples of 3-7 mg PPE-2OH or PPE-2T were measured with a heating and cooling rate of 20°C/min. The samples were heated to 300°C, kept at that temperature for 2 minutes, cooled to 50°C and reheated to 300°C. The glass transition temperature (T_g) was determined in the second heating scan.

Results and Discussion

Introduction

The depolymerisation or redistribution of commercial high molecular weight PPE (PPO-803[®]) with tetramethyl bisphenolA (TMBPA) to PPE-2OH using tetramethyl diphenoquinone (TMDPQ) as a catalyst was studied. The characterisation of the products of this reaction will be discussed first. A method to calculate the number average molecular weight and functionality of the products from the phenolic concentration measured by titration and from NMR will be presented. Then the results of the endgroup modification reaction of the phenolic endgroups of PPE-2OH with methyl chlorocarbonyl benzoate (MCCB) to the product PPE-2T will be given. The molecular weight of these segments was calculated on a similar way as that of PPE-2OH. The synthesis of PPE-2OH and PPE-2T with a narrow molecular weight distribution that can be obtained by fractionation will be discussed next. At the end the characterisation of the different PPE-2OH and PPE-2T segments by viscometry and DSC is described.

PPE-2OH

PPE-2OH is made by redistribution of PPO-803[®] with TMBPA and with TMDPQ as a catalyst. The product is obtained after precipitation of the reaction mixture in a 10-fold excess of methanol. All products are white and the yield is 66-94%, depending on the amount of TMBPA used (Table 2.1, p.22).

It was found that a major disadvantage of the product PPE-2OH of the redistribution reaction with commercial PPO-803[®] as a starting material is that this product shows a bimodal molecular weight distribution. A typical GPC curve of the starting PPO-803[®] and the product PPE-2OH that is obtained after redistribution with 10 wt% TMBPA is given in Figure 2.6.

PPO-803[®] shows a molecular weight distribution with $M_n = 11.000$ g/mol and $M_w/M_n = 2.0$. With titration the concentration of 3,5-dimethyl-4-hydroxyphenyl 'head' endgroups can be measured. It was determined that the starting functionality of PPO-803[®] is 75 $\mu\text{mol OH/gram}$. This OH endgroup concentration corresponds to a functionality of ~ 0.82 or around 82% of the chains contain a phenolic 'head' endgroup and the other 18% has no such endgroup. Based on these data, a maximum of only 82% of the chains can participate in the redistribution reaction^{15,28,30-32}. In fact there are some bifunctional chains as well, and thus the percentage of chains without a reactive endgroup is even higher. Therefore it is not possible to obtain a product that is completely depolymerised after redistribution.

With NMR analysis it can be calculated that about 50% of the PPO-803[®] chains contain a tetramethylbiphenyl unit derived from TMDPQ. Chains that contain TMDPQ can have a phenolic 'head' endgroup at both ends of the chain. Therefore the maximum phenolic functionality of PPO-803[®] is 1.5. However, about 30-40% of the 'head' endgroups is a Mannich base type endgroup. Therefore, according to NMR, about 72-81% of the chains has a phenolic endgroup and should be able to react in the redistribution reaction. The phenolic

functionality of the product as calculated by NMR is thus comparable with the functionality obtained by titration.

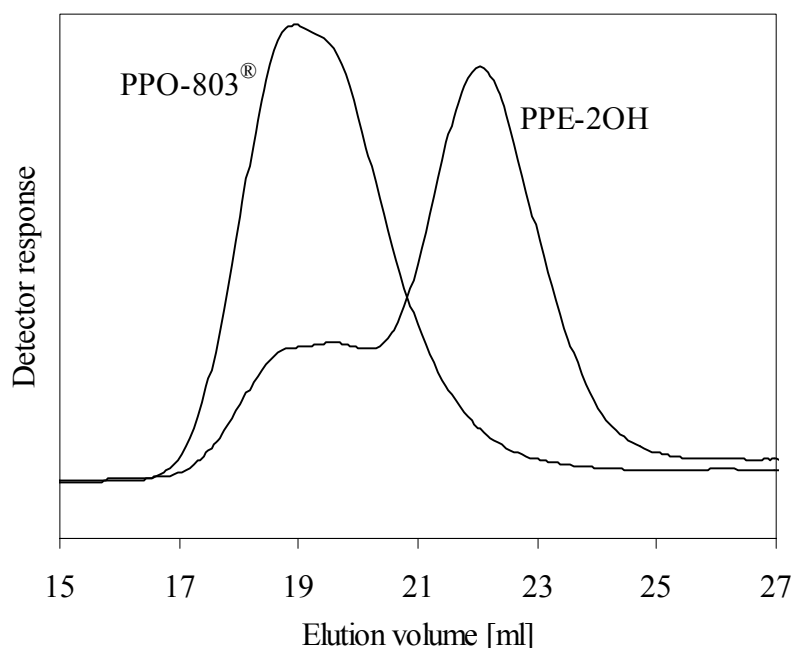


Figure 2.6: GPC molecular weight distribution of PPE-2OH product made by redistribution of PPO-803[®] with 10 wt% TMBPA.

PPE-2OH shows a bimodal molecular weight distribution as a result of the composition of PPO-803[®] starting material. Next to the low molecular weight fraction that is obtained by redistribution there is a high molecular weight fraction present. The position of the high molecular weight fraction in the GPC figure is comparable with that of the peak of the commercial PPO-803[®]. Thus the molecular weight of this high molecular weight fraction is comparable with that of the commercial PPO-803[®] starting material for redistribution (11.000 g/mol). This part of the commercial PPO-803[®] did not join in the redistribution reaction and remains unchanged in the product. The high molecular weight fraction forms about 23% of the area and the low molecular weight fraction 77% of the total area. These results correspond quite well with the expectation that around 72-81% (NMR) or 82% (titration) of the chains in PPO-803[®] have a phenolic endgroup and can be redistributed.

The presence of the high molecular weight PPE fraction that has not reacted makes characterisation of the redistribution products by NMR difficult. The redistribution product has a complicated composition. It contains both PPE chains that have not reacted and low molecular weight PPE-2OH products of the depolymerisation reaction. Different types of chains that can be found in the PPO-803[®] starting material for redistribution and in the redistribution product are given in Figure 2.7.

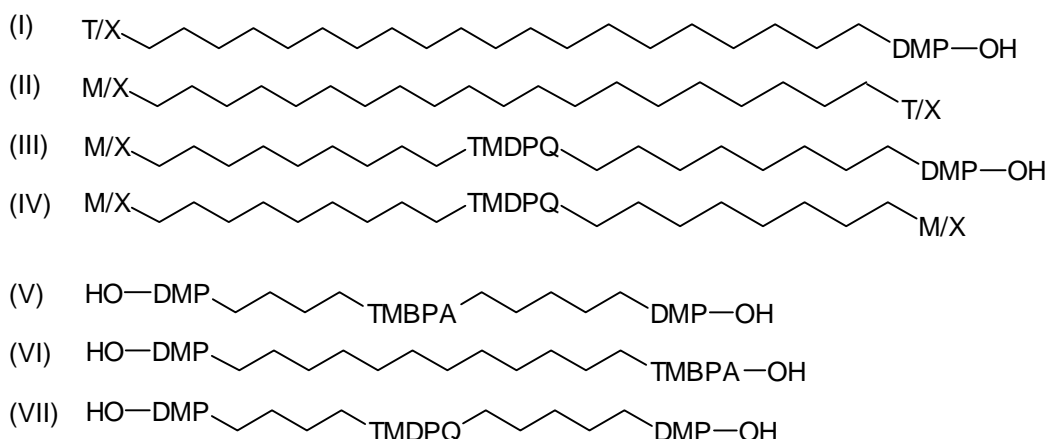


Figure 2.7: Main types of PPE chains in the product after redistribution of PPO-803[®] with TMBPA; *M* is a Mannich base type endgroup, *T* is a DMP ‘tail’ endgroup and *X* is an other endgroup.

In theory PPE (PPE-OH) has one 3,5-dimethyl-4-hydroxyphenyl ‘head’ endgroup and one 2,6-dimethylphenoxy ‘tail’ endgroup (T) (Figure 2.1) per chain (I). However several chains in commercial high molecular weight PPE contain Mannich base type endgroups (M) (Figure 2.2), tetramethylbiphenyl units (TMDPQ) and other endgroups (X) (II-IV). X endgroups can have different structures and are a result of side reactions. Only chains of type I and III with at least one ‘head’ endgroup can react in the redistribution reaction.

The redistribution product of PPE with TMBPA will contain PPE chains that have not reacted at all (II and IV), because they contain two endgroups that are not reactive in redistribution such as a Mannich base type endgroup (M), DMP ‘tail’ endgroup (T) or other endgroup (X)^{13,15,16}. Besides these chains of high molecular weight the product contains several low molecular weight chains. Redistribution of high molecular weight PPE can lead to short chains of type I. However most chains will contain a TMBPA or TMDPQ unit. There are two different types of depolymerised chains that contain TMBPA. When TMBPA is incorporated, it can be in the middle (V) or at the end of the chain (VI). And next to these types of depolymerised chains there are low molecular weight chains that contain a TMDPQ unit (VII). It is assumed that TMDPQ is mainly incorporated in the middle of the chain¹⁶. All chains can contain maximum one TMBPA or TMDPQ unit.

Besides these main chains, the product can also contain other types of chains. For example, not all the depolymerised chains (V-VII) have a phenolic endgroup at both chain ends as indicated. There will be some low molecular weight chains with Mannich base type endgroups (M), ‘tail’ endgroups (T) or other endgroups (X) instead of OH endgroups as well. Therefore, it is difficult to determine the amount of the different chain types with NMR.

The ¹H-NMR spectrum of the product after redistribution of 40 gram PPO-803[®] with 6 gram TMBPA (15 wt%) is given in Figure 2.8a. For calculation of the molecular weight of the product the aromatic part of the spectrum is used (Figure 2.8b), as the individual peaks can be seen best here. In Figure 2.9 the peak assignments for different types of chains in the product are given.

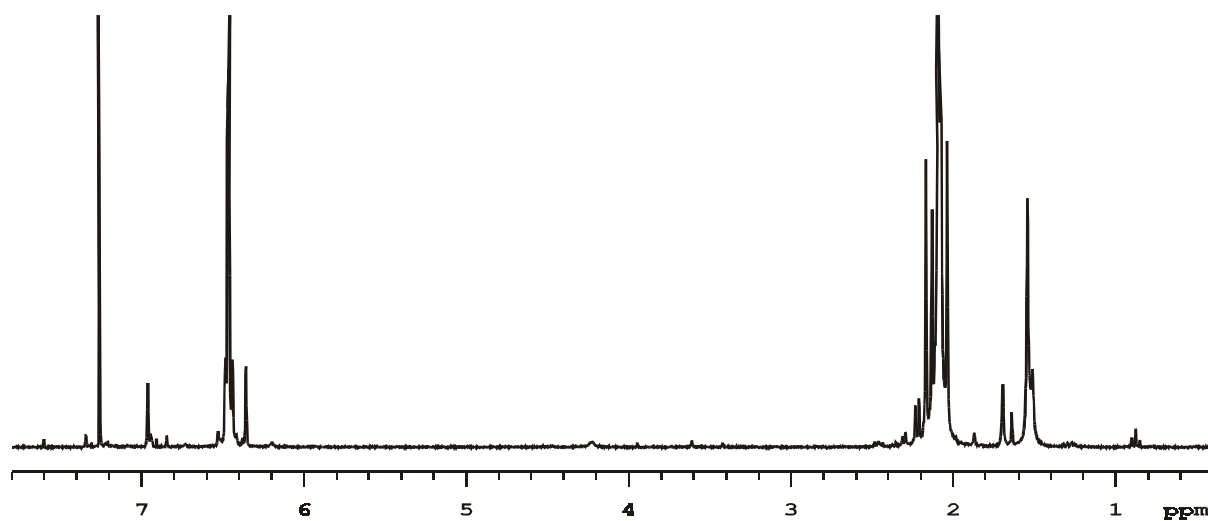


Figure 2.8a: $^1\text{H-NMR}$ spectrum of PPE-2OH, made by redistribution of PPO-803[®] with 15 wt% TMBPA.

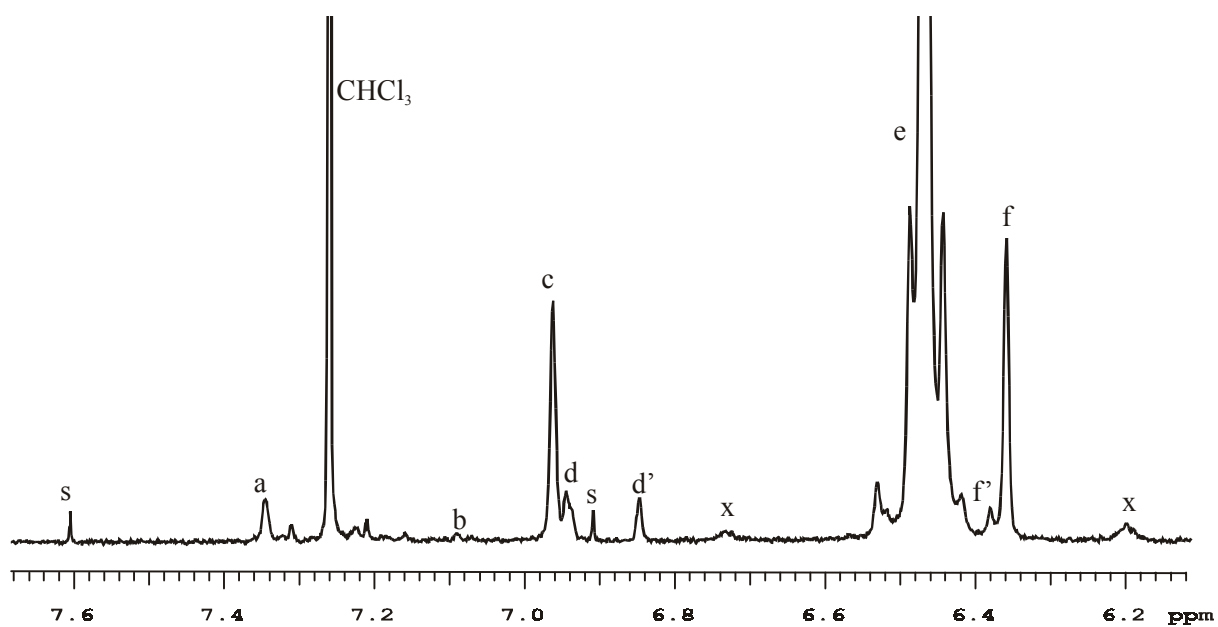


Figure 2.8b: Aromatic region of the $^1\text{H-NMR}$ spectrum of PPE-2OH, made by redistribution of PPO-803[®] with 15 wt% TMBPA (s = spinning side bands CHCl_3 and x = C^{13} satellites peak e).

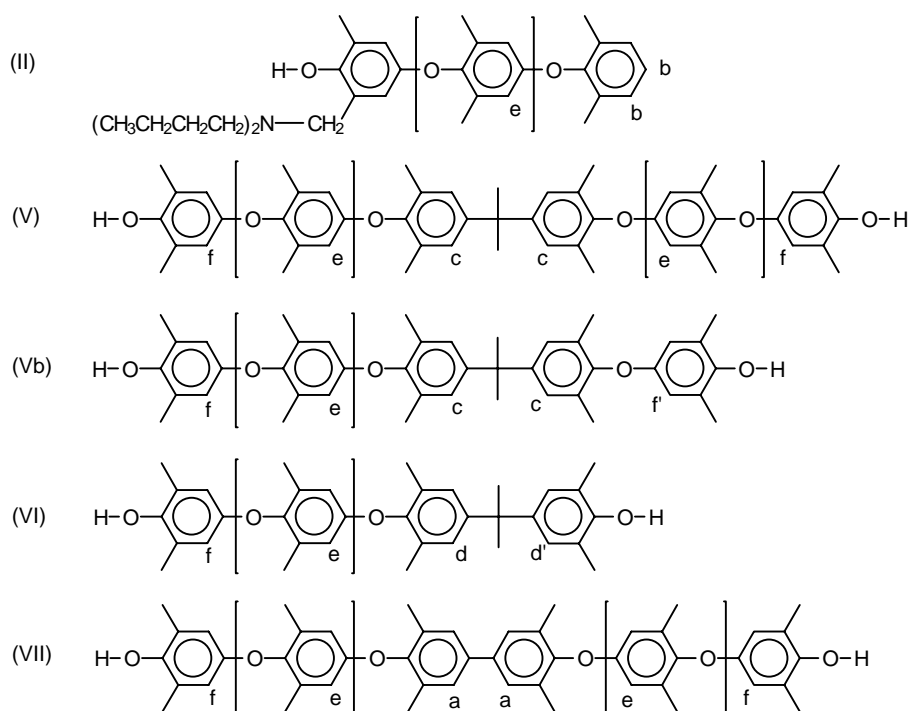


Figure 2.9: Peak assignments from the NMR spectrum given in Figure 2.8b for different chains in the product PPE-2OH, made by redistribution of PPO-803[®].

Different observations can be made from Figure 2.8 and 2.9:

- The main peak of the DMP repeating unit (peak e) can be found at 6.47 ppm; the peak spreads over the whole range of 6.4-6.55 ppm.
- The peak of the phenolic endgroup (peak f) can be found at 6.36 ppm.
- In some chains the phenolic endgroup is directly connected to the TMBPA unit in the chain (peak f', 6.38 ppm, structure Vb).
- Incorporation of TMBPA (in V, VI) is about 70% within the chain and 30% at the chain ends (peak c, 6.96 ppm, structure V vs. peak d and d', 6.94 and 6.84 ppm, structure VI). There is no unreacted TMBPA in the product (6.82 ppm)^{18,21}.
- Some chains contain a TMDPQ unit (peak a, 7.34 ppm, structure VII). The presence of the TMDPQ endgroups cannot be confirmed by NMR. Unreacted TMDPQ shows a peak at 7.72 ppm. TMDPQ is expected to give two peaks, one around 7.34 and one around 7.72 ppm. This is not the case. The number of TMDPQ units per DMP unit after redistribution is comparable with the concentration in PPO-803[®], so no extra TMDPQ units are incorporated during redistribution.
- PPE-2OH contains about 5 times as much TMBPA as TMDPQ (when 15 wt% TMBPA is used during redistribution).
- There are hardly 'tail' endgroups (peak b, multiplet 7.09 ppm, structure II) as a result of the large extent of the rearrangement reactions (Figure 2.4)²⁹ taking place.
- Mannich base type endgroups (M, structure II) are still present (see Figure 2.8a, singlet at 2.6, multiplet at 1.2-1.3 and triplet at 0.88 ppm). The number of Mannich base type endgroups per DMP unit is hardly changed after redistribution.

The average phenolic functionality (F) and the molecular weight of the bimodal PPE-2OH product can be calculated from the NMR spectrum, using the integrals of peak a and c-f'. However, an assumption is necessary to make this calculation possible. It is assumed that each chain contains one TMBPA or TMDPQ unit. By doing so the presence of monofunctional PPE chains (type I and II) is neglected. This assumption can be made because there are hardly DMP 'tail' endgroups (peak b in Figure 2.8 and 2.9) present after redistribution and because already 50% of the commercial PPE chains contain a tetramethylbiphenyl unit. As a result of this assumption the functionality and molecular weight as calculated by Equation 2.1-2.3 are a little bit too high.

The total phenolic endgroup concentration is the sum of peak d', f and f' (2H). The total expected endgroup concentration is the sum of peak a, c, d and d' (4H), assuming again that each chain contains at least one TMBPA or TMDPQ unit. The phenolic functionality can be calculated from the total phenolic endgroup concentration and the total expected endgroup concentration in the NMR spectrum. The average molecular weight can be calculated from n, the average number of repeating units per chain and the molecular mass of a repeating unit, TMBPA or TMDPQ and endgroups. The concentration of phenolic endgroups ([OH], d', f and f') can be calculated from F and M_n.

$$F \text{ (NMR)} = \frac{(d' + f + f')/2}{(a + c + d + d')/4} \quad [-] \quad \text{Equation 2.1}$$

$$n \text{ (NMR)} = \frac{(e + f + f')/2}{(a + c + d + d')/4} \quad [-] \quad \text{Equation 2.2}$$

$$M_n \text{ (NMR)} = n * M_{\text{DMP}} + M_{\text{TMBPA,TMDPQ}} + F * M_{\text{endgroup}} \quad [\text{g/mol}] \quad \text{Equation 2.3}$$

$$[\text{OH}] \text{ (NMR)} = \frac{F * 10^6}{M_n} \quad [\mu\text{mol/gram}] \quad \text{Equation 2.4}$$

$$\begin{aligned} \text{with: } M_{\text{DMP}} &= 120 \text{ g/mol} \\ M_{\text{TMBPA,TMDPQ}} &= 275 \text{ g/mol (TMBPA:TMDPQ } \sim 5:1) \\ M_{\text{endgroup}} &= 1 \text{ g/mol (H)} \end{aligned}$$

The average functionality, molecular weight and concentration of phenolic endgroups of different bimodal PPE-2OH products as calculated from the NMR spectra by Equation 2.1-2.4 are given in Table 2.1.

The average molecular weight and the phenolic functionality of the bimodal PPE-2OH product can be calculated from the phenolic concentration as measured by titration as well. By titration the concentration of the phenolic endgroups (peak d', f and f') can be determined [OH]. The starting material PPO-803[®] has 75 μmol OH/gram. Because the molecular weight of PPO-803[®] is 11.000 g/mol it contains around 182 μmol/g endgroups and thus 107 μmol/gram not titratable endgroups [M, T, X]. These endgroups will largely be present in the

product as well, except for the 2,6-dimethylphenoxy ‘tail’ endgroups (peak b) that disappear almost completely by the rearrangement reaction. The functionality of PPO-803[®] with 75 μmol OH/gram phenolic endgroups is 0.82.

The average molecular weight (M_n) and the functionality (F) of the bimodal product PPE-2OH can roughly be calculated from the phenolic concentration as measured by titration with the following equations. These equations apply only to PPO-803[®] as a starting material for redistribution with TMBPA. Again it is assumed that each chain contains a unit derived from TMBPA or TMDPQ.

$$M_n \text{ (titration)} = \frac{2 * 10^6}{[M, T, X] + [OH]} + M_{\text{TMBPA, TMDPQ}} \quad [\text{g/mol}] \quad \text{Equation 2.5}$$

$$F \text{ (titration)} = \frac{[OH] * M_n}{10^6} \quad [-] \quad \text{Equation 2.6}$$

with: [OH] = concentration of phenolic endgroups (peak d’, f and f’) measured by titration, in μmol/gram

[M,T,X] = concentration of other endgroups (not titratable) in the product (Mannich base type and 2,6-dimethylphenoxy ‘tail’ endgroups) = 107 μmol/gram (PPO-803[®])

$M_{\text{TMBPA, TMDPQ}} = 275 \text{ g/mol (TMBPA:TMDPQ } \sim 5:1)$

As a result of the assumption that each chain contains at least one unit derived from TMBPA or TMDPQ the functionality and molecular weight as calculated by Equation 2.5 and 2.6 are too high. The calculated functionality and molecular weight are further disturbed by the effect of the rearrangement reaction of ‘tail’ endgroups T. This reaction results in a decrease in the value of [M, T, X] of other endgroups that is taken as a constant in Equation 2.5. The rearranged DMP ‘tail’ endgroups are included in the [OH] that is measured by titration. As a result the concentration of rearranged endgroups is used twice in the sum of [M, T, X] and [OH] and the average molecular weight as calculated by Equation 2.5 is too low. Furthermore when almost all DMP ‘tail’ endgroups are rearranged during redistribution, the functionality as calculated by Equation 2.6 is too low. The overall effect of these two errors is probably small.

In Table 2.1 the properties of the products after redistribution of 40 gram PPO-803[®] with 4-10 grams (10-25 wt%) TMBPA are given. For product 6, TMBPA was added to the PPO-803[®] solution without dissolving in methanol first (compared to product 1). For product 7 a reaction time of only one hour was used (compared to product 2).

Table 2.1: Molecular weight and functionality of PPE-2OH made by redistribution of PPO-803[®] with different amounts of TMBPA as calculated by different methods.

			NMR			Titration			GPC		
	TMBPA	Yield	F	M _n	[OH]	[OH]	F	M _n	M _n	M _w /M _n	high
	[wt%]	[%]	(eq 2.1)	(eq 2.3)	(eq 2.4)	[μmol/g]	(eq 2.6)	(eq 2.5)	[g/mol]	[-]	M ^c
			[g/mol]	[μmol/g]		[μmol/g]	[-]	[g/mol]	[g/mol]	[-]	[%]
1	10	94	1.74	3500	503	508	1.79	3500	3250	2.7	23
2	12.5	90	1.72	3250	528	564	1.84	3250	3150	3.0	27
3	15	85	1.75	3150	554	574	1.84	3200	2850	3.3	30
4	20	74	1.84	3750	490	488	1.78	3650	2500	3.6	42
5	25	66	1.71	3400	507	510	1.79	3500	3250	4.0	50
6 ^a	10	92	1.80	4150	432	450	1.74	3850	3650	3.0	31
7 ^b	12.5	91	1.65	3400	487	537	1.82	3400	3250	3.3	32

(a), TMBPA was added without methanol; (b), a reaction time of one hour was used instead of 3 hours; (c), the area of the high molecular weight fraction as measured by GPC is given

Within the error ranges of 5-10% the molecular weight distributions as calculated from the different measuring methods are in reasonable agreement, although some data show larger deviation. In particular the [OH] and M_n from NMR and titration correspond quite well. The functionality that is calculated from the titratable OH endgroup concentration has somewhat higher values in general than that calculated from NMR measurements. The GPC data are less reliable, because the program is not well suitable for the calculation of the molecular weight of a bimodal product. It is concluded that the NMR data for average molecular weight of the bimodal product are the most accurate because here the least assumptions were used. The [OH] concentration as measured by titration can be used best to calculate quantities when the PPE segments are used in a further reaction, such as endgroup modification.

The molecular weight of the precipitated product decreases with increasing amount of TMBPA used (product 1-5), because the extent of redistribution increases. However, the products that are obtained using 20 or 25 wt% TMBPA have a higher average molecular weight than that using 15 wt% TMBPA. These results can be explained by the fact that the yield of the product decreases due to more loss of low molecular weight products as was shown by GPC measurements. So while the molecular weight of the redistributed fraction decreases further, the average molecular weight of the precipitated product increases with 20 and 25 wt% TMBPA. The molecular weight distribution of the different PPE-2OH products, as was measured by GPC, is given in Figure 2.10.

From Figure 2.10 it can be concluded that all PPE-2OH products show a bimodal molecular weight distribution. The peak of the high molecular weight fraction that has not reacted is at the same position as the peak for PPO-803[®]. However this peak broadens somewhat when the amount of TMBPA used increases. Therefore the average molecular weight of the high molecular weight fraction is probably somewhat lower when more TMBPA is used. The

relative area of the high molecular weight fraction increases with increasing amount of TMBPA from 23% (10 wt% TMBPA) to 50% (25 wt% TMBPA).

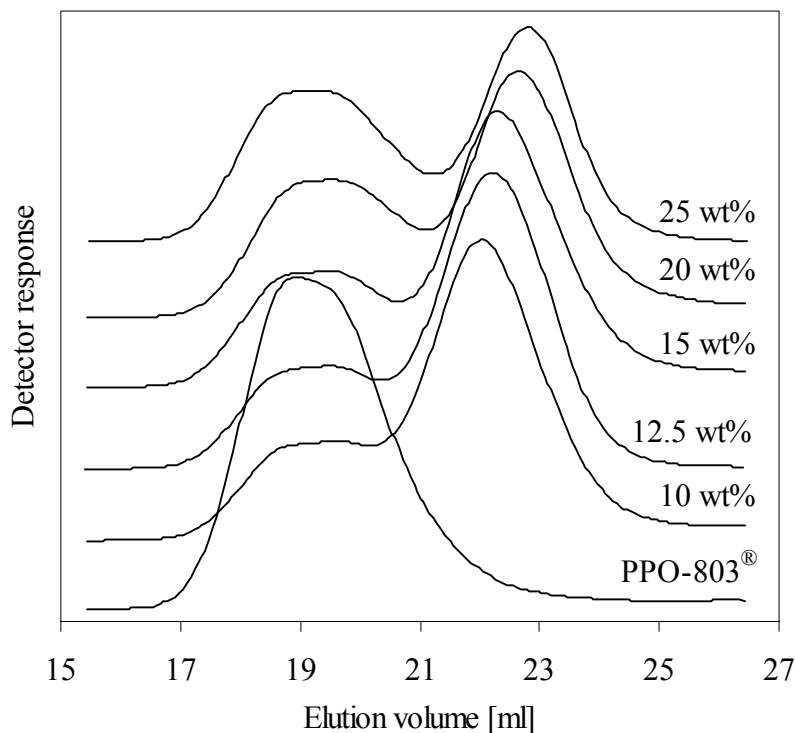


Figure 2.10: GPC molecular weight distribution of the PPE-2OH products made with different amounts of TMBPA after precipitation compared to PPO-803[®].

The peak of the low molecular weight fraction is shifted to lower value as the amount of TMBPA used increases. At the same time, with increasing amount of TMBPA, the amount of low molecular weight fraction in the precipitated product decreases compared to the high molecular weight fraction. And as is shown in Table 2.1, the yield of the product decreases with increasing amount of TMBPA as well. This can be explained by the fact that with increasing amount of TMBPA, the molecular weight of the depolymerised fraction becomes lower. The lowest molecular weight chains are lost during the precipitation step because they are soluble in the 10:1 methanol/toluene mixture that is used for precipitation. Chains with a molecular weight up to 800 g/mol are soluble in methanol^{21,32}. In a 10:1 methanol/toluene mixture, chains with a little higher molecular weight will be soluble as well, because toluene is a good solvent for PPE. So as a result of the precipitation procedure, the bimodal product that is obtained using 20 or 25 wt% of TMBPA has a higher average molecular weight than that using 15 wt% of TMBPA. When desired, this can be prevented by using evaporation as a method to obtain the product after the reaction instead of precipitation. With this method it is expected that the average molecular weight of the product will decrease further with 20 and 25 wt% TMBPA.

When the redistribution reaction is performed in toluene only (product 6), the molecular weight of the product is higher than when it is performed in a 20/1 mixture of toluene/methanol (product 1) as is shown in Table 2.1 and Figure 2.11. The peak area of the high molecular weight fraction that has not reacted is higher for PPE-2OH 6 (31%) than for 1 (23%), while the yield is approximately the same. Also the peak for the low molecular weight redistributed PPE-2OH fraction is at a higher molecular weight value for 6. Apparently the redistribution reaction is a little faster and more complete when it is performed in a reaction mixture of 20:1 toluene/methanol²⁶. Probably the phenolic endgroups are better accessible in this solvent/non-solvent mixture.

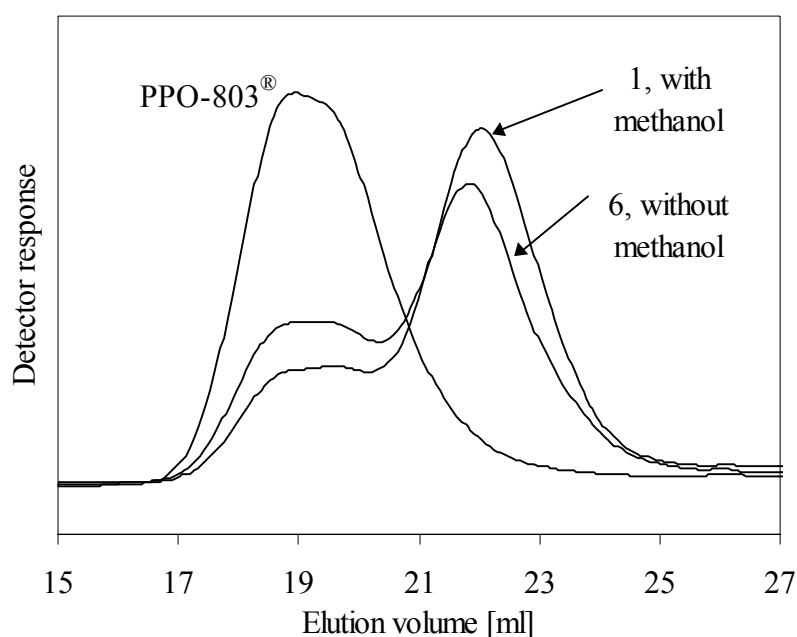


Figure 2.11: Comparing redistribution PPE-2OH product 1 and 6, synthesised by redistribution of PPO-803[®] with 10 wt% TMBPA in 20:1 toluene/methanol (1) or toluene (6).

The reaction time has little influence on the composition of the product. When a reaction time of 1 hour is used instead of 3 hours (product 7 vs. 2), the product has a little higher average molecular weight, lower functionality and larger high molecular fraction. Apparently the reaction is not fully completed after 1 hour and the equilibrium is not yet established. A reaction time of 16 hours has been studied as well, however no difference in the composition of the product was measured. Other variables that were tested include a higher amount of TMDPQ and adding the TMDPQ in three portions spread over the reaction time. These variations had no effect on the molecular weight distribution of the product.

PPE-2T

The phenolic endgroups of PPE-2OH were modified by reaction with methyl chlorocarbonyl benzoate (MCCB) to obtain PPE-2T (Figure 2.5). Next to the phenolic 'head' endgroups, also the tetramethyl bisphenol A and a part of the Mannich base type endgroups of PPE-2OH will be functionalised by reaction with MCCB. So next to the low molecular weight fraction of PPE-2OH, also some chains of the high molecular weight fraction that is not depolymerised can be functionalised.

The reaction of the phenolic endgroups with the acid chloride is a fast and complete reaction and results in the product PPE-2T that has terephthalic methyl ester endgroups at both ends of the chain. These endgroups have a higher reactivity than the original phenolic endgroups of PPE-2OH. This is preferred when the segments will be used in for example a polycondensation reaction.

The products are white and the yield of the endgroup modification reaction is over 95%. The molecular weight of the PPE chains is increased compared to the PPE-2OH starting material, as MCCB is incorporated (Figure 2.12 and Table 2.2). The position of the high molecular weight PPE fraction is unchanged after reaction with MCCB, while the depolymerised low molecular weight PPE-2OH fraction is shifted to the left -to higher molecular weight- after reaction with MCCB.

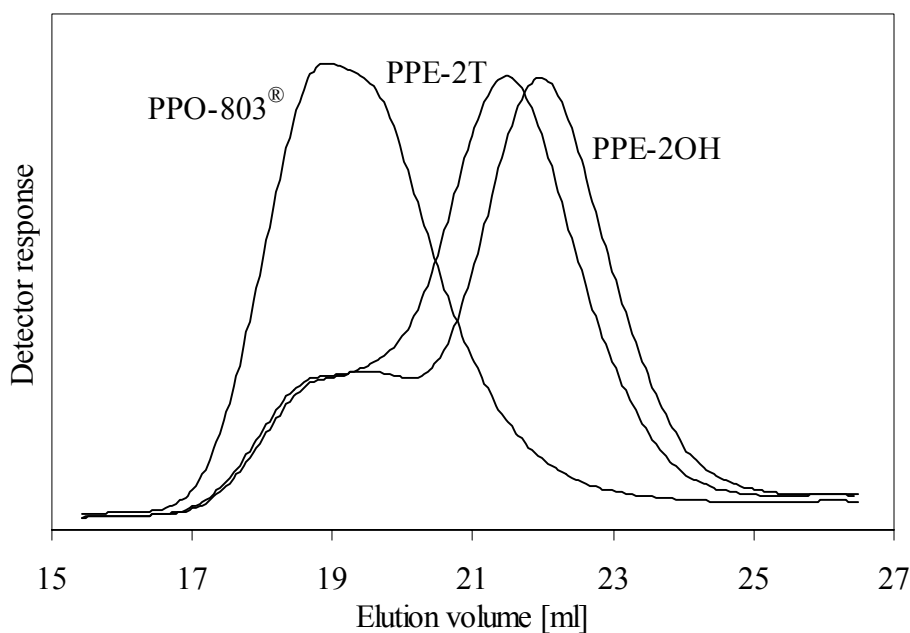


Figure 2.12: GPC molecular weight distribution of PPE-2OH-1 (10 wt% TMBPA) and PPE-2T-1 made out of this PPE-2OH.

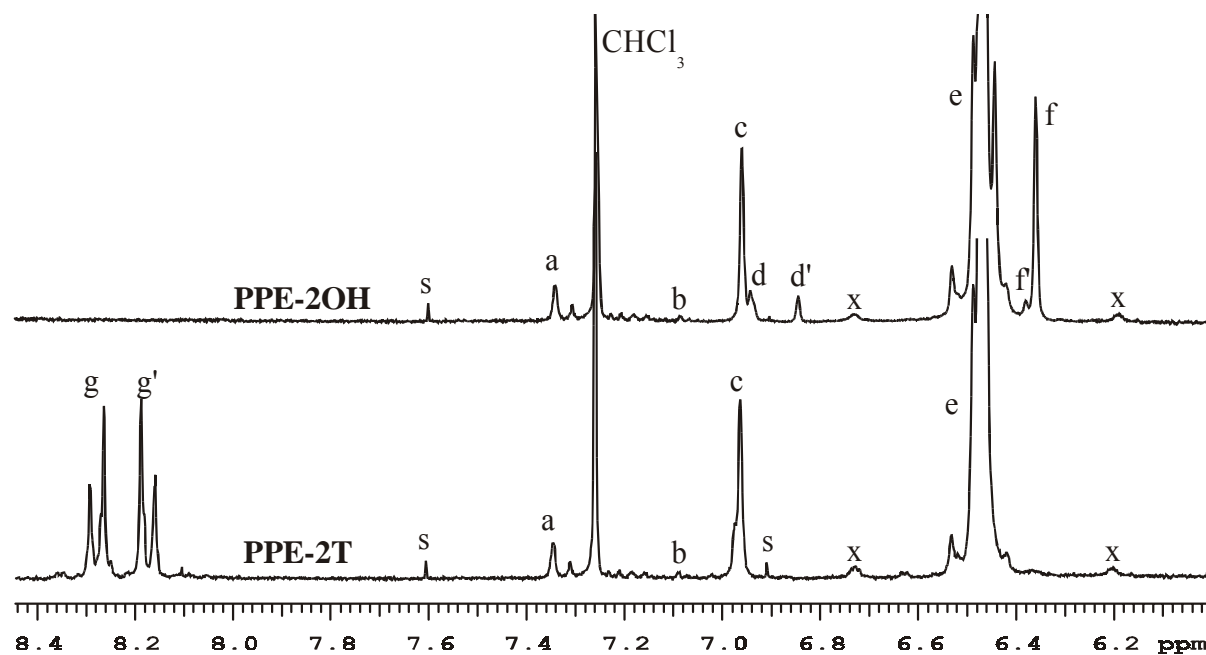


Figure 2.13: $^1\text{H-NMR}$ spectrum of PPE-2OH (10 wt% TMBPA) and PPE-2T made with this PPE-2OH.

With NMR it was shown that the peaks of the phenolic endgroup (f, f' at 6.36, 6.38 ppm) of PPE-2OH have disappeared completely (Figure 2.13) after reaction with MCCB to PPE-2T. Also the TMBPA endgroups (d, 6.84 and d', 6.94 ppm) have reacted fully with MCCB. So the endgroup modification reaction is complete and the segments preserve their high functionality. There are two new doublets at 8.18 and 8.29 ppm of the reacted MCCB and a singlet at 4.00 ppm, origination from the new methyl ester endgroups. The integral of the new endgroup peaks is approximately the same as that of the phenolic OH and TMBPA endgroups of PPE-2OH together.

The peak of the TMDPQ unit at 7.34 ppm is not effected by endgroup modification reaction. This confirms the assumption that the TMDPQ can be found mainly in the PPE chain, instead of as an endgroup. PPE-2T that is made by the two-step reaction contains about the same amount of TMDPQ groups per DMP unit as PPE-2OH.

Next to the peak of the Mannich base type endgroups at 0.88 ppm there is a new triplet at 0.75 ppm. So a part of the Mannich base type endgroups has probably reacted with MCCB, resulting in this shift of a part of the triplet. It seems that about 40-60% of the Mannich base type endgroups can react in this way. As a result the functionality of the PPE-2T segments will be increased a little compared to PPE-2OH.

The synthesis of PPE-2T was simplified by combining the redistribution and endgroup modification reaction. In this one-pot reaction the redistribution is directly followed by the endgroup modification step with MCCB. In this case the redistribution reaction is performed in toluene solution without methanol, because methanol can react with the acid chloride instead of a phenolic endgroup which is not wanted.

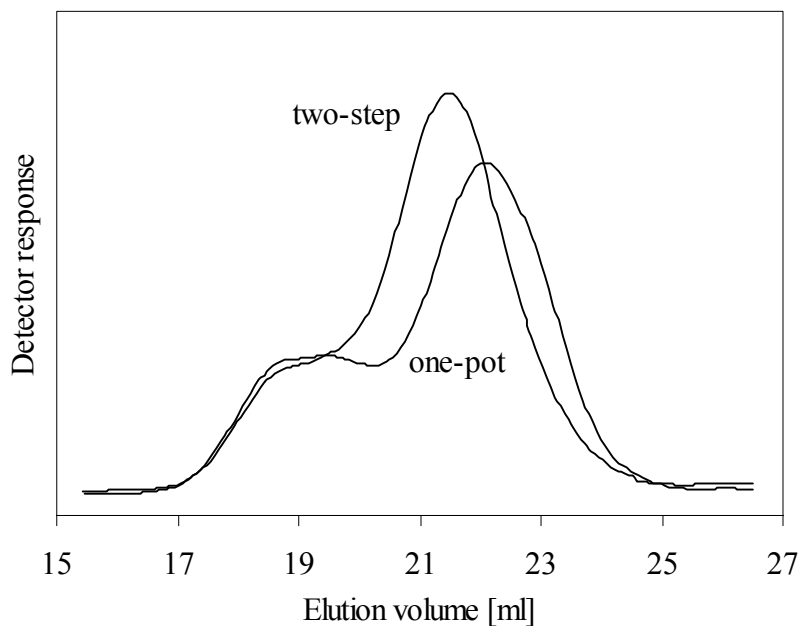


Figure 2.14: GPC molecular weight distribution of the PPE-2T (10 wt% TMBPA) precipitated product in the one-pot reaction compared to the two-step reaction.

The advantage of this one-pot reaction is in the first place that only one precipitation step is necessary. Also the yield can be higher because part of the low molecular weight PPE-2OH chains that are soluble in 10:1 methanol/toluene are insoluble after reaction with MCCB. And as a result of this, the average molecular weight of PPE-2T that can be obtained with the one-pot reaction is lower than that of PPE-2T in the two-step reaction when the same amount of TMBPA is used (Figure 2.14).

PPE-2T that is made in the one-pot reaction contains about 30-40% more TMDPQ units per DMP unit than PPE-2OH and PPO-803[®]. Probably more chains of very low molecular weight that contain TMDPQ are not lost during precipitation and washing steps, because these chains are not soluble in toluene/methanol after reaction with MCCB. In this one-pot PPE-2T also about 40-60% of the Mannich base type endgroups are modified by reaction with MCCB.

For PPE-2T the functionality and the value of n by NMR can be calculated with Equation 2.7 and 2.8. The endgroup concentration is determined by the concentration OCH_3 endgroups ($g+g'$) and the expected endgroup concentration by $a+c$ (peak d and d' have disappeared) assuming again that each chain contains a tetramethyl bisphenol or biphenyl unit. The molecular weight of PPE-2T can be calculated with Equation 2.3, using $M_{\text{endgroup}} = 163 \text{ g/mol}$ (terephthalic methyl ester endgroup).

$$F(\text{NMR}) = \frac{(g + g')/2}{(a + c)/4} \quad [-] \quad \text{Equation 2.7}$$

$$n(\text{NMR}) = \frac{e/2}{(a + c)/4} \quad [-] \quad \text{Equation 2.8}$$

In Table 2.2 the properties of the PPE-2T products after the two modification routes (two-step and one-pot reaction) are given.

Table 2.2: Molecular weight and functionality of PPE-2T made by the two-step and one-pot reaction using different amounts of TMBPA as calculated by different methods.

Reaction type	TMBPA [wt%]	Yield (%)	NMR			GPC			
			M_n (eq 2.3) [g/mol]	F (eq 2.7) [-]	[OCH ₃] (eq 2.4) [μ mol/g]	M_n [g/mol]	M_w/M_n [-]	high M^b [%]	
1	two-step	10	98 (92) ^a	3900	1.76	454	4500	2.2	17
2	two-step	15	97 (83) ^a	3700	1.79	481	4300	2.4	24
3	one-pot	10	95	3100	1.79	573	3150	3.1	27
4	one-pot	15	91	2500	1.84	733	2800	3.2	31
5	one-pot	20	87	2000	1.73	875	2450	3.6	33

(a), the yield of the second step (endgroup modification) is given first; between parenthesis the yield of the combined reaction is given; (b), the area of the high molecular weight fraction as measured by GPC is given

The yield of the endgroup modification reaction, which is the second step in the two-step reaction, is very high. However the combined yield over the two steps is lower than that of the one-pot reaction. The lowest molecular weight that can be obtained by the two-step method is 3700 g/mol. It is not well possible to obtain PPE-2T with a lower average molecular weight by this two-step method, because PPE-2OH with a lower average M_n cannot be made (Table 2.1).

In the one-pot reaction the yield decreases with increasing amount of TMBPA used. And at the same time the low molecular weight fraction is decreased compared to the high molecular weight fraction with such a high TMBPA content. The reason for this is the same as the decreasing yield for PPE-2OH with more TMBPA (Table 2.1). There are more products with a very low molecular weight that are soluble in the 10:1 methanol/toluene mixture. However it seems that PPE-2T is less soluble in the methanol/toluene mixture than PPE-2OH as the yield is higher at high TMBPA content. As a result the average molecular weight that can be obtained with high TMBPA contents is lower in the one-pot reaction.

A product with an average molecular weight of 2000 g/mol can be made when 20 wt% of TMBPA is used in the one-pot reaction. This is lower than the average molecular weight that is obtained in the two-step reaction with the same amount of TMBPA as there is less loss of low molecular weight chains. This is partly due to the fact that only one precipitation step is done and partly because PPE-2T is less soluble in the precipitation mixture than PPE-2OH. It must be noted that the PPE-2T product 5 with an average molecular weight of 2000 g/mol still contains about 33% of high molecular weight PPE that has not reacted. So the average molecular weight of the high molecular weight fraction is lower than 10.000 g/mol and the average molecular weight of the low molecular weight fraction is much lower than 2000 g/mol.

The major disadvantage of using PPO-803[®] in the redistribution reaction is that a product with a bimodal molecular weight distribution is obtained. This makes characterisation difficult. And when the PPE-2OH or PPE-2T will be used for example in a copolymerisation reaction this high molecular weight fraction will be present predominately uncoupled to the other segments (except for some Mannich base type endgroups that have reacted with MCCB). The presence of this high molecular weight PPE chains might give rise to phase separation in a copolymer. Therefore it would be nice to have a well-defined PPE-2OH or PPE-2T segment with a narrow molecular weight distribution that does not contain a high molecular weight fraction.

Fractionated PPE-2OH and PPE-2T

A way to obtain PPE-2OH or PPE-2T with a narrow molecular weight distribution after redistribution of PPO-803[®] was developed. This was done by fractionation. By precipitation in two steps it was possible to separate the high and low molecular fraction. When the reaction to PPE-2OH or PPE-2T (one-pot) is finished, a small amount of methanol is added to the reaction mixture. In this way only the high molecular weight fraction precipitates. This fraction (PPE-2OH-high or PPE-2T-high) can be obtained by filtration. Then the low molecular weight fraction (PPE-2OH-low or PPE-2T-low) that is still in solution can be obtained by precipitation by adding more methanol to get a 10:1 methanol/toluene mixture.

In Figure 2.15 the molecular weight distribution before and after fractionation of PPE-2T is given for two experiments with different amounts of methanol. It is important to add just enough methanol to precipitate the high molecular weight fraction. When too little methanol is added, the high molecular weight fraction is not completely separated and the PPE-2T-low product will still have a bimodal molecular weight distribution. When too much methanol is added (Figure 2.15b), a part of the low molecular weight fraction is precipitated together with PPE-2T-high. In this case the yield of PPE-2T-low decreases and the molecular weight distribution becomes more narrow (Table 2.3). It can be concluded that in a one-pot reaction to PPE-2T in 400 ml toluene, 175 ml methanol is just enough to precipitate the high molecular weight PPE-2T fraction selectively (Figure 2.15a).

With NMR it was shown that PPE-2OH-low contains hardly DMP ‘tail’ endgroups. PPE-2T-low contains a comparable amount of Mannich base type endgroups per DMP unit as PPO-803[®]. The TMDPQ concentration in PPE-2T-low is about 50% higher. PPE-2T-high contains about 30% less TMDPQ units per DMP unit than PPO-803[®] and a comparable amount of Mannich base type endgroups per DMP unit. However about 50% of the Mannich base type endgroups in PPE-2T-high have reacted with MCCB and give a triplet at 0.75 ppm instead of 0.88 ppm.

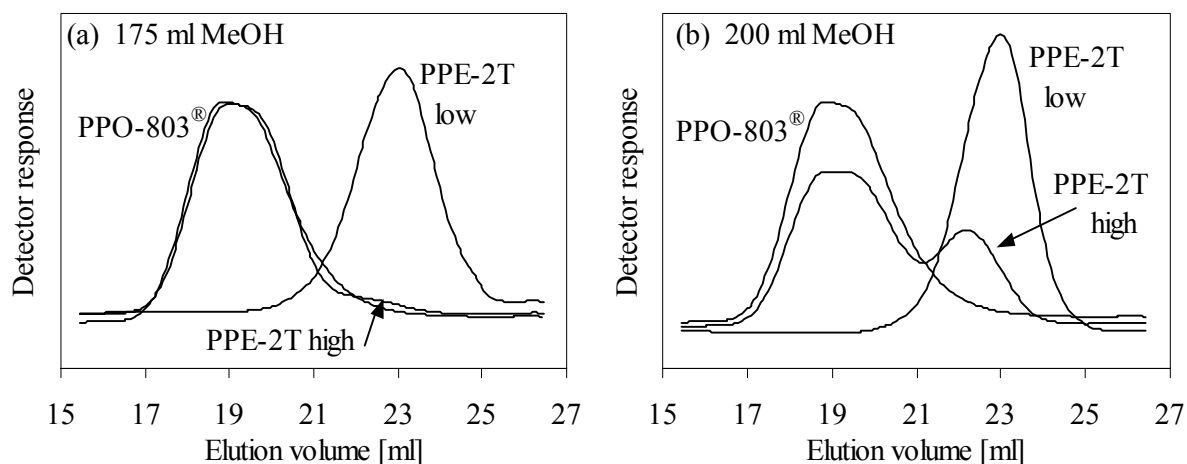


Figure 2.15: GPC molecular weight distribution of PPE-2T products made by redistribution in 400 ml toluene and obtained by partial precipitation with: (a), 175 ml methanol; (b) 200 ml methanol.

PPE-2OH was fractionated as well. When 200 ml of methanol is added at the end of the reaction the high molecular weight fraction precipitates selectively. In this case PPE-2OH-low with an optimum in yield and molecular weight distribution can be obtained. When more methanol is added after the reaction the molecular weight of PPE-2OH-high decreases and the yield increases, while the molecular weight and yield of PPE-2OH-low decrease and the molecular weight distribution becomes more narrow. For example when 800 ml methanol is added to precipitate PPE-2OH-high, a PPE-2OH-low fraction with a low molecular weight of only 1800 g/mol and a very narrow molecular weight distribution of $M_w/M_n = 1.14$ can be obtained (Table 2.3). However at the same time the yield becomes very low and most of the redistributed product will be part of PPE-2OH-high fraction. Therefore using too much methanol is not desirable.

With NMR it was shown that PPE-2OH-low contains hardly DMP ‘tail’ endgroups. PPE-2OH-low contains a comparable amount of Mannich base type endgroups per DMP units as PPO-803[®]. The TMDPQ concentration in PPE-2OH-low is about 20% higher than in PPO-803[®]. Compared to PPE-2T-low, PPE-2OH-low thus contains less TMDPQ. This is probably due to more loss during precipitation of low molecular weight chains that contain TMDPQ. PPE-2OH-high contains about 30% less TMDPQ units than PPO-803[®] and a comparable amount of Mannich base type endgroups per DMP unit. The composition of PPE-2OH-high is comparable with that of PPE-2T-high.

In Table 2.3 the properties of some PPE-2OH and PPE-2T products that were obtained after partial precipitation with different amounts of methanol to precipitate the high molecular weight fraction are given.

Table 2.3: Molecular weight and functionality by different methods of PPE-2OH and PPE-2T after fractionation (all were made with 8 gram TMBPA and 40 gram TMBPA in 400 ml toluene).

				NMR			Titration		GPC	
MeOH	Fraction	Yield	F	M _n	[OX] ^a	[OH]	M _n ^b	M _n	M _w /M _n	
[ml]		(%)	(eq 2.1/2.7)	(eq 2.3)	(eq 2.4)	(eq 2.6)				
			[-]	[g/mol]	[μmol/g]	[μmol/g]	[g/mol]	[g/mol]	[-]	
PPE-2OH										
8	200	low	27	1.70	2150	797	790	2150	1900	1.5
		high	35	-	-	-	-	-	12000	1.9
9	300	low	15	1.70	2100	794	789	2150	1600	1.6
		high	40	-	-	-	-	-	8500	2.5
10	800	low	9	1.86	1800	1018	990	1900	1400	1.14
		high	61	-	-	-	-	-	4900	3.3
PPE-2T										
6	175	low	55	1.74	1600	1088	-	-	2050	1.3
		high	28	-	-	-	-	-	10500	2.0
7	200	low	36	1.87	1550	1189	-	-	1700	1.2
		high	38	-	-	-	-	-	6500	2.8

(a), for PPE-2OH 8-10 the OH endgroup concentration and for PPE-2T 6-7 the OCH₃ endgroup concentration is given; (b), M_n was calculated from [OH] by titration by using the functionality as calculated by NMR

It is not possible to use Equation 2.5 and 2.6 to calculate M_n and F from [OH] by titration. These equations are only applicable to products that contain a concentration of M and X endgroups of 107 μmol/gram. The [M, X] after fractionation is not known. Therefore the M_n is calculated with Equation 2.6, using the functionality as calculated by NMR. The [OH] measured by titration corresponds nicely with the [OH] calculated from the NMR spectrum for PPE-2OH.

The functionality of the fractionated PPE-2OH-low and PPE-2T-low is little higher than that of bimodal PPE-2OH and PPE-2T (Table 2.1 and 2.2). The functionality of the bimodal PPE-2OH and PPE-2T is an average of the functionality of the high and low molecular weight fraction of the products. The high molecular weight fraction has a very low functionality as it has not reacted in the redistribution reaction. The low molecular weight fraction has a higher functionality. Theoretically, it is expected that the functionality of PPE-2OH of 1600 g/mol is around 1.9 after redistribution. Because the starting material contains endgroups that do not react during redistribution a functionality of 2.0 can never be obtained.

The PPE-2OH and PPE-2T-high fractions that are obtained after precipitation with 200 or 175 ml methanol hardly contain phenolic or methyl ester functional groups. These fractions have a phenolic or methyl ester functionality much lower than one.

Inherent viscosity and T_g

Next to the number average molecular weight of the different PPE-2OH and PPE-2T as given in Table 2.1-2.3, also the inherent viscosity and T_g were determined. The results are given in Table 2.4. The inherent viscosity was measured with a diluted polymer solution (0.1 dl/g in CHCl_3 , at 25°C). The T_g as measured by DSC is given as a function of molecular weight (NMR) in Figure 2.16.

Table 2.4: Inherent viscosity and T_g of PPE-2OH and PPE-2T with different number average molecular weights (taken from Table 2.1-2.3).

TMBPA		M_n	M_n	M_n	η_{inh}	T_g
[wt%]		(NMR)	(titration)	(GPC)		(DSC)
		(eq 2.3)	(eq 2.5)			
		[g/mol]	[g/mol]	[g/mol]	[dl/g]	[$^\circ\text{C}$]
PPE-2OH bimodal						
1	10	3500	3500	3250	0.19	182
2	12.5	3250	3250	3150	0.18	173
3	15	3150	3200	2850	0.18	179
4	20	3750	3650	2500	0.19	179
5	25	3400	3500	3250	0.23	173
6 ^a	10	4150	3850	3650	0.21	178
7 ^b	12.5	3400	3400	3250	0.19	173
PPE-2OH fractionated						
8-low	20	2150	2150	1900	0.09	157
8-high		-	-	12000	0.34	-
9-low	20	2100	2150	1600	0.08	160
9-high		-	-	8500	0.33	-
10-low	20	1800	1900	1400	0.07	151
10-high		-	-	4900	0.24	-
PPE-2T bimodal						
1	10	3900	-	4500	0.19	177
2	15	3700	-	4300	0.19	173
3	10	3100	-	3150	0.18	168
4	15	2500	-	2800	0.17	154
5	20	2000	-	2450	0.16	150
PPE-2T fractionated						
6-low	20	1600	-	2050	0.08	140
6-high		-	-	10500	0.36	-
7-low	20	1550	-	1700	0.07	139
7-high		-	-	6500	0.28	-

(a), TMBPA was added without methanol; (b), a reaction time of one hour was used instead of 3 hours

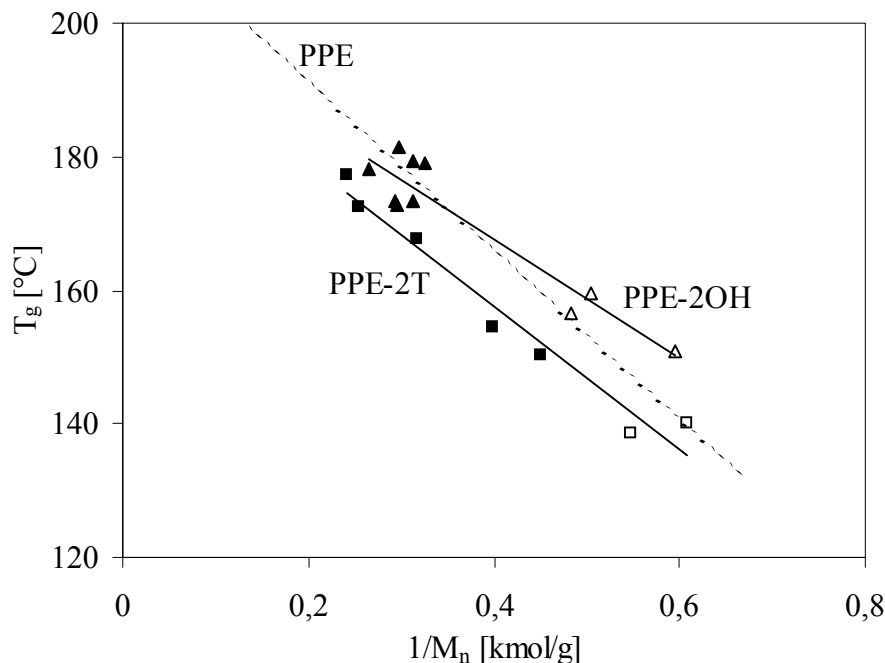


Figure 2.16: T_g as a function of the inverse value of M_n (NMR): (\blacktriangle), bimodal PPE-2OH; (\triangle), fractionated PPE-2OH; (\blacksquare), bimodal PPE-2T; (\square) fractionated PPE-2T. Also given in this figure is the T_g as function of $1/M_n$ according to Fox and Flory⁴³ for PPE (- - -).

The inherent viscosity of the bimodal products and PPO-803[®] increases with decreasing number average molecular weight. The monomodal PPE-2OH and PPE-2T have a much lower inherent viscosity than the bimodal products. The presence of the high molecular weight fraction in the bimodal products has a much larger effect on inherent viscosity than the low molecular weight fraction and as a result the inherent viscosity of a bimodal product with a certain average molecular weight is higher.

The glass transition temperature decreases with decreasing molecular weight. There are different equations to predict this dependence, the most commonly used being that of Fox and Flory⁴³ (Equation 2.9).

$$T_g = T_{g,\infty} - \frac{K}{M_n} \quad \text{Equation 2.9}$$

with: T_g = glass transition temperature of a polymer with M_n (in K)

$T_{g,\infty}$ = the T_g of a polymer of infinite chain length (PPE: $T_{g,\infty} = 490\text{K}$)⁴⁴

K = constant related to the volume of chain ends (PPE: $K = 12.73 \cdot 10^4 \text{ g} \cdot \text{K} / \text{mol}$)⁴⁴

The T_g is plotted as a function of $1/M_n$ for PPE-2OH and PPE-2T in Figure 2.16. There doesn't seem to be a difference between bimodal or monomodal PPE-2T as was seen for the effect of molecular weight on inherent viscosity. The T_g of PPE-2T is approximately 10 degrees lower than the T_g of PPE-2OH. The same was found for PPE-2OH modified with *p*-chloromethylstyrene to PPE-2VB²¹. The difference in T_g between PPE-2OH and PPE-2VB

was 10°C. This was described to the difference in hydrogen bonding of the phenolic chain ends²¹. Such a difference in hydrogen bonding of the chain ends could account for the difference between PPE-2OH and PPE-2T as well. It could also be that the introduction of terephthalic methyl ester endgroups makes the chain less stiff, resulting in a lower T_g .

The calculated T_g dependence on molecular weight according to Fox and Flory is given in Figure 2.16 as well. In this approximation the effect of the product consisting of two fractions of high and low molecular weight with higher and lower T_g is not taken into account. As a result the T_g dependence on M_n will be non-linear as can be calculated using the Fox relationship⁴⁵. When the T_g of PPE-2OH is compared with that of PPE according to Equation 2.9, we see a good agreement for the higher molecular weights (above 2500 g/mol). It could be that at lower molecular masses the ‘excess free volumes’ of the chain ends are overlapping (K smaller)⁴⁶. As a result the polymer chains are more stiff than predicted with Equation 2.9 and the glass transition temperature is higher.

Conclusions

Redistribution or depolymerisation of high molecular weight commercial PPE with tetramethyl bisphenolA is a good method to make partly bifunctional PPE-2OH. The product has a bimodal molecular weight distribution because only 70-80% of the chains of the commercial PPO-803[®] has at least one reactive endgroup that is needed to start the depolymerisation reaction. The average molecular weight of the product decreases with increasing amount of TMBPA used. However, when too much TMBPA is added, the molecular weight of the precipitated product increases because the molecular weight of the redistributed fraction in the product becomes too low and is soluble in 10:1 toluene/methanol solvent mixture that is used for precipitation.

The phenolic endgroups can be modified easily by a fast and complete reaction with methyl chlorocarbonyl benzoate. The product after endgroup modification is called PPE-2T and has terephthalic methyl ester endgroups instead of OH endgroups and a molecular weight of 3700-3900 g/mol. PPE-2T has a higher molecular weight than PPE-2OH. When PPE-2T is made in a one-pot reaction segments with a lower average molecular weight of 2000-3000 g/mol can be obtained. The functionality of all PPE-2T products is around 1.8.

The bimodal PPE-2OH and PPE-2T products can be separated in a high and low molecular weight fraction by selective precipitation of the high molecular weight fraction in ~2:1 toluene/methanol. The low molecular weight fraction has a narrow molecular weight distribution with a polydispersity between 1.2 and 1.5. The functionality of the low molecular weight fraction after partial precipitation is 1.7-1.9. The high molecular weight fraction contains hardly functional endgroups.

The inherent viscosity and the T_g decrease with the molecular weight. The T_g of the PPE-2T segments is about 10°C lower than that of PPE-2OH.

Literature

1. S.G. Allen, J.C. Bevington, 'Comprehensive polymer science', D.M. White on Poly(phenylene ether), Pergamon Press, New York, 5, 473 (1989).
2. D. Aycock, V. Abolins, D.M. White in 'Encyclopedia Of Polymer Science and Engineering', H.F. Mark, N.M. Bikales, C.G. Overberger, G. Menges, John Wiley & Sons, New York, 13, 1 (1988).
3. H.R. Kricheldorf, in 'Handbook of Polymer Synthesis', Part A, Dekker, New York, 545 (1992).
4. F.E. Karasz, J.M. O'Reilly, J. Polym. Sci. Polym. Lett. Ed., 3, 561 (1965).
5. A.S. Hay, H.S. Blanchard, G.F. Endres and J.W. Eustance, J. Am. Chem. Soc., 81, 6335 (1959).
6. A.S. Hay, J. Polym. Sci., 58, 581 (1962).
7. US 3,306,874, A.S. Hay (1967).
8. G.D. Staffin, C.C. Price, J. Am. Chem. Soc., 82, 3632 (1960).
9. C.C. Price, N.S. Chu, J. Polym. Sci., 61, 135 (1962).
10. H.S. Blanchard, H.L. Finkbeiner, G.A. Russell, J. Polym. Sci., 58, 469 (1962).
11. M.A. Semsarzadeh, C.C. Price, Macromolecules, 10, 482 (1977).
12. V. Percec, T.D. Shaffer, J. Polym. Sci., Part C, Pol. Lett., 24, 439 (1986).
13. D.M. White, S.A. Nye, Macromolecules, 23, 1318 (1990).
14. US 5,015,698, Sybert et al (1991).
15. D.M. White, J. Polym. Sci., Polym. Chem. Ed., 19, 1367 (1981).
16. US 4,140,675, D.M. White (1979).
17. H.A.M. van Aert, M.H.P. van Genderen, G.J.M.L. van Steenpaal, L. Nelissen, E.W. Meijer, J. Liska, Macromolecules, 30, 6056 (1997).
18. W. Risse, W. Heitz, D. Freitag, L. Bottenbruch, Makromol. Chem., 186, 1835 (1985).
19. W. Koch, W. Risse, W. Heitz, Makromol. Chem., Suppl., 12, 105 (1985).
20. W. Heitz, W. Stix, H. Kress, W. Koch, W. Risse, Polym. Prepr. Am. Chem. Soc. Div. Polym. Chem., 25, 136 (1984).
21. H. Nava, V. Percec, J. Polym. Sci. Polym. Chem. Ed., 24, 965 (1986).
22. US 4,665,137, V. Percec (1987).
23. H.A.M. van Aert, R. W. Venderbosch, M.H.P. van Genderen, P.J. Lemstra, E.W. Meijer, J.M.S.-Pure Appl. Chem., A32(3), 515 (1995).
24. V. Percec, J.H. Wang, Pol. Bull., 24, 493 (1990).
25. H.A.M. van Aert, M.E.M. Burkard, J.F.G.A. Jansen, M.H.P. van Genderen, E.W. Meijer, H. Oevering, G.H. Werumeus Buning, Macromolecules, 28, 7967 (1995).
26. US 5,880,221, Liska et al. (1999).
27. D.M. White, J. Org. Chem., 34, 297 (1969).
28. H.S.-I. Chao, J.M. Whalen, React. Polym. 15, 9 (1991).
29. D.M. White, J. Polym. Sci., Part A, 9, 663 (1971).
30. W. Heitz, Pure Appl. Chem., 67, 1951 (1995).
31. D.M. White, Macromolecules, 12 1008 (1979).
32. V. Percec, J.H. Wang, Pol. Bull., 24, 71 (1990).
33. V. Percec, J.H. Wang, Pol. Bull., 24, 63 (1990).
34. J. Liska, E. Borsig, J. Macromol. Sci., 35, 523 (1995)
35. T.W. Greene, 'Protective Groups in Organic Synthesis', Second Ed., Wiley Interscience, New York (1981).
36. L.F. Fieser, M.S. Fieser, 'Reagents for Organic Synthesis', Vol. 1, John Wiley and Sons, New York, 1180 (1967).
37. H.A.M. van Aert, 'Design and synthesis of reactive building blocks for multicomponent polymer systems', PhD thesis, Eindhoven University of Technology, The Netherlands (1997).

38. L.N.I.H. Nelissen, 'A novel route to blends of polystyrene and poly(2,6-dimethyl-1,4-phenylene ether)', PhD thesis, Eindhoven University of Technology, The Netherlands (1991).
39. D.M. White, G.R. Loucks, ACS Symp. Ser., 282, 187 (1985).
40. B.P. Schaffner, H. Wehrli, Helv. Chim. Acta, 55, 2563 (1972).
41. G. Höfle, W. Steglich, H. Vorbrüggen, Angew. Chem., 90, 602 (1978).
42. US 4,746,708, Sybert (1988).
43. T.G. Fox, P.J. Flory, J. Appl. Phys., 21, 581 (1950).
44. T.-P. Jauhiainen, Makromol. Chem., 183, 921 (1982).
45. T.G. Fox, Bull. Am. Phys. Soc., 1, 123 (1956).
46. M. Wicker, W. Heitz, Angew. Makromol. Chem. 185/186, 75 (1991).

Chapter 3

Copolymers of poly(2,6-dimethyl-1,4-phenylene ether) and ester units

Abstract

Amorphous copolymers of telechelic poly(2,6-dimethyl-1,4-phenylene ether) segments with terephthalic methyl ester endgroups (PPE-2T, 3700 g/mol, bimodal MWD) and different diols were made via a polycondensation reaction. The terephthalic endgroups of PPE-2T are stable during this reaction. The T_g of these polyether-ester copolymers decreases with increasing diol length and diol flexibility. The T_g can be set between 100 and 200°C by changing the type of diol. However at increasing diol length the T_g becomes broader and the test bars are less transparent because the extent of phase separation increases with increasing diol length. Only copolymers with a diol length up to C12 are homogeneous. Phase separation is probably enhanced by the bimodal molecular weight distribution of PPE-2T. Phase separation can be suppressed by using shorter PPE-2T segments with a short diol. It is even better to use fractionated, monomodal PPE-2T. Copolymerisation of PPE with a flexible diol is much more effective in decreasing the T_g of PPE and therefore its processability than blending with polystyrene. It is expected that the processability of these copolymers is much better than that of pure PPE.

Introduction

Poly(2,6-dimethyl-1,4-phenylene ether) (PPE)¹⁻³ or PPO is a linear amorphous polymer with a very high glass temperature of approximately 215°C⁴. PPE has excellent properties such as high toughness, high dimensional stability, good flame retardation and low moisture uptake. However, due to its high glass transition temperature, very high processing temperatures are required, which can lead to degradation. Only PPE with a molecular weight between 10.000 and 30.000 g/mol is just processable. By lowering the T_g , the processing temperature can be lowered and degradation free processing becomes possible. To lower the T_g , PPE is usually blended with polystyrene, as PPE and PS are fully miscible. However, possibilities for lowering the T_g of PPE by blending with other polymers than PS are limited due to the low miscibility with PPE¹⁻³.

Next to blending, also copolymerisation might change the glass transition temperature and improve the processability of PPE. Random copolymerisation with a less stiff comonomer can be a good way to decrease the T_g . However little comonomers for PPE with a lower T_g are known. More possibilities to decrease the T_g of PPE might be feasible by block copolymerisation. In block copolymers phase separation between both block types in the copolymer will occur readily, just like in a blend. However, in segmented copolymers only the low molecular weight segments have to be miscible. In general the miscibility increases with decreasing molecular weight. When phase separation occurs in copolymers with segments of low molecular weight it will be microphase separation contrary to the macrophase separation of a blend, because the segments in a copolymer are connected. Macrophase separation can lead to a material with poor properties, due to delamination. By copolymerisation of low molecular weight segments it is expected that more combinations of PPE and a second polymer are possible. However, research on copolymers based on PPE is restricted, as commercially available PPE is not well suited for copolymerisation due to the low functionality and the low reactivity of the phenolic endgroups of PPE. On segmented copolymers based on PPE even less is known because short bifunctional segments are not available.

Block copolymers that contain PPE are described mainly in patent literature. Coupling reactions with various bifunctional coupling agents, such as diacid chlorides, diisocyanates, dibromo-*p*-xylene, methylene bromide, phosgene, bischloroformates of dihydric compounds, etc., are described^{3,5-8}. Block copolymers can be prepared starting with two different polymer segments and using one of these coupling agents. Another method to prepare a block copolymer is to use a second polymer with a reactive endgroup of one of these types and couple it directly to PPE. It is also possible to start with a PPE segment and to synthesise the other polymer segment on the PPE endgroups from monomers during the reaction.

Most copolymers are prepared starting from partly monofunctional PPE-OH resulting in a mixture of ABA tri-block copolymer with A being PPE and some unreacted PPE. Sometimes also (AB)_n type multi-block copolymers are covered in which partly bifunctional PPE-2OH is made by the quinone coupling reaction⁹. Several copolymers that are described include copolymers of PPE with polyester^{8,10,11}, polystyrene¹², polycarbonate^{7,8,13-15}, polyester-polycarbonate¹³, poly(aryl ether)^{8,16}, polyurethane⁸ and polyamide¹⁷. Graft copolymers were

made from PPE macromonomers with polyester¹⁸, polyesteramide¹⁹, polystyrene²⁰, polyacrylate²⁰ or by grafting PPE on the methyl side groups, for example with nylon-6²¹. Some of these di- or tri-block type copolymers can be used as a compatibiliser in blends of PPE and a second polymer.

When segmented or multi-block copolymers are made, bifunctional PPE segments (PPE-2OH)²² with a phenolic endgroup at both chain ends are needed. These can be prepared by different methods, starting from monomers (copolymerisation), from low molecular weight PPE-OH (coupling) or from high molecular weight PPE (redistribution).

Copolymerisation, for example the co-oxidation of 2,6-dimethylphenol (DMP) and 2,2'-di(4-hydroxy-3,5-dimethylphenyl)propane (tetramethyl bisphenol A, TMBPA), leads to PPE-2OH with increased phenolic functionality of 1.6-2.0²³⁻²⁷. Another method to synthesise PPE-2OH is by halogen displacement copolymerisation of 4-bromo-2,6-dimethylphenol (BDMP) and TMBPA^{23,28}. However the products of these reactions are not so well defined and have in general a functionality lower than two.

Another method to prepare PPE-2OH is by a coupling reaction of two monofunctional PPE-OH chains of low molecular weight, such as by the quinone coupling reaction⁹ or by condensation with formaldehyde²³. However, products with two phenolic endgroups can be obtained only from a well-defined monofunctional starting PPE-OH.

A good and fast way to make short bifunctional PPE segments or PPE telechelics is by redistribution (depolymerisation) of high molecular weight PPE with bisphenols^{22,29-31}. The reaction is catalysed by tetramethyl diphenoquinone (TMDPQ). By redistribution of commercial PPE (PPO-803[®]) with tetramethyl bisphenolA (TMBPA), it is possible to make PPE-2OH segments with a number average molecular weight of 1500-4000 g/mol²². These PPE segments have a bimodal molecular weight distribution, because part of the high molecular weight starting material for redistribution does not react (~20-30%). The average phenolic functionality of these PPE segments is around 1.6-1.9²². This segment functionality should be high enough to obtain high molecular weight (>10.000 g/mol) PPE copolymers. PPE-2OH segments with a functionality of nearly 2 can only be prepared starting from well-defined PPE-OH^{22,29,30}.

In theory PPE has one 3,5-dimethyl-4-hydroxyphenyl 'head' endgroup and one 2,6-dimethylphenoxy 'tail' endgroup per chain (PPE-OH). Commercial high molecular weight PPE however has a phenolic ('head') functionality below one, due to side reactions during the polymerisation reaction²⁹⁻³². These side reactions increase with increasing molecular weight² and result in the incorporation of Mannich base type endgroups (Figure 3.1a) and TMDPQ (Figure 3.1b)³³. Mannich base type endgroups are less reactive than the normal phenolic endgroups. Incorporation of TMDPQ leads to bifunctional chains with two OH-functionalities. In linear polymers each polymer chain can contain one tetramethylbiphenyl unit derived from TMDPQ at most, predominately within the chain³⁴. In commercial high molecular weight PPE grades over 80% of the polymer chains contain a tetramethylbiphenyl unit derived from TMDPQ or a Mannich base type endgroup^{29,32}.

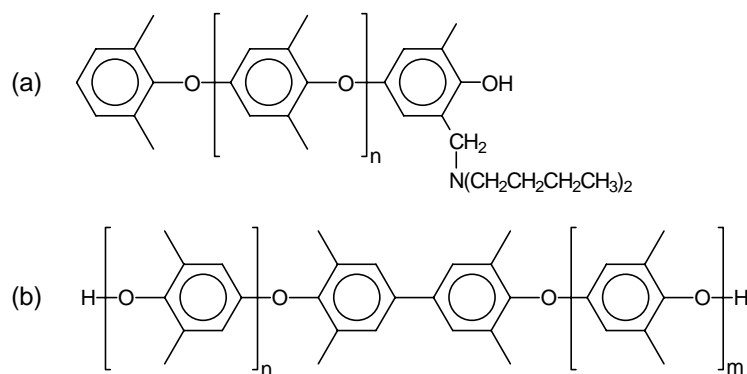


Figure 3.1: Impurities in PPE: (a) Mannich base endgroup, (b) TMDPQ incorporation.

It was found that endgroups such as the 2,6-dimethylphenoxy ‘tail’ endgroups, Mannich base type endgroups and tetramethylbiphenyl endgroups derived from TMDPQ are degradation resistant and do not react in the redistribution reaction³⁵. Only chains with at least one phenolic ‘head’ endgroup can be initiated in the redistribution reaction. Therefore, by starting with commercial PPE, only the chains with at least one phenolic ‘head’ endgroup will be depolymerised. As a result the redistribution product of commercial PPE will consist of two fractions, a low molecular weight depolymerised fraction and a high molecular weight fraction that has not reacted.

The phenolic endgroup of PPE has a low reactivity and therefore endgroup modification is preferable. In this study the phenolic endgroups of the bifunctional PPE-2OH were modified with an acid chloride. This is a fast and complete reaction. The acid chloride used was a methyl ester functional acid chloride MCCB (methyl chlorocarbonyl benzoate) (Figure 3.2). The phenolic endgroups of PPE-2OH are transferred into terephthalic methyl ester groups by reaction with MCCB^{22,32,36}. The terephthalic methyl ester endgroups have a much higher reactivity than the phenolic endgroups. This PPE segment with two methyl ester functionalities is called PPE-2T (in which T stands for the terephthalic endgroup). It is expected that next to the phenolic ‘head’ units also tetramethyl bisphenol A endgroups will be functionalised by the acid chloride. The Mannich base type endgroups have a lower reactivity and will react only partially with the acid chloride.

This PPE-2T segment can be used in a polycondensation type copolymerisation reaction. Several PPE-2T segments will then be linked via a functional coupling agent, for example a diol. It is not known if the transesterification of the ester group in this polymerisation reaction is on the methyl ester side or at the phenyl ester side of the terephthalic unit. The phenyl ester has generally a higher reactivity than the methyl ester. This is caused by the good leaving group character of phenolates, which are formed during decomposition or hydrolysis of the phenolic esters³⁷. Of course transesterification at the phenyl ester side should be absent, because otherwise the polymerisation reaction could never lead to high molecular weight polymers as the phenolic endgroups that are created by this reaction have a low reactivity. It is expected that with shielded aromatic esters like these PPE-esters with 2,6-dimethyl substitution the reactivity of the phenyl ester might be suppressed.

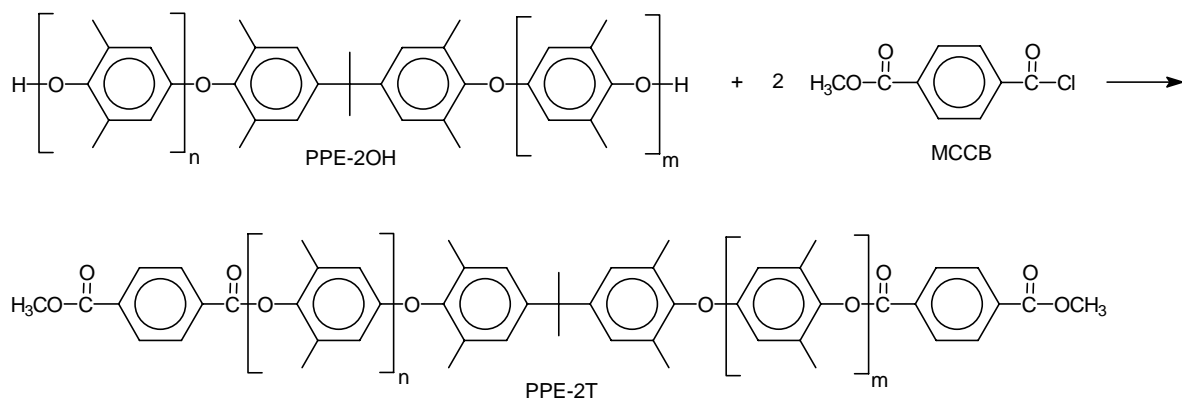


Figure 3.2: Reaction of PPE-2OH (that is obtained after redistribution of PPE with tetramethyl bisphenol A) with methyl chlorocarbonyl benzoate (MCCB) to PPE-2T.

The general structure of a PPE-2T/diol or alternating polyether-ester copolymer is given in Figure 3.3. In this PPE-2T/diol copolymer the ester segment is only one repeating unit long. The length of the ester segment can be extended by adding more diol and for example dimethyl terephthalate.

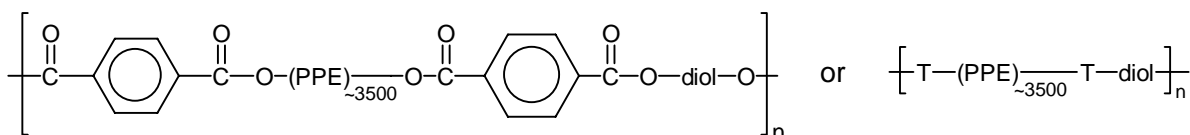


Figure 3.3: Schematic structure of a PPE-2T/diol copolymer ($T =$ terephthalic unit).

The expectation is that the low molecular weight PPE-2T segments and the diols will mix and the polymers will have one glass transition temperature. This T_g will then be lower than that of pure PPE, depending on the flexibility and length of the diol used. It is envisaged that this will lead to improved processability. However, the diol should not be too long and incompatible with the PPE segment, as this will result in partial phase separation giving a broad T_g , or more than one T_g . When there is no phase separation between polyether and ester segment, it is expected that these copolymers are transparent.

Aim

In this chapter alternating polyether-ester copolymers based on PPE-2T and different diols are studied. First, a copolymer based on PPE-2T of ~ 3700 g/mol and C36-diol will be discussed using GPC, $^1\text{H-NMR}$ and DMA. Then four different polymer series based on PPE-2T in which the structure and length of the PPE and ester segments are varied will be analysed using DMA. The effect of composition on glass transition and flow temperature will be discussed. The results are used to study the phase separation in relation with the segment length.

Experimental

Materials. Dimethyl terephthalate (DMT), 1,2-ethanediol, 1,6-hexanediol, 1,12-dodecanediol (C12) and toluene were purchased from Merck. Tetraisopropyl orthotitanate ($\text{Ti}(\text{i-OC}_3\text{H}_7)_4$), obtained from Merck, was diluted in anhydrous *m*-xylene (0.05M), obtained from Fluka. C36-dimerised fatty diol was obtained from Uniquema, Gouda (The Netherlands). Di-ethoxylated bisphenol A (Dianol220[®]) was obtained from Akzo Nobel (The Netherlands). Poly(2,6-dimethyl-1,4-phenylene ether) (PPO-803[®], 11.000 g/mol) was obtained from GE Plastics (The Netherlands). Poly(tetramethylene oxide) (PTMO, M = 650, 1000, 1400, 2000 and 2900 g/mol) was provided by DuPont. PTMO₁₀₀₀, for example, is PTMO of 1000 g/mol. All chemicals were used as received. Diphenyl terephthalate (DPT) was synthesised from terephthaloyl chloride and phenol as described in Chapter 5 of this thesis³⁸. Bimodal PPE-2OH (~3500 g/mol) was made according to the method described in Chapter 2²². Bimodal PPE-2T was made in a two-step or a one-pot reaction according to the methods described in Chapter 2²². Monomodal PPE-2T with a narrow molecular weight distribution that was obtained after fractionation was used as well²². The average molecular weight of the PPE-2T segments was between 1600 and 3700 g/mol and the segments had a functionality of 1.6-1.9 (NMR) (number of methyl ester endgroups per chain).

Synthesis of PPE-2T/diol copolymers. The PPE-2T/diol copolymers were synthesised via an ester type polycondensation reaction using PPE-2T and different diols. The preparation of a copolymer of PPE-2T (~3700 g/mol, functionality = 1.79, 480 $\mu\text{mol OCH}_3/\text{g}$ (NMR))²² and C36-diol is given as an example.

The reaction was carried out in a 50 ml glass reactor with a nitrogen inlet and mechanical stirrer. The vessel was loaded with PPE-2T (10.0 g, 4.8 mmol OCH_3), C36-diol (1.3 g, 2.4 mmol), 10 ml toluene and catalyst solution (0.3 ml of 0.05M $\text{Ti}(\text{i-OC}_3\text{H}_7)_4$ in *m*-xylene). This mixture was first heated in an oil bath to 120°C under nitrogen flow. After 30 minutes the temperature was increased in steps: 30 minutes at 180°C, 30 minutes at 220°C and 60 minutes at 250°C. The pressure was then reduced slightly ($P < 20$ mbar) for 30 minutes and then further reduced ($P < 1$ mbar) for 30 minutes. Finally, the vessel was allowed to slowly cool to room temperature whilst maintaining the low pressure. Then the polymer was cut out of the reactor and crushed.

NMR. ¹H-NMR spectra were recorded on a Bruker spectrometer at 300 MHz at 25°C. Deuterated chloroform (CDCl_3) was used as a solvent.

Viscometry. The inherent viscosity of the polymers was determined with a capillary Ubbelohde type 0C at 25°C, using a polymer solution with a concentration of 0.1 g/dl in chloroform.

GPC. GPC measurements were carried out with polymer solutions in chloroform (5 mg/ml), filtrated via 0.45 μm Schleicher&Schuell filters. The molecular weight was determined using GPC with a Waters model 510 pump, differential refractometer model 411, viscotek H502

viscometer and Waters columns HR4 + HR2 + HR0.5 and a 500Å guard column in series. A flow rate of 1.5 ml/min was used with chloroform as a solvent at 25°C. Calibration was performed with 9 monodisperse polystyrene standards (range 827-1450 g/mol).

DMA. Samples for the DMA test (70x9x2 mm) were prepared on an Arburg-H manual injection moulding machine. Before use, the samples were dried in a vacuum oven at 80°C overnight. The torsion behaviour was studied at a frequency of 1 Hz, a strain of 0.1% and a heating rate of 1°C/min using a Myrenne ATM3 torsion pendulum. The storage modulus G' and loss modulus G'' were measured as a function of temperature starting at -100°C. The glass transition temperature (T_g) was expressed as the temperature at which the loss modulus G'' has a maximum. This maximum was 0-10°C lower than the actual glass transition temperature, because with this DMA apparatus it was not possible to measure a few points around the T_g due to the very high damping. The flow temperature (T_{flow}) was determined as the temperature where the storage modulus G' reached 1 MPa. Two measures were used to get some indication of the extent of phase separation. The broadness of the T_g was defined as the temperature range over which the modulus as measured by DMA drops from 100 to 10 MPa. The drop in the storage modulus G' between -100°C and 10°C below the T_g was determined as well.

Results and Discussion

Introduction

Copolymers of PPE-2T and different diols were made in a polycondensation reaction with a maximum temperature of 250°C. A little toluene was added after putting all the reactants in the reactor to make sure that all the reactants mix well and are able to melt on increasing temperature. A clear solution is formed in toluene. After 30 minutes, when the temperature is raised to 180°C, toluene starts to evaporate. Above 220°C the reaction is in the melt. The melt is clear and the viscosity of this melt increases with reaction time.

Bifunctional PPE-2T segments were prepared from high molecular weight PPO-803[®] ($M_n \sim 11000$ g/mol) by a redistribution or depolymerisation reaction with tetramethyl bisphenolA (TMBPA) using tetramethyl diphenoquinone (TMDPQ) as a catalyst, followed by endgroup modification with MCCB²². This PPE-2T has a bimodal molecular weight distribution. The product is a mixture of a high molecular weight fraction (20-30%) and a low molecular weight depolymerised fraction (70-80%). The high molecular weight fraction is PPO-803[®] (~ 11.000 g/mol) that has not reacted due to absence of the right functional groups to initiate the redistribution reaction. This fraction is therefore hardly functionalised. It contains some methyl ester endgroups as a result of the reaction of tetramethylbiphenyl or Mannich base type endgroups with MCCB. Therefore this fraction will hardly be copolymerised. The low molecular weight fraction consists mainly of difunctionalised PPE-2T (<3000 g/mol). It is expected that this fraction will be fully copolymerised to high molecular weight copolymer in the copolymerisation reaction. The combined fractions in the

bimodal PPE-2T have an average molecular weight of 2000-3700 g/mol and a functionality of 1.6-1.9 (number of methyl ester endgroups per chain). After fractionation a low molecular weight fraction of 1600 g/mol can be obtained.

The average degree of polymerisation that can be obtained starting with a PPE-2T segment with an average molecular weight of 3500 g/mol and an average functionality of 1.7 with a stoichiometric amount of diol can be calculated with Equation 3.1, using Equation 3.2 to calculate f_{avg} (with $N_A = N_B$)³⁹.

$$\overline{X}_n = \frac{2}{2 - pf_{\text{avg}}} \quad \text{Equation 3.1}$$

$$f_{\text{avg}} = \frac{\sum N_i f_i}{\sum N_i} = \frac{N_A f_A + N_{A'} f_{A'} + N_B f_B}{N_A + N_{A'} + N_B} \quad \text{Equation 3.2}$$

With: N_A = number of molecules PPE with functionality $f_A = 2$

$N_{A'}$ = number of molecules PPE with functionality $f_{A'} = 1$

N_B = number of molecules diol with $f_B = 2$ (with $N_B = N_A + N_{A'}/2$)

The f_{avg} using PPE-2T with a functionality of 1.7 and a stoichiometric amount of diol is 1.8. With $p = 1$ a maximum average degree of polymerisation of 10 can be obtained. With an average segment length (PPE, diol) of ~2000 g/mol, this corresponds to a molecular weight of 20.000 g/mol. This is high compared to the industrial PPE (PPO-803[®], 11.000 g/mol) that was used for redistribution.

Different series of alternating polyether-ester copolymers based on PPE-2T and different diols were studied. First, a copolymer based on bimodal PPE-2T of ~3700 g/mol and C36-diol will be discussed. With GPC the molecular weight distribution of the copolymer was compared with that of PPO-803[®] and PPE-2T. A ¹H-NMR study was done to show the extent of transesterification of the phenyl ester side of the terephthalic endgroups of PPE-2T during the polymerisation reaction. The thermal-mechanical behaviour was studied by DMA.

Then the properties of three different PPE/diol copolymer series will be discussed:

1. Bimodal PPE-2T and different diols.
2. Fractionated monomodal PPE-2T and different diols.
3. PPE-2T of different lengths with C36-diol.

The effect of composition on glass transition temperature, flow temperature and phase separation was studied by DMA.

PPE-2T/C36-diol copolymer

An alternating polyether-ester copolymer based on PPE-2T and C36-diol (-T-PPE-T-C36-)_n was made. The average molecular weight of the PPE-2T segment used was 3700 g/mol and the segment has around 1.8 methyl ester endgroups per chain²². The structure of C36-diol is given in Figure 3.4.

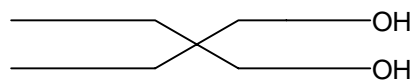


Figure 3.4: Structure of C36-diol dimerised fatty diol.

GPC

With GPC the molecular weight distribution of PPE-2T/C36 was measured. The data are compared with that of the PPE-2T segment that was used as a starting material for copolymerisation and the commercial PPO-803[®] (Figure 3.5).

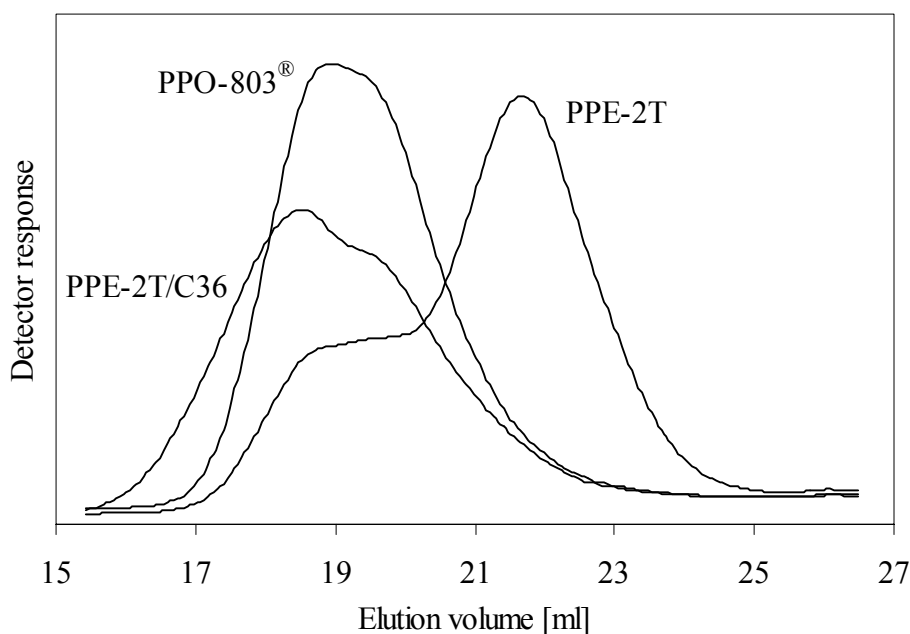


Figure 3.5: GPC data for PPE-2T/C36 copolymer compared to PPE-2T and PPO-803[®].

PPO-803[®] shows a molecular weight distribution with $M_n = 11.000$ g/mol and $M_w/M_n = 2.0$. PPE-2T shows a bimodal molecular weight distribution with a high molecular weight fraction at the position of the peak of PPO-803[®] and a low molecular weight fraction with a more narrow peak. The high molecular weight fraction forms about 24% of the area and the low molecular weight fraction 76% of the total area²². The PPE-2T/C36-diol copolymer has a broad molecular weight distribution ($M_w/M_n = 3.1$). The average molecular weight of the copolymer (14.000 g/mol) is higher than the average molecular weight of PPO-803[®] (11.000 g/mol).

The molecular weight of the copolymer was also studied by inherent viscosity determination in diluted chloroform solution. The inherent viscosity of the copolymer was 0.44 dl/g. The

commercial PPO-803[®] had an inherent viscosity of 0.37 dl/g and the PPE-2T segment 0.19 dl/g (Table 3.1).

The high molecular weight of the copolymer that is made from PPE-2T and C36-diol suggests that transesterification of the terephthalic endgroups of PPE-2T is mainly at the methyl ester side and not at the phenyl ester side. The reason for this is probably the steric hindrance of the 2,6-dimethyl groups at the phenyl unit that is linked to the terephthalic endgroup.

NMR

A ¹H-NMR study was done to determine the stability of the terephthalic endgroups of PPE-2T during the polymerisation reaction. The transesterification of the phenyl ester side of the terephthalic endgroup is an undesirable side reaction. This reaction will yield a phenolic endgroup, which has a low reactivity. The presence of the phenolic endgroup should be visible in the NMR spectrum. The ¹H-NMR spectra of PPE-2OH, PPE-2T and a PPE-2T/C36 copolymer are given in Figure 3.6.

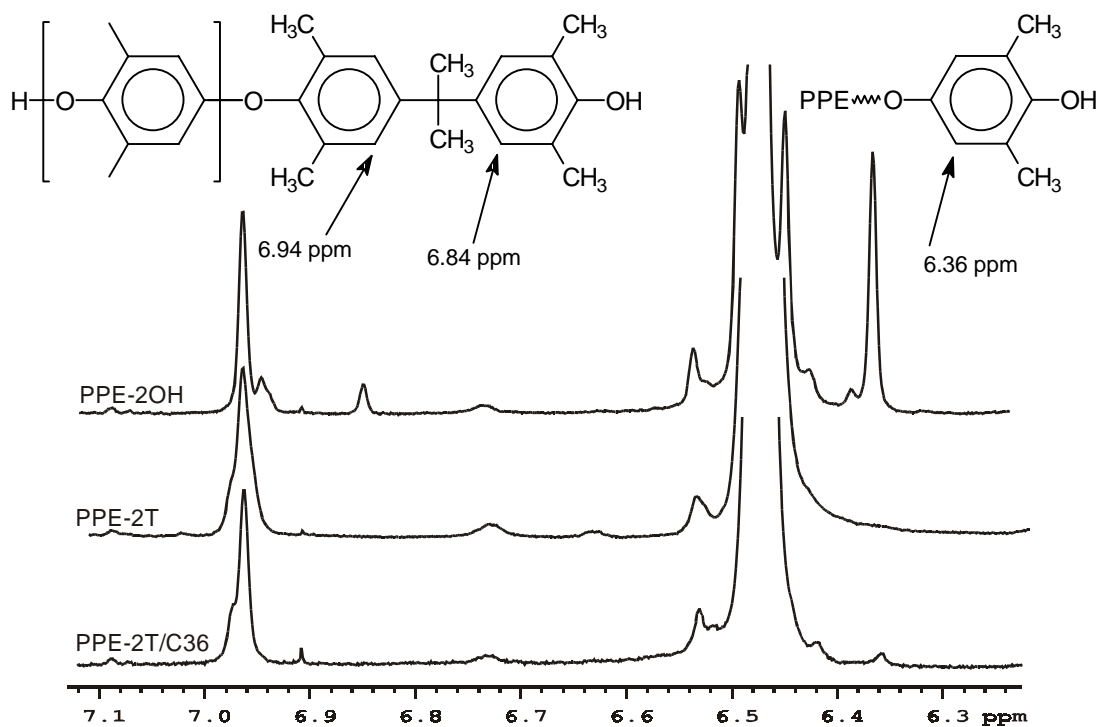


Figure 3.6: ¹H-NMR spectra of PPE-2OH, PPE-2T and the PPE-2T/C36 copolymer.

The peak at 6.36 ppm is for the aromatic H of the phenolic PPE 'head' endgroup. The bifunctional PPE-2OH shows a large peak at 6.36 ppm. After modification of the phenolic endgroups of PPE-2OH with methyl chlorocarbonyl benzoate (MCCB) to PPE-2T, this peak has disappeared completely. Also the TMBPA endgroups are transferred completely into terephthalic methyl ester endgroups by reaction with MCCB as the peaks at 6.84 and 6.94 ppm are absent in PPE-2T. Copolymerisation of PPE-2T with C36-diol results in the formation of a very small amount of new phenolic endgroups as a result of transesterification

of the phenyl ester side of the terephthalic endgroup with the diol. The transesterification of the phenyl ester side of the terephthalic endgroups in PPE-2T is less than 5%.

The phenolic endgroups are hardly reactive in this type of polycondensation reaction. The new average degree of polymerisation that can be obtained in this situation can be calculated with Equation 3.1, using Equation 3.3 to calculate the f_{avg} for the case that the B groups (diol) are in excess³⁹.

$$f_{\text{avg}} = \frac{2 * (N_A f_A + N_{A'} f_{A'})}{N_A + N_{A'} + N_B} \quad \text{Equation 3.3}$$

When 5% of the functional methyl ester endgroups is transformed into a non-reactive phenolic endgroup, the methyl ester functionality of PPE-2T decreases from 1.7 to 1.6. The f_{avg} using PPE-2T with an original functionality of 1.7 and a stoichiometric amount of diol after 5% transesterification is 1.74. With $p = 1$ a maximum average degree of polymerisation of 8 instead of 10 can be obtained. This value is still sufficient to obtain high enough molecular weight. The maximum average molecular weight of the product that can be obtained is 16.000 g/mol. In most cases there is less transesterification and the functionality of the starting material is higher, so high molecular weight copolymers can be obtained easily.

DMA

The PPE-2T/C36 copolymer was injection moulded into test bars. These bars are slightly transparent. The bars were used to measure the dynamic-mechanical behaviour by DMA. In Figure 3.7 the DMA results of the PPE-2T/C36 copolymer are compared with that of PPO-803[®].

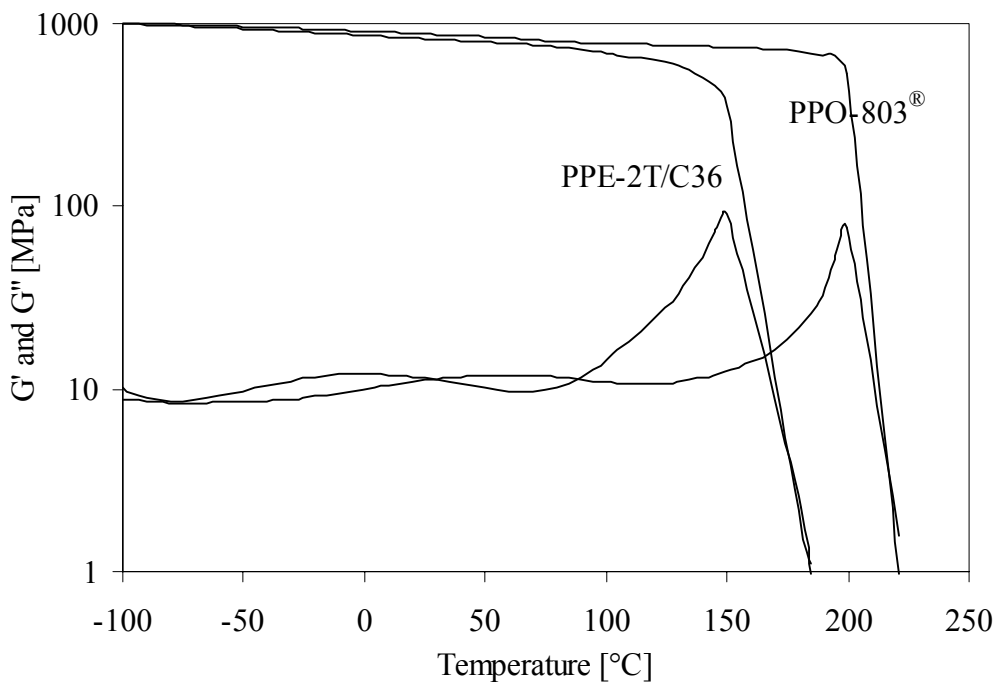


Figure 3.7: Storage and loss modulus of a PPE-2T/C36 copolymer compared to PPO-803[®].

The commercial PPO-803[®] has a high and constant modulus up to the glass transition temperature at 200°C. For the T_g the temperature at which the loss modulus G'' has its maximum is taken. This temperature is 0-10°C lower than the actual T_g of the polymer, because the DMA apparatus is unable to measure around the T_g because of the high damping. The T_g of PPO-803[®] is sharp. The flow temperature, defined as the temperature where the modulus reaches 1 MPa, is 222°C.

The copolymer of PPE-2T and C36-diol with an average PPE-2T molecular weight of 3700 g/mol consists for 83% of PPE and 17% of ester segments (-T-C36-T-). The PPE-2T/diol has a high and constant modulus up to its T_g as well. However the modulus starts to drop a little above 50°C. This is a result of the broader T_g of the copolymer compared to PPO-803[®] and can be seen as a broader peak in the loss modulus G'' . The T_g of PPE-2T/C36 is 150°C, which is 50°C lower than the T_g of PPO-803[®]. The flow temperature is 185°C.

Series 1: Bimodal PPE-2T with diols

In this polymer series, alternating polyether-ester copolymers of bimodal PPE-2T of constant length (~3700 g/mol) and different diols were synthesised. The length and type of diol were varied to change the T_g of the PPE-2T/diol copolymer. Next to different aliphatic diols (C2-C36) also poly(tetramethylene oxide) or PTMO of different lengths (650-2900 g/mol) and Dianol220[®] (bisphenolA with hydroxyethyl endgroups, Figure 3.10) were used. A copolymer of PPE-2OH (~3500 g/mol) and diphenyl terephthalate was studied as well. The synthesis was the same as described for the PPE-2T/C36 copolymer. First the copolymers with C12 and longer and than those with C12 and shorter as extender will be discussed.

All polymers had high molecular weights (>10.000 g/mol) as was measured by GPC. For other diols than C36-diol a comparable molecular weight distribution was obtained. With the longer diols the molecular weight of the copolymer was a little higher than with the shorter diols which can be expected when the molecular weight of the repeating units increases. The inherent viscosity, a measure for the molecular weight, increases with increasing diol length as well. The results for the PPE-2T/diol polymers of series 1 are given in Table 3.1.

Long diols

In Figure 3.8 the DMA results for several PPE-2T/diol copolymers based on long flexible, aliphatic diols (C12, C36 and PTMO) are compared with that of PPO-803[®].

By copolymerising PPE-2T segments with dodecanediol (C12), a PPE polymer with a lower, but still sharp T_g is obtained. The modulus of PPE-2T/C12 is high up to the T_g at 170°C. The T_g and the T_{flow} are decreased by about 30°C compared to the commercial PPO-803[®]. The broadness of the T_g is the same as that of PPO-803[®]. The test bars of this polymer are transparent. Apparently this copolymer is homogeneous. The ester segment based on dodecanediol (-T-C12-T-) is too short to phase separate.

Table 3.1: Properties of the PPE-2T/diol copolymers based on bimodal PPE-2T or PPE-2OH.

	PPE [wt%]	η_{inh} [dl/g]	T_g [°C]	T_g broadness	T_{flow} [°C]
Starting materials:					
PPO-803 [®]	100	0.37	200	8	222
PPE-2OH ^a	-	0.18	182 ^c	-	-
PPE-2T ^b	-	0.19	173 ^c	-	-
Copolymers:					
PPE-2T/C2	92	0.33	190	9	217
PPE-2T/C6	91	0.31	185	8	210
PPE-2T/C12	88	0.33	170	8	195
PPE-2T/C36	83	0.44	150	13	185
PPE-2T/PTMO ₆₅₀	82	0.40	140	18	175
PPE-2T/PTMO ₁₀₀₀	77	0.48	115	18	161
PPE-2T/PTMO ₁₄₀₀	69	0.66	80	20	145
PPE-2T/PTMO ₂₀₀₀	66	0.51	50	21	113
PPE-2T/PTMO ₂₉₀₀	57	0.66	-40	36	100
PPE-2OH/DPT	96	0.33	195	8	220
PPE-2T/Dianol220 [®]	87	0.41	185	9	211

(a), bimodal, ~ 3500 g/mol²²; (b), made by two-step synthesis, bimodal, ~ 3700 g/mol²²; (c), measured by DSC instead of DMA

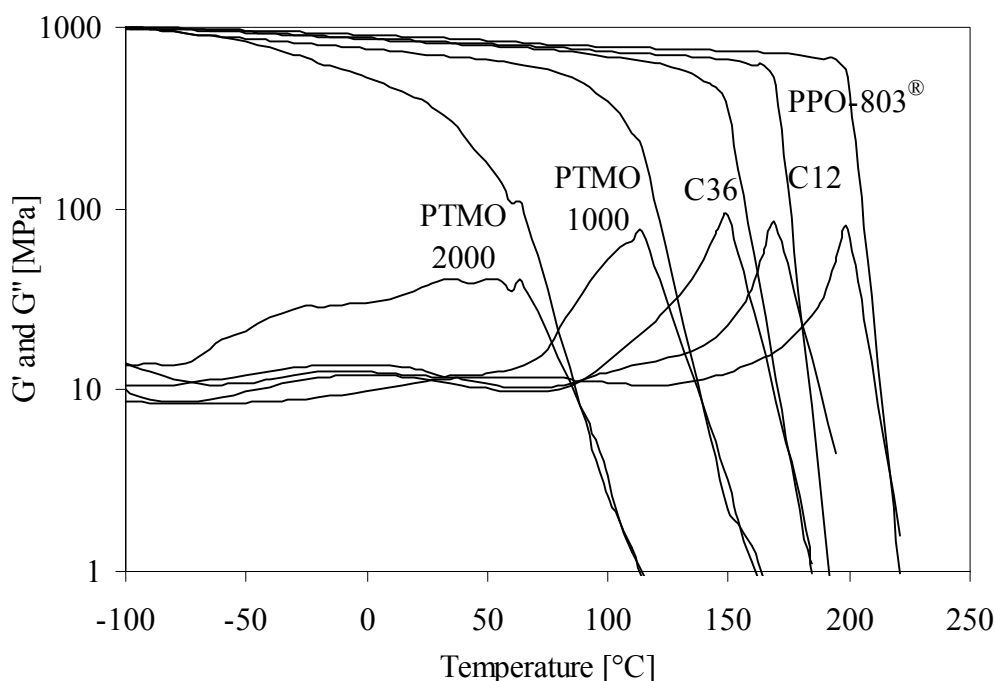


Figure 3.8: Storage and loss modulus of several PPE-2T/diol copolymers based on bimodal PPE-2T (3700 g/mol) compared to the commercial PPO-803[®] starting material for redistribution; the type of diol used in each copolymer is given in the figure.

When C36-diol is used in the copolymer the T_g is decreased by 50°C and the T_g is a little broader than for the commercial PPO-803[®]. The modulus with C36-diol is less high and constant up to the T_g as compared to the PPE-2T/C12 copolymer. However the test bars of this polymer are only slightly transparent. Therefore it can be concluded that this copolymer is nearly homogeneous. The high molecular weight PPE fraction that is present next to the PPE-2T/C36 copolymer will probably phase separate partially from the copolymer on a microscale.

With PTMO₁₀₀₀ the T_g is broadened further compared to C36-diol, but as the loss modulus start to increase above 50°C a separate PTMO phase is not present. Pure PTMO/DMT has a T_g of -65°C⁴⁰. The T_g becomes very broad with PTMO₂₀₀₀ segments. Already at -70°C the G'' starts to increase, which indicates the presence of an almost pure T-PTMO-T phase. Furthermore, PPE/PTMO mixed phases of different concentrations are present as a result of partial phase separation between PPE and PTMO. Test bars with PTMO as a diol are not transparent.

Short diols

When a copolymer with a high T_g close to that of PPO-803[®] is desired there are three approaches. The first approach is to use very short aliphatic diols. The second method is to couple PPE-2OH segments directly with diphenyl terephthalate (DPT). And a third approach is to use less flexible diols.

In Figure 3.9 the storage modulus as a function of temperature for copolymers of PPE-2T and hexanediol (C6) or ethanediol (C2) is given. In this figure the result for a copolymer of PPE-2OH and DPT is given as well. This polymer was made with doubled reaction time. In this way high enough molecular weight is obtained (0.33 dl/g), although the reactivity of the sterically hindered OH endgroups of PPE-2OH with the phenyl ester endgroups of DPT is low. The results are compared with that of PPO-803[®] and the PPE-2T/C12 copolymer.

The T_g and T_{flow} of the PPE-2T/diol copolymer increase when the diol length is decreased. With very short diols, such as hexanediol or ethanediol the effect of the flexible diol is small and the T_g is close to that of PPO-803[®]. With short diols sublimation of the diol can occur during the polymerisation reaction. Therefore care has to be taken to use the right excess of diol in order to obtain high molecular weight.

The copolymer of PPE-2OH and DPT has a T_g and T_{flow} that are almost the same as that of PPO-803[®]. The only difference between these polymers is that in PPE-2OH/DPT terephthalic groups are incorporated. The phenyl ring is not likely to effect a decrease of 5°C in the T_g of the copolymer. Therefore probably the two ester-bonds that are introduced for each DPT unit that is incorporated are responsible for the small drop of 5°C in T_g compared to PPO-803[®]. The effect of the ester bonds on the T_g is much smaller than the effect of introducing a flexible aliphatic structure.

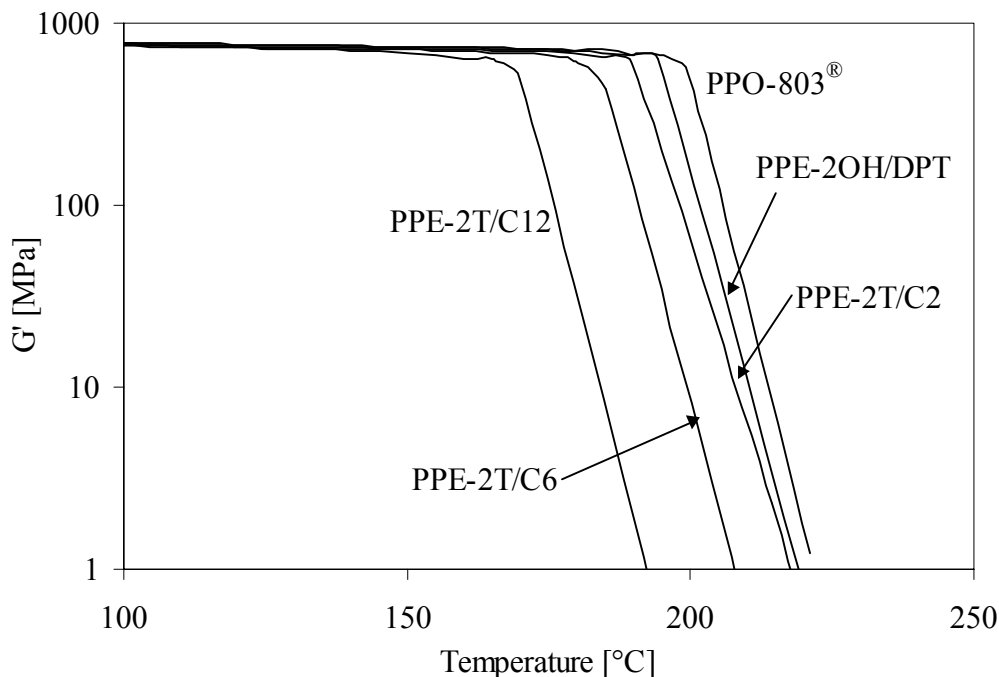


Figure 3.9: Storage modulus of the PPE-2T/diol copolymers using short diols and PPE-2OH/DPT compared to the commercial PPO-803[®] starting material for redistribution.

A third method to obtain a PPE copolymer with a T_g more close to that of PPO-803[®] is to use a less flexible diol, for example Dianol220[®], or bisphenol A with hydroxyethyl endgroups. The structure of Dianol220[®] is given in Figure 3.10.

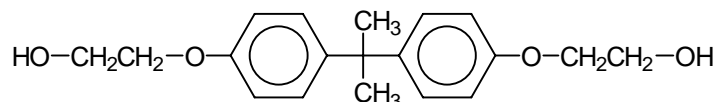


Figure 3.10. Structure of Dianol220[®].

The PPE-2T/Dianol220[®] copolymer has a T_g of 185°C and a T_{flow} of 211°C. The T_g and T_{flow} are comparable with that of a copolymer of PPE-2T and hexanediol. The T_g and T_{flow} with Dianol220[®] are higher than with an aliphatic diol of the same length (so at the same weight percentage PPE) (Table 3.1). This is the result of the low flexibility of the Dianol220[®], compared to the other, fully aliphatic, diols that were used. Next to the four CH₂ units, probably the ether bonds and the aliphatic structure in the centre of the bisphenol contribute to the flexibility of this diol. An advantage of using this diol instead of hexanediol is that no correction for sublimation of the diol to preserve stoichiometry is necessary.

It is remarkable that the polymers that show a sharp T_g , so the polymers with a diol length up to C12, turned out to be transparent, while the materials with a somewhat broadened T_g such as PPE-2T/C36-diol are only slightly transparent and the copolymers with PTMO are not transparent at all. Probably the phase separation between the PPE-2T/diol copolymer and the high molecular weight PPE fraction in the product is responsible for this. It is expected that

phase separation will occur at lower PPE content, so with increased diol length, when this high molecular weight fraction is absent.

Series 2: Fractionated PPE-2T

In this second polymer series, alternating polyether-ester copolymers of fractionated, monomodal PPE-2T of constant length (~ 1600 g/mol) and different diols were synthesised. The synthesis was the same as described for the PPE-2T/C36 copolymer. All polymers had high molecular weights as was measured by GPC and inherent viscosity. The results for the PPE-2T/diol polymers of series 2 are given in Table 3.2. In Figure 3.11 the DMA results for several PPE-2T/diol copolymers based on an aliphatic diol or PTMO are given.

Table 3.2: Properties of the PPE-2T/diol copolymers based on fractionated, monomodal PPE-2T.

	PPE [wt%]	η_{inh} [dl/g]	T_g [°C]	T_g broadness	T_{flow} [°C]
Starting materials:					
PPO-803 [®]	100	0.37	200	8	222
PPE-2T ^a	-	0.08	140 ^b	-	-
Copolymers:					
PPE-2T/C12	74	0.34	150	11	182
PPE-2T/C36	63	0.37	100	13	132
PPE-2T/PTMO ₁₀₀₀	52	0.62	35	20	95

(a), made by one-pot synthesis and fractionation, monomodal, ~ 1600 g/mol²²; (b), measured by DSC instead of DMA

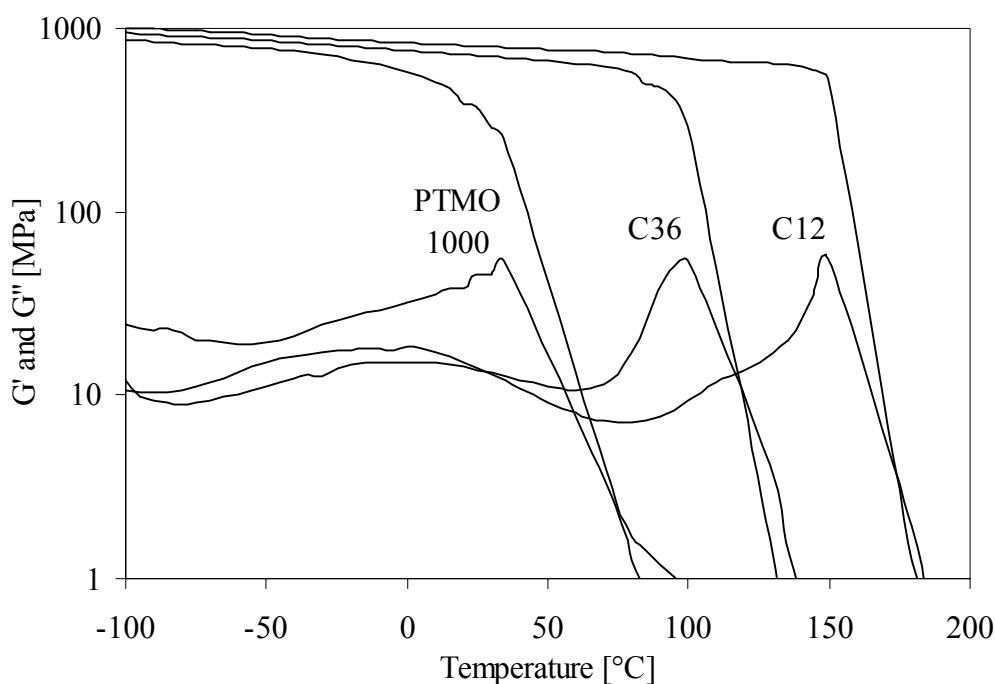


Figure 3.11: Storage and loss modulus of several PPE-2T/diol copolymers based on fractionated, monomodal PPE-2T (1600 g/mol); the type of diol used in each copolymer is given.

The T_g and T_{flow} of the PPE-2T/diol copolymer decrease with increasing diol length and decreasing PPE content. Also the broadness of the T_g increases with increasing diol length. However the T_g is much less broadened than in the copolymers based on bimodal PPE-2T of series 1. Also the loss modulus is lower up to the T_g and the storage modulus remains higher up to the T_g . The broadness of the T_g will be discussed in more detail later on.

It can be concluded that there is less phase separation between PPE and -T-diol-T- phase in these copolymers compared to the polymers of series 1. This can be attributed to the absence of the high molecular weight PPE fraction that is not redistributed in bimodal PPE-2T. This high molecular weight fraction can be copolymerised only partially and will phase separate more easily because of the higher molecular weight that reduces miscibility. The copolymers of series 2 with C12 and C36 as a diol were transparent, the copolymer based on PTMO₁₀₀₀ was not. Apparently the copolymer with PTMO₁₀₀₀ and fractionated PPE-2T has a more phase separated morphology and is not homogeneous on a microscale.

Series 3: PPE-2T length

A third series of polyether-ester copolymers was based on PPE-2T of different lengths and C36-diol. In Table 3.3 and Figure 3.12 the DMA results for these copolymers are given.

Table 3.3. Properties of the PPE-2T/C36 copolymers with PPE-2T of different lengths.

PPE-2T length [g/mol] ²²	TMBPA [gram]	PPE [wt%]	η_{inh} [dl/g]	T_g [°C]	T_g broadness	T_{flow} [°C]
3700 ^a	6	83	0.44	150	13	185
3100 ^b	4	79	0.55	140	13	180
2500 ^b	6	75	0.41	135	14	174
2000 ^b	8	69	0.50	115	18	168
1600 ^c	8	63	0.37	100	13	132

(a), bimodal PPE-2T, made by two-step synthesis²²; (b), bimodal PPE-2T, made by one-pot synthesis with different amounts of TMBPA²²; (c), monomodal PPE-2T, obtained after fractionation (series 2)²²

With decreasing length of the PPE-2T in PPE-2T/C36-diol copolymers, the T_g decreases. The T_g is hardly broadened when the C36-diol content increases. Only the copolymer with the shortest bimodal PPE-2T segment (~2000 g/mol) has a broadened T_g compared to the other three. The high molecular weight PPE fraction is probably phase separated more from the PPE-2T/C36 copolymer in this polymer, because the PPE-2T/C36 copolymer becomes less 'PPE-like' at lower molecular weight of the PPE-2T and contains relatively more high molecular weight PPE²².

When monomodal PPE-2T that is obtained after partial precipitation is used the T_g is decreased further and remains sharp. Phase separation is less likely to occur, because this PPE-2T does not contain the high molecular weight PPE fraction that phase separates more easily. Also the transparency of this PPE-2T/C36 polymer is much better than that of the polymers based on the bimodal PPE-2T.

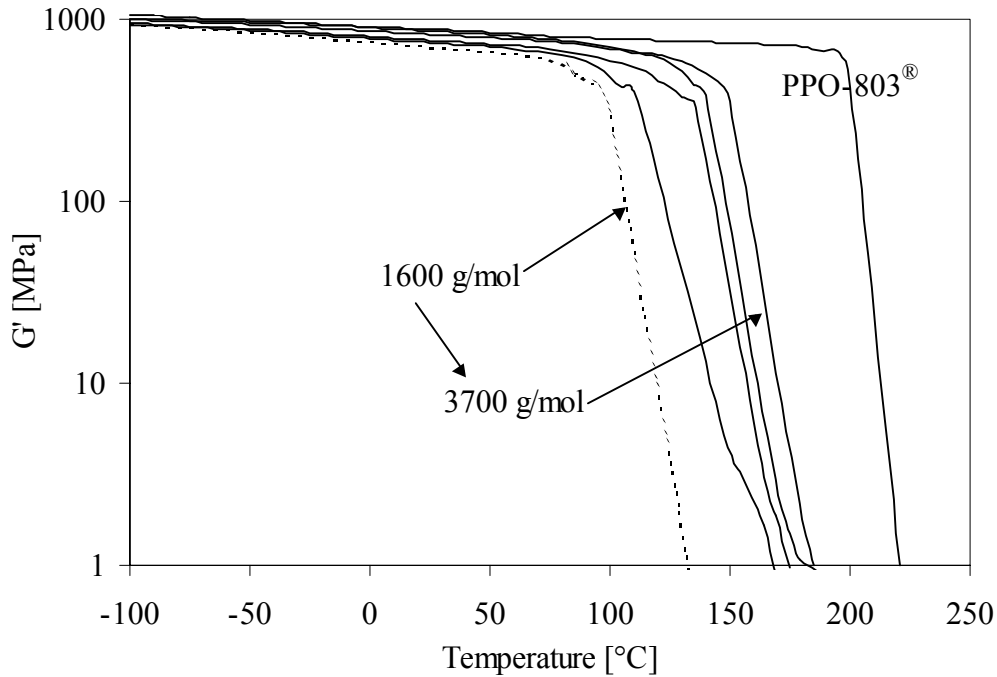


Figure 3.12: Storage modulus for PPE-2T/C36-diol copolymers with PPE-2T of different lengths as indicated (1600, 2000, 2500, 3100 and 3700 g/mol); PPE-2T of 1600 g/mol (- - -) was made by partial precipitation and has a monomodal molecular weight distribution (series 2).

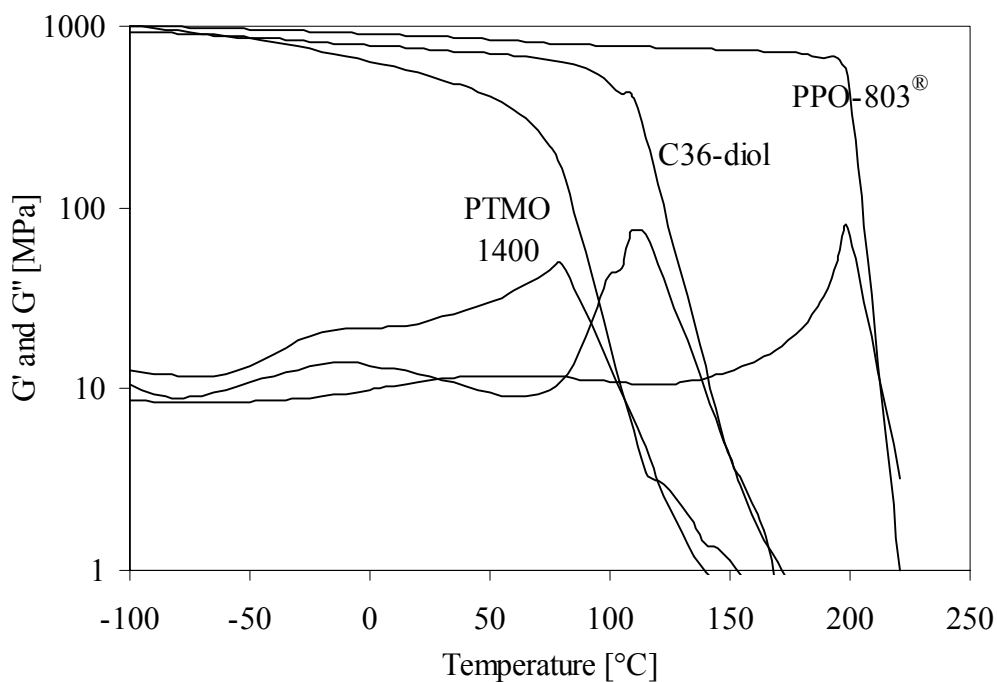


Figure 3.13: Storage and loss modulus of the PPE-2T(2000 g/mol)/C36 and PPE-2T(3700 g/mol)/PTMO₁₄₀₀ copolymer; both contain 69 wt% PPE.

In Figure 3.13 the modulus of the PPE-2T/C36 copolymer with bimodal PPE-2T segments of 2000 g/mol is compared with that of the PPE-2T/PTMO₁₄₀₀ with bimodal PPE-2T segments of 3700 g/mol. Both copolymers have a PPE content of 69 wt% (Table 3.1). The T_g is about

50°C degrees lower with PTMO₁₄₀₀ compared to C36-diol. This can be attributed to the larger flexibility of PTMO₁₄₀₀ (T_g of T-PTMO-T is -65°C)⁴⁰ as compared to C36-diol (T_g of T-C36-T is -35°C)⁴¹ in combination with increased phase separation with PTMO₁₄₀₀. The copolymer with C36-diol has a higher and more constant modulus up to the T_g and the loss modulus is lower. It can be concluded that with PTMO₁₄₀₀ some phase separation occurs, while with C36-diol there is hardly phase separation. Thus, decreasing the PPE-2T length is a better way to decrease the T_g of PPE than increasing the diol length.

Glass transition of polyether-esters

In Figure 3.14 the T_g is given as a function of the PPE content for the copolymers of series 1-3. This figure illustrates that it is better to use monomodal PPE-2T segments (series 2) or shorter PPE-2T segments with a short diol (series 3) instead of using longer PPE-2T segments with a longer diol (series 1). In this way phase separation is suppressed and the T_g remains sharp and decreases gradually with decreasing PPE content. For series 3 with varying PPE length and C36-diol the T_g decreases linearly with decreasing PPE content.

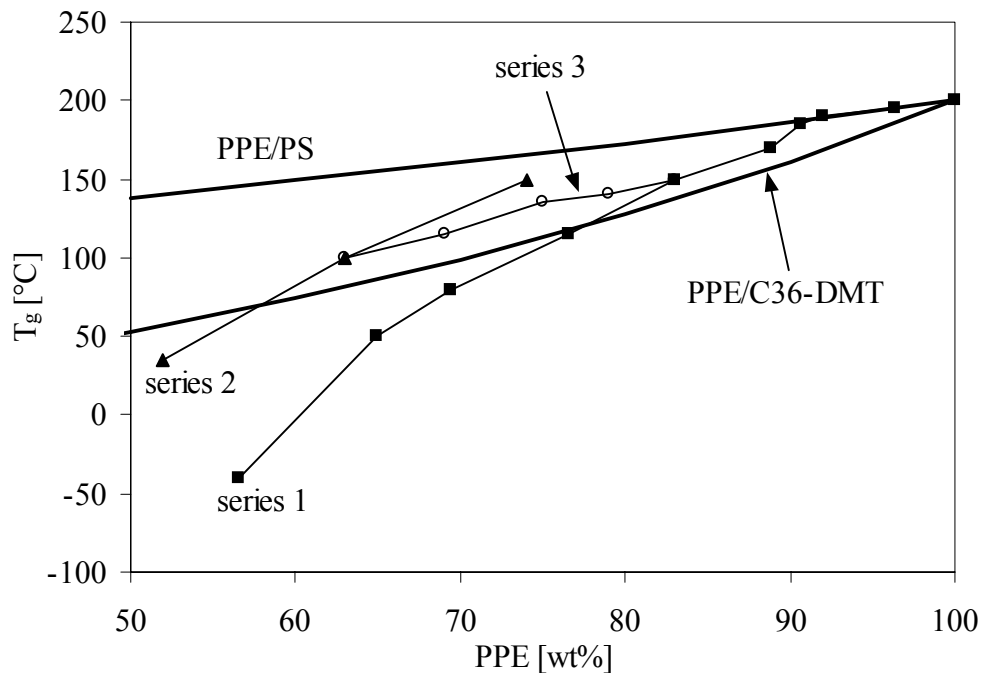


Figure 3.14. T_g for PPE-2T/diol copolymers compared with the T_g of a PPE/PS blend and that of a (theoretical) blend of PPE with the copolymer of C36-diol and DMT⁴¹ (both according to the Fox relation)⁴²: (■), PPE-2T/diol (series 1); (▲), PPE-2T/C36 with fractionated PPE-2T (series 2); (○), PPE-2T/C36 (series 3).

From Figure 3.14 it can be concluded that the effectiveness of decreasing the T_g of PPE is much higher by copolymerisation with diols to polyether-esters than by blending with polystyrene. For a polymer with a T_g of 150°C , a 50/50 blend PPE/PS can be used. The same T_g can be obtained after copolymerisation with C36-diol in a copolymer that contains 83 wt% of PPE.

Copolymerisation using flexible aliphatic diols is much more effective than blending with polystyrene, because the T_g of a homopolymer of C36-diol and dimethyl terephthalate (DMT) ($T_g = -35^\circ\text{C}$)⁴¹ is much lower than that of pure polystyrene ($T_g = 100^\circ\text{C}$). In Figure 3.14 the calculated T_g of a theoretical PPE/C36-DMT blend as function of the PPE content, based on the Fox relationship⁴², is given. This calculated line lies a little bit lower than that of the copolymer. So copolymerisation is a little less effective in lowering the T_g than a theoretical blend. The T_g of the PPE-2T/C36 polymer based on the monomodal low molecular weight fraction of PPE-2T lies on the same line as the other polymers of series 3. So using PPE-2T of narrow molecular weight distribution does not influence the value of the T_g , only its broadness (Figure 3.15).

The effect of different diols (C12, C36 and PTMO) on T_g can be seen clearly for the copolymers of series 2 that are based on fractionated, monomodal PPE-2T. The T_g of the DMT/diol copolymer decreases with decreasing diol length, thus the effectiveness of the diol after copolymerisation decreases with decreasing diol length. A homopolymer of dodecanediol and DMT with a T_g of 0°C (series 4) is less effective than C36-diol/DMT. A homopolymer of PTMO and DMT⁴⁰ has a T_g of -65°C and is the most effective. However, due to phase separation with long PTMO segments, this flexible segment is less preferred for copolymerisation with PPE, in particular when bimodal PPE-2T is used.

A definition for the broadness of the glass transition temperature was set. The broadness of the T_g was defined as the temperature range over which the modulus as measured by DMA drops from 100 to 10 MPa. The broadness of the T_g as a function of the PPE content for copolymers of series 1-3 is given in Figure 3.15a. Increasing broadness of the T_g indicates that PPE phases with different diol concentrations are present.

Another definition was set to quantify the presence of a phase separated diol 'rich' phase. When such a second phase is present, the modulus drops before the main T_g of the PPE 'rich' phase (see Figure 3.13). The drop of the modulus between -100°C and 10°C below the T_g is given as function of the PPE content in Figure 3.15b. When the modulus decreases more up to the T_g , the copolymer is more phase separated.

For the copolymers of series 1 the T_g is sharp at high PPE contents (>88 wt%), corresponding to a copolymer of PPE-2T and dodecanediol or shorter diols. When C36-diol is used the T_g becomes broader. The T_g broadness increases more sharply for the longer diols, due to partial phase separation. Also with increasing diol length the modulus decreases more before the main T_g is reached. Probably the poor miscibility with increasing diol length is due to the presence of the high molecular weight PPE fraction in the PPE-2T starting material.

When bimodal PPE-2T with a lower molecular weight is used (series 3) the broadness of the main T_g does not change compared to copolymers of series 1. However the modulus up to the T_g is higher, which indicates that there is less phase separation when the average PPE-2T length is lower.

The copolymers that were made with the low molecular weight fraction of PPE-2T only (series 2), show a much sharper T_g than the copolymers based on bimodal PPE-2T. Even the copolymer with PTMO₁₀₀₀ as a diol has a reasonably sharp T_g . Also the copolymer with C36-

diol and monomodal PPE-2T has good transparency as compared to the copolymers with C36-diol of series 3 that were only slightly transparent. So without the high molecular weight fraction in PPE-2T phase separation is suppressed and the segmented copolymers can have a sharp T_g and a higher modulus up to the T_g at much lower PPE contents.

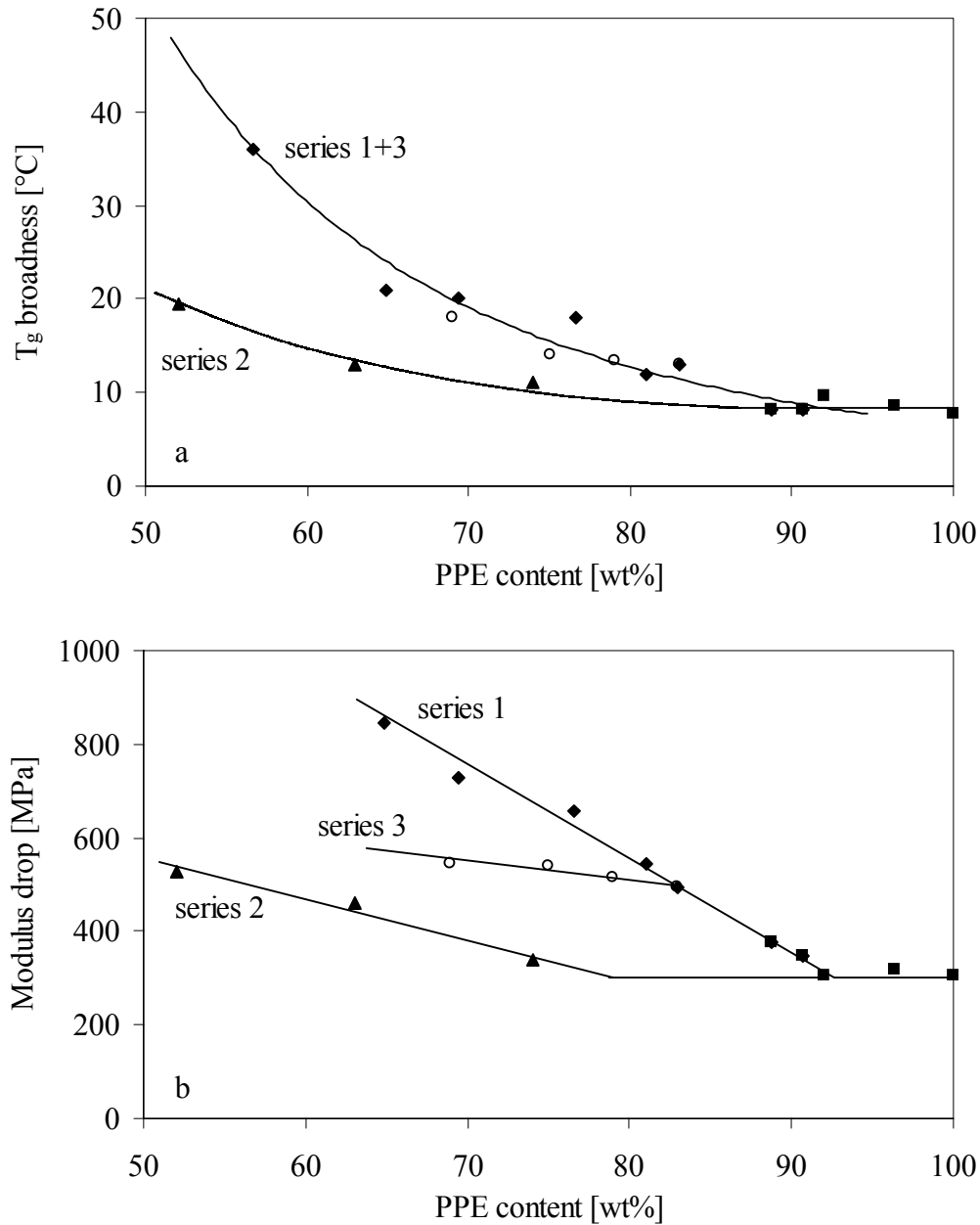


Figure 3.15: (a), broadness of the glass transition temperature (T_g broadness = $T_{(G'=10 \text{ MPa})} - T_{(G'=100 \text{ MPa})}$) is used) and (b), modulus drop between -100°C and $T_g-10^\circ\text{C}$ (b) with PPE content: (■), PPE-2T/diol up to C12 (series 1); (◆), PPE-2T/diol from C36 (series 1); (▲), PPE-2T/C36 with fractionated PPE-2T (series 2); (○), PPE-2T/C36 (series 3).

Conclusions

PPE-2T/diol polyether-ester copolymers were made via a polycondensation reaction with high molecular weights (>10.000 g/mol). Therefore the terephthalic endgroups of PPE-2T must be stable enough during the polycondensation reaction. NMR analysis confirmed that transesterification of the terephthalic endgroup occurs preferably at the methyl ester side. This is probably caused by the steric hindrance of the 2,6-dimethyl groups at the phenyl ester side of the terephthalic endgroup.

The T_g of the PPE-2T/diol copolymer with bimodal PPE-2T of 3700 g/mol decreases with increasing diol length and diol flexibility. The T_g can be set between 100 and 200°C by changing the type of diol. However at increasing diol length the T_g becomes broader and the test bars are less transparent because the extent of phase separation increases with increasing diol length. Only polymers with a diol length up to C12 are homogeneous. It is expected that the presence of the high molecular weight fraction in PPE-2T is responsible for the phase separation.

Another and better way to decrease the T_g of PPE is to use shorter bimodal PPE-2T segments with a short diol. In this way the T_g can be lowered further while phase separation is suppressed. It is even better to use fractionated, monomodal PPE-2T. Copolymers with fractionated PPE-2T phase separate less compared to copolymers based on bimodal PPE-2T.

Due to the low T_g and T_{flow} the processability of this type of PPE copolymers is expected to be improved compared to commercial PPE. Copolymerisation is much more effective in decreasing the T_g of PPE and therefore its processability than blending with polystyrene.

The PPE-2T segment can be used in copolymerisation with other bifunctional segments. All types of diol or di-ester segments or telechelics can be used. Segments can be aliphatic or aromatic, for example poly(propylene oxide) or polycarbonate telechelics.

Literature

1. S.G. Allen, J.C. Bevington, 'Comprehensive polymer science', D.M. White on Poly(phenylene ether), Pergamon Press, New York, 5, 473 (1989).
2. D. Aycok, V. Abolins, D.M. White in 'Encyclopedia Of Polymer Science and Engineering', H.F. Mark, N.M. Bikales, C.G. Overberger, G. Menges, John Wiley & Sons, New York, 13, 1 (1988).
3. H.R. Kricheldorf, in 'Handbook of Polymer Synthesis', Part A, Dekker, New York, 545 (1992).
4. F.E. Karasz, J.M. O'Reilly, J. Polym. Sci. Polym. Lett. Ed., 3, 561 (1965)
5. D.M. White, G.R. Loucks, ACS Symp. Ser., 282, 187 (1985).
6. J. Liska, E. Borsig, J. Macromol. Sci., 35, 523 (1995).
7. US 3,875,256, D.M. White (1975).
8. US 3,703,564, D.M. White (1972).
9. D.M. White, J. Polym. Sci., Polym. Chem. Ed., 19, 1367 (1981).
10. JP 57,195,122 (1982).
11. JP 58,157,819 (1984).
12. US 4,495,333, D.M. White (1985).
13. US 4,645,806, Freitag et al. (1987).
14. US 4,374,233, Loucks et al. (1983).

15. US 4,377,662, Loucks (1983).
16. US 4,536,543, Matzner et al. (1985).
17. J. Stehlicek, R. Puffr, Collect. Czech. Chem. Commun., 58, 2574 (1993).
18. M. Sato, T. Mangyo, K. Mukaida, Macromol Chem. Phys., 196, 1791 (1995).
19. M. Sato, S. Ujiie, Y. Tada, Eur. Polym. J., 34, 405 (1998).
20. M. Wicker, W. Heitz, Makromol. Chem., 192, 1371 (1991).
21. C.S. Han, S.C. Kim, Polym. Bull., 35, 407 (1995).
22. Chapter 2 of this thesis.
23. W. Risse, W. Heitz, D. Freitag, L. Bottenbruch, Makromol. Chem., 186, 1835 (1985).
24. W. Koch, W. Risse, W. Heitz, Makromol. Chem., Suppl., 12, 105 (1985).
25. W. Heitz, W. Stix, H. Kress, W. Koch, W. Risse, Polym. Prepr. Am. Chem. Soc. Div. Polym. Chem., 25, 136 (1984).
26. H. Nava, V. Percec, J. Polym. Sci. Polym. Chem. Ed., 24, 965 (1986).
27. US 4,665,137, V. Percec (1987).
28. V. Percec, J.H. Wang, Pol. Bull., 24, 493 (1990).
29. H.A.M. van Aert, M.H.P. van Genderen, G.J.M.L. van Steenpaal, L. Nelissen, E.W. Meijer, J. Liska, Macromolecules, 30, 6056 (1997).
30. H.A.M. van Aert, R. W. Venderbosch, M.H.P. van Genderen, P.J. Lemstra, E.W. Meijer, J.M.S.-Pure Appl. Chem., A32(3), 515 (1995).
31. US 5,880,221, Liska et al. (1999).
32. US 5,015,698, Sybert et al. (1991).
33. D.M. White, S.A. Nye, Macromolecules, 23, 1318 (1990).
34. US 4,140,675, D.M. White (1979).
35. H.S.-I. Chao, J.M. Whalen, React. Polym. 15, 9 (1991).
36. US 4,746,708, Sybert (1988).
37. H.A.M. van Aert, 'Design and synthesis of reactive building blocks for multicomponent polymer systems', PhD thesis, Eindhoven University of Technology, The Netherlands (1997).
38. Chapter 5 of this thesis.
39. G. Odian, 'Principles of Polymerization', John Wiley & Sons, New York, Third Edition (1991).
40. M.C.E.J. Niesten, J. Feijen, R.J. Gaymans, Polymer, 41, 8487 (2000).
41. H.J. Manuel, R.J. Gaymans, Polymer, 34, 636 (1993).
42. T.G. Fox, Bull. Am. Phys. Soc., 1, 123 (1956).

Chapter 4

Copolymers of poly(2,6-dimethyl-1,4-phenylene ether) and poly(dodecane terephthalate)

Abstract

Copolymers of telechelic poly(2,6-dimethyl-1,4-phenylene ether) segments with terephthalic methyl ester endgroups (PPE-2T, 3500 g/mol, bimodal MWD) and poly(dodecane terephthalate) (PDDT) were made via a polycondensation reaction. The T_g and T_{flow} of the PPE/PDDT polyether-ester copolymers decrease with increasing PDDT length. The T_g can be set between 90 and 170°C by changing the PDDT content between 40 and 12 wt%. However at increasing PDDT length (above 1000 g/mol, PDDT content >20 wt%) the T_g becomes broader because the extent of phase separation increases with increasing PDDT length.

A copolymer of PDDT with some PPE (27 wt%) has a modulus in the rubbery plateau that is increased by a factor three compared to pure PDDT. The material has a phase separated morphology. The amorphous PDDT phase is the continuous phase and is almost pure. PPE possibly forms rigid domains that act as reinforcing filler for the polyester. PDDT/PPE copolymers seem interesting as an alternative for glass-filled polyesters. This new approach might be of particular interest to improve the properties of polyesters such as PBT and PET.

Introduction

Poly(2,6-dimethyl-1,4-phenylene ether) (PPE)¹⁻³ or PPO is a linear amorphous polymer with a very high glass temperature of approximately 215°C⁴. PPE has excellent properties such as high toughness, high dimensional stability, good flame retardation and low moisture uptake. However, due to its high glass transition temperature, very high processing temperatures are required, which can lead to degradation. Only PPE with a molecular weight between 10.000 and 30.000 g/mol is just processable. By lowering the T_g , the processing temperature can be lowered and degradation free processing becomes possible. To lower the T_g , PPE is usually blended with polystyrene, as PPE and PS are fully miscible. However, possibilities for lowering the T_g of PPE by blending with other polymers than PS are limited due to the low miscibility with PPE¹⁻³.

It was found that copolymerisation of PPE segments with short di-ester segments is a good method to decrease the T_g of PPE and to improve the processability⁵. In segmented copolymers only the low molecular weight segments have to be miscible. In general the miscibility increases with decreasing molecular weight of the segments. When phase separation occurs in copolymers with segments of low molecular weight it will be microphase separation contrary to the macrophase separation of a blend, because the segments in a copolymer are connected. Macrophase separation can lead to a material with poor properties, due to delamination.

Thus far only di-ester segments based on terephthalic groups and aliphatic diols of varying length were incorporated in PPE by polycondensation of telechelic PPE with terephthalic methyl ester endgroups (PPE-2T, Figure 4.1) with diols⁵. Long di-ester segments were incorporated by using long diols such as the telechelic polyether poly(tetramethylene oxide) (PTMO) of 650-2900 g/mol. With these aliphatic polyethers phase separation between PPE and PTMO already starts above a PTMO length of 1000 g/mol due to the incompatibility of these two segments. It would be interesting to study copolymers of PPE with polyester segments of different lengths and to compare the phase separation with that of copolymers of PPE with PTMO.

Telechelic PPE segments (PPE-2T, Figure 4.1) can be made by redistribution or depolymerisation of high molecular weight PPE with tetramethyl bisphenol A (to PPE-2OH) followed by endgroup modification with methyl chlorocarbonyl benzoate (MCCB)⁶. These PPE segments have a bimodal molecular weight distribution because part of the high molecular weight starting material is not depolymerised^{6,7}. The product is a mixture of a high molecular weight fraction (20-30%) and a low molecular weight depolymerised fraction (70-80%). The high molecular weight fraction is PPE (~11.000 g/mol) that has not reacted due to absence of the right functional groups to initiate the redistribution reaction. The number average molecular weight of the PPE-2T segments is 2000-4000 g/mol depending on the amount of tetramethyl bisphenol A used in the redistribution reaction.

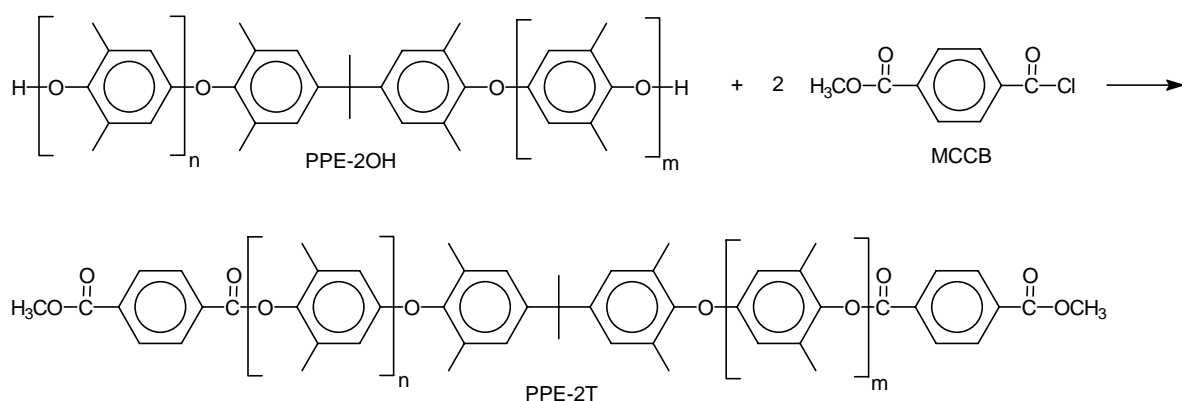


Figure 4.1: Reaction of PPE-2OH (that is obtained after redistribution of PPE with tetramethyl bisphenol A) with methyl chlorocarbonyl benzoate (MCCB) to PPE-2T.

Segmented copolymers of PPE and ester segments will be made in a polycondensation reaction using PPE-2T, dodecanediol (C12) and dimethyl terephthalate (DMT). PPE-2T with a number average molecular weight of ~ 3700 g/mol will be used. This PPE-2T contains about 24 wt% of hardly functionalised high molecular weight PPE⁶. Copolymerisation of PPE with dodecanediol and dimethyl terephthalate results in a copolymer with two types of segments, PPE (without terephthalic endgroups ~ 3500 g/mol) and C12/DMT or poly(dodecane terephthalate) (PDDT) of different lengths (Figure 4.2). In this formula, x is the average number of repeating units of the PDDT segments in the copolymer.

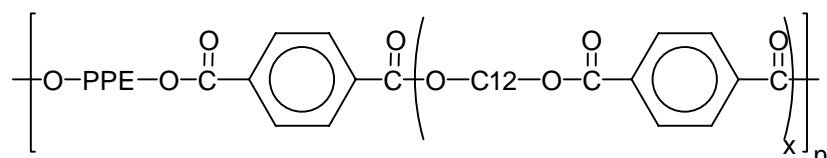


Figure 4.2: Structure of the PPE-2T/C12/DMT or PPE/PDDT copolymer in which the PPE segments are linked by poly(dodecane terephthalate) (PDDT).

The copolymer of PPE-2T, dodecanediol and dimethyl terephthalate is a mixture of this PPE/PDDT copolymer and unreacted high molecular weight PPE. Some of these unreacted PPE chains can be present in the copolymer as an endgroup because they contain a methyl ester endgroup as a result of the reaction of a Mannich base type endgroup with MCCB^{5,6}.

The expectation is that the low molecular weight PPE-2T segments and the ester segment will mix when the ester segment is short. The polymers then will have one glass transition temperature, which is lower than that of pure PPE, depending on the length of the ester segment used. It is envisaged that this will lead to improved processability. At increasing length of the ester segment, phase separation will be possible and this will give a broad T_g , or more than one T_g . PPE-2T/diol copolymers show phase separation above a diol length of ~ 1000 g/mol⁵. When there is no phase separation between polyether and ester segment, it is expected that these copolymers are transparent.

When the polyester content is high and the PPE content low, the PPE might act as a rigid modifier for the semi-crystalline polyester. In this way a system with an improved dimensional stability might be obtained. The presence of the PPE segments will probably have a negative influence on the crystallisation of the polyester.

Aim

In this chapter alternating polyether-ester copolymers based on PPE-2T and poly(dodecane terephthalate) segments are studied. The average length of the polyester segment will be varied, thereby obtaining PPE modified by polyester or polyester modified by PPE. The thermal-mechanical properties of these copolymers will be studied using DMA. The effect of composition on glass transition and flow temperature and on phase separation will be discussed.

Experimental

Materials. Dimethyl terephthalate (DMT), 1,12-dodecanediol (C12) and toluene were purchased from Merck. Tetraisopropyl orthotitanate ($\text{Ti}(\text{i-OC}_3\text{H}_7)_4$), obtained from Merck, was diluted in anhydrous *m*-xylene (0.05M), obtained from Fluka. PPO-803[®] (11.000 g/mol) was obtained from GE Plastics (The Netherlands). All chemicals were used as received. PPE-2T with an average molecular weight of 3700 g/mol (480 $\mu\text{mol OCH}_3/\text{g}$, functionality = 1.79) and a bimodal molecular weight distribution was made in a two-step reaction according to the methods described in Chapter 2⁶.

Synthesis of PPE-2T/diol copolymers. The PPE-2T/diol copolymers were synthesised by an ester type polycondensation reaction using PPE-2T, dodecanediol and dimethyl terephthalate. The preparation of a copolymer of PPE-2T (~3700 g/mol) and PDDT with $x=4$ is given as an example.

The reaction was carried out in a 50 ml glass reactor with a nitrogen inlet and mechanical stirrer. The vessel was loaded with PPE-2T (10.0 g, 4.8 mmol OCH_3), dodecanediol (1.94 g, 9.6 mmol), dimethyl terephthalate (1.40 g, 7.2 mmol), 10 ml toluene and catalyst solution (0.5 ml of 0.05M $\text{Ti}(\text{i-OC}_3\text{H}_7)_4$ in *m*-xylene). This mixture was first heated in an oil bath to 120°C under nitrogen flow. After 30 minutes the temperature was increased in steps: 30 minutes at 180°C, 30 minutes at 220°C and 60 minutes at 250°C. The pressure was then reduced slightly ($P < 20$ mbar) for 30 minutes and then further reduced ($P < 1$ mbar) for 30 minutes. Finally, the vessel was allowed to slowly cool to room temperature whilst maintaining the low pressure. Then the polymer was cut out of the reactor and crushed.

Viscometry. The inherent viscosity of the polymers was determined with a capillary Ubbelohde type 0C at 25°C, using a polymer solution with a concentration of 0.1 g/dl in chloroform.

DMA. Samples for the DMA test (70x9x2 mm) were prepared on an Arburg-H manual injection moulding machine. Before use, the samples were dried in a vacuum oven at 80°C overnight. The torsion behaviour was studied at a frequency of 1 Hz, a strain of 0.1% and a heating rate of 1°C/min using a Myrenne ATM3 torsion pendulum. The storage modulus G' and loss modulus G'' were measured as a function of temperature starting at -100°C. The glass transition temperature (T_g) was expressed as the temperature at which the loss modulus G'' has a maximum. This maximum was 0-10°C lower than the actual glass transition temperature, because with this DMA apparatus it was not possible to measure a few points around the T_g due to the very high damping. The flow temperature (T_{flow}) was determined as the temperature where the storage modulus G' reached 1 MPa.

Results and Discussion

Introduction

Bimodal PPE-2T with an average M_n of ~3700 g/mol was copolymerised with increasing amounts of dodecanediol (C12) and dimethyl terephthalate (DMT). In this way the length of the poly(dodecane terephthalate) segment was increased. All copolymers could easily be obtained with high molecular weights. When the inherent viscosity is above 0.3 dl/g (~10.000 g/mol) the molecular weight of the polymers is high enough to obtain good properties.

Table 4.1. Properties of the PPE/PDDT copolymers.

	PPE [w%]	PDDT [wt%]	x^a	PDDT length [g/mol]	η_{inh} [dl/g]	T_g PPE ^b [°C]	T_g PDDT ^b [°C]	T_{flow} [°C]
Starting materials:								
PPO-803 [®]	100	-	-		0.37	200	-	222
PPE-2T ^c	-	-	-		0.19	173 ^d	-	-
PPE-2T/C12/DMT copolymers:								
PPE-2T/C12	88	12	1	450	0.33	170	-	195
PPE/PDDT	82	18	2	800	0.70	155	-	208
PPE/PDDT	76	24	3	1150	0.56	144	85	197
PPE/PDDT	72	28	4	1450	0.65	124	45	183
PPE/PDDT	64	36	6	2150	0.58	94	35	144
PPE/PDDT	52	48	10	3500	0.59	84	30	123
PPE/PDDT	27	73	30	10000	0.65	-	9	128
PDDT	0	100	-	-	0.72	-	0	123

(a), x is the average number of repeating units in the PDDT segment as indicated in Figure 4.2; (b), both the T_g of the PPE (rich) phase and the PDDT (rich) phase are given when a two-phase morphology is present; (c), made by two-step synthesis, bimodal, M_n ~3700 g/mol⁶; (d), measured by DSC instead of DMA

The alternating polyether-ester copolymers based on bimodal PPE-2T (~3700 g/mol) and PDDT segments of different lengths were injection moulded into test bars. The effect of composition on glass transition temperature, flow temperature and phase separation was studied by DMA. The results are given in Table 4.1. First the properties of copolymers with a high PPE content will be discussed and then those with a high PDDT content.

High PPE content

Copolymers with a high PPE content were made to study the effect of the PDDT length on the T_g of PPE and to improve the processability. In Table 4.1 and Figure 4.3 the DMA results for the copolymers with high PPE content are given.

PPE (PPO-803[®]) is an amorphous polymer and has a high T_g of 200°C (maximum of G'') and a high and constant modulus up to the T_g . The glass transition is sharp and the flow temperature is 222°C. The PDDT homopolymer is a semi-crystalline polymer with a T_g of 0°C and a flow temperature of 123°C. The PPE/PDDT copolymers show a decreasing T_g and T_{flow} with increasing PDDT content. The T_{flow} can be somewhat lower when the molecular weight is lower.

The PPE-2T/C12 copolymer⁵ (PPE/PDDT with $x=1$ in Figure 4.2) that contains 12 wt% PDDT, has a high and constant modulus, up to the sharp T_g at 170°C. The T_g is decreased by 30°C compared to pure PPE. The short PDDT segments (~450 g/mol) in this copolymer are well miscible with the PPE segments. These copolymers with short PDDT segments ($x=1$, PPE-2T/C12) are slightly transparent and thus rather homogeneous.

The incorporation of little more PDDT ($x=2$, 18 wt%) in the copolymer results in a decreased and broadened T_g for the PPE phase and a lower flow temperature compared to the PPE-2T/C12 copolymer ($x=1$). The modulus is high up to the T_g . Apparently PDDT with a length of ~800 g/mol is too short to phase separate. Already at $x=2$ transparency is lost, indicating that some domains with different PPE and PDDT content might be present on a micro-scale.

When the PDDT length is increased to 1150 g/mol (24 wt% PDDT, $x=3$) the T_g and T_{flow} decrease and more phase separation between PPE and PDDT becomes possible. The modulus decreases somewhat before the T_g of the PPE rich phase. The copolymer with 24 wt% PDDT ($x=3$) seems to consist of a PPE rich phase with a high T_g and a PDDT rich phase with a lower T_g (Table 4.1). The PDDT rich phase has an increased T_g (~85°C) compared to pure PDDT (0°C) and is thus expected to contain PPE. A PPE/PDDT mixed phase with a T_g of 85°C is expected to contain about 40% PPE and 60% PDDT. When PDDT crystallises partially in the PDDT rich phase, a melting temperature somewhat below 123°C (T_m of pure PDDT) is expected. The copolymer does not show such a melting transition and is thus amorphous.

When the PDDT length is increased to 1450-2150 g/mol (28-36 wt% PDDT, $x=4-6$), more phase separation is possible. The modulus of these copolymers shows a substantial decrease before the T_g of the PPE rich phase is reached. These copolymers consist of a PPE rich phase with a high T_g and a PDDT rich phase with a lower T_g as well. The T_g of the PDDT rich phase is 35-45°C, which is higher than that of pure PDDT but lower than in the copolymer with 24

wt% PDDT ($x=3$). The PPE content of the PDDT rich phase with a T_g of 35-45°C is around 20 wt%. The PPE rich phase has a decreased T_g compared to pure PPE and PPE/PDDT copolymers with a lower PDDT content and thus contains a lot of PDDT. Thus the PDDT segment is still partially miscible with PPE. The PDDT rich phase is amorphous, as a melting transition is not observed.

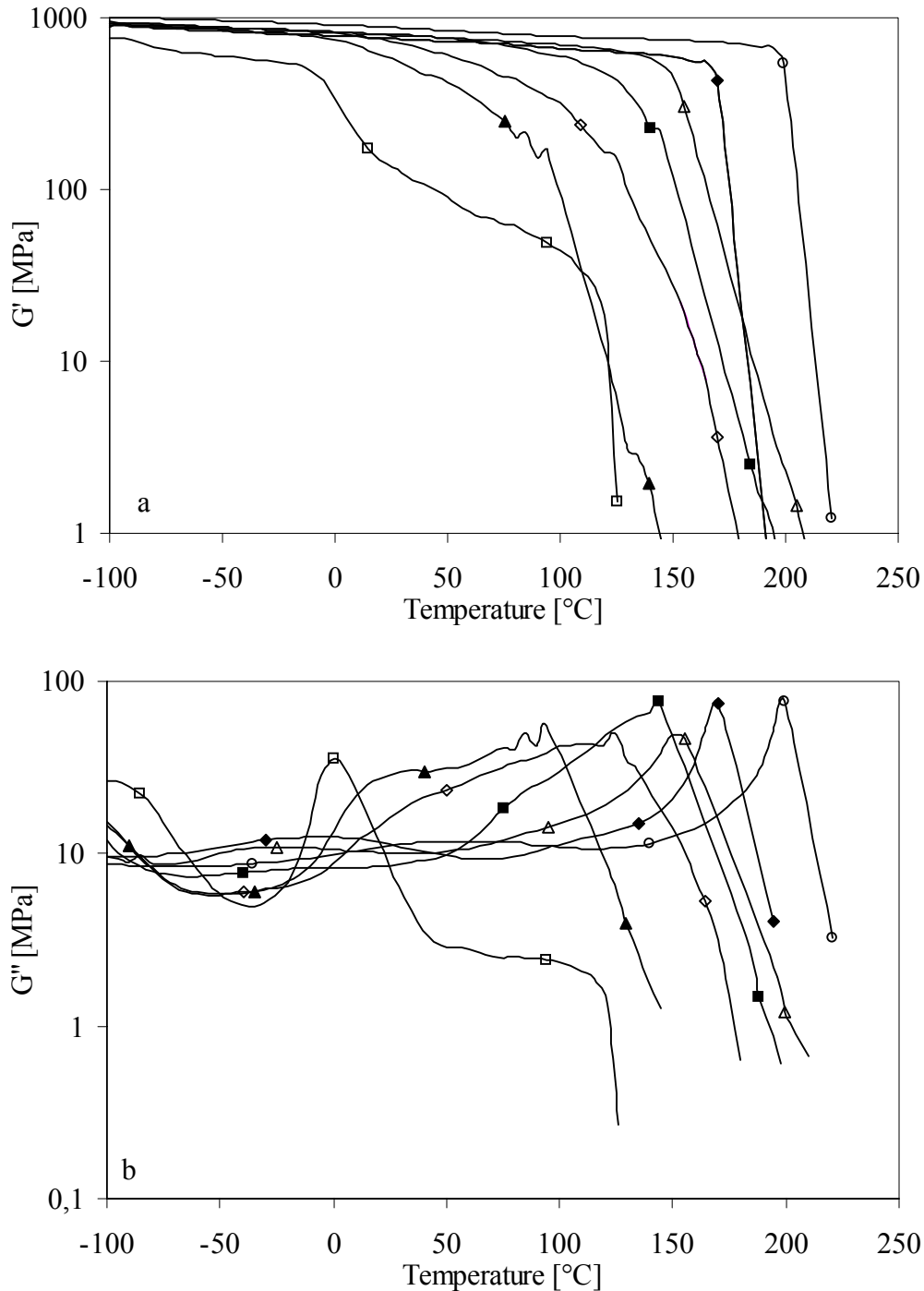


Figure 4.3. Storage (a) and loss (b) modulus of PPE/PDDT copolymers with an average PPE length of ~3500 g/mol and different PDDT contents: (○), PPE (PPO-803[®]); (◆), 12 wt% PDDT ($x=1$); (△), 18 wt% PDDT; (■), 24 wt% PDDT; (◇), 28 wt% PDDT; (▲), 36 wt% PDDT; (□), PDDT.

In Figure 4.4 the storage and loss modulus of the PPE/PDDT copolymer with a PDDT length of ~ 2150 g/mol (36 wt% PDDT, $x=6$) are compared with that of PPE-2T/PTMO₂₀₀₀ (copolymer of PPE-2T and PTMO of 2000 g/mol)⁵. Both contain around 65 wt% of PPE and the second segment (T-(C12-T)_n or T-PTMO-T) has about the same length.

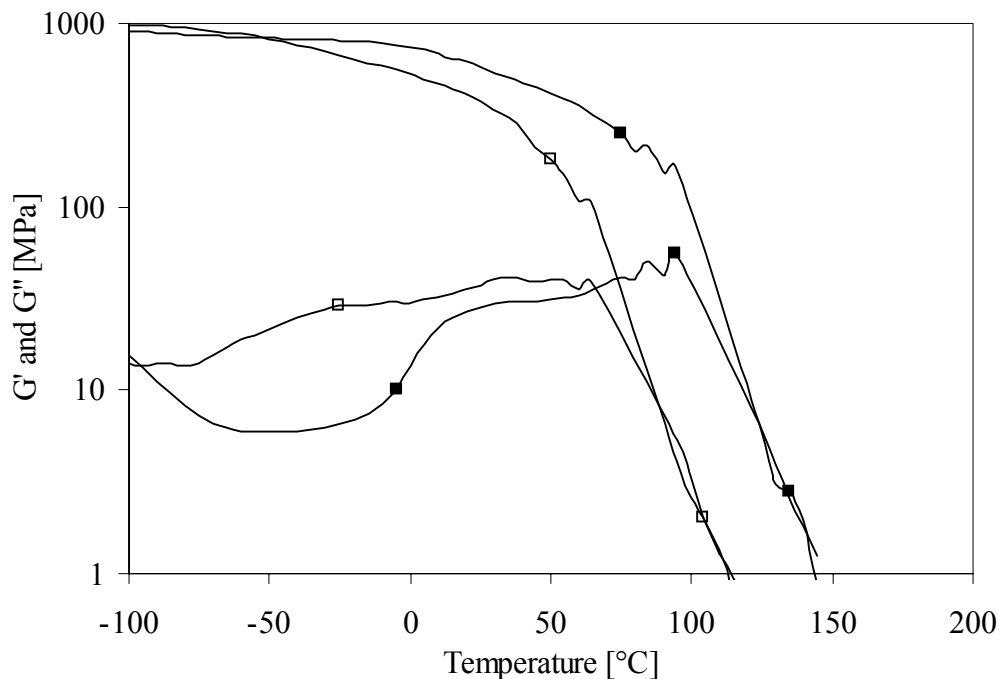


Figure 4.4. Storage and loss modulus of PPE/PDDT copolymer with 64 wt% PPE compared to PPE-2T/PTMO₂₀₀₀ with 66 wt% PPE⁵: (■), PPE/PDDT₂₁₅₀: (□), PPE-2T/PTMO₂₀₀₀.

Both copolymers of PPE with an extender segment (polyester of polyether) of ~ 2150 g/mol have a phase separated morphology consisting of a PPE rich phase and a PDDT or T-PTMO-T rich phase. The modulus of PPE-2T/PTMO₂₀₀₀ starts to decrease at a lower temperature than that of PPE/PDDT₂₁₅₀ because the T_g of the PTMO rich phase is lower than that of the PDDT rich phase. Pure PDDT has a T_g of 0°C . T-PTMO-T is more flexible and has a T_g of -65°C ⁸. Based on these T_g 's it can roughly be calculated that the PPE/PDDT copolymer with a PDDT rich phase with a T_g of $\sim 35^\circ\text{C}$ contains around 20% PPE. The PPE-2T/PTMO₂₀₀₀ copolymer with a PTMO rich phase with a T_g of about -25°C contains ~ 15 wt% of PPE. So the miscibility of PPE with PDDT and PTMO is comparable.

The decrease in T_g of the PPE rich phase is less when PDDT is used as extender instead of PTMO. This is also caused by the lower T_g and higher flexibility of PTMO compared to PDDT. As a result the T_g of the mixed PPE phase is higher after copolymerisation with PDDT. The glass transition temperatures of both copolymers have about the same broadness for PPE/PDDT₂₁₅₀ and PPE-2T/PTMO₂₀₀₀.

In Figure 4.5 the T_g of the PPE rich and the PDDT rich phase is given as a function of the PPE content for the copolymers of PPE-2T and PDDT. In this figure the calculated T_g 's of PPE/PS blend and a theoretical PPE/PDDT blend as function of the PPE content, both based on the Fox relationship⁹, are given as well.

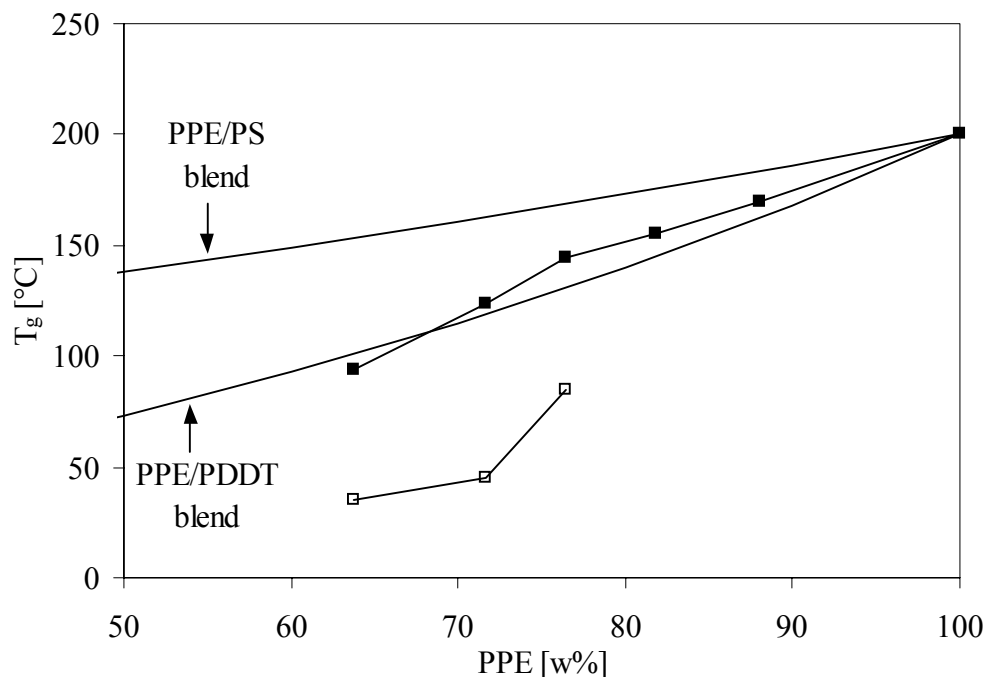


Figure 4.5. T_g for PPE/PDDT copolymers compared with the T_g of a PPE/PS blend and that of a (theoretical) blend of PPE with PDDT (both according to the Fox relation)⁹: (■), PPE rich phase; (□), PDDT rich phase.

By copolymerisation of PPE with PDDT the T_g can be set between 90 and 170°C. The T_g of the PPE rich phase in the PPE/PDDT copolymer is comparable with that of a theoretical (fully miscible) PPE/PDDT blend. Thus the PPE/PDDT copolymers are homogeneous at high PPE contents (>70 wt%, $x < 4$). Below 70 wt% PPE the T_g decreases more. Although the copolymers seem homogeneous they are not transparent, except for $x=1$ (12 wt% PPE). Apparently the copolymers are not homogeneous on a microscale.

From Figure 4.5 it can be concluded that the effectiveness of decreasing the T_g of PPE is much higher by copolymerisation with PDDT to polyether-esters than by blending with polystyrene. For a polymer with a T_g of 150°C, a 50/50 blend PPE/PS can be used. The same T_g can be obtained after copolymerisation with PDDT in a copolymer that contains ~80 wt% of PPE. Copolymerisation using PDDT is much more effective than blending with polystyrene, because the T_g of the PDDT homopolymer ($T_g = 0^\circ\text{C}$) is much lower than that of pure polystyrene ($T_g = 100^\circ\text{C}$).

The thermal behaviour of PPE/PDDT copolymers with less than 25 wt% PDDT is comparable with that of PPE-2T/diol copolymers⁵. At higher PDDT content the thermal behaviour becomes comparable with PPE-2T/PTMO copolymers. However, the effect on the T_g of

copolymerisation with PDDT is somewhat less than with PTMO due to the higher T_g of PDDT. An advantage of using long PDDT instead of PTMO as extender for PPE-2T segments is that the modulus starts to drop at a higher temperature for PPE/PDDT than PPE-2T/PTMO, because of the higher T_g of PDDT. However the phase separation between PPE and PDDT or PTMO is comparable. Therefore, when a PPE copolymer with a low T_g is needed it is probably better to decrease the PPE-2T length while keeping the (short) PDDT length constant as with PPE-2T/diol copolymers⁵. It can be concluded that copolymerisation of PPE-2T with PDDT is an alternative for copolymerisation of PPE-2T with diols. There is only one small advantage, which is that the length of the polyester segment can be adjusted continuously.

High PDDT content

Copolymers of PDDT with PPE-2T with a high PDDT content were studied as well. PDDT is a semi-crystalline polymer. The PPE can, if miscible, influence the T_g , T_m and modulus above the T_g of PDDT. In Table 4.1 and Figure 4.6 the DMA results for the copolymers with high PDDT content are given.

The PDDT homopolymer is a semi-crystalline polymer with a T_g of 0°C and a flow temperature of 123°C.

When about 27 wt% PPE is incorporated in the PDDT polymer by copolymerisation, the PDDT is still the continuous phase. The thermal behaviour as measured by DMA resembles that of the PDDT homopolymer, with a T_g , rubbery plateau and sharp flow temperature. The glass transition temperature of the PDDT phase is increased by about 9°C after copolymerisation with PPE. This indicates that only about 5 wt% of PPE is mixed with the PDDT phase. So apparently the rest of the 27 wt% PPE forms small domains in the PDDT matrix. These rigid PPE domains have a high T_g and act as rigid modifier for PDDT in its rubbery plateau. As a result the modulus in the rubbery plateau of PDDT is increased by a factor of 3. The flow temperature of the PDDT/PPE copolymer is comparable with that of pure PDDT. The average PDDT segment length is long enough to allow crystallisation.

In the PDDT/PPE copolymers with 52-64 wt% PPE the thermal behaviour is different from that of pure PDDT. The glass transition now consists of two transitions as in the PPE/PDDT copolymers with high PPE content. The first T_g is of PDDT rich phase and the second of a PPE rich phase. These two T_g 's are located close to each other, which indicates that both phases are mixed to a large extent. A rubbery plateau with a low loss modulus is not observed any more at such high PPE contents. The PDDT in the copolymer with 52 wt% PPE is probably still the continuous phase and partially crystalline as the flow temperature is still between 120 and 130°C. With 64 wt% PPE, the polyester is probably amorphous.

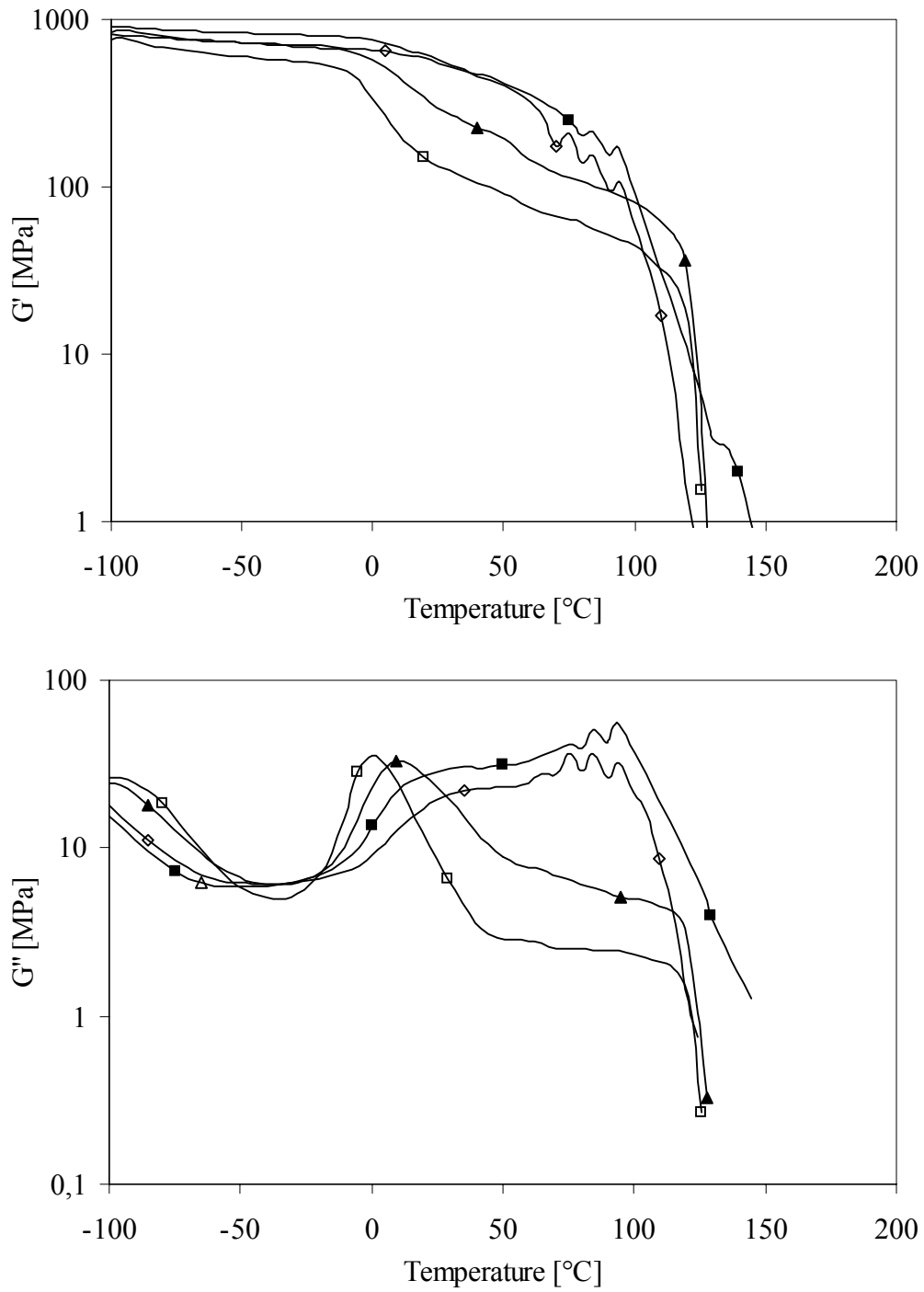


Figure 4.6. Storage (a) and loss (b) modulus of PPE/PDDT copolymers with PPE of ~ 3500 g/mol and different PDDT contents: (■), 36 wt% PDDT; (◇), 48 wt% PDDT; (▲), 73 wt% PDDT; (□), PDDT.

In Figure 4.7 the T_g 's of the PDDT and PPE rich phase and the T_{flow} are given as a function of the PDDT content. The T_g of the PDDT rich phase increases with decreasing PDDT content, but not according to the expected T_g of a theoretical, fully miscible PPE/PDDT blend. This indicates that the PDDT rich phase contains less PPE than the actual PPE content. So most of the PPE segments are in separate amorphous domains. When the PPE content is above 50 wt% these PPE contents are large enough to show a T_g of a PPE/PDDT mixed phase. At PPE contents below 50 wt% the PPE rich domains act only as rigid modifier for the semi-crystalline PDDT. The PDDT phase seems to be semi-crystalline with a flow temperature between 120 and 130°C when the PPE content is below 50 wt%.

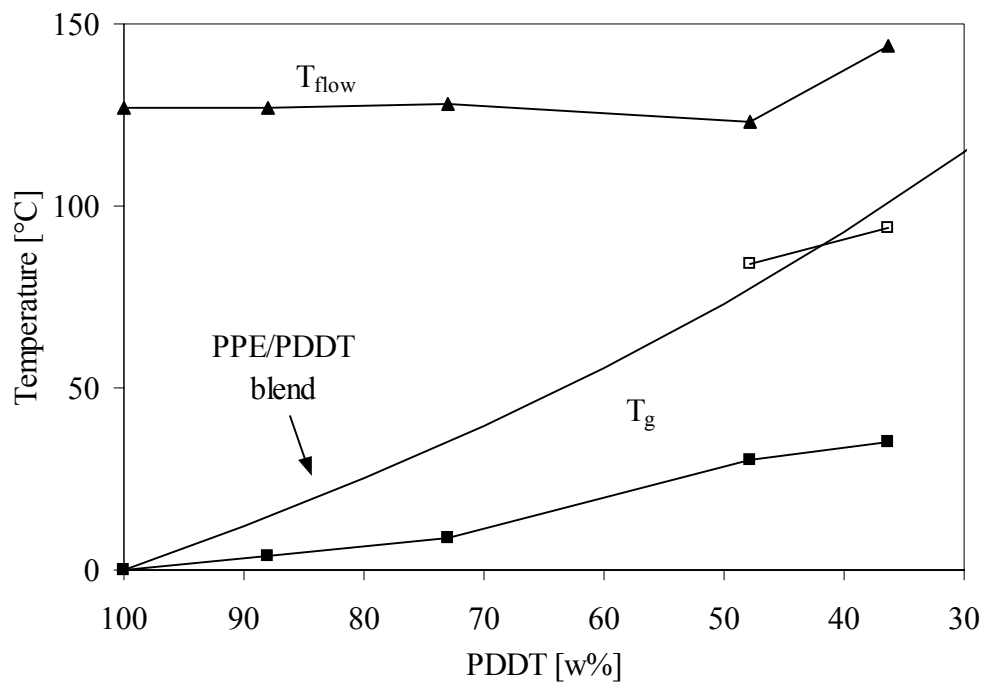


Figure 4.7. T_g and T_{flow} for PDDT/PPE copolymers compared with the T_g of a (theoretical) blend of PPE with PDDT (according to the Fox relation)⁹: (■), T_g of PDDT rich phase; (□), T_g of PPE rich phase; (▲), T_{flow} of PDDT/PPE copolymer.

Copolymerisation of PDDT with PPE segments (<50 wt%) is an interesting new approach to increase the T_g and the modulus of the rubbery plateau of the polyester, while the flow temperature remains constant. Normally glass fibres are used to increase the modulus of a polymer, but for some applications this is not so desirable.

Conclusions

PPE/PDDT polyether-ester copolymers can be made from PPE-2T, dodecanediol and dimethyl terephthalate in a polycondensation reaction with high molecular weights (>10.000 g/mol). The T_g and T_{flow} of the PPE/PDDT copolymers with bimodal PPE-2T segments with an average PPE length of 3500 g/mol decrease with increasing PDDT length. The T_g can be set between 90 and 170°C by changing the PDDT content between 40 and 12%. However at increasing PDDT length (above 1000 g/mol, PDDT content >20 wt%) the T_g becomes broader. Phase separation results in the presence of a PPE rich and a PDDT rich phase. Only copolymers with very short PDDT ($x=1$, PPE-2T/C12) are transparent and thus homogeneous. Already at $x=2$ transparency is lost, indicating that some domains with different PPE and PDDT content might be present.

Due to the low T_g and T_{flow} the processability of this type of PPE copolymers is expected to be improved compared to the commercial PPE. Copolymerisation is much more effective in decreasing the T_g of PPE and therefore its processability than blending with polystyrene. Copolymerisation of PPE-2T with PDDT is comparable with that of PPE-2T with aliphatic diols or PTMO. The T_g can be decreased less with PDDT compared to PTMO because of the larger flexibility of PTMO. The phase separation and thus the compatibility of PPE with PDDT and PTMO are comparable. The only advantage of using PDDT instead of PTMO is the flexibility to change the PDDT segment length.

By copolymerisation of PDDT with some PPE (27 wt%) a semi-crystalline material with a T_g of 9°C, a high rubbery plateau and T_{flow} of 128°C can be obtained. The amorphous PDDT phase is almost pure and is hardly mixed with PPE as the T_g is only little higher than that of pure PDDT. The rest of the PPE is in separate domains. These rigid PPE domains act as reinforcing filler for the polyester and as a result the modulus in the rubbery plateau is increased by a factor 3. PDDT/PPE copolymers seem interesting as an alternative for glass-filled polyesters. This new approach might be of particular interest to improve the properties of polyesters such as poly(butylene terephthalate) and poly(ethylene terephthalate).

Literature

1. S.G. Allen, J.C. Bevington, 'Comprehensive polymer science', D.M. White on Poly(phenylene ether), Pergamon Press, New York, 5, 473 (1989).
2. D. Aycock, V. Abolins, D.M. White in 'Encyclopedia Of Polymer Science and Engineering', H.F. Mark, N.M. Bikales, C.G. Overberger, G. Menges, John Wiley & Sons, New York, 13, 1 (1988).
3. H.R. Kricheldorf, in 'Handbook of Polymer Synthesis', Part A, Dekker, New York, 545 (1992).
4. F.E. Karasz, J.M. O'Reilly, J. Polym. Sci. Polym. Lett. Ed., 3, 561 (1965).
5. Chapter 3 of this thesis.
6. Chapter 2 of this thesis.
7. H.S.-I. Chao, J.M. Whalen, React. Polym. 15, 9 (1991).
8. M.C.E.J. Niesten, J.W. ten Brinke, R.J. Gaymans, Polymer, 42, 1461 (2001).
9. T.G. Fox, Bull. Am. Phys. Soc., 1, 123 (1956).

Chapter 5

Synthesis and characterisation of uniform bisester tetra-amide segments

Abstract

Bisester tetra-amide segments (TxTxT-dimethyl) with T is a terephthalic units and $x = n$ in $(\text{CH}_2)_n$ ($n = 2-8$) can be synthesised in a two-step reaction. These segments are based on two-and-a-half repeating units of nylon-x,T. The first step is the synthesis of xTx-diamine in the melt, followed by recrystallisation to improve the purity. TxTxT-dimethyl can then be prepared in a reaction of xTx-diamine with methyl phenyl terephthalate in solution. The structure of the products was confirmed by NMR. The purity of the tetra-amide product depends on the purity of the xTx-diamine used. The melting temperature and enthalpy of xTx-diamine and TxTxT-dimethyl and -diphenyl were determined by DSC. The melting temperature increases with decreasing length of x. For odd x the melting temperature is lower. The melting temperature and enthalpy of the products decrease with decreasing purity.

Introduction

Segmented or multi-block copolymers often consist of alternating crystallisable and amorphous segments. The high melting crystalline phase gives the material dimensional stability, heat stability and solvent resistance. If the crystallisable segment has a regular structure and a uniform length than the crystallisation of the segment is faster and more complete and the properties of the copolymer are better¹⁻⁴. Thus far the only uniform amide segments that have been described are di-amides⁵⁻¹³. A higher melting temperature can be obtained, when tetra-amide segments are formed during polymerisation by extending bisester di-amide units with a diol¹³⁻¹⁶. These extended di-amide segments have a higher melting temperature because the lamellar thickness is higher¹⁷. However, the melting temperature is broad due to a distribution in the segment lengths.

A new type of uniform amide segment that is a bisester tetra-amide segment has been developed. This tetra-amide segment can form four hydrogen bonds as compared to the di-amide segments that can only form two. The lamellar thickness of a tetra-amide segment is higher than that of a di-amide segment and as a result the melting temperature is expected to be higher than that of the corresponding di-amide units¹⁷.

Bisester tetra-amides can be synthesised from diamines and diacids or derivatives of diacids. The molecular structure of the bisester tetra-amides is given in Figure 5.1. In this Figure R_1 - R_5 are independently an aliphatic, an alicyclic or a wholly or partially aromatic group.

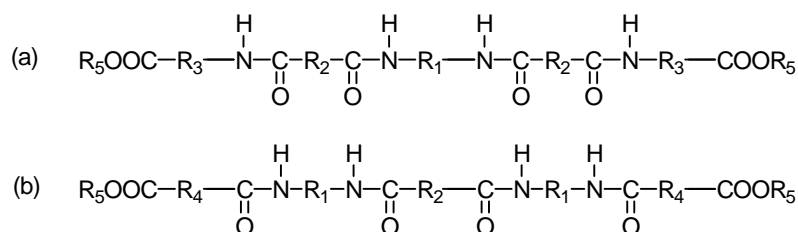


Figure 5.1: Structure of the bisester tetra-amides (R_1 - R_5 are independently an aliphatic, an alicyclic or a wholly or partially aromatic group).

In particular bisester tetra-amides of structure 5.1b in which R_2 and R_4 are a residue of a terephthalic group (T) and R_1 is an aliphatic chain $(\text{CH}_2)_n$ with $n = 2-8$ were studied. An example of a useful bisester tetra-amide segment is T6T6T-dimethyl (Figure 5.2), with R_1 is $(\text{CH}_2)_6$ and R_5 is CH_3 . These segments are based on two-and-a-half repeating unit of nylon-6,T (poly(hexamethylene terephthalamide)).

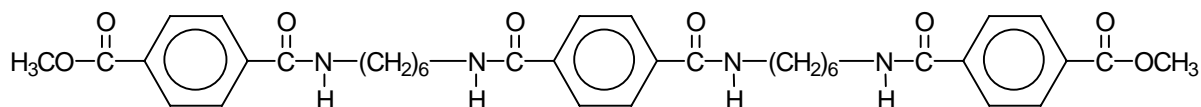


Figure 5.2: Structure of T6T6T-dimethyl.

Similar bisester tetra-amide segments were made as well and this family of half-aromatic bisester tetra-amide segments will be called TxTxT-dimethyl from now on. TxTxT-dimethyl can be made with other x, in which $x = (\text{CH}_2)_n$ with $n = 2-8$. The endgroups (R_5) can be changed as well, for example into phenyl (TxTxT-diphenyl), if desirable.

The bisester tetra-amides can be synthesised quite easily in two steps. For example in the case of T6T6T-dimethyl, first 6T6-diamine (di-(4-aminohexyl)terephthalamide) is made from dimethyl terephthalate (DMT) and 1,6-hexanediamine. The synthesis of 6T6-diamine is derived from the synthesis of 4T4-diamine. The synthesis of 4T4-diamine or di-(4-aminobutyl)terephthalamide (DABT) was described before⁵. Then 6T6-diamine is reacted with methyl phenyl terephthalate (MPT) to obtain the corresponding bisester tetra-amide.

Aim

In this chapter the synthesis and characterisation of different bisester tetra-amide segments (TxTxT-dimethyl or TxTxT-diphenyl) and precursors thereof (xTx-diamine) are described. The structure, purity and melting behaviour of these segments were analysed using NMR and DSC. The bisester tetra-amides were studied by IR and WAXD as well.

Experimental

Materials. Dimethyl terephthalate (DMT), 1,2-ethanediamine, 1,3-propanediamine, 1,4-butanediamine, 1,6-hexamethylenediamine (HMDA), 1,7-heptanediamine, 1,8-octanediamine, terephthaloylchloride (TCI), triethylamine, phenol, n-butyl acetate, diethyl ether and N-methyl-2-pyrrolidone (NMP) were purchased from Merck. Methyl-(4-chlorocarbonyl) benzoate (MCCB) was obtained from Dalian (no.2 Organic Chemical Works P.R.O.C.). All chemicals were used as received.

Synthesis of methyl phenyl terephthalate (MPT). A mixture of phenol (150 g, 1.6 mol) and triethylamine (73 g, 0.7 mol) was heated to 60°C in a 500 ml flask equipped with magnetic stirrer, condenser, calcium chloride tube and nitrogen inlet. Then MCCB (100 g, 0.5 mol), previously dissolved in 200 ml NMP, was added dropwise. After 3 hours the product was precipitated in 2 L of warm water (70°C). The precipitate was separated using a glass filter and washed twice with 50/50 water/ethanol (50°C). The product was subsequently dried in a vacuum oven at 50°C. The yield was 93%. The purity as determined by ¹H-NMR was >98% and the product had a melting temperature of 114°C and a melting enthalpy of 135 J/g.

Synthesis of diphenyl terephthalate (DPT). A mixture of TCI (100 g, 0.5 mol) and phenol (140 g, 1.5 mol) was heated to 50°C in a 500 ml flask equipped with magnetic stirrer, condenser, nitrogen inlet and HCl outlet. The HCl that was formed was lead through a NaOH solution (40 g, 1.0 mol in 1 L water). After 1 hour the reaction mixture was partly solidified. After 3 hours the product was washed with 2 L of warm water (70°C). The product was separated with a glass filter and washed twice with warm ethanol (50°C). The product was

subsequently dried in a vacuum oven at 50°C. The yield was 91%. The purity as determined by ¹H-NMR was >99% and the product had a melting temperature of 206°C and a melting enthalpy of 155 J/g.

Synthesis of di-(6-aminohexyl)terephthalamide (DAHT or 6T6-diamine)⁵. A mixture of DMT (39 g, 0.20 mol) and HMDA (139 g, 1.2 mol) was heated to 120°C in a 1 L stirred round bottomed flask with nitrogen inlet and a reflux condenser. At 80°C a clear solution was formed and methanol started boiling off. When a temperature of 120°C was reached, precipitation had started. After 4 hours at 120°C 500 ml toluene was added to the thick suspension and the mixture was allowed to cool to 100°C under stirring. The product was collected by filtration with a glass filter and washed twice with hot toluene (80°C). Finally the product was washed with diethyl ether and dried at room temperature.

The product that contained some 6(T6)_n-diamine (with n≥2) and other impurities, was recrystallised from n-butyl acetate at 110°C (15 g/l).

Synthesis of other xTx-diamine segments. Other xTx-diamine segments were prepared according to the method for the synthesis of 6T6-diamine. The amine:ester ratio and the reaction time and temperature were changed for some reactions. Also the recrystallisation step was modified for some of the xTx-diamine segments (Table 5.1).

Table 5.1: Reaction conditions for the synthesis of different xTx-diamine segments.

	Excess amine [mol]	Temperature [°C]	Time [hours]	Yield [%]	Recrystallisation (n-butyl acetate)
2T2-diamine	5	60	5	83	50 g/l
3T3-diamine	3	80	4	96	50 g/l
4T4-diamine	3	100	4	77	20 g/l
6T6-diamine	5	120	4	94	15 g/l
7T7-diamine	5	100	4	81	10 g/l
8T8-diamine	3	120	4	76	10 g/l

Synthesis of T6T6T-dimethyl. A mixture of 6T6-diamine (7.24 g, 0.02 mol) and MPT (20.5 g 0.08 mol) was dissolved in 400 ml NMP in a 1 L stirred round bottomed flask with nitrogen inlet and a reflux condenser. The mixture was warmed to 120°C and kept at that temperature for 16 hours. After cooling, the precipitated product was collected by filtration using a glass filter and washed with NMP, warm toluene (70°C) and warm acetone (50°C). The product was dried in a vacuum oven at 50°C.

Synthesis of other TxTxT-dimethyl segments. Other TxTxT-dimethyl segments were prepared according to the procedure for the synthesis of T6T6T-dimethyl using 0.02 mol of different xTx-diamines.

Synthesis of T6T6T-diphenyl. A mixture of 6T6-diamine (7.24 g, 0.02 mol) and DPT (38 g, 0.12 mol) was dissolved in 400 ml NMP in a 1 L stirred round bottomed flask with nitrogen inlet and a reflux condenser. The mixture was warmed to 120°C and kept at that temperature for 16 hours. After cooling, the precipitated product was collected by filtration using a glass filter and washed with NMP, warm toluene (70°C) and warm acetone (50°C). The product was dried in a vacuum oven at 50°C.

The product that contained some T(6T6T)_n-diphenyl (with $n \geq 2$) as well, was recrystallised from NMP (120°C, 40 g/l). The product was dried in a vacuum oven at 50°C.

¹H-NMR. ¹H-NMR spectra were recorded on a Bruker spectrometer at 300 MHz. Deuterated trifluoro acetic acid (D-TFA) was used as a solvent.

DSC. DSC spectra were recorded on a Perkin Elmer DSC7 apparatus, equipped with a PE7700 computer and TAS-7 software. Dried samples of 3-7 mg were heated to 340°C at a rate of 20°C/min. The peak temperature of the melting peak of the first heating scan was taken as the melting temperature, the peak area was used to calculate the melting enthalpy.

WAXD. X-ray diffraction data of different TxTxT-dimethyl were collected with a Philips PW3710 based X'Pert-1 diffractometer in Bragg-Brentano geometry, using a Θ compensating divergence slit (12.5 mm length). Powder diffraction data collection was performed at room temperature, using a low-background spinning (1 r/s) specimen holder. CuK $_{\alpha 1}$ radiation of 1.54056 Å was obtained, using a curved graphite monochromator. The data were collected in a range of $2\Theta = 4-60^\circ$.

IR. FTIR data were obtained using a Bio-Rad Model FTS-60 spectrometer with a resolution of 4 cm⁻¹. Samples were prepared by pressing tablets of dry KBr that was milled together with some sample.

Results and Discussion

Introduction

The synthesis and characterisation by NMR and DSC of 6T6-diamine, T6T6T-diphenyl and T6T6T-dimethyl will be described in detail. The results for other xTx-diamine and TxTxT-dimethyl segments will be given more briefly. The purity of the different products was calculated from the ¹H-NMR spectra. The melting endotherms of the different segments as measured by DSC give an indication of the purity as well. A pure product has a high melting temperature, a high heat of fusion (ΔH_m) and a sharp melting peak. The WAXD spectra of different TxTxT-dimethyl segments and the IR spectra of 6T6-diamine and T6T6T-dimethyl will be discussed as well.

6T6-diamine

The melt reaction between dimethyl terephthalate and 1,6-hexamethylenediamine to synthesise 6T6-diamine was fast. Before the reaction temperature of 120°C was reached, precipitation had caused solidification of the reaction mixture. The yield of this reaction was 94%. The product was a white powder. The product that was obtained in this melt reaction had a low purity (70-80%). After recrystallisation from boiling n-butyl acetate the purity was >97%. The yield of the recrystallisation step was 48%.

NMR

In Figure 5.3 the ¹H-NMR spectra of 6T6-diamine before and after recrystallisation are given. The peak assignments are given in Figure 5.4 and in Table 5.2 the integrals and peak assignments for the product after synthesis and the product and residue after recrystallisation are given.

The integrals of the peaks of the product after recrystallisation correspond well with the theoretical number of protons. The NMR spectrum of this product contains no peaks of side products. Therefore it can be concluded that 6T6-diamine with a very high purity is obtained after recrystallisation.

The product directly after synthesis contains some side products. Peak a and c (two doublets) in the spectrum of the product are from a side product. The structure of this side product is not known. Next to this side product, also further reacted 6T6-diamine, for example 6T6T6-diamine and 6T6T6T6-diamine, will be present. The purity of the product directly after synthesis is approximately 70-80%. By recrystallisation of the product after synthesis from boiling n-butyl acetate 6T6-diamine of high purity can be obtained. The side product (peak a and c) and all further reacted 6T6-diamine do not dissolve in boiling n-butyl acetate and can be found in the residue after recrystallisation.

The uniformity of 6T6-diamine after recrystallisation can be calculated when several assumptions are made. In the first place it is assumed that no products with a lower molecular weight than 6T6-diamine are present, as these compounds will be removed from the product mixture during the washing steps. Secondly it is assumed that the only other products present are 6(T6)_n. No products like 6T6T are present, otherwise a peak originating from the methyl ester endgroup on the terephthalic side (4.1 ppm) should be visible in the spectrum and this is not the case. The side product (peak a and c) remains in the residue during recrystallisation. A last assumption that is made, is that after recrystallisation only 6T6T6-diamine will be present next to the product 6T6-diamine, because further reacted 6T6-diamine such as 6T6T6T6-diamine is not likely to dissolve in n-butyl acetate.

Based on these assumptions the uniformity of the recrystallised product can be calculated by Equation 5.1. The ratio between the CH₂ group next to the amide bond (peak e) and the CH₂ group that is coupled to the NH₂ endgroup (peak f) is used to calculate the uniformity. For the product 6T6-diamine this ratio is 1:1, for 6T6T6-diamine the ratio amide-side:amine-side = 2:1.

$$\text{purity 6T6-diamine} = (2 - e/f) * 100\% \quad [\%] \quad \text{Equation 5.1}$$

Based on Equation 5.1 it can be concluded that the product after recrystallisation has a purity of >99%, and thus contains only up to 1% of the further reacted 6T6T6-diamine.

DSC

With DSC the melting endotherms of 6T6-diamine before and after recrystallisation were measured. In Figure 5.5 the first heating scans of 6T6-diamine before and after recrystallisation are compared. In Table 5.3 the peak temperature of the melting peak and the heat of fusion of 6T6-diamine are given.

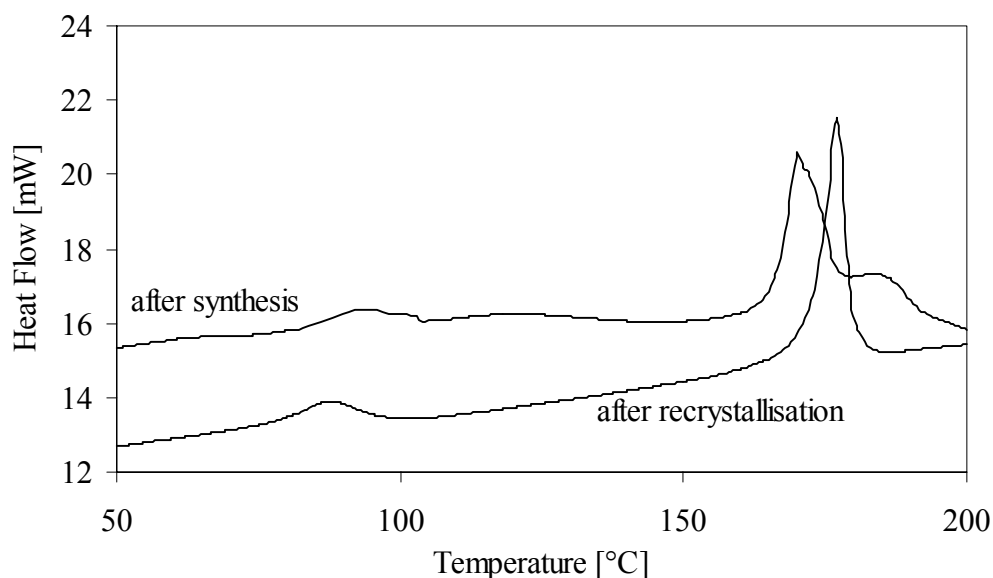


Figure 5.5: First heating scan of 6T6-diamine after synthesis and after recrystallisation.

The DSC heating curve of recrystallised 6T6-diamine shows a sharp melting peak with a peak temperature of 178°C and a melting enthalpy of 130 J/g. The product after synthesis shows a double melting transition. The presence of further reacted products (6(T6)_n with n ≥ 2) and side products next to 6T6-diamine disturb the regular packing of 6T6-diamine and thus lowers the enthalpy and the melting point. Further reacted 6(T6)_n has a higher melting temperature because the lamellar thickness is higher¹⁷.

At 80-100°C there is a broad peak that is possibly due to a transition in the crystalline structure of the 6T6-diamine. This phenomenon is well known polyamides, for example nylon-6,6^{18,19}.

Other xTx-diamine segments

The other xTx-diamine segments could be prepared easily in a fast melt reaction according to the same method as for 6T6-diamine. The yield and purity of the products before and after recrystallisation and the melting temperatures and enthalpies of the recrystallised products are given in Table 5.3.

Table 5.3: Properties of different xTx-diamine, compared to 6T6-diamine.

Amine		After synthesis		After recrystallisation			
(CH ₂) _n	T _m	Yield	Purity	Yield ^a	Purity	T _m	ΔH _m
n =	[°C]	[%]	[%]	[%]	[%]	[°C]	[J/g]
2	10	83	67	6	99	234	400
3	-22	96	78	8	98	209	300
4	27	77	68	11	96	210	150
6	39	94	71	48	99	178	130
7	28	81	79	64	96	168	100
8	53	90	93	43	98	173	130

(a), yield of the recrystallisation step

All xTx-diamine segments can be obtained with a high yield between 77 and 96%. The purity of the products after synthesis is above 67% and seems to increase with increasing length of the diamine.

Recrystallisation of xTx-diamines with n = 6-8 from n-butyl acetate gives the highest yields. Recrystallisation of the other xTx-diamines from n-butyl acetate was possible, but with lower yields. The use of other recrystallisation solvents may further improve the yields of these xTx-diamines.

With DSC it was shown that the xTx-diamine segments after synthesis all show multiple melting transitions. After recrystallisation all xTx-diamines have a high purity and show a sharp melting peak. The melting temperature increases with decreasing length of x for even x. For odd numbers of x the melting temperature is lower because these segments are less ordered. The melting enthalpy of 2T2-diamine and 3T3-diamine is very high. Probably degradation starts upon melting.

T6T6T-diphenyl

T6T6T-diphenyl was synthesised from diphenyl terephthalate (DPT) and 6T6-diamine using NMP as a solvent. During the reaction at 120°C a part of the product precipitated and more product precipitated on cooling. The yield of this reaction was 90%. The product was a white powder. Despite the large excess of DPT used, the product had a low purity or uniformity. DPT can react at both ends and therefore further reacted products, such as T6T6T6T6T-diphenyl, can be formed easily. After recrystallisation from hot NMP the uniformity was excellent. The yield of the recrystallisation step was 53%.

NMR

In Figure 5.6 the ¹H-NMR spectrum of T6T6T-diphenyl after recrystallisation is given. The peak assignments are given in Figure 5.7 and in Table 5.4 the integrals and peak assignments for the product after synthesis and for the product and residue after recrystallisation are given.

The purity or uniformity of T6T6T-diphenyl can be calculated by comparing the integrals of the peaks of the aromatic protons of the ester-amide and amide-amide terephthalic groups. In this calculation it is assumed that there are no products with a lower molecular weight as these products are expected to be soluble in NMP. This assumption can be made because T6T6T-diphenyl itself is soluble in NMP when it is heated to at least 60°C. Products with a lower molecular weight are therefore probably soluble in NMP at room temperature. Another assumption is that all products are endcapped by a terephthalic group. This assumption was made because in the spectrum of T6T6T-diphenyl no peaks of the amine endgroup (6.8 ppm) and the CH₂ group next to the amine endgroup (3.3 ppm) of 6T6-diamine can be found.

In pure T6T6T-diphenyl the ratio between the integral of peak a and peak b and c together is 1:2. For the hexa-amide T6T6T6T this ratio is 1:3 and for the octa-amide T6T6T6T6T 1:4. When the reaction is performed using 6T6-diamine of high purity it is expected that the product will only consist of tetra-amide and a little octa-amide.

$$\text{purity T6T6T-diphenyl} = (4 - (b+c)/a)/2 * 100\% \quad [\%] \quad \text{Equation 5.2}$$

The purity of the T6T6T-diphenyl after recrystallisation as calculated by Equation 5.2 is 99%. So the product consists for 99% of T6T6T-diphenyl and only 1% of the octa-amide.

DSC

With DSC the melting endotherms of T6T6T-diphenyl of different purities were measured. In Figure 5.8 the melting endotherms for T6T6T-diphenyl before and after recrystallisation (product and residue) are compared. In Table 5.5 the peak temperature of the melting peak and the heat of melting are given for T6T6T-diphenyl of different purities.

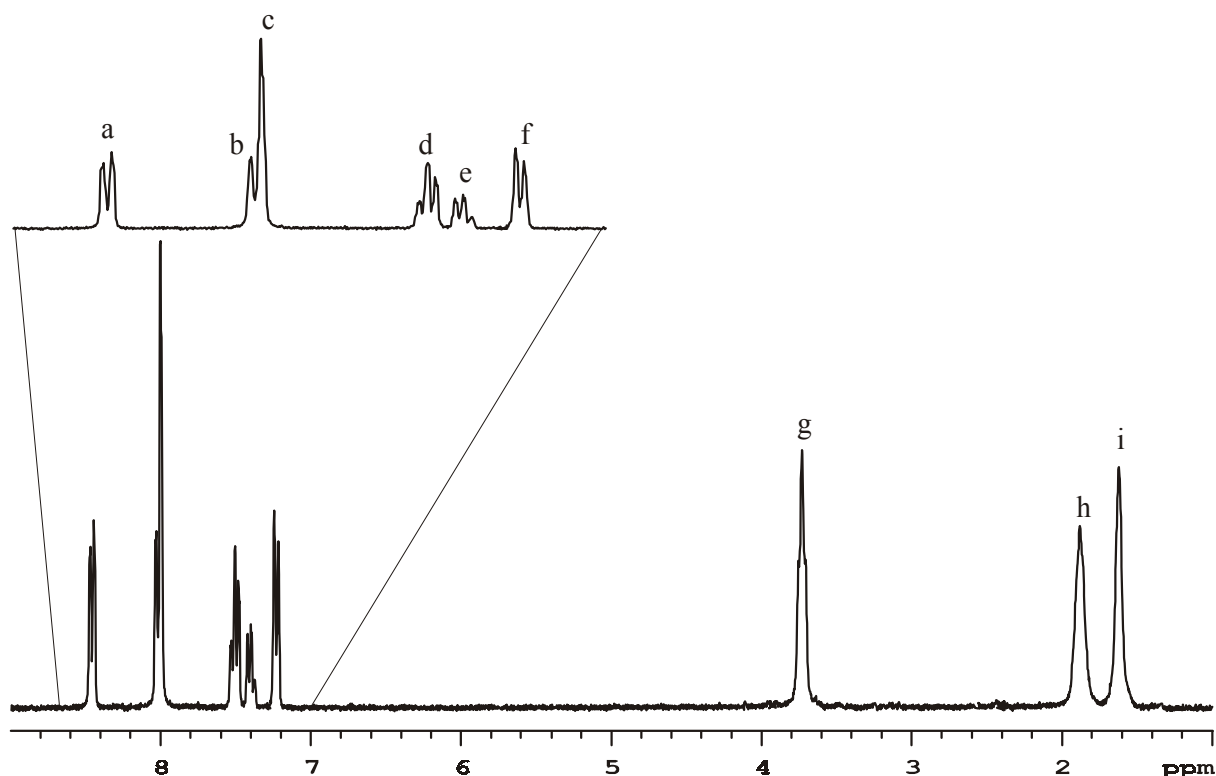
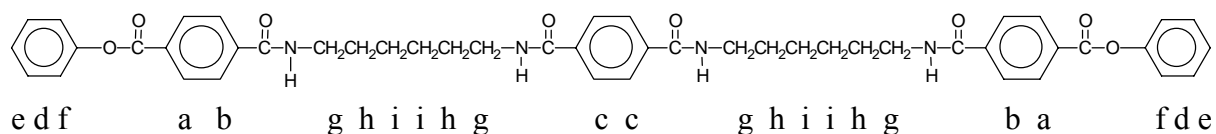

 Figure 5.6: ^1H -NMR spectrum of T6T6T-diphenyl.


Figure 5.7: Peak assignment of protons of T6T6T-diphenyl.

 Table 5.4: Chemical shifts δ and assignment of protons of T6T6T-diphenyl.

Peak	δ [ppm]	Type	Theor. # protons	Integral after synthesis	Integral after recryst. (product)	Integral after recryst. (residu)	Description ^b
a	8.46	doublet	4	4.00	4.00	4.00	terephthalic H , EA, ester side
b	8.01	doublet	4	4.00 ^a	4.00 ^a	4.00 ^a	terephthalic H , EA, amide side
c	7.99	singlet	4	5.18 ^a	4.02 ^a	8.15 ^a	terephthalic H , AA
d	7.50	multiplet	4	4.03	4.04	4.04	phenyl ester endgroup H 3 and 5
e	7.40	triplet	2	2.01	2.01	2.02	phenyl ester endgroup H 4
f	7.23	doublet	4	4.08	4.02	4.06	phenyl ester endgroup H 2 and 6
g	3.73	triplet	8	9.15	8.10	12.23	1 st and 6 th CH_2 HMDA
h	1.88	singlet	8	9.20	8.28	12.36	2 nd and 5 th CH_2 HMDA
i	1.61	singlet	8	9.17	8.26	12.40	3 rd and 4 th CH_2 HMDA

(a), with the sum of the integrals of peak b and c, peak c was calculated by assuming peak a = peak b; (b), EA = ester-amide substituted terephthalic group, AA = amide-amide substituted terephthalic group, HMDA = hexamethylenediamine

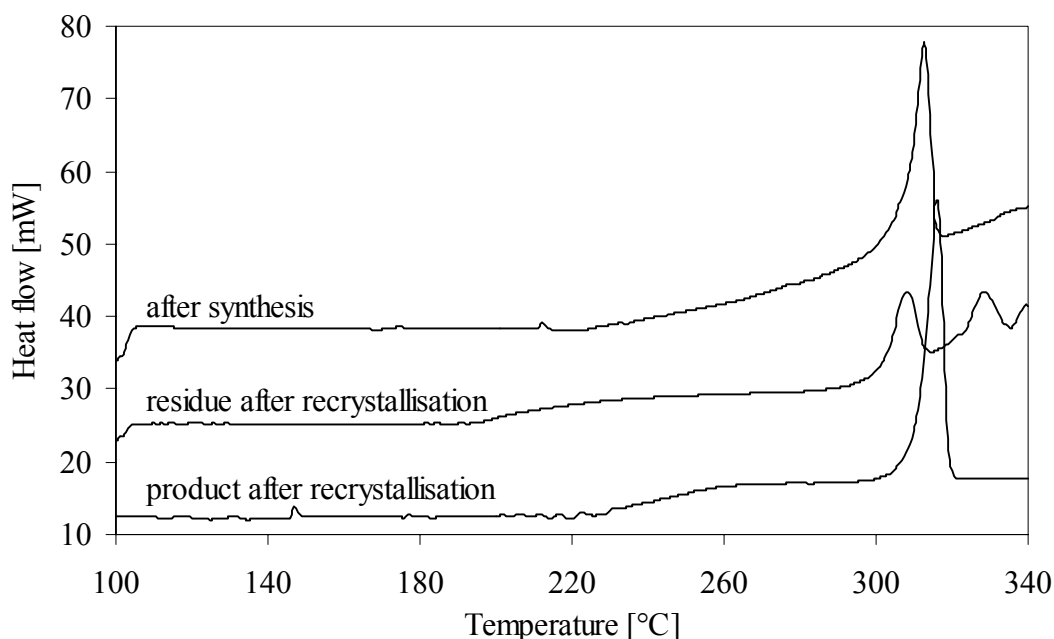


Figure 5.8: First heating scan of T6T6T-diphenyl before and after recrystallisation (product and residue).

Table 5.5: Properties of T6T6T-diphenyl before and after recrystallisation synthesised from 6T6-diamine of high and low purity.

Purity 6T6-diamine [%]	Product	Yield [%]	Purity [%]	T_m (peak) [°C]	ΔH_m [J/g]
98	after synthesis	90	89	312	123
	after recrystallisation	53	99	316	129
71	after synthesis	83	70	308	105
	after recrystallisation	28	97	316	128

The yield of the reaction decreases when 6T6-diamine of a lower purity is used to synthesise T6T6T-diphenyl. As a result of the lower purity of the 6T6-diamine used, the purity of the T6T6T-diphenyl after synthesis also decreases. The purity of both products could be improved to >97% by recrystallisation from NMP. The melting temperature of T6T6T-diphenyl is 316°C and the melting enthalpy is 129 J/g. The melting temperature and the heat of melting decrease with decreasing purity of the product. The presence of longer products than T6T6T-diphenyl disturb the regular packing of T6T6T-diphenyl and thus lower the enthalpy and the melting point. The residue after recrystallisation shows a melting transition with two peaks.

T6T6T-dimethyl

The reaction between methyl phenyl terephthalate (MPT) and 6T6-diamine was done in NMP solution according to the procedure for T6T6T-diphenyl. The excess of MPT that was used was smaller than that of DPT for the synthesis of T6T6T-diphenyl. The phenyl ester side of MPT will react better with the amine endgroup of 6T6-diamine than the methyl ester side. Therefore it is less likely that in this reaction a lot of further reacted products will be created. When the reaction was carried out using 6T6-diamine of high purity (recrystallised) no further recrystallisation step was required. The yield of the reaction was 85%. The product was a white powder.

NMR

The molecular structure of the product T6T6T-dimethyl was verified by $^1\text{H-NMR}$ in D-TFA. The $^1\text{H-NMR}$ spectrum is given in Figure 5.9. The peak assignments are given in Figure 5.10 and in Table 5.6 the integrals and peak assignments for the product after synthesis are given.

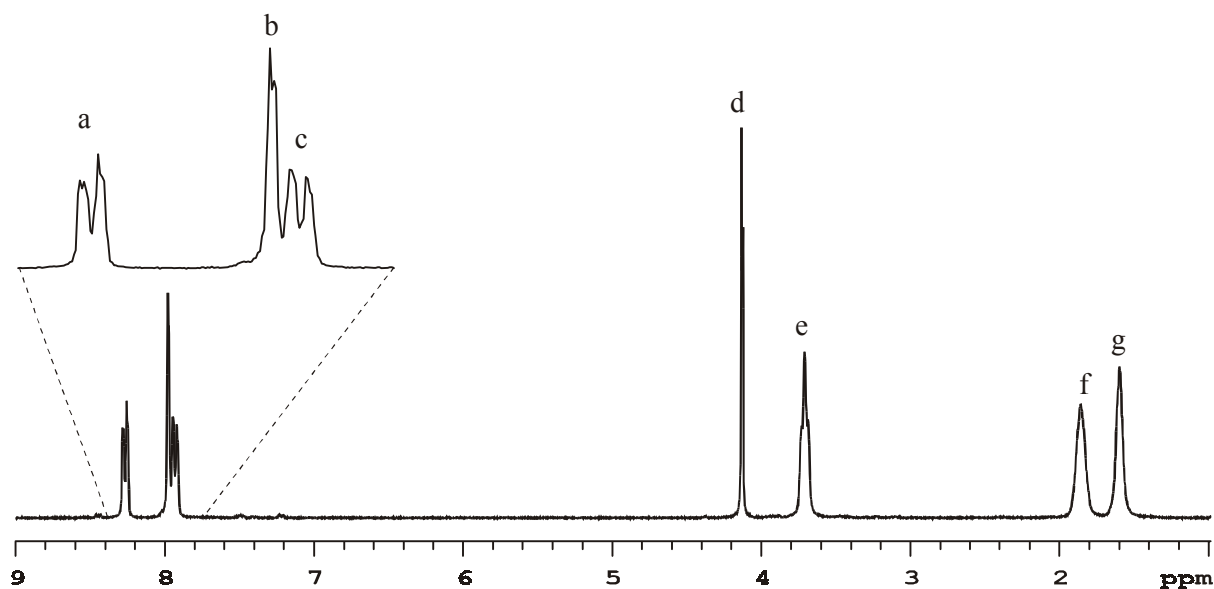


Figure 5.9: $^1\text{H-NMR}$ spectrum of T6T6T-dimethyl.

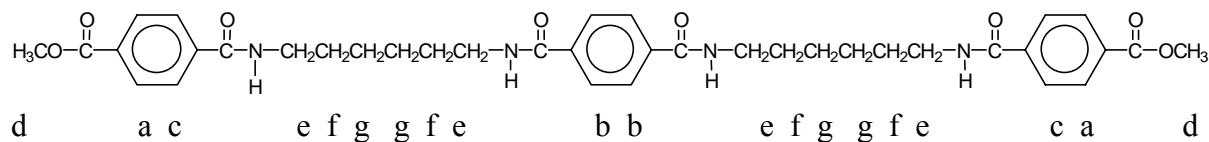


Figure 5.10: Peak assignment of protons of T6T6T-dimethyl.

Table 5.6: Chemical shifts δ and assignment of protons of T6T6T-dimethyl.

Peak	δ [ppm]	Type	Theor. # protons	Integral	Description ^c
a	8.27	doublet	4	4.00	terephthalic H , methyl ester-amide, ester side
a'	8.46	doublet	4 ⁺	0.12	terephthalic H , phenyl ester-amide, ester side
b	7.98	singlet	4	4.16 ^b	terephthalic H , amide-amide
c	7.94	doublet	4	4.00 ^b	terephthalic H , methyl ester-amide, amide side
c'	8.01	doublet	4 ^a	0.12 ^b	terephthalic H , phenyl ester-amide, amide side
q	7.50	multiplet	4 ^a	0.12	phenyl ester endgroup H 3 and 5
q	7.40	triplet	2 ^a	0.06	phenyl ester endgroup H 4
q	7.23	doublet	4 ^a	0.12	phenyl ester endgroup H 2 and 6
d	4.14	singlet	6	5.96	methyl ester endgroup CH ₃
e	3.72	triplet	8	8.36	1 st and 6 th CH ₂ HMDA
f	1.87	singlet	8	8.52	2 nd and 5 th CH ₂ HMDA
g	1.60	singlet	8	8.50	3 rd and 4 th CH ₂ HMDA

(a), protons of phenyl ester endgroups of T6T6T-diphenyl; (b), the sum of the integrals of peak b, c and c' was 8.28, the integral of peak b was calculated by assuming peak c = peak a and peak c' = peak a'; (c), HMDA = hexamethylenediamine

The aromatic region of Figure 5.9 shows a few very small peaks next to peak a-c. In Figure 5.11 the aromatic region of Figure 5.9 is enlarged to compare the positions of these small peaks with that of T6T6T-diphenyl. It is clear that there is an exact overlap. So the product that is obtained after reaction of 6T6-diamine with MPT contains a little T6T6T-diphenyl next to T6T6T-dimethyl. This is a result of the fact that MPT is able to react at the methyl ester side as well, although at a very low rate compared to the phenyl ester side.

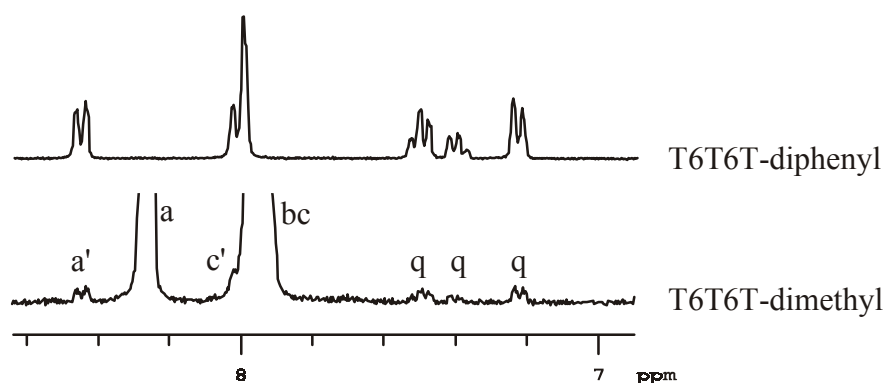


Figure 5.11: Comparison of the aromatic region of T6T6T-dimethyl and T6T6T-diphenyl.

The purity or uniformity of T6T6T-dimethyl can be calculated in the same way as for T6T6T-diphenyl by comparing the integrals of the peaks of the aromatic protons of the ester-amide and amide-amide terephthalic groups. The same assumptions as for T6T6T-diphenyl are applicable for T6T6T-dimethyl.

The amount of T6T6T-diphenyl present can be calculated from the ratio between the terephthalic phenyl ester-amide peak and the terephthalic methyl ester-amide peak according to Equation 5.3.

$$\text{percentage T6T6T-diphenyl} = (a'/(a+a')) * 100\% \quad [\%] \quad \text{Equation 5.3}$$

With Equation 5.3 it was calculated that the product T6T6T-dimethyl contains 3% of T6T6T-diphenyl.

In pure T6T6T-dimethyl the ratio between the integral of peak a and peak b and c together is 1:2. For the hexa-amide T6T6T6T this ratio is 1:3 and for the octa-amide T6T6T6T6T 1:4. When the reaction is performed using 6T6-diamine of high purity it is expected that the product will consist of tetra-amide and a little octa-amide. The presence of T6T6T-diphenyl next to T6T6T-dimethyl is not harmful to the purity of the product, because this side product will give the same structure in a polymer after a polycondensation reaction. So the peaks resulting from the terephthalic phenyl ester-amide, can be added to that of the terephthalic methyl ester-amide and the purity of T6T6T-dimethyl can be calculated with Equation 5.4.

$$\text{purity T6T6T-dimethyl} = (4 - (b+c+c')/(a+a'))/2 * 100\% \quad [\%] \quad \text{Equation 5.4}$$

The purity of the T6T6T-dimethyl after synthesis as calculated by Equation 5.4 is 99%. So the product consists for 99% of T6T6T-dimethyl (including 3% T6T6T-diphenyl) and only 1% of the octa-amide.

DSC

The melting endotherms of T6T6T-dimethyl of different purities were measured with DSC. In Figure 5.12 the melting endotherms for T6T6T-dimethyl of high and low purity are compared. In Table 5.7 the peak temperature of the melting peak and the heat of fusion are given for T6T6T-dimethyl segments of different purities.

The yield of the reaction decreases when 6T6-diamine of a lower purity is used to synthesise T6T6T-dimethyl. The purity of the T6T6T-dimethyl decreases with decreasing purity of the 6T6-diamine used. The melting temperature and the heat of melting decrease with decreasing purity of the product.

Pure T6T6T-dimethyl has a melting temperature of 303°C and a melting enthalpy of 152 J/g. The melting temperature of T6T6T-dimethyl is in between that of T6T-dimethyl (232-235°C)^{7,8}, and that of nylon-6,T (371°C)²⁰. The melting temperature of T6T6T-dimethyl is 13°C lower than that of T6T6T-diphenyl, due to decreased stiffness of the endgroups. If desired, the melting temperature of the T6T6T segment can be further decreased by using more flexible endgroups, such as ethyl or butyl. For example, the melting temperature of T6T-dimethyl is 232°C and that of T6T-dibutyl is 187°C⁷.

Table 5.7: Properties of T6T6T-dimethyl synthesised from 6T6-diamine of different purities.

Purity 6T6-diamine	Yield	Purity	T_m	ΔH_m
[%]	[%]	[%]	[°C]	[J/g]
98	85	99	303	152
85	79	88	298	144
77	70	83	295	142
71	64	76	291	138

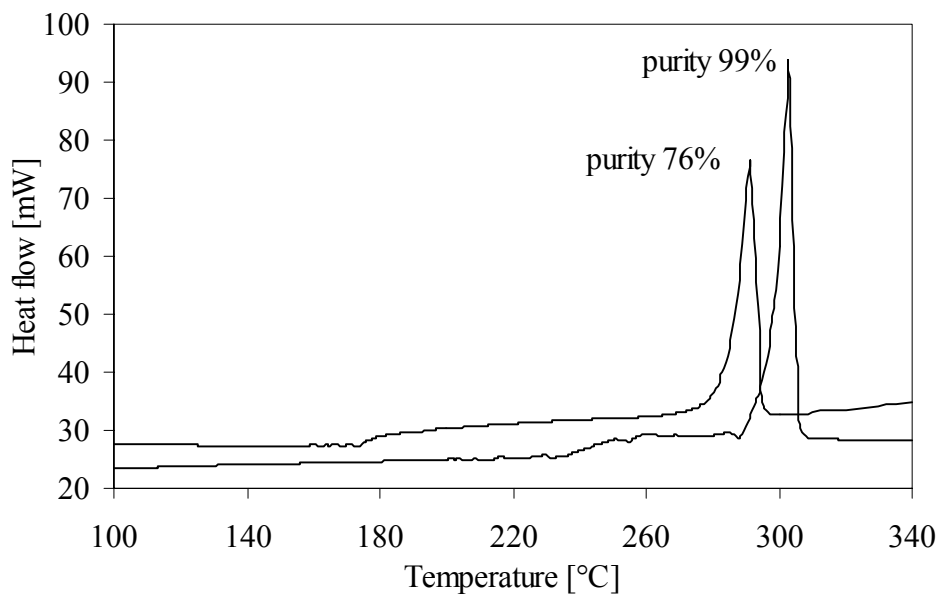


Figure 5.12: First heating scan of T6T6T-dimethyl of low and high purity.

Other TxTxT-dimethyl segments

The other TxTxT-dimethyl segments were prepared according to the method for T6T6T-dimethyl. The yield and purity of the products and the melting temperatures and enthalpies are given in Table 5.8.

Table 5.8: Properties of different TxTxT-dimethyl segments.

TxTxT- dimethyl	Yield	Purity	T_m	ΔH_m
	[%]	[%]	[°C]	[J/g]
T2T2T	74	97	>340 ^a	-
T3T3T	43	97	307	128
T4T4T	71	97	>340 ^a	-
T6T6T	85	99	303	152
T7T7T	69	96	262	99
T8T8T	73	93	268	163

(a), 340°C is the maximum temperature for the DSC apparatus used

All TxTxT-dimethyl could be prepared from recrystallised xTx-diamine with high yield and purity. No recrystallisation step was required as for T6T6T-diphenyl.

The melting temperature of TxTxT-dimethyl decreases with increasing amine length for even n. The melting temperature of T2T2T-dimethyl and T4T4T-dimethyl could not be determined because these were above 340°C. The melting temperature and heat of crystallisation of TxTxT with odd n ($x=(\text{CH}_2)_n$) is lower because these segments are less ordered.

WAXD

With wide angle X-ray diffraction the diffraction patterns of the different purified TxTxT-dimethyl segments were measured. The results are given in Figure 5.13.

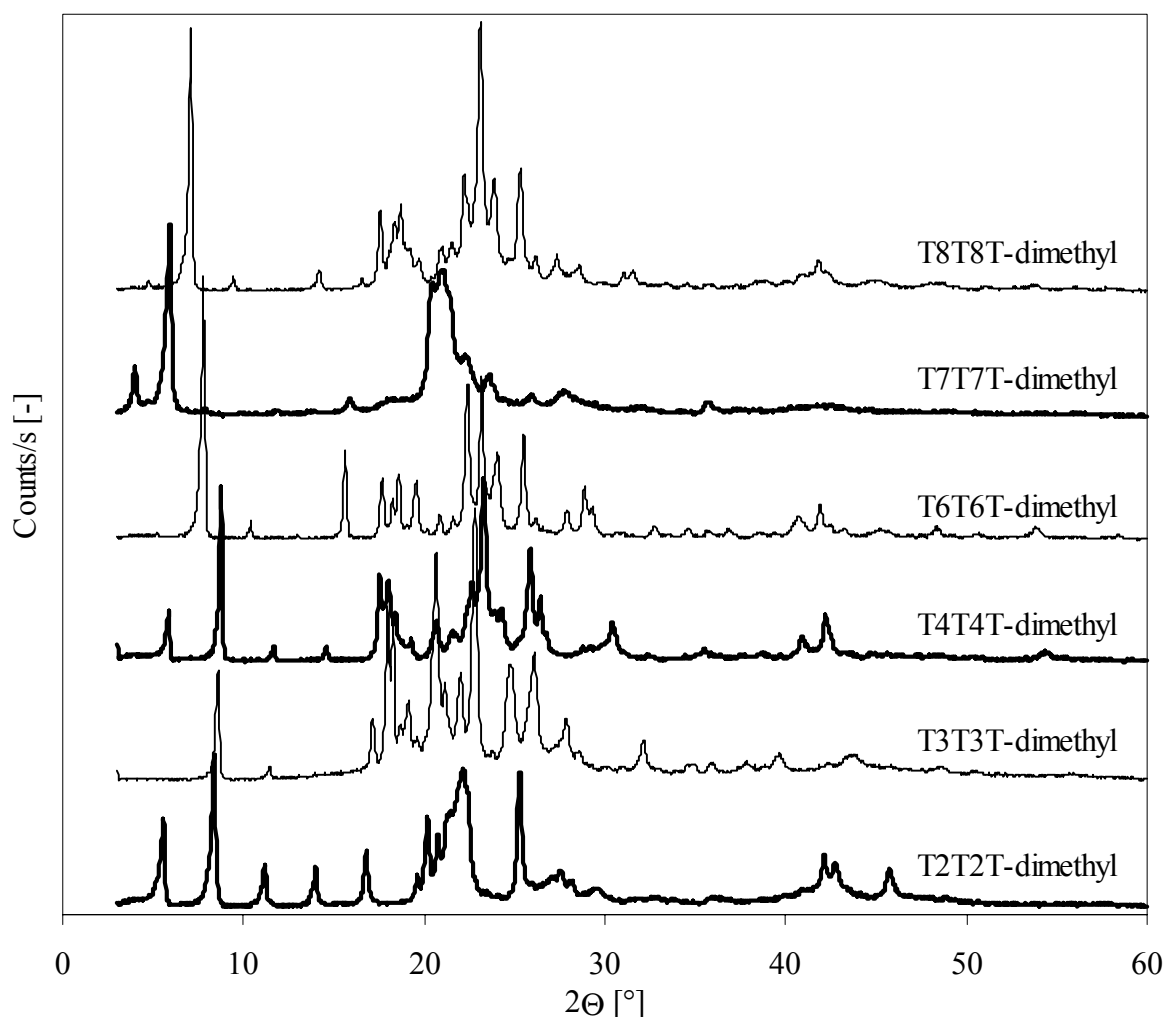


Figure 5.13: WAXD spectrum of different TxTxT-dimethyl segments of high purity.

The WAXD diagrams in Figure 5.13 are typical for crystalline substances of low molecular weight and comparable to di-amide segments such as T4T-dimethyl¹⁶. The different TxTxT-dimethyl segments show a broad spectrum of peaks, indicating the presence of different crystalline structures. It can be noted that the large peak at $2\Theta = 6-8^\circ$ shifts to lower values with increasing length of the diamine in the tetra-amide, indicating an increasing lamellar

thickness in the chain direction. T7T7T-dimethyl deviates from this trend and has this peak at a lower value indicating higher lamellar thickness. This is a result of the odd number of CH₂ groups between the terephthalic groups, which decreases the crystalline order. The other main peaks at $2\Theta = 15\text{-}30^\circ$ do not show such a shift. These peaks may be attributed to the lateral crystal sizes. These sizes are expected to be comparable for different TxTxT-dimethyl segments. In each sample, crystallites of different sizes are present. Only T2T2T-dimethyl and T7T7T-dimethyl show one broad peak instead of a spectrum of many sharp peaks.

IR

With IR spectroscopy the formation of amide and ester groups can be observed. In Figure 5.14 the IR spectrum of 6T6-diamine and T6T6T-dimethyl are compared.

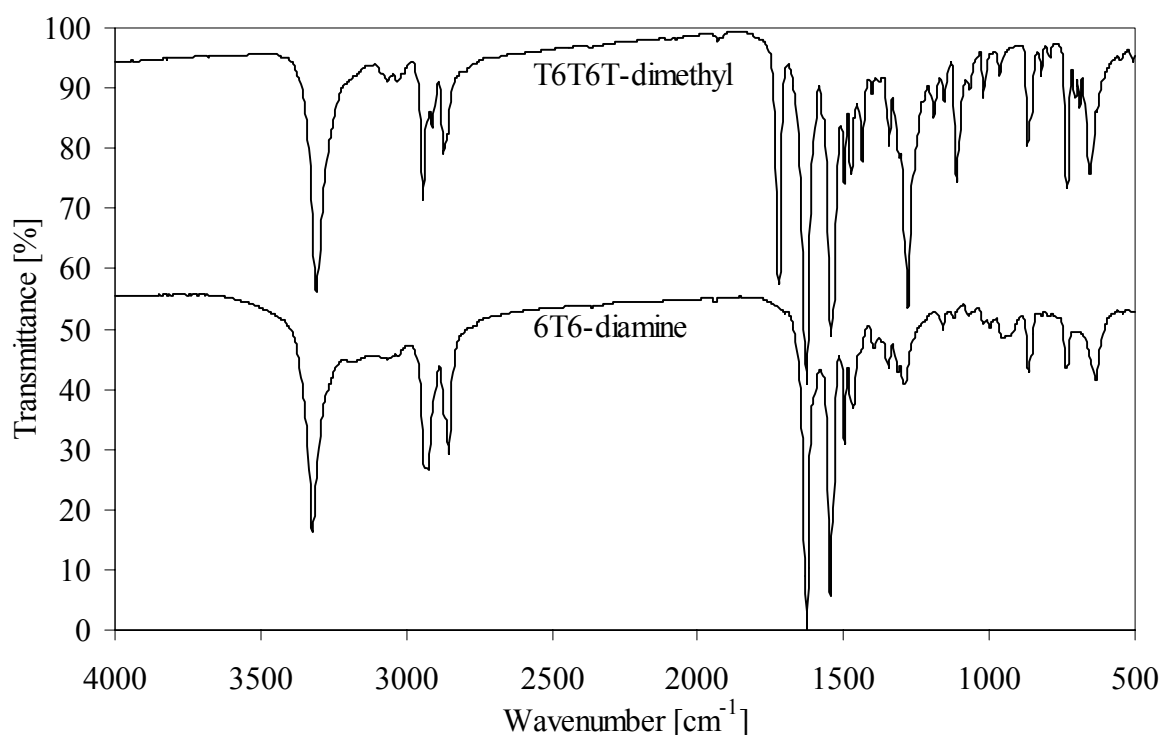


Figure 5.14: IR spectrum of 6T6-diamine and T6T6T-dimethyl; the spectrum of 6T6-diamine is shifted by 40% on the y-axis.

Both 6T6-diamine and T6T6T-dimethyl show the amide carbonyl band at 1628 cm^{-1} . T6T6T-dimethyl shows an ester carbonyl band at 1721 cm^{-1} next to this amide carbonyl band. T6T6T-dimethyl also shows a peak of the CH₃ methyl ester endgroup at 1112 cm^{-1} . The fact that 6T6-diamine does not show a peak at 1721 cm^{-1} and 1112 cm^{-1} confirms the assumption that 6T6-diamine does not contain any DMT that has reacted at only one side, such as 6T or 6T6T.

Conclusions

Bisester tetra-amide TxTxT-dimethyl segments with $x = (\text{CH}_2)_n$ and $n = 2-8$ can be synthesised in a two-step reaction. The first step is the synthesis of xTx-diamine in the melt, followed by recrystallisation to improve the purity. TxTxT-dimethyl can then be prepared in a reaction of xTx-diamine with methyl phenyl terephthalate in solution. The structure of the products could be confirmed by NMR. The purity of the tetra-amide product depends on the purity of the xTx-diamine used. The product xTx-diamine does not contain any side products such as xT or xTxT.

The melting temperature and enthalpy of xTx-diamine and TxTxT-dimethyl and -diphenyl were determined by DSC. The melting temperature increases with decreasing length of x. For odd x the melting temperature is lower. The melting temperature and enthalpy of the products decrease with decreasing purity.

Literature

1. L.L. Harrell, *Macromolecules*, 2, 607 (1969).
2. H.N. Ng, A.E. Allegrazza, R.W. Seymour, S.L. Cooper, *Polymer*, 14, 255 (1973).
3. C.D. Eisenbach, M. Baumgartner, G. Gunter, in 'Advances in Elastomer and Rubber Elasticity, proc. Symposium', J. Lal and J. E. Mark Eds., Plenum Press, New York, 51 (1985).
4. J.A. Miller, B.L. Shaow, K.K.S. Hwang, K.S. Wu, P.E. Gibson, S.L. Cooper, *Macromolecules*, 18, 32 (1985).
5. R.J. Gaymans, S. Aalto, F.H.J. Maurer, *J. Polym. Sci.: Part A: Pol. Chem.*, 27, 423 (1989).
6. J.L.R. Williams, T.M. Laakso, K.R. Dunham, D.G. Borden, J. VandenBerghe, J.A. VanAllan, D.D. Reynolds, *Chem. Soc.*, 55, 4161 (1933).
7. US 1,365,952, Cicero et al. (1970).
8. US 4,614,815, Cognigni et al. (1986).
9. J. Brisson, F. Brisse, *Macromolecules*, 19, 2632 (1986).
10. M.C.E.J. Niesten, J. Feijen, R.J. Gaymans, *Polymer*, 41, 8487 (2000).
11. P.J.M. Serrano, A.C.M. van Bennekom, R.J. Gaymans, *Polymer*, 39, 5773 (1998).
12. K. Bouma, J.H.G.M. Lohmeijer, R.J. Gaymans, *Polymer*, 41, 2719 (2000).
13. E. Sorta, G. della Fortuna, *Polymer*, 21, 728 (1980).
14. M.C.E.J. Niesten, H. Bosch, R.J. Gaymans, *J. Appl. Polym. Sci.*, 81, 1605 (2001).
15. G. Perego, M. Cesart, G. della Fortuna, *J. Appl. Polym. Sci.*, 29, 1141 (1984).
16. L. Guang, R.J. Gaymans, *Polymer*, 38, 4891 (1997).
17. J.D. Hoffman, J.J. Weeks, *J. Res. Nat. Bur. Stand., Sect. A*, 66, 13 (1962).
18. M. Todoki, T. Kawaguchi, *J. Polym. Sci. Phys. Ed.*, 15, 1067 (1977).
19. J. Hirschinger, H. Miura, K.H. Gardner, A.D. English, *Macromolecules*, 23, 2153 (1990).
20. P.W. Morgan, S.L. Kwolek, *Macromolecules*, 8, 104 (1975).
21. P.F. van Hutten, R.M. Mangnus, R.J. Gaymans, *Polymer*, 34, 4193 (1993).

Chapter 6

Synthesis and properties of copolymers of PPE, dodecanediol and uniform tetra-amide units

Abstract

Copolymers of telechelic poly(2,6-dimethyl-1,4-phenylene ether) segments with terephthalic methyl ester endgroups (PPE-2T, 3500 g/mol, bimodal MWD), uniform crystallisable T6T6T units (two-and-a-half repeating unit of nylon-6,T, 13 wt%) and dodecanediol as an extender were made via a polycondensation reaction. The maximum reaction temperature was 280°C. The PPE-2T/C12/T6T6T copolymers are semi-crystalline materials with a T_g around 170°C, a melting temperature of 264-270°C and a very high T_g/T_m ratio above 0.8. The modulus is high up to the T_g and the modulus in the rubbery plateau after injection moulding is 7-12 MPa. It is particular that the T6T6T units can actually crystallise in these copolymers despite the very high T_g/T_m ratio. The materials are slightly transparent and have good solvent resistance, low water absorption and good processability. From DSC and DMA results it was calculated that the crystallinity of T6T6T in the copolymers is between 60 and 75%. The part of the T6T6T units that does not crystallise mixes with the amorphous PPE matrix or forms sort of “frozen-in” ordered T6T6T nano-phases. These T6T6T nano-phases have a thermal transition around 100°C. The crystallinity of T6T6T in a test bar can be improved by a heat treatment step. The crystallinity decreases with increasing molecular weight and is very sensitive to processing conditions. The undercooling ($T_m - T_c$) as measured by DSC is 18°C at a cooling rate of 20°C/min. The undercooling increases with increasing cooling rate. With WAXD it was shown that the copolymer contains ordered T6T6T above its melting temperature (at 300°C). These results indicate that the tetra-amide units remain organised in the melt.

Introduction

Poly(2,6-dimethyl-1,4-phenylene ether) (PPE)¹⁻³ or PPO is a linear amorphous polymer with a glass temperature of approximately 215°C⁴. PPE has excellent properties such as high toughness, high dimensional stability, good flame retardation and low moisture uptake. However, PPE is amorphous and has a low solvent resistance. And due to its high glass transition temperature (T_g), very high processing temperatures are required, which can lead to degradation. To improve its processability PPE is usually blended with polystyrene. PPE is fully miscible with polystyrene¹⁻³. To obtain solvent resistance, some crystallinity is necessary.

The solvent resistance of PPE can be increased by blending with a semi-crystalline polymer, for example polyamide-6,6 (Noryl-GTX[®]). This blend contains around 40% polyamide that crystallises partially and has good solvent resistance and improved processability. Noryl-GTX[®] has a phase separated morphology. A compatibiliser is added to obtain a fine phase structure that gives better tensile and impact properties. The amorphous PPE phase has a T_g at 200°C. The semi-crystalline polyamide phase shows a T_g at 70°C and a melting temperature (T_m) at 265°C. As a result the modulus of the blend is only high up to ~50°C instead of 200°C. Thus a disadvantage of Noryl-GTX[®] is that the dimensional stability is high only up to the lower T_g of the amorphous part of the semi-crystalline polyamide.

A system with dimensional stability up to high temperatures can possibly be obtained when PPE is blended with a miscible semi-crystalline polymer. The T_g of the mixed amorphous phase will then be in between the T_g 's of the two polymers that form the mixed phase. Such a blend will have one T_g and one T_m and have dimensional stability up to the T_g of the mixed amorphous phase. An example of such a blend is PPE and syndiotactic polystyrene (sPS)⁵. Pure sPS is semi-crystalline, has a T_g of 100°C, a T_m of 270°C and can obtain a maximum degree of crystallinity of 60%. By blending sPS and PPE the T_g of the amorphous phase (sPS/PPE) increases with increasing PPE content. However, at the same time the crystallinity decreases with increasing PPE content and crystallisation during melt processing is difficult at high PPE levels. So for most applications this blend does not result in a polymer system with a high T_g and a good solvent resistance. Few other polymer combinations are known that are fully miscible and in which one of the polymers is semi-crystalline.

In a blend of PPE with polyamide-6,6 a high polyamide content (~40%) is needed in order to obtain enough crystallinity and a co-continuous morphology for a good solvent resistance. And due to the phase separation and crystallisation into spherulites this blend is not transparent.

Copolymerisation might be a good method to improve the solvent resistance of PPE. Some blockcopolymers of PPE and polyamide-6 are known⁶⁻⁹. The problem with these PPE/PA-6 copolymers is that the melting temperature is close to the T_g with as a result that the crystallisation of the PA-6 is slow and incomplete. These copolymers have a phase separated morphology, show hardly crystallinity and can be used as compatibiliser in PPE/PA blends.

It would be very interesting to copolymerise PPE with a crystallisable segment with which it is miscible to a copolymer with one high T_g , a high melting temperature, fast crystallisation upon cooling from the melt and a high T_g/T_m ratio. It is expected that this combination of

properties can be obtained in a segmented copolymer consisting of bifunctional PPE segments and short, fast crystallising, uniform crystallisable segments. Thus far only such segmented copolymers based on amorphous segments with a low T_g are known. Especially segmented copolymers consisting of poly(tetramethylene oxide) and uniform di-amide units were found to crystallise very fast and complete upon cooling from the melt^{10,11}. These materials have a good solvent resistance and are transparent. It will be interesting to study the synthesis, phase structure and crystallisability of such uniform crystallisable units in segmented copolymers with PPE as an amorphous segment that have a high T_g/T_m ratio.

Crystallisation

The rate of crystallisation of a semi-crystalline polymer system is known to decrease dramatically upon increasing T_g/T_m ratio^{12,13}. The rate of crystallisation is influenced by the temperature of crystallisation. At the melting and the glass transition temperature the rate of growth of crystals is nearly zero. Between T_g and T_m the rate of crystallisation has a maximum. The maximum growth rate will be obtained about halfway between T_g and T_m (Figure 6.1)¹². Basically the rate of crystallisation is determined by the rate of diffusion and nucleation. The diffusion of the polymer chains is more difficult when the temperature is more close to the T_g where the melt viscosity is high, and therefore the rate of crystallisation is reduced. Close to the melting temperature however, the rate of crystallisation is reduced as well because nucleation is less likely to occur and the driving force for crystallisation is smaller.

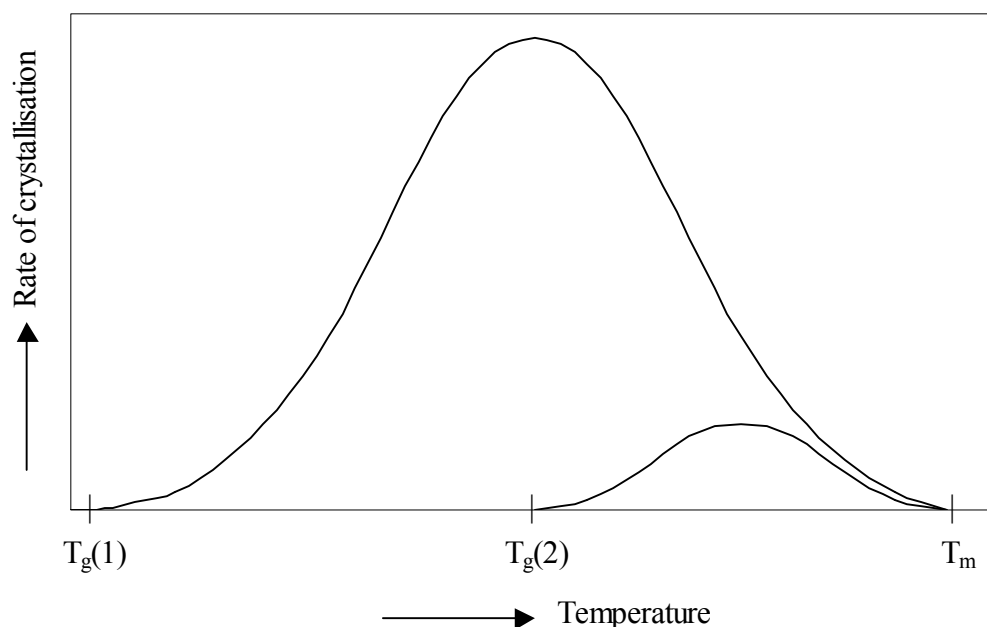


Figure 6.1: Schematic rate of crystallisation as a function of temperature for two copolymers with low $T_g(1)$ and high $T_g(2)$ having the same melting temperature.

With increasing T_g/T_m ratio, the temperature gap between T_g and T_m decreases. As a result the maximum rate of crystallisation is more close to the T_g and T_m and therefore the maximum rate of crystallisation decreases with increasing T_g/T_m (Figure 6.1). The maximum attainable degree of crystallisation depends to a great extent on the maximum rate of crystallisation and is therefore also determined by T_g/T_m . The maximum extent of crystallisation for a semi-crystalline polymer decreases with T_g/T_m ratio^{12,13}. The average polymers that have a T_g/T_m ratio of 0.6-0.7 can obtain a crystallinity between 40 and 60%. Semi-crystalline polymers with a T_g/T_m ratio above 0.8 crystallise very slowly and hence will be amorphous under non-ideal crystallisation conditions.

Niessen et al^{10,14} found that crystallisable amide segments of uniform length in segmented copolymers with aliphatic polyethers having a T_g/T_m ratio around 0.5 crystallise almost completely. Apparently, such segmented copolymers with uniform di-amide segments are able to crystallise faster and to a higher extent than expected based on their T_g/T_m ratio and the theory of Van Krevelen for “normal” polymers¹². It was found that the di-amide units already organise in the melt¹⁵⁻¹⁷ and thus the rate of diffusion is not limiting the rate of crystallisation. As a result fast crystallisation is possible upon cooling. Based on these results it is expected that the uniform crystallisable segments also crystallise fast in systems based on PPE that have a relatively high T_g/T_m ratio.

Segmented copolymers

PPE segments

No semi-crystalline segmented or multi-block copolymers based on PPE are known because short bifunctional PPE segments are not available. In literature different methods to prepare bifunctional PPE segments (PPE-2OH) are described. These methods include coupling of two monofunctional low molecular weight chains^{18,19}, copolymerisation with a bisphenol (from monomers)¹⁹⁻²⁴ and redistribution of high molecular weight PPE with a bisphenol²⁵⁻²⁷.

Redistribution or depolymerisation of high molecular weight, commercial PPE (PPO-803[®], $M_n \sim 11000$ g/mol) with tetramethyl bisphenolA (TMBPA), using tetramethyl diphenoquinone (TMDPQ) as a catalyst is a simple and fast method to make bifunctional PPE segments²⁷. PPO-803[®] contains around 75 $\mu\text{mol OH/gram}$ ²⁷ and only ~80% of the chains in this starting material have a phenolic endgroup and can be redistributed. Examples of a non-reactive endgroups are the Mannich base type endgroups and the 2,6-dimethylphenoxy ‘tail’ endgroups^{28,29}. Therefore PPE-2OH has a bimodal molecular weight distribution. The product is a mixture of a high molecular weight fraction (20-30%) and a low molecular weight depolymerised fraction (70-80%). The high molecular weight fraction is PPO-803[®] (~11.000 g/mol) that has not reacted due to absence of the right functional groups to initiate the redistribution reaction. The redistribution reaction leads to bimodal PPE segments with a number average molecular weight of 1500-4000 g/mol, depending on the amount of TMBPA used²⁷. The average phenolic functionality of these PPE segments is around 1.6-1.9²⁷. PPE-2OH segments with a functionality of nearly 2 can only be prepared starting from well-defined PPE-OH²⁶.

As the phenolic endgroup has low reactivity, endgroup modification is preferable. In this study the phenolic endgroups of the bifunctional PPE-2OH were modified by a fast and complete reaction with the functional acid chloride MCCB (methyl chlorocarbonyl benzoate), into terephthalic methyl ester groups^{27,30,31}. This PPE segment with two methyl ester functionalities is called PPE-2T (Figure 6.2).

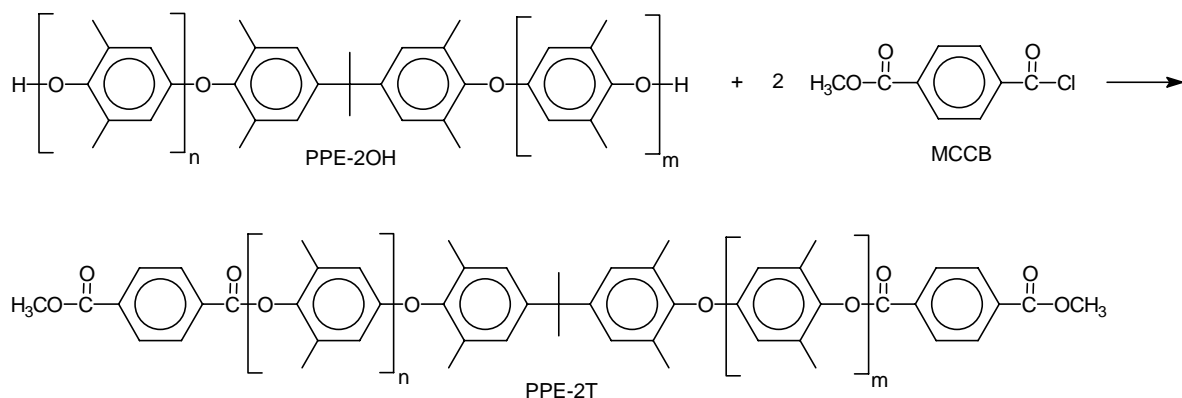


Figure 6.2: Reaction of PPE-2OH (that is obtained after redistribution of PPE with tetramethyl bisphenol A) with methyl chlorocarbonyl benzoate (MCCB) to PPE-2T.

The terephthalic methyl ester endgroups of PPE-2T have a much higher reactivity than the phenolic endgroups of PPE-2OH. This PPE-2T segment can therefore be used in a polycondensation reaction with for example a diol³². It is expected that the functionality of the bimodal PPE-2T is little higher than that of PPE-2OH, because part of the Mannich base type endgroups will react with the highly reactive MCCB as well.

Tetra-amide segments

In this study segmented copolymers based on PPE as an amorphous segment will be made. In order to obtain some crystallinity the T_m of the crystallisable segment should be above the T_g of the amorphous phase (215°C). Segmented copolymers with fully aromatic di-amide units and amorphous poly(tetramethylene oxide) segments of 2900 g/mol (9 wt% amide) have a melting temperature of 170°C¹⁰.

For copolymerisation with PPE a crystallisable segment with a higher melting temperature is needed. Di-amide units with a higher melting temperature are not known. The melting temperature can be increased by using a di-amide segment that is extended via a diol³³⁻³⁶. Copolymers with diol-extended di-amides have a higher melting temperature, because the lamellar thickness is higher³⁷. However the melting temperature is broadened due to length distribution in the diol-extended di-amides and also melt phasing can take place.

The melting temperature can also be increased by using uniform tetra-amide units³⁸ instead of di-amide units. The lamellar thickness of a tetra-amide segment is higher and as a result the melting temperature is expected to be higher than that of the corresponding di-amide units³⁷.

As a crystallisable segment bisester tetra-amides TxTxT (with T = terephthalic unit and $x = n$ in $(CH_2)_n$) will be used³⁸. The melting temperature of these segments increases with decreasing length x , because the stiffness increases. These amide units can be prepared in two

steps from dimethyl terephthalate and a diamine³⁸. The structure of the tetra-amide T6T6T-dimethyl ($x=6$) which is based on two-and-a-half repeating units of nylon-6,T with methyl ester endgroups is given in Figure 6.3. The length of this segment (without the endgroups) is ~ 4 nm.

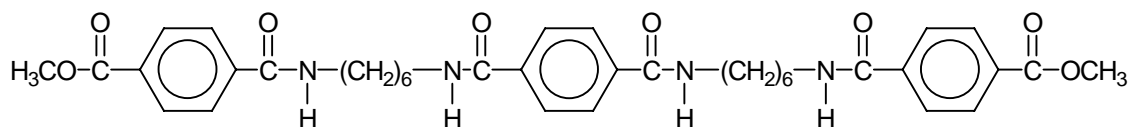


Figure 6.3: Molecular structure of the uniform crystallisable segment T6T6T-dimethyl.

The crystallisation is faster and more complete when uniform crystallisable units are used³⁹⁻⁴². Uniform di-amide units are known to crystallise fast and complete^{10,14}. It is expected that uniform tetra-amide units will crystallise even faster, as they can form four hydrogen bonds as compared to the di-amide units that can only form two.

Copolymerisation

Segmented copolymers of PPE-2T and TxTxT-dimethyl segments can be made via a polycondensation reaction. Several PPE-2T segments will then be linked via a functional coupling agent, for example a diol, to the TxTxT-dimethyl segment. Amorphous copolymers of PPE-2T with different diols³² or polyester segments⁴³ were studied before. It was shown that transesterification of the terephthalic endgroups of PPE-2T occurs preferably at the methyl ester side during polycondensation³². The phenyl ester side has a higher reactivity but is sterically hindered by the 2,6-dimethyl groups. The general structure of an alternating copolymer (T = terephthalic unit) of PPE-2T, a diol and T6T6T is given in Figure 6.4.

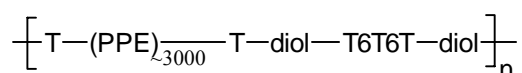


Figure 6.4: Schematic structure of an alternating PPE-2T/diol/T6T6T copolymer.

The low molecular weight fraction of the bimodal PPE-2T consists mainly of difunctionalised PPE-2T (< 3000 g/mol). It is expected that this fraction will be fully copolymerised to high molecular weight copolymer in the copolymerisation reaction. The high molecular weight fraction of PPE-2T (~ 10000 g/mol) contains only few methyl ester endgroups. Therefore this fraction will hardly be copolymerised, and may then occur as a chain end in the copolymer. The combined fractions in the bimodal PPE-2T have a number average molecular weight of 2000-3700 g/mol and a functionality of 1.7-1.9 (number of methyl ester endgroups per chain). This segment functionality is high enough to obtain high molecular weight ($M_n > 10.000$ g/mol) PPE copolymers³².

The expectation is that the PPE-2T segments and the short TxTxT units will form a homogeneous melt. Upon cooling crystallisation of the TxTxT units might take place. The diol extenders will probably mix with the amorphous PPE phase thereby decreasing its T_g as was shown in Chapter 3³² or they might crystallise together with the tetra-amide units.

Morphology

It is expected that the morphology of segmented copolymers based on PPE and uniform tetra-amide units is comparable with that of PTMO/(DMT) with uniform di-amide units⁴⁴ or tetra-amide units⁴⁵. A model for the crystalline structure of segmented copolymers that contain a low content (<20 wt%) of fast crystallising short uniform di-amide segments was proposed by Niesten et al⁴⁴.

The uniform di-amide crystalline segments form thread or ribbon-like structures with a thickness of ~2 nm and a very high aspect ratio⁴⁴⁻⁴⁷. This morphology for PTMO with T6T6T was confirmed by AFM measurements⁴⁵. The crystalline ribbons act as physical crosslinks and reinforcing fibres for the amorphous phase. With such a morphology the degree of crystallinity has a strong effect on the modulus. When the ribbons are not stacked into spherulites then the copolymer will be transparent. At high amide contents and long length of the crystallisable segments spherulitic structures can be formed and transparency will be lost⁴⁷.

Aim

In this chapter the synthesis and structure-property relationships of semi-crystalline segmented copolymers based on PPE-2T and tetra-amide units using dodecanediol as an extender are described. In particular the crystallisation of these segmented copolymers with a high T_g/T_m ratio is studied. The goal of this work is to obtain segmented copolymers with a high T_g/T_m ratio of above 0.8 that have a high glass transition temperature (150-200°C) in combination with a not too high melting temperature (250-300°C). The expectation is that these new semi-crystalline polymers will combine high dimensional stability up to the T_g , a good solvent resistance and a good processability. Furthermore the materials are expected to be transparent. When the crystallisation at such high T_g/T_m is still very fast, injection moulding with low cycling times will be possible.

Experimental

Materials. 1,12-Dodecanediol (C12) and N-methyl-2-pyrrolidone (NMP) were purchased from Merck. Tetraisopropyl orthotitanate ($Ti(i-OC_3H_7)_4$), obtained from Merck, was diluted in anhydrous *m*-xylene (0.05M), obtained from Fluka. PPO-803[®] (11.000 g/mol) and Noryl-GTX[®] (GTX914) were obtained from GE Plastics (The Netherlands). All chemicals were used as received. T6T6T-dimethyl and T4T4T-dimethyl were synthesised as described in Chapter 5³⁸. Bimodal PPE-2T of 3100 g/mol (573 μ mol OCH₃/gram) was made in a one-pot reaction as described in Chapter 2²⁷.

Synthesis of PPE-2T/C12/T6T6T. The PPE-2T/C12/T6T6T copolymers were synthesised via a polycondensation reaction. The preparation of a copolymer of PPE-2T (~3100 g/mol, 573 μ mol OCH₃/gram), dodecanediol and 13 wt% of T6T6T-dimethyl is given as an example.

The reaction was carried out in a 50 ml glass reactor with a nitrogen inlet and mechanical stirrer. The vessel was loaded with PPE-2T (10.0 g, 5.73 mmol OCH₃), dodecanediol (1.15 g, 5.73 mmol), T6T6T-dimethyl (1.97 g, 2.87 mmol), 20 ml NMP and catalyst solution (0.6 ml of 0.05M Ti(i-OC₃H₇)₄ in *m*-xylene). This mixture was first heated in an oil bath to 180 °C under nitrogen flow. Then the temperature was raised in steps: 30 min 180°C, 30 min 220 °C, 60 min 250°C and 60 min 280°C. The pressure was then carefully reduced (P<20 mbar) to distil off the remaining NMP and then further reduced (P<1 mbar) for 60 minutes. Finally, the vessel was allowed to slowly cool to room temperature whilst maintaining the low pressure. Then the polymer was cut out of the reactor and crushed.

Viscometry. The inherent viscosity of the polymers was determined with a capillary Ubbelohde type 1B at 25°C, using a polymer solution with a concentration of 0.1 g/dl in phenol/1,1,2,2-tetrachloroethane (50/50, mol/mol).

DMA. Samples for the DMA test (70x9x2 mm) were prepared on an Arburg-H manual injection moulding machine. Before use, the samples were dried in a vacuum oven at 80°C overnight. The torsion behaviour was studied at a frequency of 1 Hz, a strain of 0.1% and a heating rate of 1°C/min using a Myrenne ATM3 torsion pendulum. The storage modulus G' and loss modulus G'' were measured as a function of temperature starting at -100°C. The glass transition temperature (T_g) was expressed as the temperature at which the loss modulus G'' has a maximum. This maximum was 0-10°C lower than the actual glass transition temperature, because with this DMA apparatus it was not possible to measure a few points around the T_g due to the very high damping. The modulus of the rubbery plateau was determined at 40°C above the T_g. The flow temperature (T_{flow}) was defined as the temperature where the storage modulus G' reached 0.5 MPa. The flow temperature indicates the onset of melting. When the T_{flow} is sharp it is only a few degrees below the melting temperature (T_m) and the T_g/T_{flow} ratio (K/K) is about the same as the T_g/T_m ratio.

DSC. DSC spectra were recorded on a Perkin Elmer DSC7 apparatus, equipped with a PE7700 computer and TAS-7 software. Dried samples of 5-10 mg polymer in aluminium pans were measured with a heating rate of 20°C/min and different cooling rates (5-160°C/min). The samples were heated to 300°C, kept at that temperature for 2 minutes, cooled to 100°C and reheated to 300°C. The (peak) melting temperature and enthalpy were obtained from the second heating scan. The crystallisation temperature was defined as the maximum of the peak in the cooling scan. For comparison with other data the onset of the crystallisation peak was determined as well.

To account for the thermal lag between a point in the sample and the calorimeter furnace, the recorded temperatures in non-isothermal crystallisation experiments must be corrected. For Perkin Elmer DSC7 with aluminium pans the actual temperature was calculated from the display temperature and cooling rate λ (°C/min) with Equation 6.1^{48,49}.

$$T_{\text{actual}} = T_{\text{display}} + 0.089\lambda \quad [^{\circ}\text{C}] \quad \text{Equation 6.1}$$

WAXD. X-ray diffraction data of melt-pressed samples were collected with a Philips PW3710 based X'Pert-1 diffractometer in Bragg-Brentano geometry, using a Θ compensating divergence slit (12.5 mm length). Diffraction data collection was performed at room temperature, using a low-background spinning (1 r/s) specimen holder. $\text{CuK}_{\alpha 1}$ radiation of 1.54056 Å was obtained using a curved graphite monochromator. The data were collected in a range of $2\Theta = 4\text{-}60^\circ$.

Melt-pressed samples of 10x15x1 mm were prepared from an injection moulded test bar in a mould at 300°C for 5 minutes with a pressure of 10 bar, after which the samples were slowly cooled with 5°C/min. Melt-pressed samples of ~0.1 mm thickness were prepared from polymer powder between two Teflon sheets (5 min at 300°C, 10 bar), after which the thin film was directly quenched in ice-water, with a cooling rate of >5000°C/min.

WAXD as function of temperature. Diffraction patterns at different temperatures were obtained using a Philips X'Pert-MPD diffractometer. With a curved graphite monochromator $\text{CuK}_{\alpha 1}$ radiation of 1.54056 Å was obtained. Melt-pressed samples of approximately 1 mm thickness were mounted in a sample holder in an Anton Paar HTK-16 temperature chamber. The measurements were carried out in nitrogen atmosphere and the heating and cooling rate were 2°C/min. The data were collected in a range of $2\Theta = 4\text{-}60^\circ$. The experiment started with a measurement at room temperature and then the temperature was raised to 175°C and further to 300°C with a measurement every 25°C. Measurements were also performed during cooling with the same temperature steps.

Water absorption. The absorption of water was measured as the weight gain after conditioning. DMA test bars were dried at 70°C in a vacuum oven for several days and weighed (w_0). Then the samples were conditioned in a dessicator over water at room temperature for 28 days (100% RH). The samples were reweighed after 7 and 28 days (w). The water absorption was calculated using Equation 6.2.

$$\text{water absorption} = \frac{w - w_0}{w_0} \times 100\% \quad [\%] \quad \text{Equation 6.2}$$

Melt viscosity. The melt viscosity was measured using a Kayeness capillary flow rheometer. The length and diameter of the capillary were 20.32 and 1.016 mm respectively. The diameter of the barrel was 9.525 mm. The pressure was measured at different flow rates by applying varying piston speeds of 10, 20, 50, 100, 130, 200 and 500 mm/min. These piston speeds correspond to shear rates of 115, 230, 576, 1154, 1499, 2304 and 5760 sec^{-1} respectively. The temperature was set at 300°C.

Results and Discussion

The synthesis of copolymers based on PPE-2T, dodecanediol and TxTxT-dimethyl will be discussed first. Then the thermal-mechanical properties of two polyether-esteramide copolymers of PPE-2T and dodecanediol as an extender with T4T4T-dimethyl and T6T6T-dimethyl will be compared. The properties of PPE-2T/C12/T6T6T copolymer with 13 wt% T6T6T are discussed in more detail using DSC, WAXD, water absorption and rheology experiments. Particular attention is given to the crystallisation of these new segmented copolymers.

Synthesis

Copolymers of PPE-2T, dodecanediol (C12) and TxTxT-dimethyl were made via a polycondensation reaction with a maximum temperature of 280°C. During the first part of the reaction NMP was used as a solvent because of the high melting temperature of the tetra-amide segment. The melting temperature of T6T6T-dimethyl is 303°C and that of T4T4T-dimethyl is above 340°C³⁸. After one hour at 250°C, the reaction had progressed enough to allow the final part of the reaction to be performed in the melt. Most of the NMP was stripped off at 280°C. The rest of the NMP was stripped off when the vacuum was applied. During the last hour a vacuum of <1 mbar was applied to strip off any methanol formed and to obtain polymers with high molecular weights. For copolymers with T6T6T-dimethyl as crystallisable segment the reaction mixture was gradually transferred from a clear solution into a clear melt. The clear melt indicates that melt phasing or liquid-liquid demixing between both segments is absent or only present at a nano-scale level. With T4T4T-dimethyl the polymerisation continued in the solid state after NMP removal.

The copolymers could be easily obtained with inherent viscosities comparable to PPO-803[®]. PPO-803[®], the starting material for redistribution, has an inherent viscosity of 0.37 dl/g (determined in chloroform) and average molecular weight M_n of 11.000 g/mol. A molecular weight above 10.000 g/mol is preferred for good toughness of the material. The PPE segments that are used have a number average molecular weight around 3100 g/mol. The molecular weight of the dodecanediol unit in the copolymer is 200 g/mol and that of T6T6T is 624 g/mol. The average molecular weight of these three segments in the copolymer is ~1300 g/mol. Thus a degree of polymerisation of above 10 is sufficient to obtain copolymers with good properties (see Chapter 3)³².

With PPE-2T of 3100 g/mol, dodecanediol and T4T4T-dimethyl, the amide content is 12 wt% and with T6T6T-dimethyl 13 wt%. The amide content was calculated, assuming that the ester carbonyl does not crystallise and belongs to the amorphous phase¹⁵. The uniformity of the TxTxT-dimethyl that was used was >95%. The uniformity is the amount of TxTxT-dimethyl in the starting material. When the uniformity is below 100% the crystallisable segment contains TxTxTxT-dimethyl and TxTxTxTxT-dimethyl as well³⁸. When the uniformity is 100%, TxTxT-dimethyl does not contain T(xT)_n units with n>2. It was not possible to measure the uniformity of the TxTxT units in the polymer after copolymerisation, because the

copolymers are insoluble in appropriate solvents. The copolymers swell in good solvents for PPE such as chloroform and toluene. T6T6T-dimethyl is soluble in deuterated trifluoro acetic acid (TFA-D), however the copolymers of PPE and T6T6T are insoluble in this solvent. For T6T6T-PTMO/(DMT) copolymers that are soluble in TFA-D it was found that the uniformity of the T6T6T units is preserved during the polymerisation reaction⁴⁵.

In the copolymers based on PPE-2T with a number average molecular weight of 3100 g/mol, dodecanediol and TxTxT-dimethyl (12-13 wt%) the PPE-2T endgroup and TxTxT endgroup molar contents are equal. As a result of the random reaction between PPE-2T, diol and TxTxT-dimethyl some PPE-2T will be coupled directly via dodecanediol (-PPE-C12-PPE-) as well as some TxTxT segments (-C12-TxTxT-C12-TxTxT-C12-). The product is a mixture of PPE-2T/C12/TxTxT copolymer and high molecular weight PPE chains that were not redistributed. Some of these high molecular weight PPE chains can be present in the copolymer as an endgroup because some of their Mannich base type endgroups are transferred into methyl ester endgroups²⁷.

Morphology of PPE-2T/diol/TxTxT copolymers

The possible morphology of a PPE-2T/C12/TxTxT copolymer in which the PPE-2T and TxTxT-dimethyl endgroup concentrations are equal (copolymer with 12-13 wt% TxTxT) is schematically drawn in Figure 6.5. The morphology of PPE-2T/C12/TxTxT will be comparable with that of PTMO/di-amide⁴⁴ or PTMO/tetra-amide⁴⁵. Most TxTxT units will crystallise to threads or ribbon-like structures (I) of ~4 nm thickness with high aspect ratio and some will be amorphous and mixed with the amorphous PPE phase (II). In PTMO/tetra-amide⁴⁵ the length of the crystalline ribbons can be 500 nm, as was measured by AFM experiments.

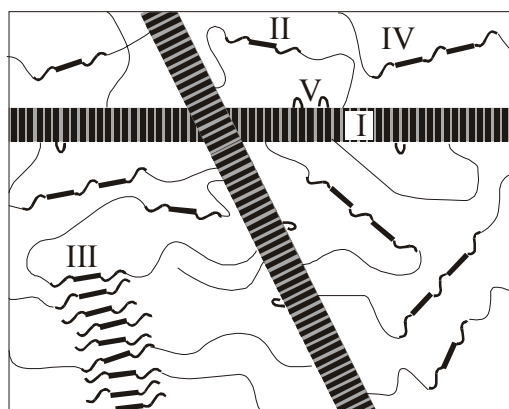


Figure 6.5: Different possible morphologies for PPE-2T/C12/TxTxT copolymers: (I), crystalline TxTxT ribbons; (II), amorphous TxTxT units, mixed with PPE; (III), ordered TxTxT phase; (IV), amorphous diol-extended TxTxT units; (V), chain-folded crystalline diol-extended TxTxT units.

Possibly the tetra-amide units are still ordered in the melt^{50,51}, like the di-amides in PTMO/di-amide¹⁵⁻¹⁷. It is thought that crystallisation of TxTxT takes place from these ordered TxTxT in the melt upon cooling. However, due to the high T_g/T_m ratio for PPE-2T/C12/TxTxT,

crystallisation is incomplete. Therefore it can be expected that after cooling the non-crystalline TxTxT units are still ordered in a sort of frozen-in TxTxT nano-phases (III). The dimensions of such ordered TxTxT domains will be comparable with that of the crystalline lamellae I, which is at a nano-scale.

It is expected that the diol-extended TxTxT segments are still miscible with PPE and are present in the amorphous PPE phase (IV). It is also possible that some diol-extended TxTxT units crystallise after chain folding (V) or over their full length. Crystallisation of diol-extended TxTxT over their full length will lead to crystals with increased lamellar thickness (thicker ribbons) with a higher melting temperature³⁷. In PTMO/di-amide copolymers diol-extended di-amide units crystallise over their full length with a higher melting temperature for diol lengths up to ~500 g/mol³³. Chain folding should be possible with butanediol and longer diols.

The T_g of the amorphous PPE phase will be reduced due to the presence of the amorphous TxTxT units (II and IV) and the dodecanediol extender. Also the dodecanediol that is at the interphase between amorphous PPE and TxTxT crystalline ribbons will probably decrease the T_g of the PPE phase.

When the segment lengths (PPE and TxTxT/diol) are long enough, phase separation (melt phasing or liquid-liquid demixing) can occur. Phase separation will occur more readily when the segment length increases, thus with long diols or long diol-extended TxTxT segments. Such phase separated domains already exist in the melt and have a spherical shape and dimensions >100 nm (not shown in Figure 6.5). As a result of the presence of phase separated domains light is scattered and the material will not be transparent.

Thermal-mechanical properties

The thermal-mechanical properties of segmented copolymers based on PPE-2T, dodecanediol and TxTxT-dimethyl were measured by DMA. Two crystalline segments, T4T4T-dimethyl and T6T6T-dimethyl were compared. With T6T6T-dimethyl copolymers with different molecular weights were made. The polymers were injection moulded into bars and dried in a vacuum oven at 80°C. Injection moulding was done at 50-100°C above the melting temperature with a manual injection moulding machine in an unheated mould.

The test bars of the copolymers based on T6T6T or T4T4T are slightly transparent. When the material is transparent this indicates that no spherulites are present⁴⁷. Light scattering also occurs when phase separated domains with a size above 100 nm are present. Apparently such domains are not present in PPE-2T/C12/TxTxT with 12-13 wt% TxTxT.

Table 6.1: Properties of the PPE-2T/C12/TxTxT copolymers.

	T6T6T content [wt%]	η_{inh} [dl/g]	T_g [°C]	G' (at T_g + 40°C) [MPa]	T_{flow} [°C]	T_g/T_{flow} [-]
PPE-2T ^a	-	0.18 ^b	168 ^c	-	-	-
PPO-803 [®]	-	0.37 ^b	200	-	222	-
PPE-2T/C12	0	0.31 ^b	169	-	193	-
PPE-2T/C12/T4T4T	12	0.31	175	6	>300	<0.78
PPE-2T/C12/T6T6T	13	0.41	169	10	269	0.82
PPE-2T/C12/T6T6T ^d	13	0.41	179	12	270	0.83
PPE-2T/C12/T6T6T	13	0.52	164	7	264	0.81

(a), bimodal product made by one-pot synthesis (3100 g/mol)²⁷; (b), chloroform was used as a solvent instead of phenol/tetrachloroethane; (c), measured by DSC instead of DMA; (d), properties of test bar after heat treatment in a press (10 bar) for 5 minutes at 240°C and then slowly (5°C/min) cooled down to room temperature

T4T4T and T6T6T

In Figure 6.6 the storage and loss moduli as measured by DMA are given for the PPE-2T/C12/TxTxT copolymers with T4T4T and T6T6T as crystallisable segment. The results can also be found in Table 6.1.

Copolymers of PPE-2T, dodecanediol and T4T4T- or T6T6T-dimethyl are semi-crystalline materials. Both show a rubbery plateau above the glass transition temperature of the amorphous PPE phase. This result is very surprising, because the T_g/T_{flow} ratios of these copolymers are very high (up to 0.82). In general the rate of crystallisation and therefore the extent of crystallisation decreases dramatically when the T_g/T_{flow} ratio increases^{12,13}. The fast cooling rates in the unheated mould after injection moulding does not seem to limit the crystallisability of these copolymers. It could be that the crystallisation is somewhat lower at the surface of the test bars due to the higher cooling rates there.

Both copolymers have a high and constant modulus up to the T_g . However for both copolymers the modulus drops somewhat above 70°C and the loss modulus shows a peak around 100°C. This peak is larger for the copolymer based on T6T6T. This small effect can be attributed to a crystalline transition in the crystalline TxTxT ribbons (I), to the presence of phase separated amorphous TxTxT/C12 domains or to the presence of frozen-in ordered TxTxT nano-phases (Figure 6.5, III). It could be that the transition at 100°C is a crystalline transition. Such a transition was also found for example for 6T6-diamine³⁸ and polyamide^{52,53}. However the T6T6T-dimethyl segment did not show such a crystalline transition³⁸.

Both the phase separated amorphous TxTxT domains and the non-crystalline ordered TxTxT nano-phases will have a glass transition temperature close to that of the corresponding polyamide. The T_g of nylon-6,T is 125°C⁵⁴ and that of nylon-4,T is 133°C⁵⁴. So the peak in the loss modulus at 100°C in the copolymer with T6T6T is probably originating from T6T6T/C12 that has a little lower T_g than pure nylon-6,T. The T_g of such C12-T4T4T-C12 is expected to be somewhat higher and will probably located close to the T_g of PPE. The

presence of phase separated amorphous TxTxT/C12 rich domains in PPE-2T/C12/TxTxT is not likely because these materials are slightly transparent and phase separated domains with dimensions below 100 nm are not expected. Therefore the peak in the loss modulus can probably be attributed to the presence of frozen-in TxTxT nano-phases.

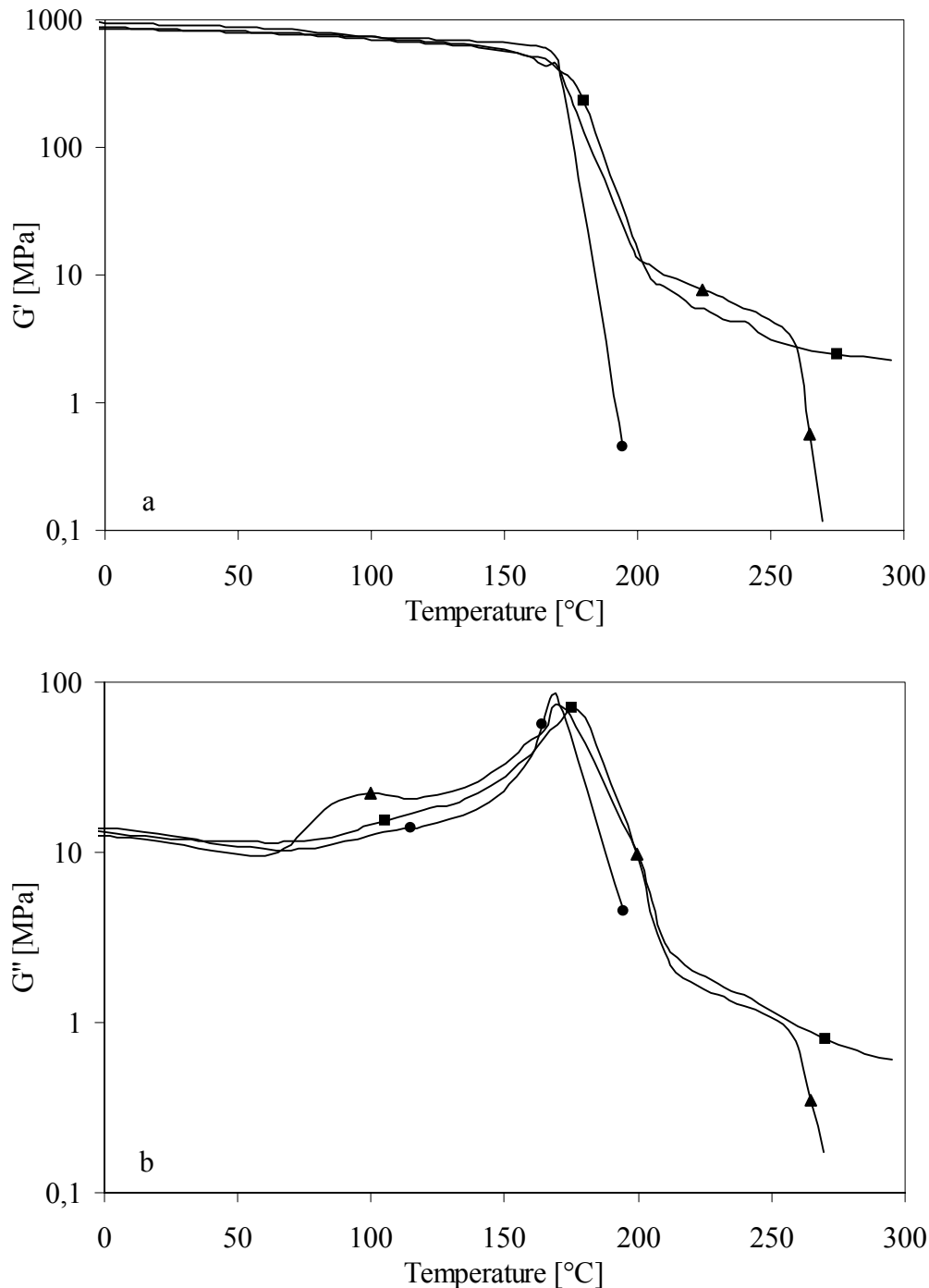


Figure 6.6: Storage (a) and loss (b) modulus for copolymers of PPE-2T, dodecanediol and TxTxT-dimethyl: (■), 12 wt% T4T4T-dimethyl (0.31 dl/g); (▲), 13 wt% T6T6T-dimethyl (0.41 dl/g); (●), PPE-2T/C12 (0.31 dl/g).

The main T_g 's of PPE in these two copolymers with TxTxT are comparable. The T_g 's of the copolymers with TxTxT are higher than the T_g of the amorphous PPE-2T/C12 copolymer, although the dodecanediol content is doubled. In the amorphous PPE-2T/C12 copolymer without TxTxT all dodecanediol mixes with the PPE because dodecanediol is too short (T-C12-T) to form a separate amorphous phase³². In the copolymers with TxTxT the presence of both dodecanediol and amorphous TxTxT (Figure 6.5, II and IV) will lower the T_g of PPE, but the effect of TxTxT is much weaker than that of dodecanediol that is more flexible. It can therefore be concluded that less dodecanediol mixes with the PPE phase in the PPE/C12/TxTxT copolymers. Most dodecanediol is at the interface of the amorphous PPE and crystalline and ordered TxTxT nano-phases. Dodecanediol at this interphase it is not likely to effect the T_g of PPE as much as mixed PPE/C12, because the two are not really mixed and the mobility of the PPE phase is not increased.

The rubber moduli of the copolymers with T4T4T and T6T6T are 6 and 10 MPa respectively. The height of the rubber modulus is mainly determined by the crystallinity. So the crystallinity in the copolymer based on T6T6T is higher. It is not possible to conclude directly what the exact degree of crystallinity of the TxTxT in these copolymers is. Copolymers of PTMO/DMT and T6T6T (12 wt%) with almost 100% crystallinity of T6T6T have a rubber modulus of 18 MPa⁴⁵. It can be assumed that the effect of crystallinity on rubber modulus for T6T6T is comparable with PTMO/DMT and PPE when the morphology is the same. The logarithm of the rubber modulus then increases linearly with the crystallinity⁵⁵. Therefore it can roughly be concluded that the crystallinity of T6T6T is around 75% and that of T4T4T around 60%. Thus the crystallinity of TxTxT is quite high despite the high T_g of the amorphous PPE phase and the high T_g/T_m ratio (>0.8).

The flow temperature of the copolymers with 13 wt% T6T6T and dodecanediol is 269°C. The flow temperature is sharp, which indicates that ribbons with a constant thickness are present. Thus few extended T6T6T-C12-T6T6T segments have crystallised. The diol extended units crystallise by chain folding or are amorphous and mixed with the amorphous PPE phase. With 12 wt% T4T4T as crystallisable segment the flow temperature is above 300°C, which is the maximum for the DMA apparatus. To obtain copolymers with PPE that can be processed at not too high temperatures, thereby preventing degradation, the use of T6T6T is preferred. These copolymers will be studied in more detail.

Influence of molecular weight

Two alternating PPE-2T/C12/T6T6T copolymers with inherent viscosities of 0.41 ($M_n = \sim 12000$ g/mol)³² and 0.52 dl/g ($M_n = \sim 16000$ g/mol) were made. The thermal-mechanical behaviour of these two copolymers is compared in Figure 6.7.

The presented data in Figure 6.7 are used to show a trend. When the thermal-mechanical properties of two copolymers with the same inherent viscosity and T6T6T content are compared the crystallinity can sometimes be higher or lower. The crystallinity of T6T6T of all copolymers seems to be dependent on several factors, especially processing conditions

such as the injection moulding temperature and the cooling rate. The crystallinity might be improved by increasing the injection moulding temperature and by using a heated mould.

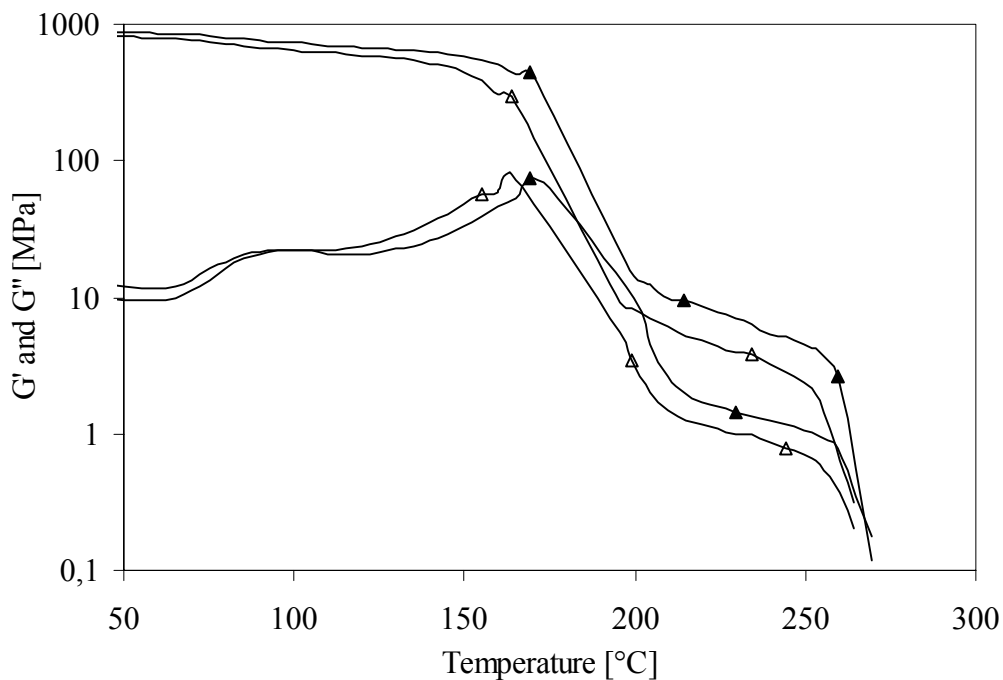


Figure 6.7: Storage and loss modulus of PPE-2T/C12/T6T6T (13 wt%) copolymers: (▲), 0.41 dl/g; (△), 0.52 dl/g.

With increasing molecular weight the crystallinity decreases as is indicated by a decreasing rubber modulus and flow temperature. At an inherent viscosity of 0.41 dl/g the crystallinity of T6T6T is ~75% relatively to T6T6T in copolymers with PTMO/DMT as amorphous segment⁴⁵. At 0.52 dl/g the relative crystallinity is ~60%.

With the higher inherent viscosity the main T_g is about 5°C lower, which can be attributed to the presence of a less pure PPE phase as a result of more mixing between PPE and T6T6T/C12 (Figure 6.5, II and IV). Thus the high melt viscosity does not only reduce crystallisation of T6T6T in crystalline ribbons but also the formation of ordered T6T6T nano-phases. Probably the T6T6T was already less ordered in the melt for the copolymer with the higher molecular weight.

Influence of heat treatment

Part of the T6T6T units, probably especially those at the surface of the test bar, seem unable to crystallise due to the high T_g/T_m ratio and the high cooling rate during injection moulding in an unheated mould. Therefore, the effect of heat treatment was investigated. A test bar of the PPE-2T/C12/T6T6T copolymer with 13 wt% T6T6T and an inherent viscosity of 0.41 dl/g was heated in a press at 240°C for 5 minutes and then slowly cooled (5°C/min) to room temperature. The thermal-mechanical behaviour before and after heat treatment is compared in Figure 6.8.

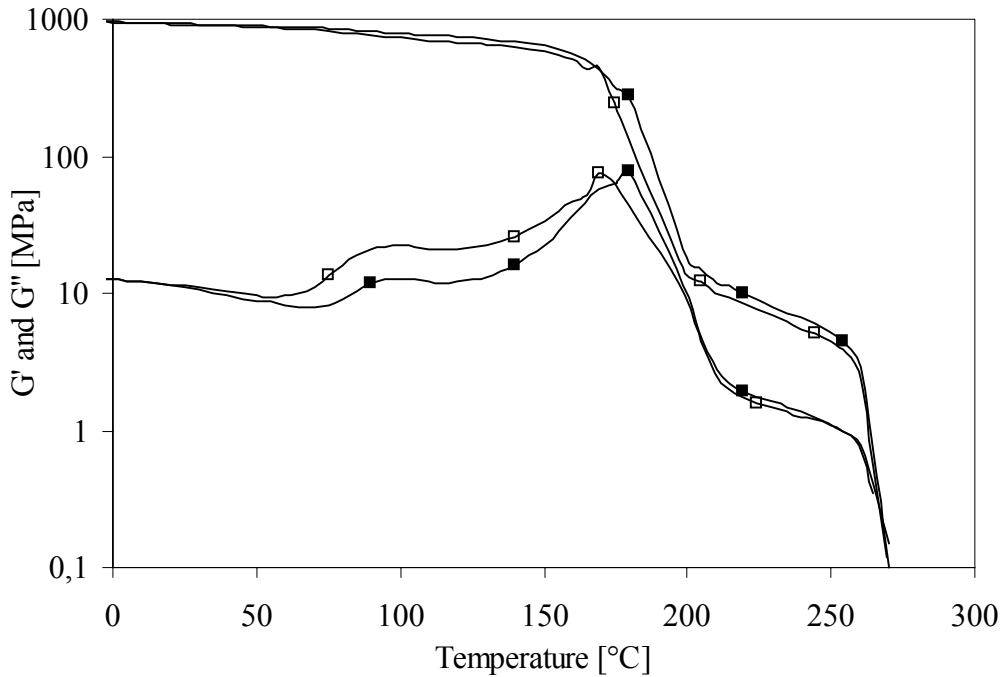


Figure 6.8: Storage and loss modulus of PPE-2T/C12/T6T6T (13 wt%, 0.41 dl/g) copolymer: (□), after injection moulding in an unheated mould; (■), after heat treatment in a press at 240°C.

After heat treatment the T_g and modulus of the rubbery plateau increase. The area and height of the peak in the loss modulus around 100°C decreases and therefore the storage modulus is somewhat higher between 100 and 170°C for the test bar after heat treatment. Apparently a part of the frozen-in ordered T6T6T nano-phases crystallises during the heat treatment step. From the modulus in the rubbery plateau it can be calculated that the crystallinity of T6T6T is ~80% relatively to T6T6T in copolymers with PTMO/DMT as amorphous segment⁴⁵.

Test bars with a high crystallinity such as after heat treatment can probably be obtained directly after injection moulding when the cooling rate is decreased by using a heated mould.

Comparison with commercial materials

By copolymerising PPE-2T/C12 with T6T6T-dimethyl a material is obtained that fulfils the requirements that were set as a goal for this project. The polymers have a high and constant modulus up to the T_g of PPE, a sharp glass transition and melting temperature and a rubbery plateau. The height of the rubbery plateau can probably be adjusted by optimising the processing conditions or by changing the amount of T6T6T in the copolymer. Crystallisation is possible, despite the very high T_g/T_{flow} ratio of >0.8.

In Figure 6.9 the modulus of the copolymer PPE-2T/C12/T6T6T with 13 wt% uniform T6T6T (after heat treatment) and an inherent viscosity of 0.41 dl/g (~13.000 g/mol) is compared with the modulus of PPO-803[®] and Noryl-GTX[®]. Noryl-GTX[®] is a blend of PPE, polyamide-6,6 (~40%) and a rubber (~10%).

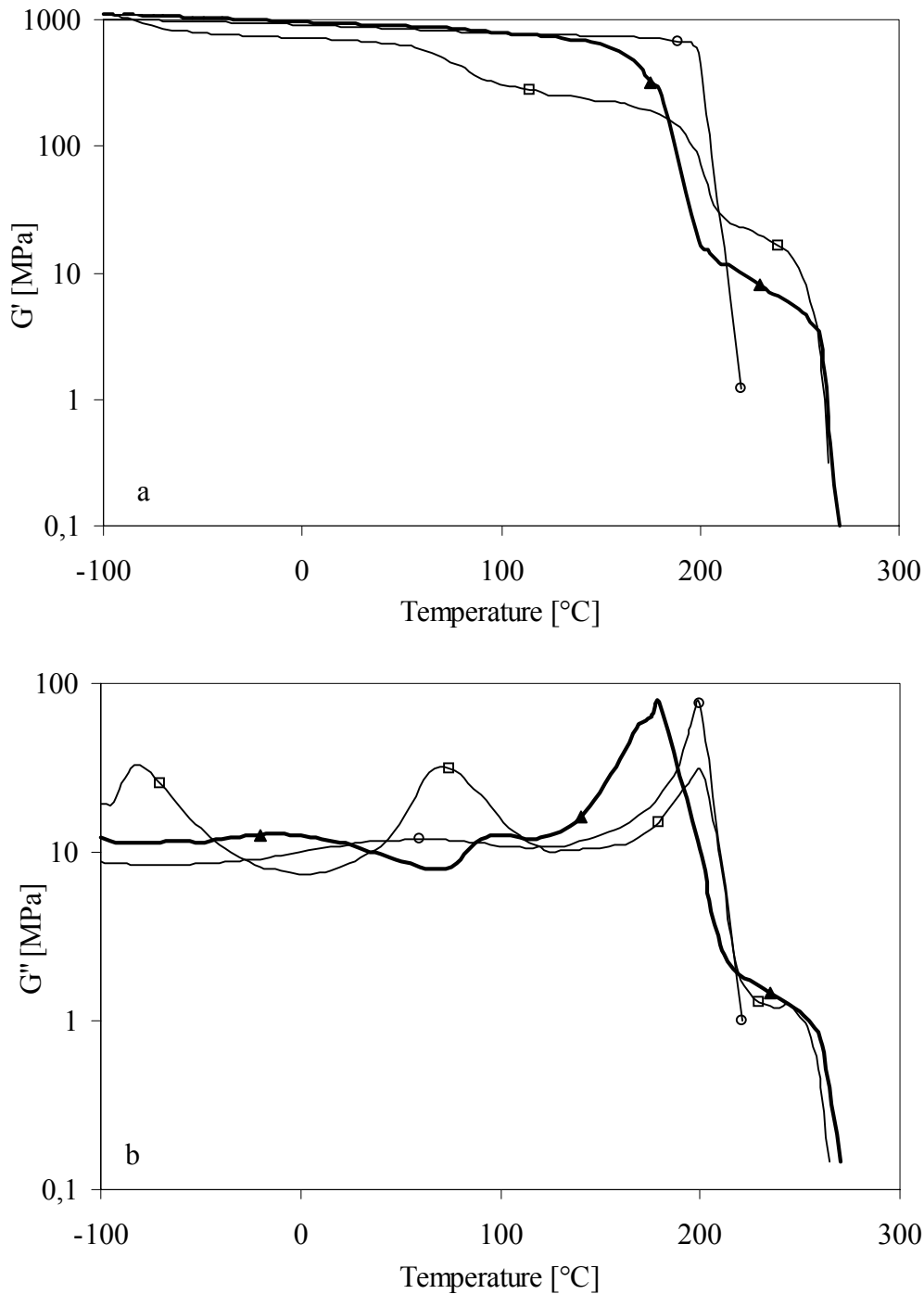


Figure 6.9: Storage (a) and loss (b) modulus of PPE-2T/C12/T6T6T compared to commercial materials: (\blacktriangle), PPE-2T/C12/T6T6T (13 wt%, 0.41 dl/g); (\square), Noryl-GTX[®]; (\circ), PPO-803[®].

The amorphous homopolymer PPO-803[®] has a high and constant modulus up to the T_g at 200°C (determined as the maximum of the loss modulus). The blend of PPE with ~40% polyamide-6,6 and rubber (~10%) as an impact modifier shows a much different behaviour. The blend has a phase separated morphology. The blend shows a T_g of the PPE phase at 200°C as does the pure PPE. This indicates that this PPE phase is almost pure and does not contain any polyamide-6,6 or rubber. At -80°C the modulus drops due to the presence of the

rubber impact modifier. At 70°C the modulus drops because the amorphous part of the semi-crystalline polyamide has its T_g at this temperature. As a result the modulus of the blend is only very high up to 50°C instead of 200°C. The crystalline part of the semi-crystalline polyamide gives a melting temperature (T_m) at 265°C. Between the T_g of the PPE phase and the T_m of the crystalline part of the polyamide phase is a rubbery plateau with a modulus of ~20 MPa.

The copolymer with 13 wt% T6T6T (after heat treatment) has a higher modulus up to the glass transition temperature at 179°C. For good impact properties some rubber might be added to the copolymer as well and as a result the modulus will then drop somewhat above – 80°C. The copolymer with 13 wt% T6T6T after heat treatment has a rubbery plateau with a modulus of 12 MPa. The flow temperature is 270°C and the T_g/T_{flow} ratio 0.82. The height of the rubbery plateau and flow temperature can be increased by increasing the crystallinity. The crystallisation of T6T6T is dependent on the molecular weight of the copolymer and on the cooling rate during processing. The crystallinity can probably also be increased by increasing the T6T6T content.

The height of the rubbery plateau and flow temperature are important properties of the PPE/C12/T6T6T copolymers and are related to the crystallinity. The solvent resistance is also dependent on the crystallinity. The solvent resistance of the material is of major importance in applications comparable to Noryl-GTX[®], which is mainly used in the automotive industry. As yet we do not know how much crystallinity is needed for good solvent resistance in PPE/C12/T6T6T copolymers. The presence of crystallites also increases the chain interaction and good tensile and impact properties can be obtained at a lower molecular weight and thus at a lower melt viscosity. This is important for the processability. Also less rubber might be needed to improve the impact properties.

These new copolymers of PPE and tetra-amide units could also be useful as compatibiliser for blends of PPE and polyamide. And when PPE-2T segments are copolymerised with other segments, suitable compatibilisers for other PPE blends can also be obtained.

DSC

With DSC the melting and crystallisation behaviour of PPE-2T/C12/T6T6T with 13 wt% uniform T6T6T was studied. Polymers with different inherent viscosities were used. The influence of molecular weight and cooling rate on crystallisation was studied.

Molecular weight

The crystallisation behaviour of PPE-2T/C12/T6T6T polymers with 13 wt% uniform T6T6T with different molecular weights (inherent viscosity) was studied. The peak melting temperature, melting enthalpy, peak crystallisation temperature, crystallisation enthalpy and undercooling are given in Table 6.2. The data were corrected for the thermal lag. For a cooling rate of 20°C/min the thermal lag is ~2°C^{48,49} (Equation 6.1).

Table 6.2: Melting and crystallisation behaviour of PPE-2T/C12/T6T6T with 13 wt% T6T6T and two different inherent viscosities.

η_{inh} [dl/g]	$T_m(\text{peak})$ [°C]	ΔH_m [J/g]	ΔH_m [J/g T6T6T]	x_c [%]	$T_c(\text{peak})$ [°C]	$T_m - T_c(\text{peak})$ [°C]	ΔH_c [J/g]
0.41	268	14	109	70	250	18	13
0.52	264	12	93	60	241	23	12

With increasing molecular weight the melting temperature and enthalpy decrease a little. Polymers with a lower melting temperature at a constant amide content have a lower crystallinity. The solvent effect of the amorphous phase increases when the degree of crystallinity decreases and therefore the melting temperature decreases with decreasing crystallinity⁵⁶. When the molecular weight increases the viscosity of the melt increases and therefore crystallisation is suppressed.

The peak melting temperature as measured by DSC is 268°C with an enthalpy of 14 J/g (109 J/g T6T6T) at an inherent viscosity of ~0.41 dl/g. The undercooling is only 18°C. The T_m of T6T6T-dimethyl is 303°C with an enthalpy of 152 J/g³⁸. When it is assumed that the melting enthalpy of T6T6T in the copolymer and T6T6T-dimethyl are comparable it can be calculated that about 70% of the T6T6T has crystallised. At an inherent viscosity of 0.52 dl/g the melting and crystallisation temperature and enthalpy decrease, while the undercooling increases. The crystallinity of T6T6T as calculated from the melting enthalpy of T6T6T-dimethyl is ~60%. The calculated crystallinities of T6T6T correspond quite well with the crystallinities that were calculated from the rubber modulus relatively to T6T6T-PTMO(/DMT) copolymers.

These data corroborate the results of dynamic mechanical analysis. The rate of crystallisation of these segmented copolymers is dependent on the molecular weight of the polymer and therefore the crystallinity of T6T6T decreases with increasing molecular weight.

Cooling rate

The crystallisation of the polymer with an inherent viscosity of 0.42 dl/g was studied at different cooling rates. The data were corrected for the thermal lag. For low cooling rates (5-10°C/min) the thermal lag is less than 1°C^{48,49} (Equation 6.1). At higher cooling rates (above 50°C/min) the error in the temperature increases because of a delay in the heat transfer to the sample in the DSC pan. At 160°C/min the thermal lag increases to 14°C/min.

The corrected crystallisation data as measured by DSC are given in Figure 6.10. The onset and peak crystallisation temperature at different cooling rates are given in Table 6.3. The relative crystallinity as a function of the corrected temperature at different cooling rates is given in Figure 6.11.

Table 6.3: Crystallisation temperature at different cooling rates for PPE-2T/C12/T6T6T with 13 wt% T6T6T and $\eta_{inh} = 0.42$ dl/g that has a peak melting temperature of 268°C.

Cooling rate [°C/min]	T _c (onset) [°C]	T _m (peak)-T _c (onset) [°C]	T _c (peak) [°C]	T _m (peak)-T _c (peak) [°C]
5	257	11	253	15
10	256	12	252	16
20	255	13	250	18
40	254	14	248	20
80	252	16	241	27
120	251	17	236	32
160	244	24	230	38

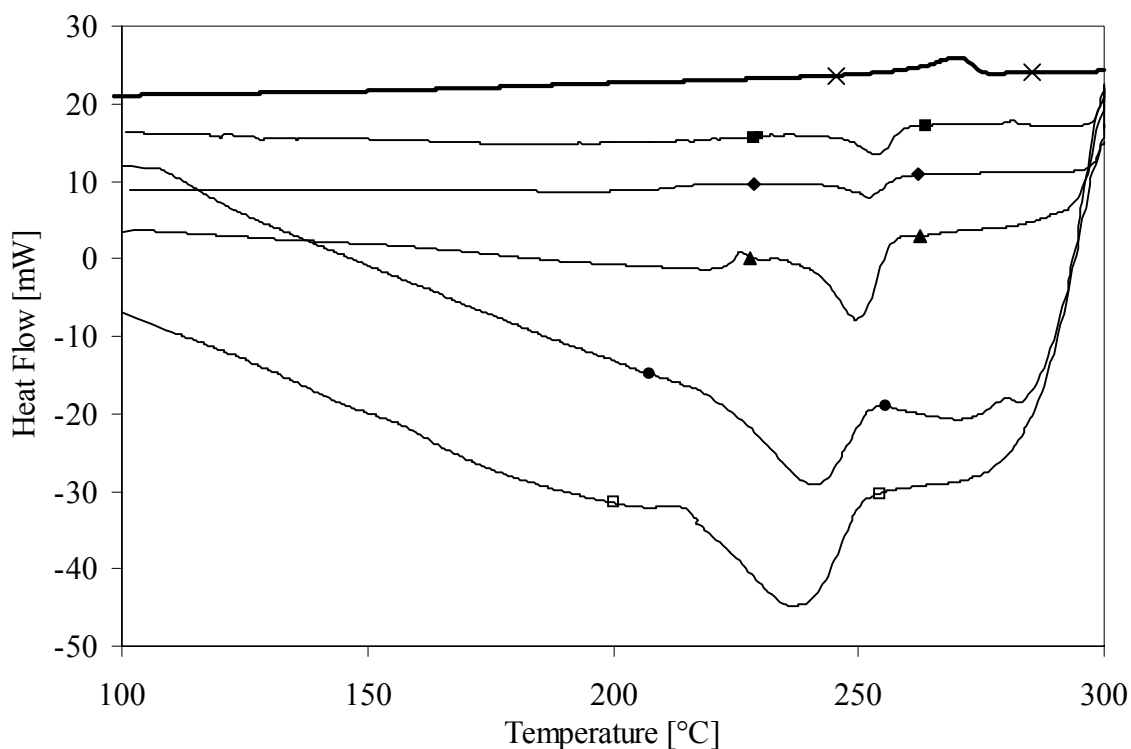


Figure 6.10: Melting and crystallisation curves (after correction) of PPE-2T/C12/T6T6T with 13 wt% T6T6T (0.42 dl/g) as measured by DSC at different rates: (x), +20°C/min; (■), -10°C/min, (◆), -20°C/min; (▲), -40°C/min; (●), -80°C/min; (□), -120°C/min.

The crystallisation peak shifts to lower temperatures and becomes broader when the cooling rate increases. At all cooling rates the onset of crystallisation is sharp, while the peak broadens at the end.

The undercooling values of 15-38°C ($T_m(\text{peak})-T_c(\text{peak})$) at cooling rates of 5-160°C are very low. Other semi-crystalline polymers such as PBT or nylon-4,6 that are known to crystallise fast have higher undercooling values.

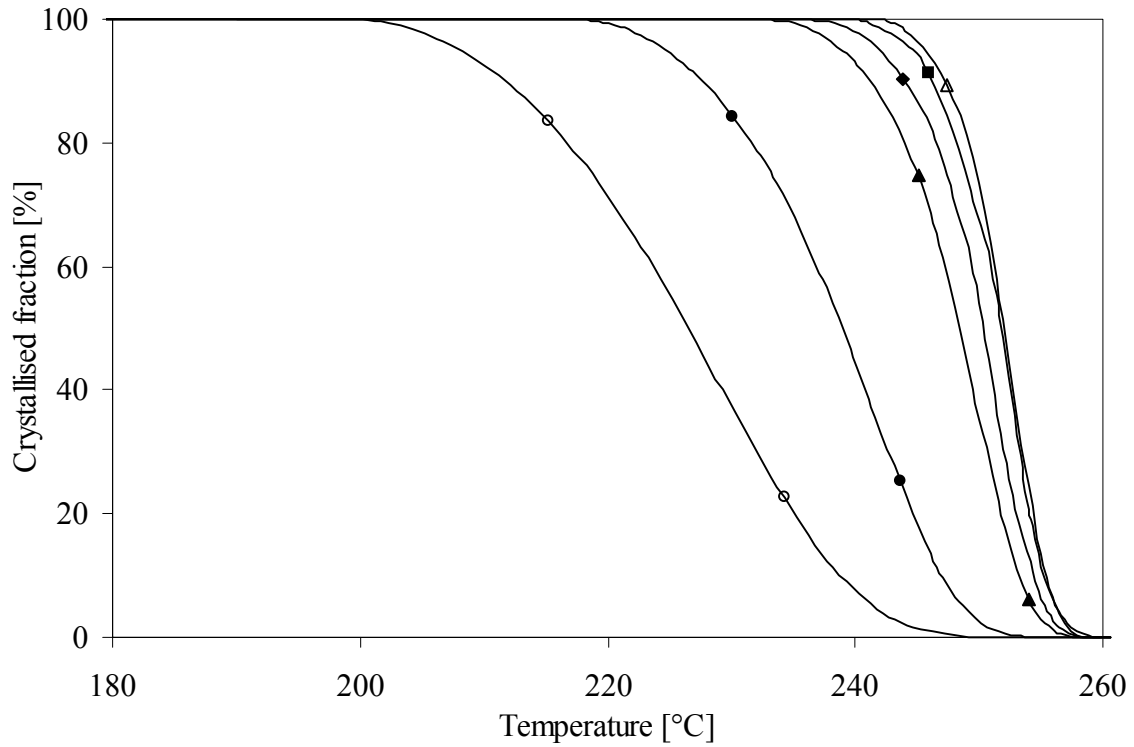


Figure 6.11: Corrected crystallised fraction of PPE-2T/C12/T6T6T with 13 wt% T6T6T (0.42 dl/g) as measured by DSC at different cooling rates: (Δ), $-5^{\circ}\text{C}/\text{min}$; (\blacksquare), $-10^{\circ}\text{C}/\text{min}$; (\blacklozenge), $-20^{\circ}\text{C}/\text{min}$; (\blacktriangle), $-40^{\circ}\text{C}/\text{min}$; (\bullet), $-80^{\circ}\text{C}/\text{min}$; (\circ), $-160^{\circ}\text{C}/\text{min}$.

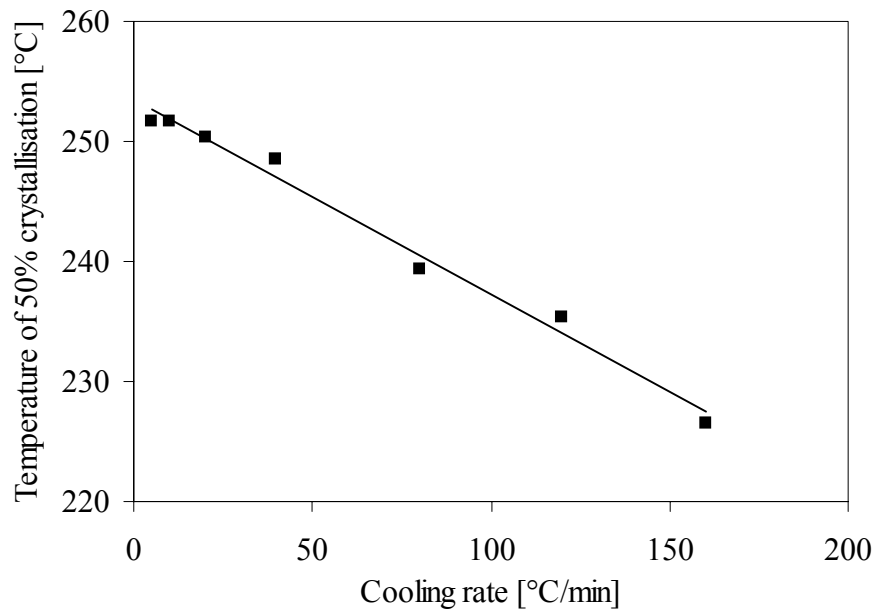


Figure 6.12: Temperature at which 50% of the crystallisation of PPE-2T/C12/T6T6T with 13 wt% T6T6T (0.42 dl/g) is completed as a function of cooling rate as measured by DSC.

The temperature at which 50% of the crystallisation is reached is given as a function of temperature in Figure 6.12. The temperature of 50% crystallisation decreases linearly with increasing cooling rate. This data show that the cooling rate influences the rate of crystallisation of T6T6T. These results suggest that the observed difference between PPE-2T/C12/T6T6T copolymers with the same molecular weight and T6T6T content in DMA can be a result of difference in cooling rate.

A simple method to characterise the crystallisability of polymers and their sensitivity towards processing conditions, mainly cooling rates, was proposed by Nadkarni et al^{57,58}. The variation of the undercooling ΔT ($T_{m,peak} - T_{c,onset}$) with cooling rate (λ) can be fitted to a linear equation (Equation 6.3).

$$\Delta T = P * \lambda + \Delta T^0 \quad [^{\circ}\text{C}] \quad \text{Equation 6.3}$$

The degree of undercooling required in the limit of zero cooling rate (ΔT^0) signifies the inherent crystallisability of the polymer. This value is related to the thermodynamic driving force for nucleation. The slope P ([min]) of this line is a process sensitivity factor that accounts for kinetic effects. The variation of the degree of undercooling with cooling rate indicates the ability of polymer molecules to respond to thermal changes. For the data in Table 6.3 the slope P is 0.07 min and $\Delta T^0 = 11^{\circ}\text{C}$. These values are very low and confirm the fast crystallisation of T6T6T in these copolymers.

The rate of crystallisation as expressed by Equation 6.3 of the PPE-2T/C12/T6T6T copolymer is compared with several other polymers in Table 6.4. To compare the P and ΔT^0 values the undercooling was calculated as $T_{m,peak} - T_{c,peak}$ because onset of crystallisation data are not available. Therefore the values of P and ΔT^0 are larger for PPE-2T/C12/T6T6T than mentioned before.

Table 6.4: Slope P and intercept ΔT^0 for several polymers using $\Delta T = T_{m,peak} - T_{c,peak}$.

	P	ΔT^0
	[min]	[$^{\circ}\text{C}$]
PPE-2T/C12/T6T6T	0.15	15
Nylon-4,6 ^{59,60}	0.28	24
Nylon-6 ^{59,60}	0.55	33
PBT ⁶⁰⁻⁶²	0.40	26
PET ⁶¹	1.3	40

From Table 6.4 it can be concluded that the crystallisation of PPE-2T/C12/T6T6T is very fast and less sensitive to changes in cooling rate compared to polyamides and polyesters.

It was not possible to determine isothermal crystallisation data that can be used in the Avrami equation to calculate the rate of crystallisation because the crystallisation was too fast. Ozawa derived a non-isothermal crystallisation kinetics model for crystallisation at a constant cooling

rate by extending the Avrami equation^{58,63,64}. According to this theory, the relative crystallinity θ at temperature T can be calculated with Equation 6.4.

$$\theta(T) = 1 - \exp\left[\frac{-K^*(T)}{\lambda^n}\right] \quad [-] \quad \text{Equation 6.4}$$

In this equation λ is the cooling rate, n is the Avrami exponent and $K^*(T)$ is the cooling crystallisation function at temperature T for non-isothermal crystallisation. The K^* is related to the overall crystallisation rate and indicates how fast crystallisation occurs.

After rewriting and taking the logarithm of the Ozawa equation, Equation 6.5 is obtained.

$$\log\{-\ln[1-\theta(T)]\} = \log K^*(T) - n \log \lambda \quad [-] \quad \text{Equation 6.5}$$

The value of n at a certain temperature can be obtained as the slope of a straight line of a plot of the left term of Equation 6.5 versus $\log \lambda$. When Equation 6.5 is applied to the data of Figure 6.11 at different temperatures the value of n as a function of temperature can be calculated. The results are given in Figure 6.13.

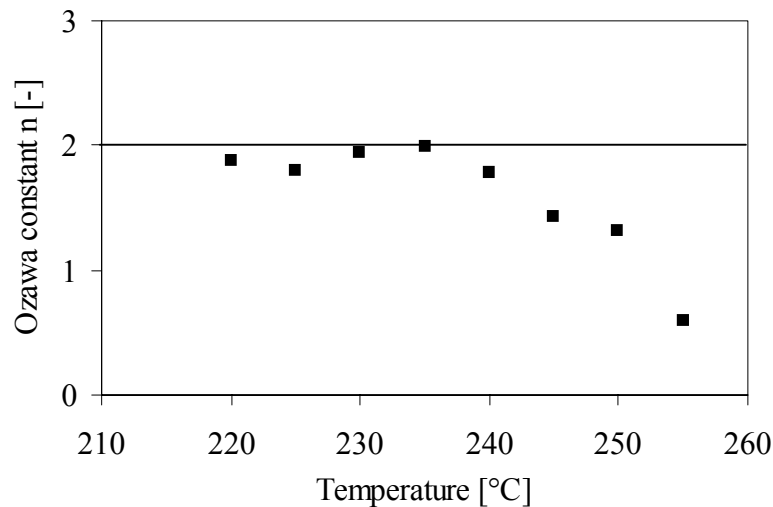


Figure 6.13: Ozawa constant n as a function of temperature as calculated by Equation 6.5.

The Ozawa or Avrami constant n has a value of 2 below 240°C. Above 240°C the value of n is lower, but these data are not so reliable because the error in the relative crystallinity is very high at low cooling rates as the crystallisation peak becomes very small. A value of 2 for n is indicative for 1-dimensional crystal growth with sporadic nucleation and contact as the rate determining step⁶⁵. When n decreases to 1.5 diffusion becomes the rate determining step and for $n=1$ the nucleation mode becomes simultaneous.

WAXD

The crystalline structure of PPE-2T/C12/T6T6T with 13 wt% uniform T6T6T (0.41 dl/g) was studied with WAXD. A melt-pressed sample of 1 mm thickness was prepared in a press at 300°C during 5 minutes with a pressure of 10 bar. Then the sample was cooled down under pressure with a cooling rate of 5°C/min. The strip that was obtained was slightly transparent. A similar strip of PPO-803[®] was prepared according to the same procedure. This strip was transparent. In Figure 6.14 the data of the WAXD experiment on these two strips are given. The difference between the semi-crystalline PPE-2T/C12/T6T6T and the amorphous PPO-803[®] data is given in this figure as well. The data are compared with the WAXD spectrum of the T6T6T-dimethyl segment³⁸.

PPE-2T/C12/T6T6T shows a number of small peaks at $2\Theta = 8, 19, 25, 29$ and 42° . There is one large peak at $2\Theta = 23^\circ$. These peaks become better visible when the spectrum of the amorphous PPO-803[®] is subtracted from the spectrum of the copolymer. In this way the amorphous contribution to the spectrum can roughly be filtered out. It is clear that the peaks that can be found in the spectrum of the copolymer correspond nicely with a peak or a group of peaks of T6T6T-dimethyl³⁸. Peaks of T6T6T can be found at the same positions in the WAXD figure for T6T6T-PTMO/DMT⁴⁵. This suggests that the crystalline structure of T6T6T in PPE and PTMO/DMT is comparable.

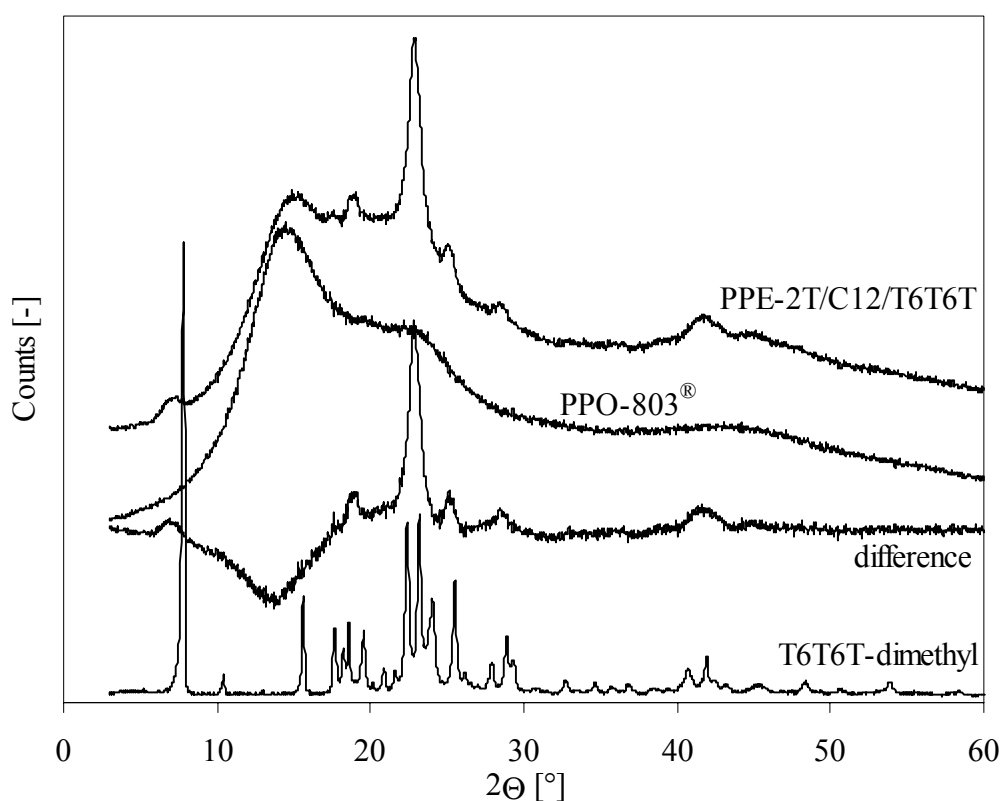


Figure 6.14: WAXD data of PPE-2T/C12/T6T6T, PPO-803[®] and PPO-803[®] subtracted from PPE-2T/C12/T6T6T (difference) compared to T6T6T-dimethyl³⁸.

It was expected that crystallinity would be absent at very high cooling rates. The effect of very high cooling rates on the crystalline structure was studied on a melt-pressed (5 minutes at 300°C) film of 0.1 mm thickness that was quenched in ice-water. The polymer film was prepared between two Teflon sheets and was fluid up to the moment that it was quenched in the ice-water bath. The cooling rate therefore was above 5000°C/min. This thin polymer film was transparent. The expectation was that this film was amorphous.

The WAXD data of this quenched film are compared with the melt-pressed sample of PPE-2T/C12/T6T6T of 1 mm thickness that was obtained after cooling with 5°C/min in Figure 6.15.

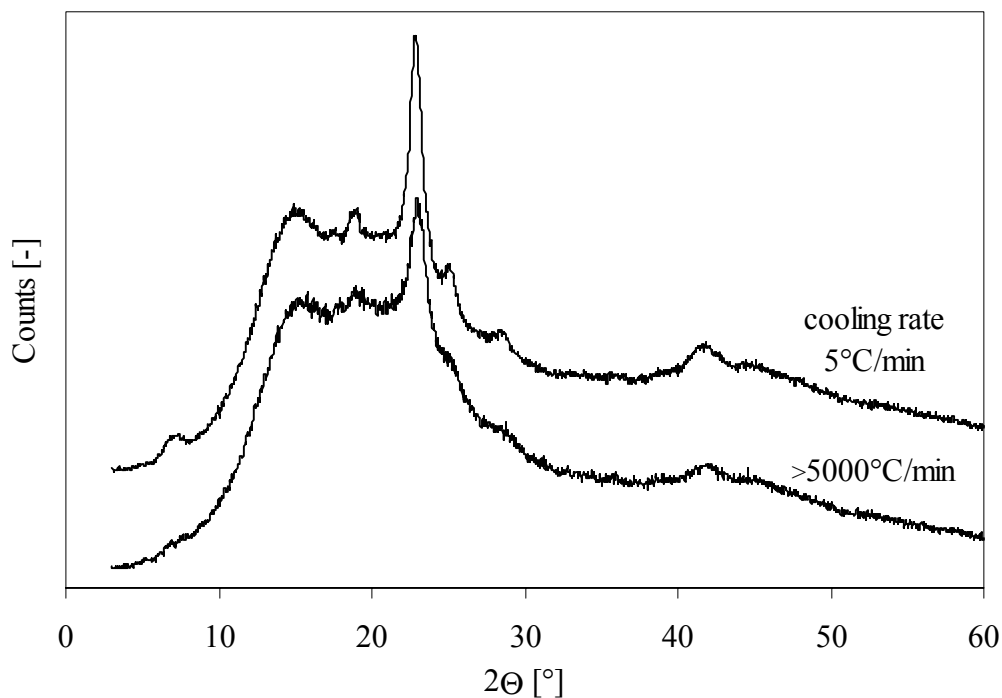


Figure 6.15: WAXD data two PPE-2T/C12/T6T6T melt-pressed sample at 300°C for 5 minutes; one with a thickness of 1 mm and a cooling rate of 5°C/min and one with a thickness of 0.1 mm that was quenched in an ice-water bath (>5000°C/min).

WAXD data show that the quenched sample shows crystalline order despite the very high cooling rate. The peak height of the main peak at $2\Theta = 23^\circ$ is reduced to 60% of the peak in the sample that was cooled with 5°C/min. This can be explained by the fact that the T6T6T units remain largely ordered in the melt and as a result can form ordered structures after fast cooling (Figure 6.5, III).

The influence of temperature on the crystalline structure of T6T6T in PPE-2T/C12/T6T6T with 13 wt% uniform T6T6T was studied by WAXD as well. A melt-pressed sample of 1 mm thickness (at 300°C, cooling rate of 5°C/min) was used for this measurement. The experiment started with a measurement at room temperature and then the temperature was raised to 175°C and further to 300°C with a measurement every 25°C. The sample was measured during cooling with the same temperature steps. The heating and cooling rate were 2°C/min.

The results after heating to 250°C and 300°C are given in Figure 6.16 together with the data for a measurement at room temperature. The relative peak height of the peak at $2\Theta = 22-23^\circ$ is given in Figure 6.17 with the peak height at 25°C at the beginning of the experiment set at 100%.

The peak at $2\Theta = 22-23^\circ$ shifts to lower position and decreases in height when the temperature is increased. This indicates an increase in crystal dimensions and a decrease in crystalline order with increasing temperature respectively.

It is remarkable that the crystalline order at 25°C is higher than that at 175°C with heating as well as cooling. The T_g of this polymer as determined by DMA is 180°C, which means that the modulus of this polymer is high up to this temperature. Nevertheless the order is decreasing (upon heating) or increasing (upon cooling) a little between room temperature and the T_g .

At 300°C, which is well above the melting temperature of $\sim 268^\circ\text{C}$, the peak at $2\Theta = 22-23^\circ$ has still 30% of its original height. So in the melt there is still an ordered T6T6T fraction present. This is probably an ordered T6T6T phase in which the length of the hydrogen bonds is increased and the distance between the T6T6T units is larger than in crystalline T6T6T. For copolymers of PTMO(/DMT) and aromatic di-amide units¹⁵ it was found by IR experiments that the di-amide units remain hydrogen bonded in the melt and that the average hydrogen bond strength decreases with increasing temperature. In the melt these di-amide units are thought to form a smectic crystalline structure.

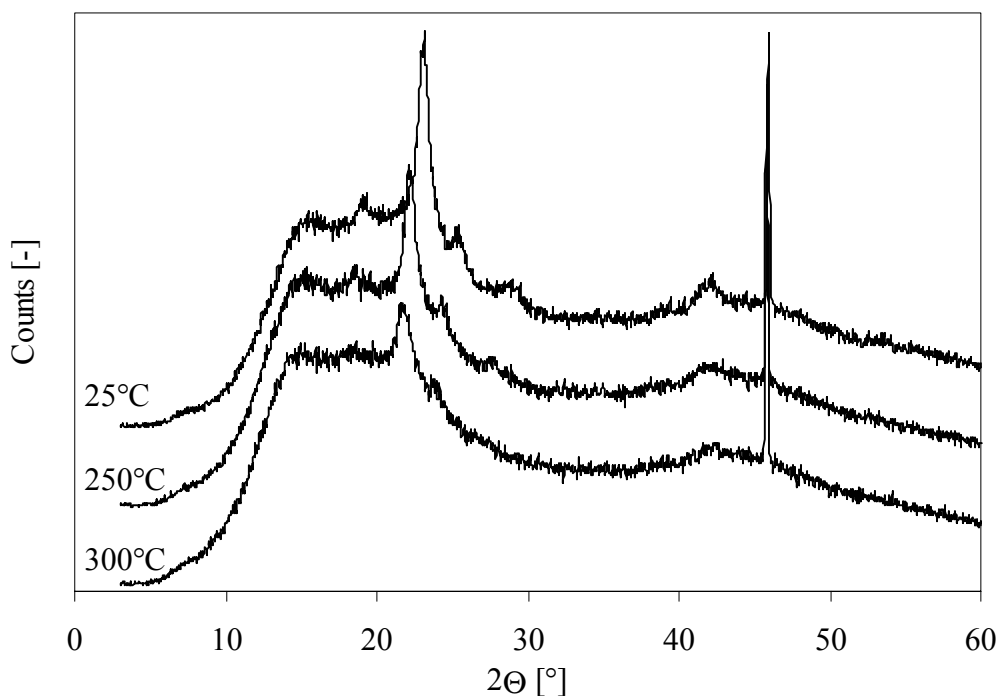


Figure 6.16: WAXD data for a measurement on PPE-2T/C12/T6T6T (13 wt%) at different temperatures; room temperature, 250°C and 300°C as indicated in the figure.

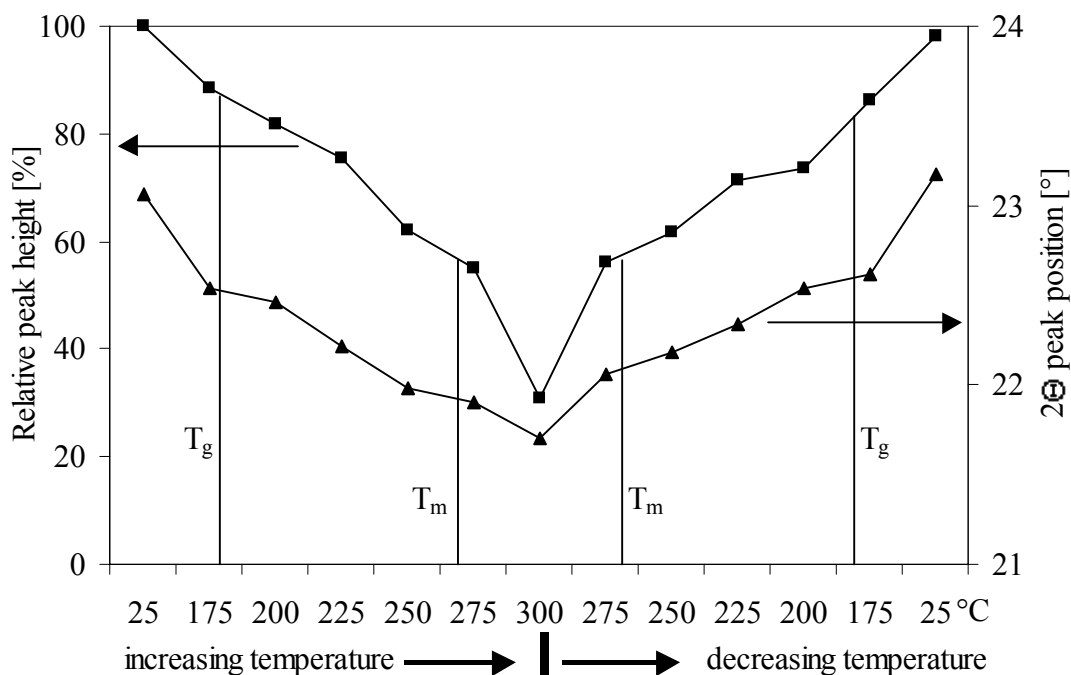


Figure 6.17: Relative peak height (■) and 2θ peak position (▲) of the crystalline peak at $2\theta = 22-23^\circ$.

Water absorption

The water absorption of DMA test bars of PPE-2T/C12/T6T6T with 13 wt% uniform T6T6T and an inherent viscosity of 0.41 dl/g was measured. The water absorption is compared with that of Noryl-GTX[®] and PPO-803[®]. The results are given in Table 6.5.

Table 6.5: Water absorption of PPE-2T/C12/T6T6T with 13 wt% uniform T6T6T compared to Noryl-GTX[®] and PPO-803[®] (20°C, 100% RH).

	7 days [%]	28 days [%]
PPE-2T/C12/T6T6T	0.48	0.48
Noryl-GTX [®]	2.1	3.3
PPO-803 [®]	0.24	0.24

PPO-803[®] has a very low water absorption of 0.24% after one week. The water absorption of the PPE-2T/C12/T6T6T copolymer is 0.48% after one week. The water absorption does not increase further after 7 days. The water absorption of Noryl-GTX is 2.1% after 7 days and 3.3% after 28 days. The maximum water absorption is not reached after 1 week.

PPE-2T/C12/T6T6T copolymer with 13 wt% T6T6T has a lower water absorption than Noryl-GTX[®]. Polyamides are known to have high water absorption. In Noryl-GTX[®] the polyamide content is about three times larger than that of the copolymer. The water absorption of Noryl-GTX is 4 times that of the copolymer after 7 days and almost 7 times after 28 days. So the higher water absorption of Noryl-GTX cannot be ascribed to an

increased polyamide content alone. Probably the fact that a larger part of the polyamide in Noryl-GTX[®] is amorphous accounts for these results. The amorphous polyamide absorbs more water.

Solvent resistance

Next to a low water absorption the copolymer has very good resistance to various solvents as well. The copolymers are not soluble in good solvents for PPE such as toluene and chloroform. Good solvents for the tetra-amide units and polyamides such as the strong acids sulphuric acid, trifluoro acetic acid and hexafluoroisopropanol are not suitable to dissolve the polymers either. Only in the 50/50 phenol/tetrachloroethane mixture that is used to measure the inherent viscosity of the polymers they dissolve after one night stirring at very low concentration (1 g/l). The polymers are also soluble in NMP, the solvent for the polymerisation reaction, but only at low concentration (<5 g/l) and high temperature (>100°C).

Rheology

The melt viscosity of PPE-2T/C12/T6T6T with 13 wt% uniform T6T6T (0.41 and 0.52 dl/g dl/g; resp. 12000 and 16000 g/mol) was studied using a capillary flow rheometer at 300°C. The data of the copolymer are compared with that of Noryl-GTX[®] (GTX914) and PPO-803[®] in Figure 6.18.

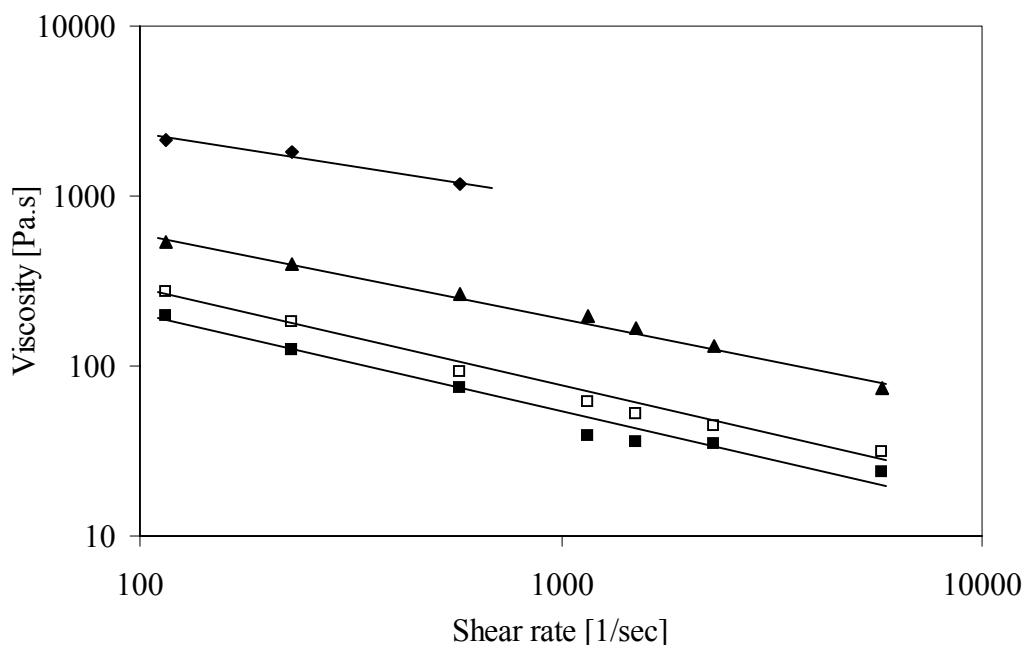


Figure 6.18: Melt viscosity at 300°C as a function of shear rate: (■), PPE-2T/C12/T6T6T (13 wt%, 0.41 dl/g); (□), PPE-2T/C12/T6T6T (13 wt%, 0.52 dl/g); (▲), Noryl-GTX[®]; (◆), PPO-803[®].

The melt viscosity of PPO-803[®] is very high. By blending with polyamide as in Noryl-GTX[®] the processability is improved a lot. At 300°C the PPE-2T/C12/T6T6T copolymers have a much lower melt viscosity than Noryl-GTX[®]. The melt viscosity increases slightly with increasing molecular weight. It can be concluded that the processability of a copolymer of PPE and T6T6T with only 13 wt% of T6T6T is much better than that of PPO-803[®] and Noryl-GTX[®] with 40 wt% of polyamide.

Conclusions

Copolymerisation of PPE with uniform, crystallisable T6T6T units and dodecanediol as an extender is a good method to obtain a semi-crystalline material with a very high T_g/T_{flow} ratio, good solvent resistance and good processability. T6T6T units have a length of ~4 nm. T6T6T is preferred as crystallisable unit over T4T4T because it has a melting temperature of 264-270°C in the copolymer at 13 wt% content. It is particular that the T6T6T units can actually crystallise in these copolymers despite the very high T_g/T_{flow} ratio above 0.8 and low hard segment concentration. The modulus in the rubbery plateau after injection moulding is 7-12 MPa.

The polymers have a high and constant modulus up to their T_g at about 170°C. The T_g is decreased compared to pure PPE due to the incorporation of the flexible dodecanediol as linking unit between the PPE-2T and T6T6T segments. The modulus decreases slightly above 100°C. This is probably due to the presence of a glass transition in the frozen-in ordered T6T6T nano-phases. The materials based on bimodal PPE-2T and 13 wt% T6T6T are slightly transparent, which indicates that no liquid-liquid demixing has taken place.

The crystallinity of T6T6T in a test bar can be improved by a heat treatment step. After heat treatment at 240°C the T_g is increased from 269 to 279°C and the rubber modulus from 10 to 12 MPa. The area peak in the loss modulus around 100°C decreases after heat treatment, which indicates that some T6T6T that is in frozen-in ordered T6T6T nano-phases has crystallised.

It was found that the molecular weight of the product seems to have a large effect on the rate of crystallisation of the polymer. The rubber modulus and flow temperature decrease with increasing molecular weight. With DSC it was measured that the temperature of crystallisation decreases a little while the undercooling increases strongly when the molecular weight increases. From DMA and DSC it was calculated that the crystallinity of T6T6T in the copolymers is between 60 and 80%. The rate of crystallisation decreases dramatically when the cooling rate increases. However with WAXD it was shown that even at very high cooling rates ordered T6T6T is still present. Also the copolymer contains ordered T6T6T above its melting temperature (at 300°C). These results indicate that the tetra-amide units remain organised in the melt.

The PPE-2T/C12/T6T6T copolymers are interesting for applications where a high modulus up to the T_g of PPE is essential in combination with good solvent resistance and good processability. The segmented copolymers can also be useful as compatibiliser for blends of PPE with polyamide.

The tetra-amide segments can also be used in copolymerisation with other amorphous polymers. For example copolymers of polycarbonate with tetra-amide units will be very interesting new materials that are expected to be solvent resistant, semi-crystalline and transparent at the same time.

Literature

1. S.G. Allen, J.C. Bevington, 'Comprehensive polymer science', D.M. White on Poly(phenylene ether), Pergamon Press, New York, 5, 473 (1989).
2. D. Aycock, V. Abolins, D.M. White in 'Encyclopedia Of Polymer Science and Engineering', H.F. Mark, N.M. Bikales, C.G. Overberger, G. Menges, John Wiley & Sons, New York, 13, 1 (1988).
3. Kricheldorf, H.R. in 'Handbook of Polymer Synthesis', Part A, Dekker, New York, 545 (1992).
4. F.E. Karasz, J.M. O'Reilly, J. Polym. Sci. Polym. Lett. Ed., 3, 561 (1965).
5. S. Duff, S. Tsuyama, T. Iwando, F. Fujibayashi, C. Birkinshaw, Polymer, 42, 991 (2001).
6. J. Stehlicek, J. Kovarova, F. Lednicky, Collect. Czech. Chem. Commun., 58, 2437 (1993).
7. J. Stehlicek, R. Puffr, Collect. Czech. Chem. Commun., 58, 2574 (1993).
8. C.S. Han, S.C. Kim, Polym. Bull., 35, 407 (1995).
9. M. Sato, S. Ujiie, Y. Tada, Eur. Polym. J., 34, 405 (1998).
10. M.C.E.J. Niesten, J. Feijen, R.J. Gaymans, Polymer, 41, 8487 (2000).
11. R.J. Gaymans, J. de Haan, Polymer, 34, 4360 (1993).
12. D.W. van Krevelen, 'Properties of Polymers', Elsevier, Amsterdam, Ch. 19, 585 (1990).
13. J. Bicerano, J. Macromol. Sci., C38, 391 (1998).
14. M.C.E.J. Niesten, J.W. ten Brinke, R.J. Gaymans, Polymer, 42, 1461 (2001).
15. M.C.E.J. Niesten, S. Harkema, E. van der Heide, R.J. Gaymans, Polymer, 42, 1131 (2001).
16. A.C.M. van Bennekom, R.J. Gaymans, Polymer, 38, 657 (1997).
17. P.F. van Hutten, R.M. Mangnus, R.J. Gaymans, Polymer, 35, 4193 (1993).
18. D.M. White, J. Polym. Sci., Polym. Chem. Ed., 19, 1367 (1981).
19. W. Risse, W. Heitz, D. Freitag, L. Bottenbruch, Makromol. Chem., 186, 1835 (1985).
20. W. Koch, W. Risse, W. Heitz, Makromol. Chem., Suppl., 12, 105 (1985).
21. W. Heitz, W. Stix, H. Kress, W. Koch, W. Risse, Polym. Prepr. Am. Chem. Soc. Div. Polym. Chem., 25, 136 (1984).
22. H. Nava, V. Percec, J. Polym. Sci. Polym. Chem. Ed., 24, 965 (1986).
23. US 4,665,137, V. Percec (1987).
24. V. Percec, J.H. Wang, Pol. Bull., 24, 493 (1990).
25. H.A.M. van Aert, R. W. Venderbosch, M.H.P. van Genderen, P.J. Lemstra, E.W. Meijer, J.M.S.-Pure Appl. Chem., A32(3), 515 (1995).
26. H.A.M. van Aert, M.H.P. van Genderen, G.J.M.L. van Steenpaal, L. Nelissen, E.W. Meijer, J. Liska, Macromolecules, 30, 6056 (1997).
27. Chapter 2 of this thesis.
28. H.S.-I. Chao, J.M. Whalen, React. Polym. 15, 9 (1991).
29. H.S.-I. Chao, T.W. Hovetter, Polym. Bull., 17, 423 (1987).
30. US 5,015,698, Sybert et al (1991).
31. US 4,746,708, Sybert (1988).
32. Chapter 3 of this thesis.
33. M.C.E.J. Niesten, H. Bosch, R.J. Gaymans, J. Appl. Polym. Sci., 81, 1605 (2001).
34. E. Sorta, G. della Fortuna, Polymer, 21, 728 (1980).
35. G. Perego, M. Cesart, G. della Fortuna, J. Appl. Polym. Sci., 29, 1141 (1984).

36. L. Guang, R.J. Gaymans, *Polymer*, 38, 4891 (1997).
37. J.D. Hoffman, J.J. Weeks, *J. Res. Nat. Bur. Stand., Sect. A*, 66, 13 (1962).
38. Chapter 5 of this thesis.
39. L.L. Harrell, *Macromolecules*, 2, 607 (1969).
40. H.N. Ng, A.E. Allegrazza, R.W. Seymour, S.L. Cooper, *Polymer*, 14, 255 (1973).
41. C.D. Eisenbach, M. Baumgartner, G. Gunter, in 'Advances in Elastomer and Rubber Elasticity, Proc. Symposium', J. Lal and J. E. Mark Eds., Plenum Press, New York, 51 (1985).
42. J.A. Miller, B.L. Shaow, K.K.S. Hwang, K.S. Wu, P.E. Gibson, S.L. Cooper, *Macromolecules*, 18, 32 (1985).
43. Chapter 4 of this thesis.
44. M.C.E.J. Niesten, R.J. Gaymans, *Polymer*, 42, 6199 (2001).
45. Chapter 9 of this thesis.
46. L. Zhu, G. Wegner, *Makromol. Chem.*, 182, 3625 (1981).
47. B.B. Sauer, R.S. McLean, R.R. Thomas, *Polym. Int.*, 49, 449 (2000).
48. Y. Mubarak, E.M.A. Harkin-Jones, P.J. Martin, M. Ahmad, III Jordanian Chemical Engineering Conference, vol. I, 49 (1999).
49. Y. Mubarak, E.M.A. Harkin-Jones, P.J. Martin, M. Ahmad, *Polymer*, 42, 3171 (2001).
50. D. Garcia, H. Starkweather, *J. Polym. Sci. Phys. Ed.*, 32, 537 (1985).
51. C. Ramesh, A. Keller, S.J.E.A. Eltink, *Polymer*, 35, 5293 (1994).
52. M. Todoki, T. Kawaguchi, *J. Polym. Sci. Phys. Ed.*, 15, 1067 (1977).
53. J. Hirschinger, H. Miura, K.H. Gardner, A.D. English, *Macromolecules*, 23, 2153 (1990).
54. P.W. Morgan, S.L. Kwolek, *Macromolecules*, 8, 104 (1975).
55. G. Wegner, Chapter 12 in: 'Thermoplastic Elastomers', N.R. Legge, G. Holden, H.E. Schroeder, First Ed., Carl Hanser Verlag, Munich (1987).
56. P.J. Flory, *Trans. Faraday Soc.*, 51, 848 (1955).
57. V.M. Nadkarni, N.N. Bulakh, J.P. Jog, *Adv. Polym. Technol.*, 12, 73 (1993).
58. M.L. Di Lorenzo, C. Silvestre, *Prog. Polym. Sci.*, 24, 917 (1999).
59. E. Roerdink, J.M.M. Warnier, *Polymer*, 26, 1582 (1984).
60. C. Koning, G.W. Buning, *Recent Res. Devel. Macromol. Res.*, 4, 1 (1999).
61. K. Bouma, R.J. Gaymans, *Polym. Eng. Sci.*, 41, 466 (2001).
62. A.C.M. van Bennekom, R.J. Gaymans, *Polymer*, 38, 657 (1997).
63. T. Ozawa, *Polymer*, 12, 150 (1971).
64. Y. Mubarak, E.M.A. Harkin-Jones, P.J. Martin, M. Ahmad, *Polymer*, 42, 3171 (2001).
65. P.C. Hiemenz, 'Polymer Chemistry', Marcel Dekker Inc., New York, p. 227 (1984)

Chapter 7

Thermal-mechanical properties of copolymers of PPE, dodecanediol and tetra-amide units

Abstract

Copolymers of telechelic poly(2,6-dimethyl-1,4-phenylene ether) segments with terephthalic methyl ester endgroups (PPE-2T), uniform crystallisable T6T6T units (two-and-a-half repeating unit of nylon-6,T, 8-20 wt%) and dodecanediol as an extender were made via a polycondensation reaction. The maximum reaction temperature was 280°C. The products are semi-crystalline materials with a high T_g/T_m ratio above 0.8. The modulus is high and constant up to the T_g around 170-180°C. The modulus of the rubbery plateau increases with increasing crystalline T6T6T (3-15 MPa) content and can be tuned by changing the amount of T6T6T in the copolymer or by improving the crystallinity of T6T6T. With increasing amount of crystalline T6T6T the flow temperature increases slightly as well (260-275°C). The materials are transparent when the T6T6T content is below 15 wt%. The crystallinity of T6T6T in PPE-2T/C12/T6T6T based on bimodal PPE-2T as calculated from DMA is between 54 and 94%. In copolymers based on fractionated, monomodal PPE-2T segments the crystallinity of T6T6T is very low (<30%). This is probably the result of better interaction between short monomodal PPE-2T and T6T6T as compared to bimodal PPE-2T and T6T6T. The uniformity of the T6T6T units seems to have little effect on the properties of the copolymer, as long as it is above 70%. At very low uniformity (<50%) the flow temperature is considerably broadened.

Introduction

Segmented copolymers consisting of amorphous poly(2,6-dimethyl-1,4-phenylene ether) (PPE) segments and crystallisable T6T6T units (13 wt%) with dodecanediol as an extender have very good properties¹. Surprisingly these copolymers are semi-crystalline materials. The polymers have a high T_g of $\sim 170^\circ\text{C}$, a high melting temperature of $\sim 270^\circ\text{C}$ and an extremely high T_g/T_m ratio above 0.8. Despite this high T_g/T_m ratio a rubbery plateau is observed with a modulus of $\sim 7\text{-}12$ MPa. This is very particular because normally crystallisation is absent at such a high T_g/T_m ratio^{2,3}. It was concluded that the crystallisation of the T6T6T units in the copolymer is extremely fast and that these units already order in the melt. The copolymers are also slightly transparent and have good processability, good solvent resistance and low water absorption¹.

The segmented polyether-esteramide copolymers were made via a polycondensation reaction using telechelic PPE-2T, T6T6T-dimethyl and dodecanediol (C12) as an extender (Figure 7.1)¹. The PPE-2T segments were made by redistribution or depolymerisation of high molecular weight PPE with tetramethyl bisphenol A followed by endgroup modification with methyl chlorocarbonyl benzoate (MCCB)⁴. These PPE segments have a bimodal molecular weight distribution because part of the high molecular weight starting material was not depolymerised^{4,5}. The number average molecular weight of the PPE-2T segments is around 3000 g/mol. The T6T6T-dimethyl segments were made in a two-step reaction⁶.

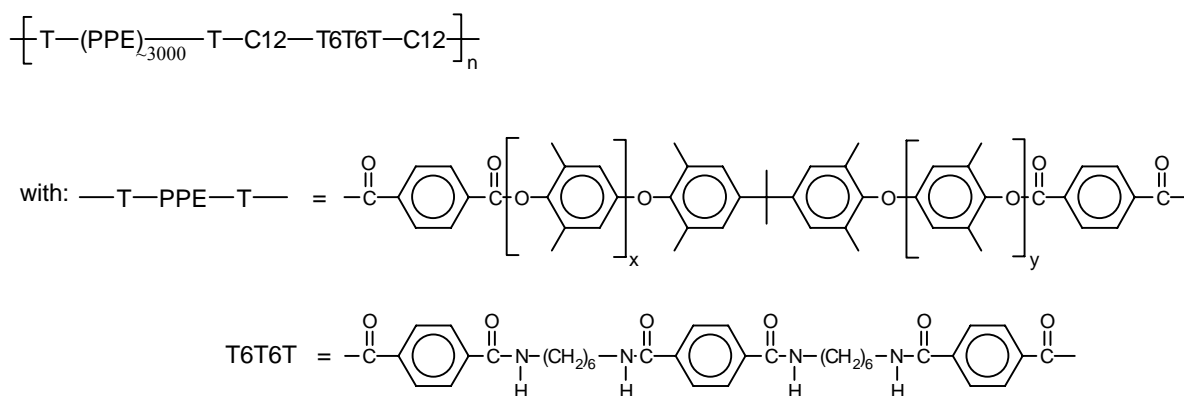


Figure 7.1: Schematic structure of a PPE-2T/C12/T6T6T copolymer.

The copolymer of PPE-2T, a diol and T6T6T-dimethyl is a mixture of PPE-2T/diol/T6T6T copolymer and unreacted high molecular weight PPE. Some of these unreacted PPE chains can be present in the copolymer as an endgroup because they contain a methyl ester endgroup as a result of the reaction of a Mannich base type endgroup with MCCB^{4,7}.

Morphology

It is expected that the morphology of segmented copolymers based on PPE and uniform tetra-amide units is comparable with that of PTMO with uniform di-amide units⁸ or tetra-amide units⁹. The uniform crystalline segments form thread or ribbon-like structures with a very

high aspect ratio⁸⁻¹¹. This morphology was confirmed by AFM experiments⁹. The crystalline ribbons act as physical crosslinks and reinforcing fibres for the amorphous phase. With such a morphology the crystalline content has a strong effect on the modulus. When the ribbons are not stacked into spherulites then the copolymer will be transparent. At high amide contents spherulitic structures can be formed and transparency will be lost¹¹.

A model for the crystalline structure of a PPE-2T/C12/T6T6T segmented copolymer based on bimodal PPE-2T with an average length of 3100 g/mol that contains ~13 wt% T6T6T is given in Figure 7.2¹. In these copolymers the PPE-2T endgroup and T6T6T endgroup molar contents are equal. As a result of the random reaction between PPE-2T, diol and T6T6T-dimethyl some PPE-2T will be coupled directly via dodecanediol (-PPE-C12-PPE-) as well as some T6T6T segments (-C12-T6T6T-C12-T6T6T-C12-). The product is a mixture of PPE-2T/C12/T6T6T copolymer and high molecular weight PPE chains that were not redistributed. Some of these high molecular weight PPE chains can be present in the copolymer as an endgroup because some of their Mannich base type endgroups are transferred into methyl ester endgroups^{4,7}.

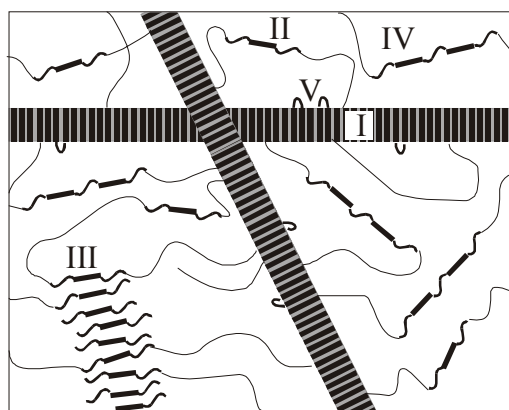


Figure 7.2: Different possible morphologies for PPE-2T/C12/T6T6T copolymers: (I), crystalline T6T6T ribbons; (II), amorphous T6T6T units, mixed with PPE; (III), ordered T6T6T phase; (IV), amorphous diol-extended T6T6T units; (V), chain-folded crystalline diol-extended T6T6T units.

Most T6T6T units will crystallise to threads or ribbon-like structures (I) of ~4 nm thickness with high aspect ratio and some will be amorphous and mixed with the amorphous PPE phase (II). In PTMO/tetra-amide⁹ the length of the crystalline ribbons can be 500 nm.

It was found that the tetra-amide units are still ordered in the melt¹, like the di-amides in PTMO/di-amide¹²⁻¹⁶. It is thought that crystallisation of T6T6T takes place from these ordered T6T6T in the melt upon cooling. However, due to the high T_g/T_m ratio, crystallisation is incomplete. Therefore it can be expected that after cooling the non-crystalline T6T6T units are still ordered in a sort of frozen-in T6T6T domains. The dimensions of such ordered T6T6T domains (III) will be comparable with that of the crystalline lamellae I, which is at a nano-scale.

It is expected that the diol-extended T6T6T segments are still miscible with PPE and are present in the amorphous PPE phase (IV). It is also possible that some diol-extended T6T6T

units crystallise after chain folding (V) or over their full length. Crystallisation of diol-extended T6T6T over their full length will lead to crystals with increased lamellar thickness (thicker ribbons) with a higher melting temperature¹⁷. In PTMO/di-amide copolymers diol-extended di-amide units crystallise over their full length with a higher melting temperature for diol lengths up to ~ 500 g/mol¹⁸. Chain folding should be possible with butanediol and longer diols.

The T_g of the amorphous PPE phase will be reduced due to the presence of the amorphous T6T6T units (II and IV) and the dodecanediol extender. Also the dodecanediol that is at the interphase between amorphous PPE and T6T6T crystalline ribbons will probably decrease the T_g of the PPE phase.

When the segment lengths (PPE and T6T6T/diol) are long enough, phase separation (melt phasing or liquid-liquid demixing) can occur. Phase separation will occur more readily when the segment length increases, thus with long diols or long diol-extended T6T6T segments (at high T6T6T concentration). Such phase separated domains already exist in the melt and have a spherical shape and dimensions >100 nm (not shown in Figure 7.2). As a result of the presence of phase separated domains light is scattered and the material will not be transparent. Phase separated amorphous T6T6T(/C12) domains are not present in PPE-2T/C12/T6T6T¹ that contain 13 wt% T6T6T because these copolymers are slightly transparent, which indicates that only T6T6T nano-phases (I and III) can be present.

Aim

In this chapter the synthesis and thermal-mechanical properties of semi-crystalline segmented copolymers based on PPE-2T ($M_n \sim 3100$ g/mol), dodecanediol and T6T6T-dimethyl units are described. Different polymer series in which the T6T6T content was varied were studied. Polymers made from either bimodal or fractionated, monomodal PPE-2T will be compared and the influence of the uniformity of T6T6T on the properties will be discussed. The influence of crystallinity on the rubber modulus and flow temperature will be discussed as well.

Experimental

Materials. 1,12-Dodecanediol (C12) and N-methyl-2-pyrrolidone (NMP) were purchased from Merck. Tetraisopropyl orthotitanate ($Ti(i-OC_3H_7)_4$), obtained from Merck, was diluted in anhydrous *m*-xylene (0.05M), obtained from Fluka. PPO-803[®] (11.000 g/mol) and Noryl-GTX[®] (GTX914) were obtained from GE Plastics (The Netherlands). All chemicals were used as received. T6T6T-dimethyl was synthesised as described in Chapter 5⁶. Bimodal PPE-2T of 3700 g/mol (480 μ mol OCH_3 /gram) was made in a two-step reaction and bimodal PPE-2T of 3100 g/mol (573 μ mol OCH_3 /gram) was made in a one-pot reaction as described in Chapter 2⁴. Monomodal PPE-2T that was obtained after partial precipitation (1600 g/mol, 1088 μ mol OCH_3 /gram) was used as well⁴. The PPE-2T/C12/T6T6T copolymers were synthesised according to the method described in Chapter 6¹.

Viscometry. The inherent viscosity of the polymers was determined with a capillary Ubbelohde type 1B at 25°C, using a polymer solution with a concentration of 0.1 g/dl in phenol/1,1,2,2-tetrachloroethane (50/50, mol/mol).

DMA. Samples for the DMA test (70x9x2 mm) were prepared on an Arburg-H manual injection moulding machine. Before use, the samples were dried in a vacuum oven at 80°C overnight. The torsion behaviour was studied at a frequency of 1 Hz, a strain of 0.1% and a heating rate of 1°C/min using a Myrenne ATM3 torsion pendulum. The storage modulus G' and loss modulus G'' were measured as a function of temperature starting at -100°C. The glass transition temperature (T_g) was expressed as the temperature at which the loss modulus G'' has a maximum. This maximum was 0-10°C lower than the actual glass transition temperature, because with this DMA apparatus it was not possible to measure a few points around the T_g due to the very high damping. The modulus of the rubbery plateau was determined at 40°C above the T_g . The flow temperature (T_{flow}) was defined as the temperature where the storage modulus G' reached 0.5 MPa. The flow temperature indicates the onset of melting. When the T_{flow} is sharp it is only a few degrees below the melting temperature (T_m) and the T_g/T_{flow} ratio (K/K) is about the same as the T_g/T_m ratio.

Results and Discussion

Copolymers of PPE-2T, dodecanediol (C12) and T6T6T-dimethyl were made via a polycondensation reaction using a maximum temperature of 280°C as was discussed in Chapter 6¹. All copolymers could be obtained easily with high molecular weights as compared to PPO-803[®]. The thermal-mechanical properties of different series of copolymers will be discussed successively:

1. Bimodal PPE-2T (PPE-2T(B), 3100 g/mol), dodecanediol and varying T6T6T content.
2. Fractionated, monomodal PPE-2T (PPE-2T(A), 1600 g/mol), dodecanediol and varying T6T6T content.
3. Bimodal PPE-2T (PPE-2T(B), 3100 g/mol and PPE-2T(C), 3700 g/mol), dodecanediol and varying T6T6T uniformity at constant T6T6T content.

In particular the effect of composition on glass transition temperature, rubber modulus, flow temperature and crystallinity will be studied.

Thermal-mechanical properties

The polymers were injection moulded into bars and dried in a vacuum oven at 80°C. Injection moulding was done at 50-100°C above the melting temperature with a manual injection moulding machine in an unheated mould. The thermal-mechanical properties were measured by DMA. The results are given in Table 7.1.

The T6T6T content was calculated, assuming that the ester carbonyl does not crystallise and belongs to the amorphous phase¹². The uniformity of T6T6T (Table 7.1) is the uniformity of the starting material T6T6T-dimethyl⁶. The uniformity is the amount of T6T6T-dimethyl in

the starting material. When the uniformity is below 100% the crystallisable segment contains T6T6T6T-dimethyl and T6T6T6T6T-dimethyl as well⁶. When the uniformity is 100%, T6T6T does not contain T(6T)_n units with n>2. It is assumed that the uniformity of the T6T6T units is preserved during the polymerisation reaction^{1,9}.

Table 7.1: Properties of the PPE-2T/C12/T6T6T copolymers (series 1-3).

	M _n PPE-2T [g/mol]	Purity T6T6T [%]	T6T6T content [wt%]	η _{inh} [dl/g]	T _g [°C]	G' (at T _g + 40°C) [MPa]	T _{flow} [°C]	T _g /T _{flow} [-]
Starting materials:								
PPO-803 [®]	-	-	-	0.37 ^d	200	-	222	-
PPE-2T(A) ^a	1600	-	-	0.08 ^d	148 ^c	-	-	-
PPE-2T(B) ^b	3100	-	-	0.18 ^d	168 ^c	-	-	-
PPE-2T(C) ^c	3700	-	-	0.19 ^d	173 ^c	-	-	-
Series 1: Bimodal PPE-2T								
PPE-2T(B)/C12	3100	-	0	0.31	169	-	193	-
PPE-2T(B)/C12/T6T6T	3100	>98	6	0.32	173	-	209	-
PPE-2T(B)/C12/T6T6T	3100	>98	8	0.53	179	4	263	0.84
PPE-2T(B)/C12/T6T6T	3100	>98	10	0.56	179	6	265	0.84
PPE-2T(B)/C12/T6T6T	3100	>98	11	0.48	178	5	264	0.84
PPE-2T(B)/C12/T6T6T ¹	3100	>98	13	0.52	164	7	264	0.81
PPE-2T(B)/C12/T6T6T ¹	3100	>98	13	0.41	169	10	269	0.82
PPE-2T(B)/C12/T6T6T	3100	>98	15	0.47	179	11	267	0.84
PPE-2T(B)/C12/T6T6T	3100	>98	20	0.46	180	13	275	0.83
Series 2: Fractionated, monomodal PPE-2T								
PPE-2T(A)/C12 ⁷	1600	-	0	0.34	150	-	182	-
PPE-2T(A)/C12/T6T6T	1600	>98	5	0.38	148	-	197	-
PPE-2T(A)/C12/T6T6T	1600	>98	7	0.40	144	1	208	0.87
PPE-2T(A)/C12/T6T6T	1600	>98	9	0.40	142	2	212	0.86
PPE-2T(A)/C12/T6T6T	1600	>98	11	0.39	143	2	220	0.84
PPE-2T(A)/C12/T6T6T	1600	>98	14	0.41	143	3	232	0.82
Series 3: Uniformity T6T6T								
PPE-2T(B)/C12/T6T6T	3100	>98	11	0.48	179	5	262	0.84
PPE-2T(B)/C12/T6T6T	3100	87	11	0.55	179	5	259	0.85
PPE-2T(B)/C12/T6T6T	3100	80	11	0.46	179	9	268	0.84
PPE-2T(C)/C12/T6T6T	3700	76	12	0.41	184	14	274	0.84
PPE-2T(B)/C12/T6T6T	3100	35	11	0.44	179	8	277	0.82

(a), monomodal product obtained after fractionation⁴; (b), bimodal product made by one-pot synthesis⁴; (c), bimodal product made by two-step synthesis⁴; (d), measured in chloroform instead of phenol/1,1,2,2-tetrachloroethane; (e), measured by DSC instead of DMA

Series 1: Bimodal PPE-2T; T6T6T content

In this polymer series, copolymers of PPE-2T(B) (bimodal, ~3100 g/mol), dodecanediol and uniform T6T6T-dimethyl (>98%) with varying T6T6T content were synthesised. These polymers are based on uniform T6T6T-dimethyl and therefore do not contain T(6T)_n units with n>2⁶.

With 13 wt% of T6T6T the number of methyl ester endgroups of PPE-2T and T6T6T-dimethyl are equal. At this concentration some diol-extended T6T6T (-T6T6T-C12-T6T6T-) will be formed next to alternating PPE/T6T6T (-PPE-C12-T6T6T-C12-) as well because of the random reaction of dodecanediol with PPE-2T or T6T6T-dimethyl. At lower T6T6T content more T6T6T will be linked with PPE on both sides and at higher T6T6T content more diol-extended T6T6T will be formed.

The test bars for DMA of these copolymers with low T6T6T content (<10 wt%) were transparent, but the transparency becomes less at high T6T6T contents (>15 wt%). Probably at higher T6T6T content the ribbons can no longer be randomly distributed and are ordered into spherulites. It is also possible that some phase separation occurs during the copolymerisation reaction (melt phasing or liquid-liquid dimixing), because the number of diol-extended T6T6T segments increases with increasing T6T6T content. With increasing segment length the miscibility decreases. When the phase separated domains are large enough (>100 nm) the polymer will lose its transparency too.

The inherent viscosity and thus the molecular weight of the copolymers in series 1 varies between 0.31 and 0.56 dl/g. In chapter 6¹ it was concluded that the molecular weight influences the crystallisation of T6T6T. Also processing conditions were thought to influence the crystallisation. Therefore differences in DMA behaviour may occur that are not related to the T6T6T content only.

The DMA results for the PPE-2T(B)/C12/T6T6T copolymers of series 1 are given in Table 7.1 and Figure 7.3.

The PPE-2T(B)/C12/T6T6T copolymers show a rubbery plateau above 8 wt% T6T6T content. In this series there is a broad range in molecular weight of the copolymers and this was found to influence the crystallisability of T6T6T¹. Also other factors such as processing conditions can influence the crystallinity of T6T6T¹. When the crystallinity increases, the rubber modulus and flow temperature increase. The rubber modulus and flow temperature increase with increasing T6T6T content for most copolymers of this series. However some copolymers clearly have a lower crystallinity than expected based on their T6T6T content.

The T_g's of the copolymers of series 1 are higher than that of the amorphous fully miscible PPE-2T(B)/C12 copolymer, although the dodecanediol content is higher. With dodecanediol the mobility in the amorphous PPE phase increases and as a result the T_g decreases. So when T6T6T is incorporated less dodecanediol is mixed with the amorphous PPE phase. Most dodecanediol is at the interphase between T6T6T crystalline ribbons and the PPE phase. Some dodecanediol is at the interphase of the ordered T6T6T nano-phases and the PPE phase. Probably the dodecanediol interphase between PPE and the T6T6T does not influence the T_g of PPE as much as when it is completely mixed with PPE as in the PPE-2T/C12 copolymer. As a result the PPE phase is more pure and has a T_g more close to that of PPE (~200°C)⁷.

With increasing T6T6T content the dodecanediol content increases while the T_g remains approximately constant. Apparently the amount of -C12-T6T6T-C12- and C12-extended T6T6T in the PPE phase remains constant with increasing T6T6T content. When more dodecanediol and T6T6T would mix with the amorphous PPE phase a decrease in T_g with increasing T6T6T content should be found⁷.

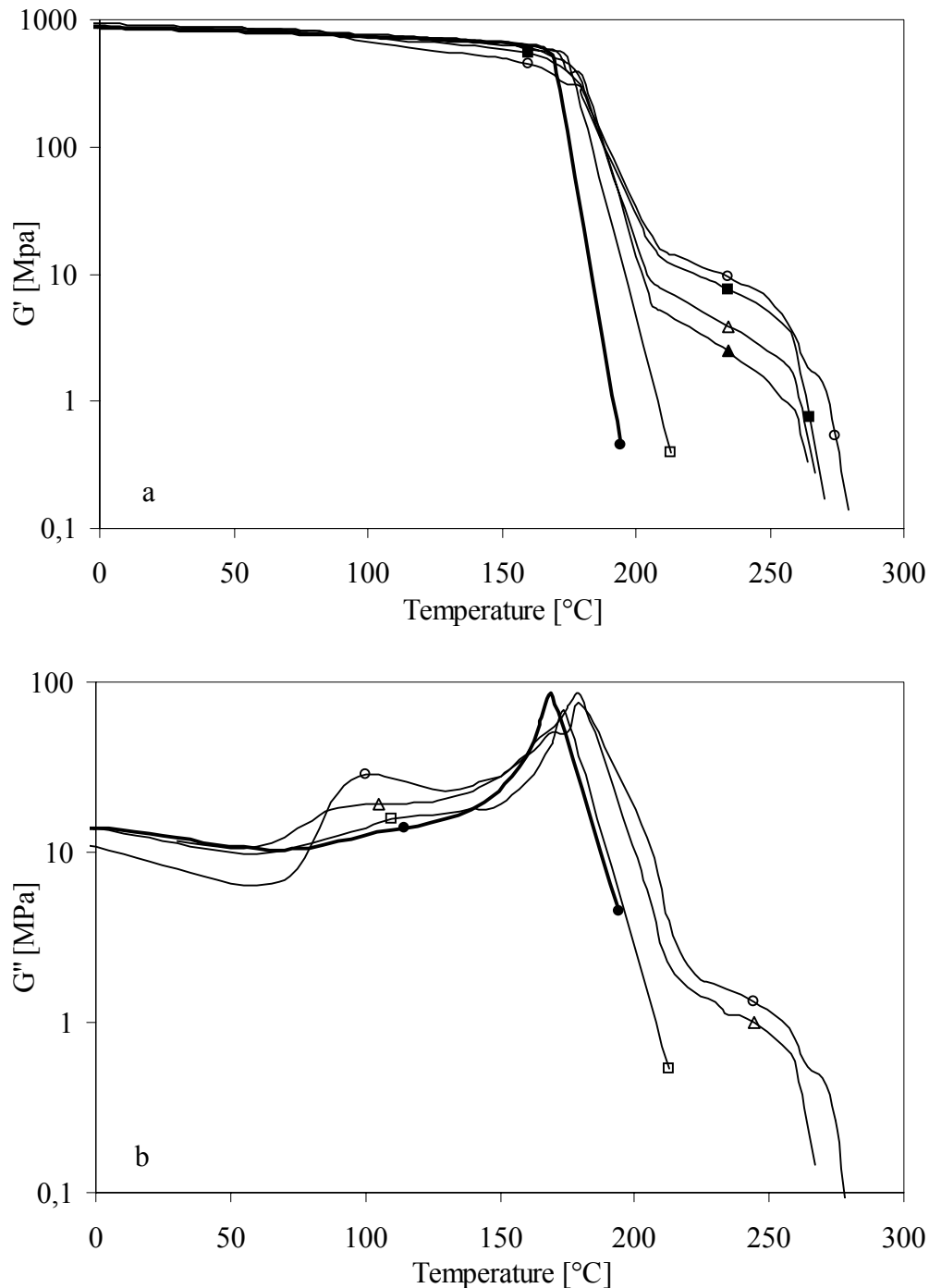


Figure 7.3: Storage (a) and loss (b) modulus for PPE-2T(B)/C12/T6T6T copolymers with 0-20 wt% of uniform T6T6T and bimodal PPE-2T (series 1): (●), 0 wt%; (□), 6 wt%; (▲), 8 wt%; (△), 10 wt%; (■), 15 wt%; (○), 20 wt%.

The modulus of the polymers of series 1 is high up to the T_g . Above 70°C the modulus drops slightly and there is a peak in the loss modulus around 100°C. This effect, which can probably be attributed to a crystalline transition in the T6T6T ribbons or a thermal transition in the ordered T6T6T/C12 nano-phase¹, increases with increasing T6T6T content. For PPE-2T/C12/T6T6T copolymers with 13 wt% T6T6T¹ it was concluded that a crystalline transition is not likely to occur.

Only for the polymer with a high T6T6T content of 20 wt% the decrease of the modulus before the T_g and the height of the peak in the loss modulus become substantial. With such a high T6T6T content a lot of T6T6T segments will be linked to each other via dodecanediol to double or triple blocks. Apparently these extended blocks can also be found in the liquid crystalline T6T6T nano-phases. It can also be that these C12-extended T6T6T segments phase separate in spherical domains because they are less miscible with PPE. This phase separation already takes place in the melt (melt phasing) and will occur more readily at long segment lengths¹⁸. The occurrence of melt phasing did not prevent the formation of polymers with a high molecular weight, so melt phasing can only take place on a small scale or during the final stage of the polymerisation reaction. The presence of these amorphous T6T6T/C12 rich domains can also account for the absence of transparency at high T6T6T contents. Copolymers with more than 15 wt% of T6T6T were not transparent. The decreasing transparency with increasing T6T6T content can also be explained by the formation of a spherulitic crystalline morphology at high T6T6T content¹¹.

The modulus of the rubbery plateau increases with increasing T6T6T content, due to increased crystallinity. The effect of T6T6T content on the rubber modulus is strong. The polymer with only 6 wt% of T6T6T does not show a rubbery plateau. Apparently a T6T6T content of at least 8 wt% is necessary to allow crystallisation and to obtain a crystalline structure of ribbons with high aspect ratio that is able to give the material enough dimensional stability above its T_g . Also at low T6T6T content, the crystallisation is low because the melting temperature is lower and as a result the window for crystallisation is more narrow.

The flow temperature increases slightly with increasing T6T6T content, due to increased crystallinity. The copolymer with 20 wt% T6T6T seems to show a double melting transition. Apparently some crystalline lamellae of extended T6T6T-C12-T6T6T are present as well. These extended T6T6T lamellae have a somewhat higher melting temperature than normal T6T6T lamellae because of the increased lamellar thickness^{17,18}.

The influence of T6T6T content and crystallinity on the rubber modulus and flow temperature will be discussed in more detail later on (Figure 7.8).

Series 2: Fractionated, monomodal PPE-2T; T6T6T content

In this polymer series, copolymers of fractionated, monomodal PPE-2T(A) (~1600 g/mol), dodecanediol and uniform T6T6T-dimethyl (>98%) with varying T6T6T content were synthesised. These polymers are based on uniform T6T6T-dimethyl and therefore do not contain T(6T)_n units with $n > 2$ ⁶. The test bars of copolymers of this series were transparent for

all T6T6T contents. The transparency of this copolymer series was much better than that of the copolymers of series 1.

A polymer with equal endgroup concentration of PPE-2T(A) and T6T6T-dimethyl contains 20 wt% T6T6T. With T6T6T contents up to only 14 wt% the polymers in this series will not contain a lot of diol-extended T6T6T segments. The DMA results for these PPE-2T(A)/C12/T6T6T copolymers are given in Table 7.1 and Figure 7.4.

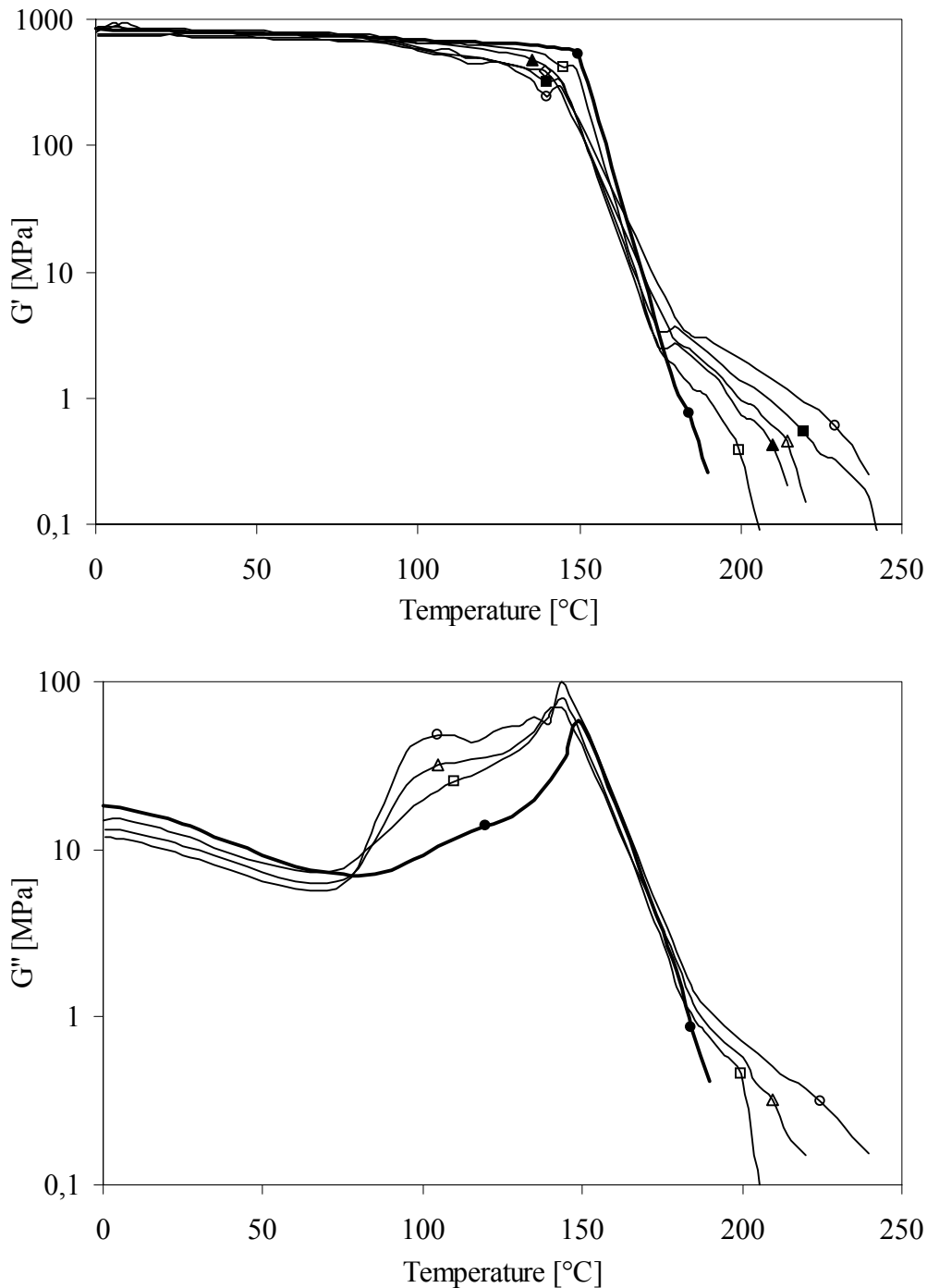


Figure 7.4: Storage (a) and loss (b) modulus for PPE-2T(A)/C12/T6T6T copolymers with 0-14 wt% of uniform T6T6T and fractionated, monomodal PPE-2T (series 2): (●), 0 wt%; (□), 5 wt%; (▲), 7 wt%; (△), 9 wt%; (■), 11 wt%; (○), 14 wt%.

The inherent viscosity of the polymers of series 2 is constant (0.38-0.41 dl/g), which rules out molecular weight or viscosity of the polymer melt as a factor that influences the crystallisation. Therefore we see a gradual increase of modulus of the rubbery plateau and flow temperature with increasing T6T6T content.

The glass transition temperature is rather constant. The T_g is only little lower for copolymers with T6T6T as compared to the amorphous PPE-2T(A)/C12 copolymer. Thus the PPE phase in copolymers with T6T6T does contain a comparable amount of dodecanediol as does the amorphous copolymer. This is in contrast with the polymers of series 1 that show an increased T_g when T6T6T is incorporated. Therefore in series 2 more T6T6T/C12 mixes with the amorphous PPE phase compared to the copolymers of series 1. This can be a result of the absence of the high molecular weight PPE fraction in PPE-2T(A).

In Figure 7.4b the copolymers show a peak in the loss modulus at $\sim 100^\circ\text{C}$ and the height of this peak increases with increasing T6T6T content. This peak in the loss modulus is higher than for series 1. Again this peak can be ascribed to a glass transition of the frozen-in ordered T6T6T nano-phases. So also in series 2 probably not all T6T6T units that are ordered in the melt are able to crystallise upon cooling. Some T6T6T forms frozen-in ordered T6T6T nano-phases in the amorphous PPE phase after processing.

It was expected that the crystallisation of T6T6T in copolymers of series 2 would be better than that of series 1 because of the reduced viscosity of the polymer melt that does not contain the high molecular weight unreacted PPE fraction. The decreased T_g of copolymer based on short, monomodal PPE-2T(A)⁷ is another factor that can enhance the crystallisability. However, the opposite is true. The rubber modulus and flow temperature and thus the crystallinity of T6T6T in this polymer series are much lower than that of series 1. It seems that the miscibility of the PPE-2T(A) segments and the C12-T6T6T-C12 units is better, because the high molecular weight PPE fraction is absent. Also the concentration of terephthalic ester units and dodecanediol units in the copolymers based on PPE-2T(A) is higher, which can influence the miscibility. A better miscibility of PPE and C12-T6T6T-C12 reduces the driving force for crystallisation of T6T6T with as a result a slower crystallisation. The assumed increased interaction between PPE and T6T6T also explains the low flow temperature of copolymers of series 2²⁵. The influence of T6T6T content and crystallinity on rubber modulus and flow temperature will be discussed in more detail later on (Figure 7.8).

In Figure 7.5 the storage and loss modulus of PPE-2T/C12/T6T6T of series 1 and series 2 with 13 and 14 wt% T6T6T respectively are compared.

Figure 7.5 shows what has already been discussed. The rubbery plateau and flow temperature are lower for copolymers based on monomodal PPE-2T (series 2) as compared to bimodal PPE-2T (series 1). Also the glass transition temperature is lower for series 2, because the PPE content is lower and because more C12(-T6T6T-C12) units are mixed with the amorphous PPE phase. The figure also shows that the polymer of series 2 has a larger peak in the loss modulus at $\sim 100^\circ\text{C}$. Thus a larger part of the T6T6T units is not crystallised and is present in ordered T6T6T nano-phases. Both the increased concentration of amorphous T6T6T units in the PPE phase and the larger amount of ordered T6T6T/C12 nano-phase lead to decreased

crystallinity of T6T6T in the copolymers with PPE-2T(A) in series 2. Apparently the better miscibility of short, monomodal PPE and T6T6T for the copolymers of series 2 reduces the driving force for crystallisation.

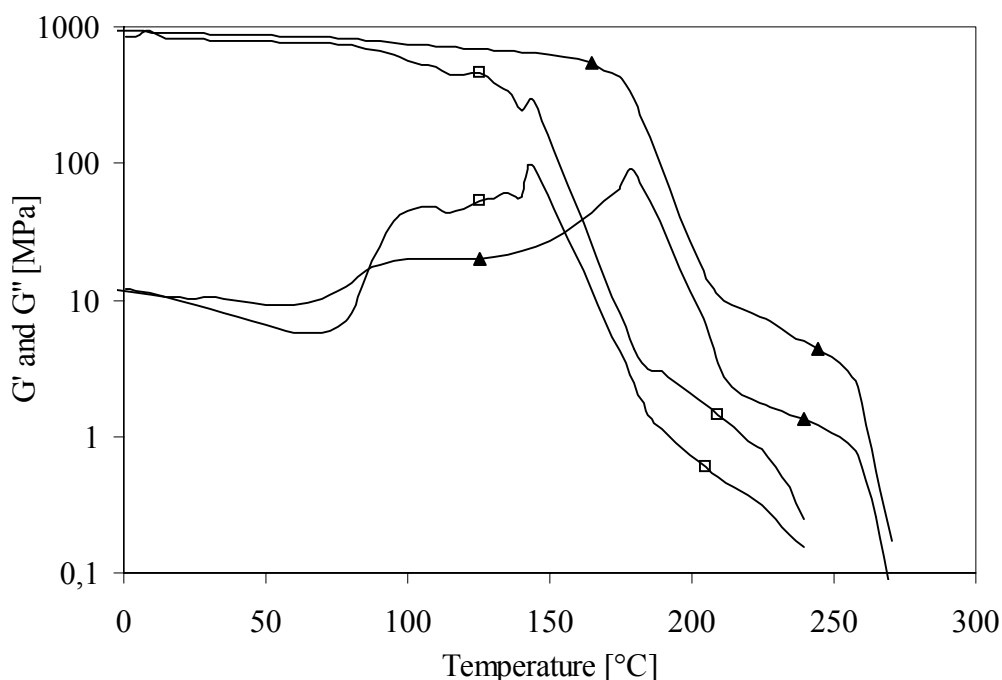


Figure 7.5: Storage and loss modulus for copolymers of series 1 and 2: (▲), bimodal PPE-2T with 13 wt% T6T6T; (□), fractionated, monomodal PPE-2T with 14 wt% T6T6T.

Series 3: Bimodal PPE-2T; T6T6T uniformity

In this polymer series, copolymers of bimodal PPE-2T(B) with an average molecular weight of ~ 3100 g/mol, dodecanediol and T6T6T-dimethyl with varying T6T6T uniformity were synthesised. At a T6T6T content of 13 wt% the PPE-2T and T6T6T-dimethyl endgroup concentration are equal. With decreasing uniformity of T6T6T the number of further reacted $T(6T)_n$ units with $n > 2$ next to T6T6T increases⁶. Because it was not possible to measure the uniformity of the T6T6T units in the polymer after polymerisation, it is assumed that the T6T6T units in the polymers have the same uniformity as the T6T6T-dimethyl that was used as a starting material⁹.

The DMA results for these PPE-2T(B)/C12/T6T6T copolymers are given in Table 7.1. In Figure 7.6 only the storage modulus is given, because the loss modulus does not show large differences between these polymers.

There is no simple relationship between the uniformity of T6T6T and modulus of the rubbery plateau and flow temperature of the polymer. When the rubbery plateau and flow temperature are higher, the degree of crystallinity is higher. The polymers with a uniformity around 80% (that contain 80% of T6T6T and 20% of $T(6T)_n$ units with $n > 2$) seem to have the highest crystallinity as their rubbery plateau and flow temperature are higher. This is unexpected, because it is generally accepted that the crystallisation is better and more complete with

uniform crystallisable units¹⁹⁻²². Therefore, it is more probable that these differences are in fact a result of other parameters such as the molecular weight of the polymer and the conditions for injection moulding. Most copolymers with a higher rubbery plateau were found to have a lower molecular weight (Table 7.1).

The peak in the loss modulus (not given) is comparable to that of PPE-2T/C12/T6T6T copolymers of series 1. The area of this peak decreases somewhat when the height of the rubbery plateau - and thus the crystallinity - increases.

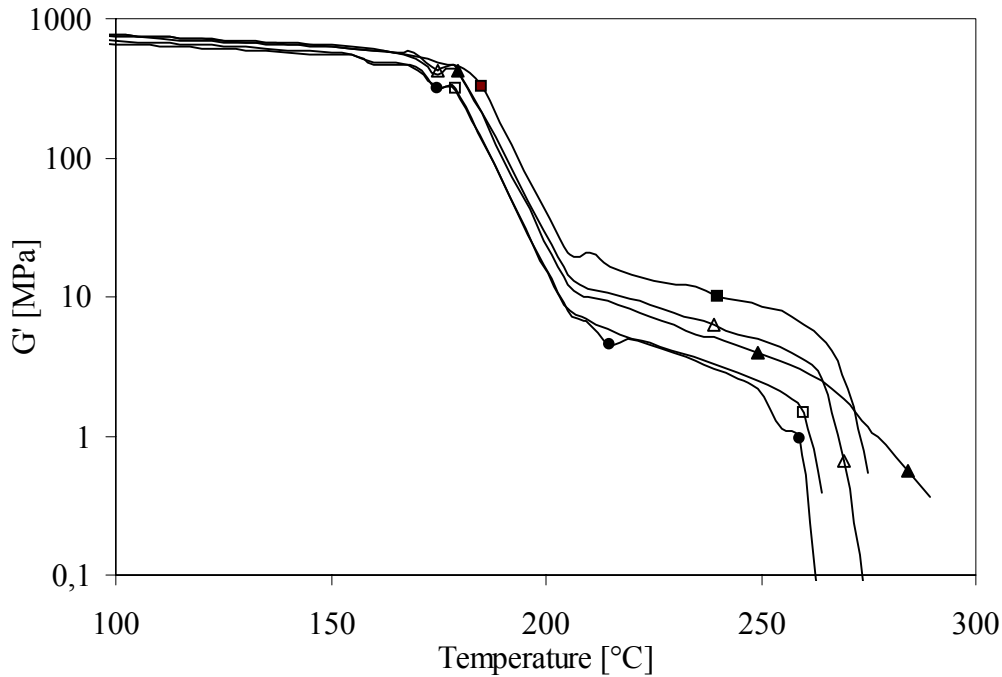


Figure 7.6: Storage modulus for PPE-2T(B)/C12/T6T6T copolymers with 11 wt% of T6T6T of different uniformities: (●), 87% (0.55 dl/g); (□), 98% (0.48 dl/g); (▲), 35% (0.44 dl/g); (△), 80% (0.46 dl/g); (■), 76% (12 wt% T6T6T, PPE-2T(C), 0.41 dl/g).

The flow temperature is only little broadened when the uniformity is decreased to 76%. Apparently there are hardly crystalline lamellae based on T(6T)_n units with n=3 or n=4 present. Only in the polymer with T6T6T with a uniformity of 35% the flow temperature is significantly broadened. In this polymer many hexa-amide and octa-amide units are present. These units are able to crystallise in this polymer and these lamellae have a higher melting temperature¹⁷. T6T6T-PTMO/DMT copolymers show already at a T6T6T uniformity of 76% a broadening of the flow temperature⁹.

The PPE-2T(C)/C12/T6T6T copolymer with 12 wt% T6T6T with a uniformity of 76% (series 3) and an inherent viscosity of 0.41 dl/g (~13.000 g/mol) has the highest modulus and flow temperature of all copolymers discussed in this chapter. It is remarkable that this copolymer is based on bimodal PPE-2T with a higher average molecular weight than that of the other copolymers of series 1 and 3. So probably the interaction between PPE-2T and T6T6T is lower for this copolymer and as a result the driving force for crystallisation is higher.

It can be concluded that copolymers with good thermal-mechanical properties can be obtained when the uniformity of T6T6T is at least 70% and the T6T6T content is 11-12 wt%. The inherent viscosity should preferably be around 0.4 dl/g when a high cooling rate during injection moulding is applied.

Compared to Noryl-GTX[®] (GTX914)¹, which contains about 40% PA-6,6, the rubbery plateau of the PPE-2T(C)/C12/T6T6T copolymer with 12 wt% T6T6T with a uniformity of 76% is almost as high (14 vs. 20 MPa) and the flow temperature is higher (274 vs. 265°C) at only 12 wt% T6T6T. This means that the copolymer has probably enough crystallinity for good solvent resistance¹. Also important is the fact that the copolymer has a very high T_g of 184°C and a high and nearly constant modulus up to this T_g .

Rubber modulus

In Figure 7.7 the logarithm of the rubber modulus at 40°C above the T_g is given as a function of the T6T6T content for copolymers of series 1-3 and T6T6T-PTMO(/DMT)⁹.

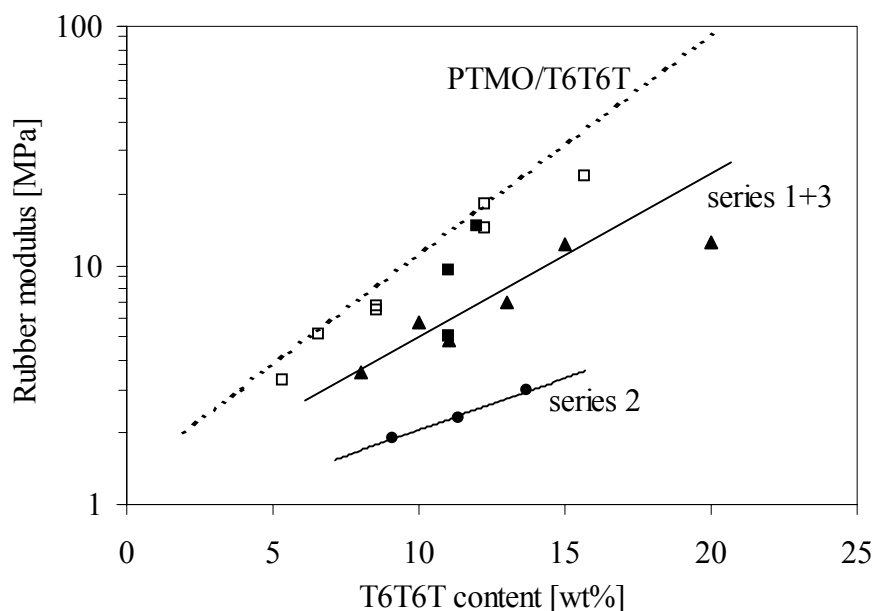


Figure 7.7: Rubber modulus at $T_g + 40^\circ\text{C}$ as a function of T6T6T content: (\blacktriangle), series 1 (bimodal PPE-2T, uniform T6T6T); (\bullet), series 2 (monomodal PPE-2T, uniform T6T6T); (\blacksquare), series 3 (bimodal PPE-2T, non-uniform T6T6T); (\square), T6T6T-PTMO(/DMT) copolymers⁹

A linear increase of the rubber modulus with the amide content was found for T6T6T-PTMO(/DMT)⁹ and other segmented polymers with uniform crystallisable units²³ having a low glass transition temperature below room temperature. According to Wegner²⁴, the logarithm of the modulus in the rubbery plateau of a segmented copolymer follows such a linear relationship with the crystallinity. Equation 7.1 describes this relationship where E is the modulus, E_c is the modulus of the crystalline fraction, E_a is the modulus of the amorphous fraction and x_c is the crystallinity.

$$\log E = \log E_a + x_c \log \frac{E_c}{E_a} \quad \text{Equation 7.1}$$

The rubber modulus shows a strong increase with T6T6T content for T6T6T-PTMO(/DMT) copolymers⁹. The effect of T6T6T content on rubber modulus is strong because the ribbons with a high aspect ratio have a strong reinforcing effect. The rubber modulus increases somewhat less with increasing T6T6T content for PPE-2T/C12/T6T6T copolymers of series 1 and 3 (bimodal PPE-2T), because the crystallinity is probably lower. The logarithm of the rubber modulus increases approximately linear with T6T6T content, but shows large variation. There is a larger variation in the modulus of PPE-2T/C12/T6T6T copolymers compared to T6T6T-PTMO(/DMT) because in Figure 7.7 the rubber modulus is given as function of the T6T6T content. For PPE-2T/C12/T6T6T the crystallisation of T6T6T is not always complete and therefore cannot be related directly to the T6T6T content. The crystallinity will be discussed later on (Equation 7.2).

The modulus in the rubbery plateau for PPE-2T/C12/T6T6T copolymers is much higher for copolymers of series 1 and 3 using bimodal PPE-2T of 3100 g/mol than that of series 2 using short monomodal PPE-2T (1600 g/mol). The rubber modulus of T6T6T-PTMO(/DMT)⁹ is even higher. The rubber modulus is expected to increase with increasing degree of crystallinity or changing crystalline morphology. A difference in morphology is not likely. Most probably the crystallisation of T6T6T in PTMO(/DMT) is more complete because the T_g/T_m ratio is much lower and the window for crystallisation is larger. Also the rubber modulus is higher of T6T6T in bimodal PPE-2T (series 1+3) and thus the crystallisation is more complete than in monomodal PPE-2T (series 2). The PPE-2T used in series 2 does not contain the high molecular weight unreacted PPE fraction and the amount of terephthalic ester units and dodecanediol in this copolymer is higher. Therefore probably the interaction between PPE-2T and T6T6T is higher. As a result the driving force for crystallisation is smaller and the crystallinity of T6T6T is lower.

At higher T6T6T contents (>15 wt%) the rubber modulus is lower than expected according to the linear increase of the rubber modulus with the T6T6T content for both PPE-2T/C12/T6T6T and T6T6T-PTMO(/DMT)⁹ copolymers. This could be explained by the fact that more T6T6T units are extended via dodecanediol for PPE-2T/C12/T6T6T and C12-extended T6T6T is probably less crystallisable. However T6T6T-PTMO(/DMT) does not contain such extended T6T6T units. Therefore this effect above 15 wt% T6T6T can probably be ascribed best to a change in the morphology. At higher T6T6T concentration the T6T6T crystalline ribbons can less easily be randomly distributed and become stacked or ordered in spherulitic structures. The reinforcing effect and therefore the influence on rubber modulus of spherulites is lower than that of ribbons with a high aspect ratio.

Flow temperature

In Figure 7.8 the flow temperature is given as function of the T6T6T content and rubber modulus for copolymers of series 1-3 and T6T6T-PTMO/DMT⁹.

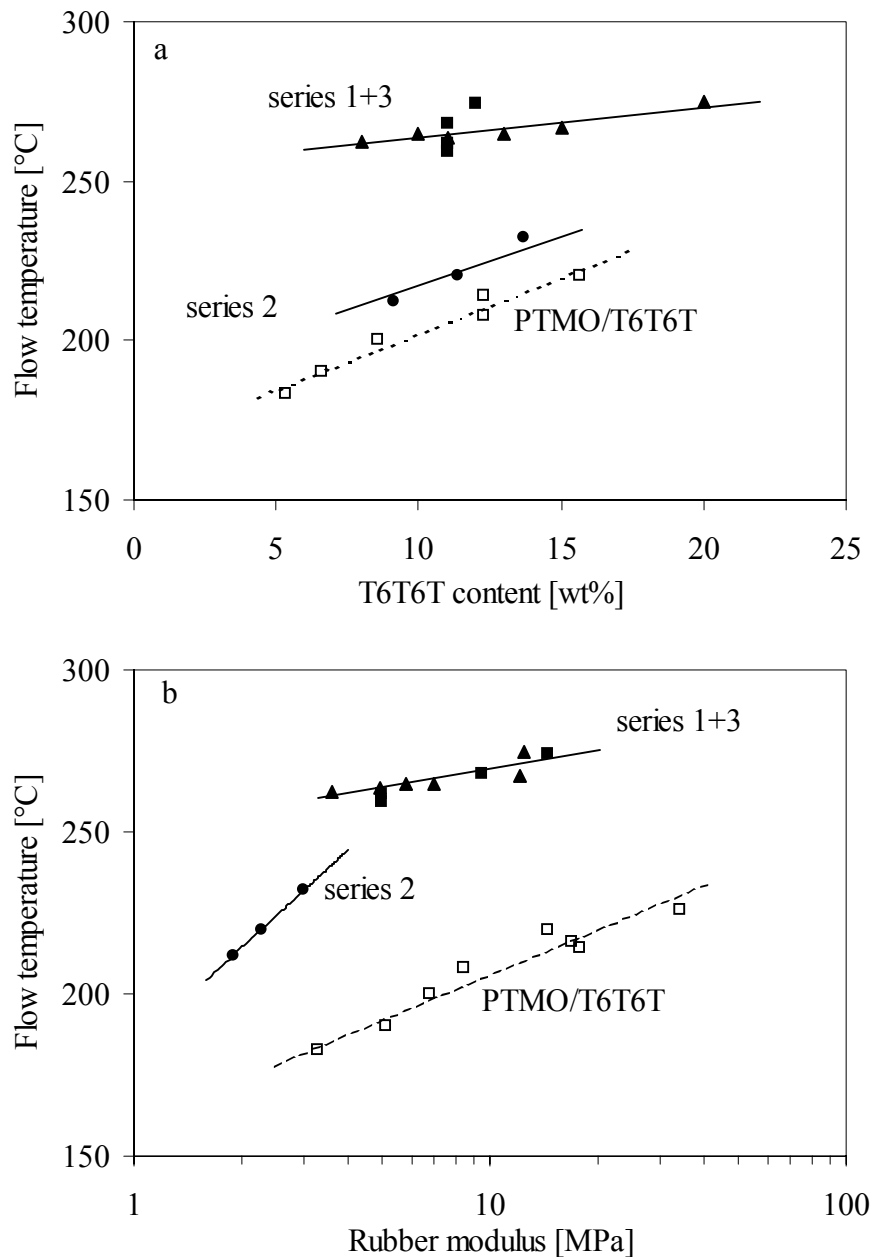


Figure 7.8: Flow temperature as function of (a) the T6T6T content and (b) the logarithm of the rubber modulus at 40°C above T_g : (\blacktriangle), series 1 (bimodal PPE-2T, uniform T6T6T); (\bullet), series 2 (monomodal PPE-2T, uniform T6T6T); (\blacksquare), series 3 (bimodal PPE-2T, non-uniform T6T6T); (\square), T6T6T-PTMO/(DMT) copolymers⁹.

Above 8 wt% T6T6T, when a rubbery plateau is present in series 1 and 3, the flow temperature increases slightly with increasing T6T6T content. The increase is approximately linear with T6T6T content, but the data points show some variation. This variation indicates

that the crystallinity is not directly related to the T6T6T content and that the crystallinity of T6T6T is incomplete and not the same for all copolymers. When the flow temperature is related to the rubber modulus, which is a measure for the crystallinity, the data points show less variation. This can be explained by the fact that the rubber modulus depends in the same way on the crystallinity as the flow temperature.

The flow temperature of the copolymers of series 1 and 3 (bimodal PPE) increases only slightly with T6T6T content. Therefore the solvent effect²⁵ of PPE on the T6T6T crystalline melting point seems small. T6T6T-dimethyl has a melting temperature of 303°C⁶. The flow temperature of T6T6T in the copolymer is 260-275°C and thus the melting temperature is only little lowered by copolymerisation with PPE-2T/C12.

PPE/T6T6T copolymers based on both types of PPE-2T have a higher flow temperature than T6T6T-PTMO(/DMT) copolymers⁹. The flow temperature is expected to increase with increasing lamellar thickness, increasing degree of crystallinity and decreasing interaction. The lamellar thickness is expected to be constant. The degree of crystallinity in PPE-2T/C12/T6T6T is probably lower than in T6T6T-PTMO(/DMT) at a certain T6T6T content. Thus probably a difference in interaction accounts for the much higher flow temperature of T6T6T in PPE. Then the interaction of PPE and T6T6T should be much smaller than that between PTMO(/DMT) and T6T6T. The low compatibility of PPE and T6T6T also explains the fact that crystallisation of T6T6T is possible, despite the high T_g/T_m ratio.

The copolymers of series 2 based on monomodal PPE-2T have a much lower flow temperature than that of series 1 and 3 based on bimodal PPE-2T. It seems that the crystallinity is very low for the copolymers of series 2, as a well-developed rubbery plateau is not present either.

From the difference in height of the rubber modulus (Figure 7.7) it was concluded that the crystallinity of T6T6T is higher for bimodal PPE-2T (series 1+3) than for monomodal PPE-2T (series 2) and as a result the flow temperature is higher for bimodal PPE-2T. However this cannot be the only effect, because then at a certain rubber modulus the flow temperature should be the same for series 1+3 and 2. This is not the case, as is shown in Figure 7.8b. The flow temperature of the copolymers of series 2 is lower at a certain rubber modulus than that of series 1 and 3. A difference in interaction between PPE and T6T6T is thought to be the reason for this behaviour²⁵. Probably the interaction between monomodal PPE-2T/C12 and T6T6T is higher than that between bimodal PPE-2T/C12 and T6T6T. The absence of the high molecular weight PPE fraction in monomodal PPE-2T and the higher concentration of terephthalic ester units and dodecanediol (because of the lower length of the monomodal PPE-2T) in the copolymers of series 2 enhances the miscibility.

Crystallinity

The actual degree of crystallinity of the copolymers can (roughly) be estimated from their rubber modulus and the dependence of the rubber modulus on the T6T6T content for T6T6T-PTMO(/DMT) copolymers^{1,9}. It is assumed that the crystallinity of T6T6T in these T6T6T-PTMO(/DMT) copolymers is 100% and that the crystallinity increases linearly with the

logarithm of the rubber modulus (dashed line Figure 7.7). It is also assumed that the morphology of the PPE-2T/C12/T6T6T copolymers is the same as that of the T6T6T-PTMO(/DMT) copolymers and thus that the effect of crystalline content on rubber modulus is the same. Equation 7.2 gives the relationship between rubber modulus (G' in MPa) and degree of crystallinity (x_c in wt%) for T6T6T-PTMO(/DMT) copolymers⁹. This equation is for copolymers with more than 3 wt% crystallinity.

$$G'(\text{plateau}) = 1.3 \exp(0.21 * x_c) \quad [\text{MPa}] \quad \text{Equation 7.2}$$

The calculated degree of crystallinity and the percentage of the T6T6T that has crystallised for the PPE-2T/C12/T6T6T copolymers of series 1-3 relatively to T6T6T-PTMO(/DMT) are given in Table 7.2.

Table 7.2: Degree of crystallinity and crystallinity of T6T6T in PPE-2T/C12/T6T6T copolymers (series 1 and 3) compared to T6T6T-PTMO(/DMT) copolymers.

	T6T6T content [wt%]	Purity T6T6T [%]	η_{inh} [dl/g]	G' (at T_g + 40°C) [MPa]	Degree of cryst. ^a [wt%]	Crystallinity T6T6T ^b [%]
Series 1: Bimodal PPE-2T						
PPE-2T(B)/C12/T6T6T	8	>98	0.53	4	4.8	60
PPE-2T(B)/C12/T6T6T	10	>98	0.56	6	7.0	70
PPE-2T(B)/C12/T6T6T	11	>98	0.48	5	6.2	56
PPE-2T(B)/C12/T6T6T	13	>98	0.41	10	9.6	74
PPE-2T(B)/C12/T6T6T	13	>98	0.52	7	7.9	61
PPE-2T(B)/C12/T6T6T	15	>98	0.47	11	10.0	67
PPE-2T(B)/C12/T6T6T	20	>98	0.46	13	10.8	54
Series 2: Fractionated, monomodal PPE-2T						
PPE-2T(A)/C12/T6T6T	9	>98	0.40	2	1.8	20
PPE-2T(A)/C12/T6T6T	11	>98	0.39	2	2.7	23
PPE-2T(A)/C12/T6T6T	14	>98	0.41	3	3.9	29
Series 3: Uniformity T6T6T						
PPE-2T(B)/C12/T6T6T	11	>98	0.48	5	6.3	56
PPE-2T(B)/C12/T6T6T	11	87	0.55	5	6.3	56
PPE-2T(B)/C12/T6T6T	11	80	0.46	9	9.3	83
PPE-2T(C)/C12/T6T6T	12	76	0.41	14	11.3	94

(a), the degree of crystallinity of the copolymer was calculated with Equation 7.2 and the rubber modulus relatively to T6T6T-PTMO(/DMT)⁹; (b), the crystallinity of T6T6T (relatively to T6T6T-PTMO(/DMT)) was calculated from the degree of crystallinity in the copolymer and the total T6T6T content of the copolymer

The data in Table 7.2 show that the relative crystallinity of T6T6T in PPE is high for series 1 and 3, despite the high T_g/T_m ratio. The relative crystallinity of T6T6T in PPE for series 1 and 3 is between 54 and 94%. As was concluded before, the crystallinity of T6T6T is much lower (<30%) for series 2 than for series 1 and 3 (>50%).

For series 1 and 3 the crystallisation of the T6T6T units was found to be very sensitive to factors such as molecular weight (viscosity) and processing conditions. The sensitivity of the crystallisation process was already measured by DSC experiments on PPE-2T/C12/T6T6T with 13 wt% uniform T6T6T¹. As a result the crystallinity of T6T6T in the copolymers of series 1 and 3 shows variation. The copolymer with 12 wt% of T6T6T with an uniformity of 76% and bimodal PPE-2T (series 3) has a relative crystallinity of 94%. Therefore it can be concluded that it is possible to obtain PPE/T6T6T copolymers with a very high crystalline T6T6T content, provided that the molecular weight and processing conditions are optimised. The calculated crystallinity of 94% is probably too high, because this copolymer also shows a peak in the loss modulus at ~100°C, which indicates that not all T6T6T has crystallised.

Conclusions

Copolymerisation of PPE with crystallisable T6T6T tetra-amide units with a uniformity above 70% is a good method to obtain a semi-crystalline material with a very high T_g/T_{flow} ratio. It is particular that the T6T6T units can actually crystallise in these copolymers despite the very high T_g/T_{flow} ratio above 0.8 and low T6T6T concentration (8-20 wt%).

Copolymers based on bimodal PPE-2T, dodecanediol and T6T6T have a high and constant modulus up to their T_g around 170-180°C. The T_g is decreased compared to pure PPE due to the incorporation of dodecanediol to link the PPE-2T and T6T6T segments. The moduli of the copolymers decrease slightly above 80°C due to the presence of ordered T6T6T nano-phases. Ordered T6T6T is already present in the melt, but part of it is not able to crystallise during injection moulding. Therefore part of the ordered T6T6T is frozen-in upon cooling from the melt. When the T6T6T content is above 15 wt%, some phase separation of (diol-extended) T6T6T domains might occur as well. As a result the material is not transparent at such high T6T6T concentrations. Another explanation of the decreasing transparency at high T6T6T content is that crystallites become stacked and scatter light at high T6T6T concentration.

The modulus of the rubbery plateau increases strongly with increasing crystalline T6T6T content and can be tuned by changing the amount of T6T6T in the copolymer or by improving the crystallinity of T6T6T. With increasing amount of crystalline T6T6T the flow temperature increases slightly as well. With increasing crystallinity the solvent resistance is expected to increase which is important for many applications.

It is not possible to obtain a nice rubbery plateau with a high modulus and high flow temperature with copolymers based on fractionated, monomodal PPE-2T segments. The reason for this is the very low crystallinity, which is probably the result of better interaction between short monomodal PPE-2T and T6T6T as compared to bimodal PPE-2T and T6T6T. When no high molecular weight PPE is present and with decreasing average length of the PPE segment the crystallinity of T6T6T seems to decrease due to increasing miscibility of PPE-2T and T6T6T. This is probably also due to the increasing amount of terephthalic ester groups and dodecanediol with decreasing average PPE-2T length. As a result of increasing interaction the flow temperature is lower.

The uniformity of the T6T6T units seems to have little effect on the properties of the copolymer, as long as it is above 70%. This is in contrast with other studies on segmented copolymers. Only at very low uniformity (<50%) the flow temperature is considerably broadened.

The crystallinity of T6T6T in PPE-2T/C12/T6T6T, relatively to T6T6T-PTMO/DMT, is between 54 and 94% for the copolymers with bimodal PPE-2T and below 30% for the copolymers based on monomodal PPE-2T. So it is possible to obtain a high crystallinity despite the high T_g/T_m ratio.

The PPE-2T/C12/T6T6T copolymers with a T6T6T content of 10-15 wt% with >70% uniformity are interesting for applications where a high modulus up to high temperatures in combination with solvent resistance and thus a certain amount of crystallinity is essential. The segmented copolymers can also be useful as compatibiliser for blends of PPE with polyamide.

Literature

1. Chapter 6 of this thesis.
2. D.W. van Krevelen, 'Properties of Polymers', Elsevier, Amsterdam, Ch. 19, 585 (1990).
3. J. Bicerano, J. Macromol. Sci., C38, 391 (1998).
4. Chapter 2 of this thesis.
5. H.S.-I. Chao, J.M. Whalen, React. Polym. 15, 9 (1991).
6. Chapter 5 of this thesis.
7. Chapter 3 of this thesis.
8. M.C.E.J. Niesten, R.J. Gaymans, Polymer, 42, 6199 (2001).
9. Chapter 9 of this thesis.
10. L. Zhu, G. Wegner, Makromol. Chem., 182, 3625 (1981).
11. B.B. Sauer, R.S. McLean, R.R. Thomas, Polym. Int., 49, 449 (2000).
12. M.C.E.J. Niesten, S. Harkema, E. van der Heide, R.J. Gaymans, Polymer, 42, 1131 (2001).
13. D. Garcia, H. Starkweather, J. Polym. Sci. Phys. Ed., 32, 537 (1985).
14. C. Ramesh, A. Keller, S.J.E.A. Eltink, Polymer, 35, 5293 (1994).
15. A.C.M. van Bennekom, R.J. Gaymans, Polymer, 38, 657 (1997).
16. P.F. van Hutten, R.M. Mangnus, R.J. Gaymans, Polymer, 35, 4193 (1993).
17. J.D. Hoffman, J.J. Weeks, J. Res. Nat. Bur. Stand., Sect. A, 66, 13 (1962).
18. M.C.E.J. Niesten, H. Bosch, R.J. Gaymans, J. Appl. Polym. Sci., 81, 1605 (2001).
19. L.L. Harrell, Macromolecules, 2, 607 (1969).
20. H.N. Ng, A.E. Allegrazza, R.W. Seymour, S.L. Cooper, Polymer, 14, 255 (1973).
21. C.D. Eisenbach, M. Baumgartner, G. Gunter, in 'Advances in Elastomer and Rubber Elasticity, Proc. Symposium', J. Lal and J. E. Mark Eds., Plenum Press, New York, 51 (1985).
22. J.A. Miller, B.L. Shaow, K.K.S. Hwang, K.S. Wu, P.E. Gibson, S.L. Cooper, Macromolecules, 18, 32 (1985).
23. M.C.E.J. Niesten, J. Feijen, R.J. Gaymans, Polymer, 41, 8487 (2000).
24. G. Wegner, Chapter 12 in: 'Thermoplastic Elastomers', N.R. Legge, G. Holden, H.E. Schroeder, First Ed., Carl Hanser Verlag, Munich (1987).
25. P.J. Flory, Trans. Faraday Soc., 51, 848 (1955).

Chapter 8

Thermal-mechanical properties of copolymers of PPE, different extenders and uniform tetra-amide units

Abstract

Copolymers of telechelic poly(2,6-dimethyl-1,4-phenylene ether) segments with terephthalic methyl ester endgroups (PPE-2T), uniform crystallisable T6T6T units (two-and-a-half repeating unit of nylon-6,T, 8-20 wt%) and different diols (C2-C36, PTMO) as an extender were made via a polycondensation reaction. The maximum reaction temperature was 280°C. The products are semi-crystalline materials with a high T_g/T_m ratio above 0.8. The modulus is high and constant up to the T_g around 170°C. The modulus of the rubbery plateau increases with increasing crystalline T6T6T content. With increasing amount of crystalline T6T6T the flow temperature increases slightly as well (260-275°C). The materials are transparent when the T6T6T content is below 15 wt% or the diol length is C12 or lower. Copolymers based on PPE-2T and T6T6T-dimethyl (10-15 wt%) with dodecanediol or hexanediol as an extender have the best combination of properties. With longer diols, the T_g is decreased and broadened a lot, while the modulus starts decreasing before the T_g . Also the modulus in the rubbery plateau is not as high as with C6 and C12. With shorter diols or by coupling PPE and T6T6T directly the T_g can be increased, which is desirable. However at the same time the crystallinity of the copolymer decreases. Both the increased T_g/T_m ratio and the decreased flexibility of the units that link PPE and T6T6T are thought to be responsible for this behaviour.

Introduction

Segmented copolymers consisting of amorphous poly(2,6-dimethyl-1,4-phenylene ether) (PPE) segments and crystallisable T6T6T units (8-20 wt%) with dodecanediol as an extender have very good properties^{1,2}. Surprisingly these copolymers are semi-crystalline materials. The polymers have a high T_g of ~ 170 - 180°C , a high melting temperature of ~ 260 - 275°C and an extremely high T_g/T_m ratio of >0.8 . Despite this high T_g/T_m ratio a rubbery plateau is observed with a modulus of ~ 3 - 15 MPa. This is very particular because normally crystallisation is absent at such high T_g/T_m ratio^{3,4}. It was concluded that the crystallisation of the T6T6T units in these copolymers is extremely fast and that these units already order in the melt. The copolymers have good processability, good solvent resistance and low water absorption and those with <13 wt% T6T6T are slightly transparent^{1,2}. The crystallisation is very sensitive to molecular weight and processing conditions and, as a result, the crystallinity² of T6T6T in different copolymers is roughly between 50 and 95%.

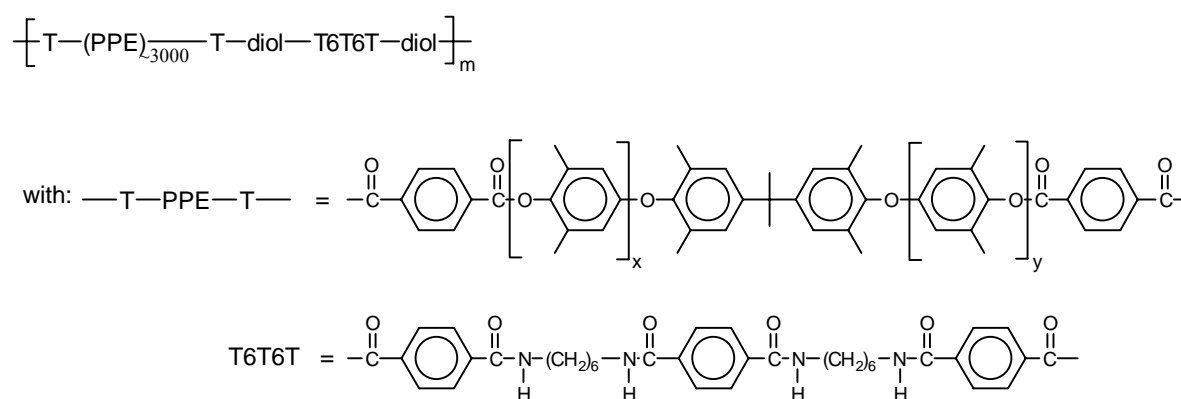


Figure 8.1: Schematic structure of a PPE-2T/diol/T6T6T copolymer.

Segmented copolymers were made via a polycondensation reaction using bimodal PPE-2T, T6T6T-dimethyl and a diol as an extender (Figure 8.1)¹. The PPE-2T segments were made by redistribution or depolymerisation of high molecular weight PPE with tetramethyl bisphenol A followed by endgroup modification with methyl chlorocarbonyl benzoate (MCCB)⁵. These PPE segments have a bimodal molecular weight distribution because part of the high molecular weight starting material was not depolymerised^{5,6}. The number average molecular weight of the PPE-2T segments is around 3000 g/mol. The T6T6T-dimethyl segments were made in a two-step reaction⁷.

The copolymer of PPE-2T, a diol and T6T6T-dimethyl is a mixture of PPE-2T/diol/T6T6T copolymer and unreacted high molecular weight PPE. Some of these unreacted PPE chains can be present in the copolymer as an endgroup because they contain a methyl ester endgroup as a result of the reaction of a Mannich base type endgroup with MCCB^{5,8}.

Thus far only copolymers of PPE-2T and tetra-amides that were linked via dodecanediol were studied^{1,2}. It will be interesting to study the crystallisability of such uniform crystallisable units in segmented copolymers with other diols as extender. When the diol length is decreased

the glass transition temperature increases⁸, and thus the T_g/T_m ratio increases. The rate and extent of crystallisation are known to decrease dramatically upon increasing the T_g/T_m ratio^{3,4}. Also, it is expected that the length and flexibility of the diol between PPE and tetra-amide will influence the rate and the extent of crystallisation. Moreover T6T6T units that are extended via diols shorter than butanediol can probably not crystallise by chain folding.

A disadvantage of the polymerisation using PPE-2T is that the synthesis of PPE-2T is probably not economically feasible. It is also possible to start from PPE-2OH and to react this directly with T6T6T-diphenyl⁷ (Figure 8.2, with $n=2$). PPE-2OH with a bimodal molecular weight distribution is the product of the redistribution reaction before endgroup modification with MCCB. Polymerisation using PPE-2OH can be performed in the melt when 6T6-diamine⁷ and diphenyl terephthalate (DPT) are used instead of T6T6T-diphenyl, which makes this route even more interesting. However by starting with 6T6-diamine the length of the $T(6T)_n$ units is no longer uniform and n has values of 2, 4, 6, etc. These copolymers in which PPE and T6T6T are linked directly have no flexible unit between the PPE and the T6T6T segment and therefore the T_g will be higher⁸. Consequently it is expected that these copolymers crystallise to a smaller extent. The absence of a flexible diol between PPE and T6T6T could also have a negative influence on the crystallisation of T6T6T.

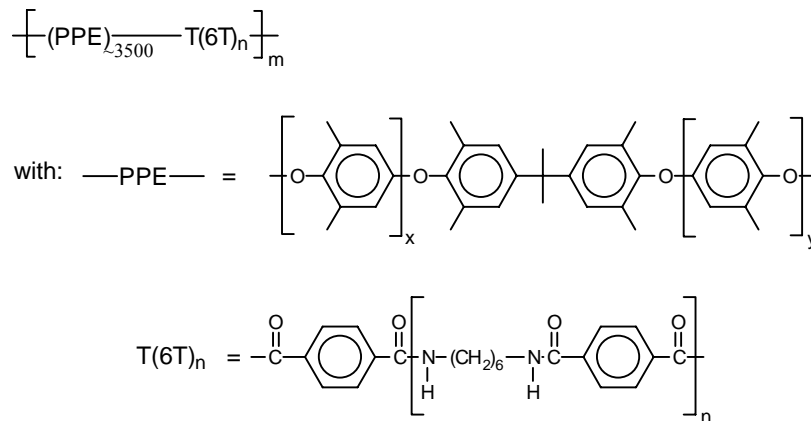


Figure 8.2: Schematic structure of a PPE-2OH/ $T(6T)_n$ copolymer.

Morphology

It is expected that the morphology of segmented copolymers based on PPE and uniform tetra-amide units is comparable with that of PTMO with uniform di-amide units⁹ or tetra-amide units¹⁰. The effect of degree of crystallinity on modulus of T6T6T in PPE² was comparable with that of T6T6T in PTMO¹⁰ and both are transparent materials at low hard segment content (<15 wt%). The uniform crystalline segments form thread or ribbon-like structures with a very high aspect ratio⁹⁻¹². This morphology was confirmed by AFM experiments¹⁰. The crystalline ribbons act as physical crosslinks and reinforcing fibres for the amorphous phase. With such a morphology the crystalline content has a strong effect on the modulus. When the ribbons are not stacked into spherulites then the copolymer will be transparent. At high amide contents spherulitic structures can be formed and transparency will be lost¹².

A model for the crystalline structure of a PPE-2T/diol/T6T6T segmented copolymer based on bimodal PPE-2T with an average length of 3100 g/mol that contains ~13 wt% T6T6T is given in Figure 8.3¹. In these copolymers the PPE-2T endgroup and T6T6T endgroup molar contents are equal. As a result of the random reaction between PPE-2T, diol and T6T6T-dimethyl some PPE-2T will be coupled directly via the diol (-PPE-diol-PPE-) as well as some T6T6T segments (-diol-T6T6T-diol-T6T6T-diol-). The product is a mixture of PPE-2T/diol/T6T6T copolymer and high molecular weight PPE chains that were not redistributed. Some of these high molecular weight PPE chains can be present in the copolymer as an endgroup because some of their Mannich base type endgroups are transferred into methyl ester endgroups^{5,8}.

Most T6T6T units will crystallise to threads or ribbon-like structures (I) of ~4 nm thickness with high aspect ratio and some will be amorphous and mixed with the amorphous PPE phase (II). In PTMO/tetra-amide¹⁰ the length of the crystalline ribbons can be 500 nm.

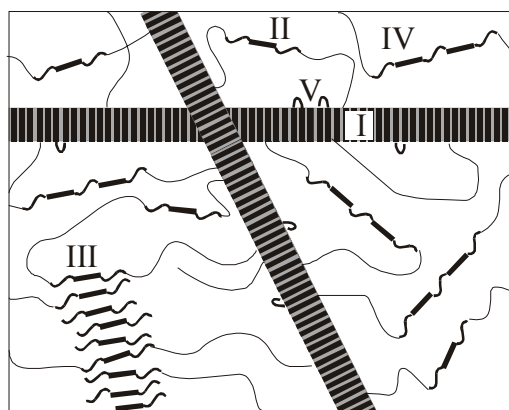


Figure 8.3: Different possible morphologies for PPE-2T/diol/T6T6T copolymers: (I), crystalline T6T6T ribbons; (II), amorphous T6T6T units, mixed with PPE; (III), ordered T6T6T phase; (IV), amorphous diol-extended T6T6T units; (V), chain-folded crystalline diol-extended T6T6T units.

It was found that the tetra-amide units are still ordered in the melt¹, like the di-amides in PTMO/di-amide¹³⁻¹⁷. It is thought that crystallisation of T6T6T takes place from these ordered T6T6T structures in the melt upon cooling. However, due to the high T_g/T_m ratio, crystallisation is incomplete. Therefore it can be expected that after cooling the non-crystalline T6T6T units are still ordered in a sort of frozen-in T6T6T domains. The dimensions of such ordered T6T6T domains (III) will be comparable with that of the crystalline lamellae I, which is at a nano-scale.

It is expected that the diol-extended T6T6T segments are still miscible with PPE and are present in the amorphous PPE phase (IV). It is also possible that some diol-extended T6T6T units crystallise after chain folding (V) or over their full length. The possibility of chain folding depends on the length and flexibility of the diol. Chain folding should be possible with butanediol and longer diols. Crystallisation of diol-extended T6T6T over their full length will lead to crystals with increased lamellar thickness (thicker ribbons) with a higher melting temperature¹⁸. In PTMO/di-amide copolymers diol-extended di-amide units crystallise over their full length with a higher melting temperature for diol lengths up to ~500 g/mol¹⁹. Other

diol-extended di-amide units showed comparable behaviour²⁰⁻²². The melting temperature of PPE-2T/C12/T6T6T copolymers with 8-15 wt% T6T6T with a uniformity above 70% was sharp and it was concluded that C12-extended T6T6T units do not crystallise as extended unit over their full length².

The T_g of the amorphous PPE phase will be reduced due to the presence of the amorphous T6T6T units (II and IV) and the dodecanediol extender. Also the dodecanediol that is at the interphase between amorphous PPE and T6T6T crystalline ribbons will probably decrease the T_g of the PPE phase.

When the segment lengths (PPE and T6T6T/diol) are long enough, phase separation (melt phasing or liquid-liquid demixing) can occur. Phase separation will occur more readily when the segment length increases, thus with long diols or long diol-extended T6T6T segments (at high T6T6T concentration). Phase separation increases with increasing diol length, because the miscibility of the PPE and diols was found to decrease with increasing diol length⁸.

Phase separated domains already exist in the melt and have spherical shape and dimensions >100 nm. As a result of the presence of phase separated domains light is scattered and the material will not be transparent. Phase separated amorphous T6T6T(/C12) domains are not present in PPE-2T/C12/T6T6T² at T6T6T contents below 13 wt% because the copolymers are transparent, which indicates that only T6T6T nano-phases (I and III) can be present. For PPE-2T/C12/T6T6T some phase separation was probably present at high T6T6T contents of 15-20 wt%². This is due to an increasing concentration of C12-extended T6T6T units that are less miscible with PPE.

Aim

The aim of this chapter is to investigate the influence of the length and flexibility of the extender between PPE and T6T6T on the T_g/T_m ratio and crystallisability of T6T6T. Therefore several series of polyether-esteramide copolymers based on PPE-2T ($M_n \sim 3100$ g/mol) and T6T6T that were linked via different diols were studied. Also copolymers based on PPE-2OH and T6T6T-diphenyl or 6T6-diamine/DPT will be made. For each series, the T6T6T content was varied. The effect of composition on glass transition and flow temperature and rubber modulus was studied with DMA for all copolymers.

Experimental

Materials. 1,2-Ethandiol, 1,6-hexandiol, 1,12-dodecanediol and N-methyl-2-pyrrolidone (NMP) were purchased from Merck. Tetraisopropyl orthotitanate ($Ti(i-OC_3H_7)_4$), obtained from Merck, was diluted in anhydrous *m*-xylene (0.05M), obtained from Fluka. C36-dimerised fatty diol was obtained from Uniquema, Gouda (The Netherlands). Poly(tetramethylene-oxide) (PTMO, $M = 1000$ g/mol) was provided by DuPont. PPO-803[®] (11.000 g/mol) was obtained from GE Plastics (The Netherlands). All chemicals were used as received. T6T6T-dimethyl, T6T6T-diphenyl, 6T6-diamine and diphenyl terephthalate (DPT) were synthesised as described in Chapter 5⁷. Bimodal PPE-2OH with an average molecular

weight of 3500 g/mol and 450 $\mu\text{mol OH/gram}$ was made according to the method described in Chapter 2⁵. Bimodal PPE-2T (3100 g/mol, 573 $\mu\text{mol OCH}_3/\text{gram}$) was made according to the one-pot method⁵. The PPE-2T/diol/T6T6T copolymers were synthesised according to the method described in Chapter 6¹.

Synthesis of PPE-2OH/T6T6T copolymers. The PPE-2OH/T6T6T and PPE-2OH/DPT/6T6 copolymers were synthesised by a slightly different method using longer reaction times. The preparation of an alternating copolymer of PPE-2OH (~3500 g/mol, 450 $\mu\text{mol OH/gram}$) and T6T6T-diphenyl is given as an example. For a lower T6T6T content part of the T6T6T-diphenyl was replaced by DPT to retain stoichiometry.

The reaction was carried out in a 50 ml glass reactor with a nitrogen inlet and mechanical stirrer. The vessel was loaded with PPE-2OH (10.0 g, 4.50 mmol OH), T6T6T-diphenyl (1.82 g, 2.25 mmol), 20 ml NMP and catalyst solution (0.6 ml of 0.05M $\text{Ti}(\text{i-OC}_3\text{H}_7)_4$ in *m*-xylene). This mixture was first heated in an oil bath to 180°C under nitrogen flow. Then the temperature was raised in steps: 30 min 180°C, 30 min 220°C, 60 min 250°C and 120 min 280°C. The pressure was then carefully reduced ($P < 20$ mbar) to distil off the remaining NMP in 60 minutes and then further reduced ($P < 1$ mbar) for 60 minutes. Finally, the vessel was allowed to slowly cool to room temperature whilst maintaining the low pressure. Then the polymer was cut out of the reactor and crushed.

Viscometry. The inherent viscosity of the polymers was determined with a capillary Ubbelohde type 1B at 25°C, using a polymer solution with a concentration of 0.1 g/dl in phenol/1,1,2,2-tetrachloroethane (50/50, mol/mol).

DMA. Samples for the DMA test (70x9x2 mm) were prepared on an Arburg-H manual injection moulding machine. Before use, the samples were dried in a vacuum oven at 80°C overnight. The torsion behaviour was studied at a frequency of 1 Hz, a strain of 0.1% and a heating rate of 1°C/min using a Myrenne ATM3 torsion pendulum. The storage modulus G' and loss modulus G'' were measured as a function of temperature starting at -100°C. The glass transition temperature (T_g) was expressed as the temperature at which the loss modulus G'' has a maximum. This maximum was 0-10°C lower than the actual glass transition temperature, because with this DMA apparatus it was not possible to measure a few points around the T_g due to the very high damping. The modulus of the rubbery plateau was determined at 40°C above the T_g . The flow temperature (T_{flow}) was defined as the temperature where the storage modulus G' reached 0.5 MPa. The flow temperature indicates the onset of melting. When the T_{flow} is sharp it is only a few degrees below the melting temperature (T_m) and the T_g/T_{flow} ratio (K/K) is about the same as the T_g/T_m ratio.

DSC. DSC spectra were recorded on a Perkin Elmer DSC7 apparatus, equipped with a PE7700 computer and TAS-7 software. Dried samples of 5-10 mg polymer in aluminium pans were measured with a heating and cooling rate of 20°C/min. The samples were heated to 300°C, kept at that temperature for 2 minutes, cooled to 100°C and reheated to 300°C. The

(peak) melting temperature and enthalpy were obtained from the second heating scan. The crystallisation temperature was defined as the maximum of the peak in the cooling scan.

To account for the thermal lag between a point in the sample and the calorimeter furnace, the recorded temperatures in non-isothermal crystallisation experiments must be corrected. For Perkin Elmer DSC7 with aluminium pans the actual temperature was calculated from the display temperature and cooling rate λ ($^{\circ}\text{C}/\text{min}$) with Equation 8.1^{23,24}.

$$T_{\text{actual}} = T_{\text{display}} + 0.089\lambda \quad [^{\circ}\text{C}] \quad \text{Equation 8.1}$$

Results and Discussion

Copolymers of PPE-2T, a diol and T6T6T-dimethyl were made in a polycondensation reaction with a maximum temperature of 280°C as was discussed in Chapter 6¹. All copolymers could be easily obtained with high molecular weights as compared to PPO-803[®]. It was more difficult to obtain high molecular weight copolymers using PPE-2OH. The reaction between the phenolic endgroups of PPE-2OH and the phenyl ester endgroups of T6T6T-diphenyl is slow⁸. To overcome this problem, the reaction times with PPE-2OH were almost doubled. The low reactivity is due to the aromatic nature and steric hindrance of the 2,6-dimethyl groups on the phenolic endgroups of PPE-2OH. Furthermore, the average functionality of PPE-2OH is lower than that of PPE-2T, because some of the endgroups of lower reactivity such as Mannich base type endgroups^{5,6} in PPE-2T have reacted with the highly reactive acid chloride during endgroup modification. As a result, the high molecular weight PPE fraction in PPE-2OH has no reactive endgroups at all and will be present as such in the copolymer.

In this chapter the thermal-mechanical properties of several series of copolymers based on PPE-2T (~ 3100 g/mol) and varying T6T6T content with different diols as an extender will be discussed. The effect of the diol length will be studied using poly(tetramethylene oxide) (PTMO) of 1000 g/mol, C36-diol, dodecanediol^{1,2}, hexanediol and ethanediol. Two series in which PPE and T6T6T are coupled directly using PPE-2OH (~ 3500 g/mol) and T6T6T-diphenyl or 6T6-diamine/DPT will be discussed next. The effect of composition on glass transition, flow temperature and rubber modulus as studied by DMA will be discussed for all copolymers. The effect of the diol length on the thermal behaviour, in particular the undercooling ($T_m - T_c$) for crystallisation, was studied with DSC.

Table 8.1: Properties of the PPE/T6T6T copolymers with varying extender between PPE and T6T6T.

	PPE	T6T6T	η_{inh}	T_g	G' (at T_g + 40°C)	T_{flow}	T_g/T_{flow}	Calc. cryst. ^f
	[g/mol]	[wt%]	[dl/g]	[°C]	[MPa]	[°C]	[-]	[%]
Starting materials:								
PPO-803 [®]	-	-	0.37 ^c	200	-	222	-	-
PPE-2T ^a	3100	-	0.17 ^c	173 ^d	-	-	-	-
PPE-2OH ^b	3500	-	0.19 ^c	182 ^d	-	-	-	-
Series 1: PTMO₁₀₀₀								
PPE-2T/PTMO ₁₀₀₀	3100	0	0.50	115	-	165	-	-
PPE-2T/PTMO ₁₀₀₀ /T6T6T	3100	9	0.54	165	1	260 ^e	0.82	<10
Series 2: C36-diol								
PPE-2T/C36 ⁸	3100	0	0.55	140	-	180	-	-
PPE-2T/C36/T6T6T	3100	6	0.53	135	0.7	225	0.82	<10
PPE-2T/C36/T6T6T	3100	8	0.57	130	2.0	267	0.75	22
PPE-2T/C36/T6T6T	3100	10	0.60	128	2.2	267	0.74	23
PPE-2T/C36/T6T6T	3100	11	0.65	126	2.2	266	0.74	21
Series 3: Dodecanediol^{1,2}								
PPE-2T/C12	3100	0	0.31	169	-	193	-	-
PPE-2T/C12/T6T6T	3100	6	0.32	173	-	209	-	-
PPE-2T/C12/T6T6T	3100	8	0.53	179	4	263	0.84	59
PPE-2T/C12/T6T6T	3100	10	0.56	179	6	266	0.84	71
PPE-2T/C12/T6T6T	3100	13	0.41	169	10	269	0.82	76
PPE-2T/C12/T6T6T	3100	15	0.47	179	12	267	0.84	69
Series 4: Hexanediol								
PPE-2T/C6	3100	0	0.30	185	0	210	-	-
PPE-2T/C6/T6T6T	3100	7	0.33	184	0	228	-	-
PPE-2T/C6/T6T6T	3100	9	0.33	178	1	236	0.89	<10
PPE-2T/C6/T6T6T	3100	11	0.32	183	4	263	0.85	48
PPE-2T/C6/T6T6T	3100	14	0.37	184	4	266	0.85	37
Series 5: Ethanediol								
PPE-2T/C2	3100	0	0.36	190	0	217	-	-
PPE-2T/C2/T6T6T	3100	7	0.29	188	0	220	-	-
PPE-2T/C2/T6T6T	3100	9	0.30	185	1	232 ^g	0.91	<10
PPE-2T/C2/T6T6T	3100	11	0.31	188	2	261 ^g	0.86	16
PPE-2T/C2/T6T6T	3100	14	0.30	189	2	278 ^g	0.84	13
Series 6: PPE-2OH/T6T6T								
PPE-2OH/DPT	3500	0	0.33	195	0	220	-	-
PPE-2OH/DPT/T6T6T	3500	7	0.31	183	0	230	-	-
PPE-2OH/DPT/T6T6T	3500	9	0.38	183	2	262	0.85	20
PPE-2OH/DPT/T6T6T	3500	10	0.35	188	1	251	0.88	<10
PPE-2OH/T6T6T	3500	11	0.34	183	1	254	0.87	<10
Series 7: PPE-2OH/DPT/6T6								
PPE-2OH/DPT	3500	0	0.33	195	0	220	-	-
PPE-2OH/DPT/6T6	3500	7	0.40	188	0	235	-	-
PPE-2OH/DPT/6T6	3500	9	0.37	192	2	284 ^g	0.83	20
PPE-2OH/DPT/6T6	3500	11	0.42	188	1	264 ^g	0.86	<10
PPE-2OH/DPT/6T6	3500	14	0.44	193	2	290 ^g	0.83	13

(a), bimodal PPE-2T made by one-pot synthesis⁵; (b), bimodal PPE-2OH⁵; (c), chloroform was used as a solvent instead of phenol/1,1,2,2-tetrachloroethane; (d) measured by DSC instead of DMA; (e) the T_g of the PPE rich phase is given instead of the maximum of G'' ; (f) calculated crystallinity, relatively to T6T6T-PTMO(/DMT) copolymers¹⁰, according to $G'(\text{plateau}) = 1.3 \cdot \exp(0.21x_c)$ with x_c the crystalline content in wt% and crystallinity is $x_c / (\text{T6T6T content})^{2,10}$; (g) the flow temperature is not well defined because there is not a sharp decrease in modulus

Thermal-mechanical properties

The polymers were injection moulded into bars and dried in a vacuum oven at 80°C. Then the thermal-mechanical properties were measured by DMA. The results are given in Table 8.1.

The T6T6T content was calculated, assuming that the ester carbonyl does not crystallise and belongs to the amorphous phase¹³. The polymers were made with either T6T6T-dimethyl or T6T6T-diphenyl of high uniformity (>95%) and it is assumed that the uniformity of the T6T6T units is preserved during the polymerisation reaction^{1,10}. A high uniformity of T6T6T means that the product consists almost solely of T6T6T⁷. T(6T)_n units with n>2 are hardly present. The results of the different series will be discussed successively. The results of series 3 were discussed before^{1,2}.

Series 1: PTMO₁₀₀₀

A copolymer with PTMO₁₀₀₀ (PTMO of 1000 g/mol) as extender between PPE-2T (~3100 g/mol) and T6T6T-dimethyl was made. The copolymer in which the PPE-2T and T6T6T-dimethyl endgroup concentration are equal contains 9 wt% T6T6T. As a result of the random reaction of PTMO₁₀₀₀ with PPE-2T and T6T6T-dimethyl there will be some PPE units that are linked directly to other PPE units (-PPE-PTMO₁₀₀₀-PPE-) as well as T6T6T units that are coupled with PTMO₁₀₀₀ to form extended T6T6T units (-T6T6T-PTMO₁₀₀₀-T6T6T-). Extended T6T6T is not likely to crystallise as extended segment, because PTMO₁₀₀₀ is too long and flexible and will chain fold. Therefore a sharp melting temperature of crystallised T6T6T is expected. The copolymer based on PTMO₁₀₀₀ and T6T6T has a high inherent viscosity of 0.53 dl/g. The test bars of the polymers with and without T6T6T that are discussed are not transparent. In Figure 8.4 the storage and loss modulus as measured by DMA are given. The results can also be found in Table 8.1.

The amorphous polyether-ester copolymer based on PPE-2T and PTMO₁₀₀₀ has a high and constant modulus up to the T_g at 115°C. When PTMO₁₀₀₀ is used as an extender between PPE and T6T6T the PTMO content is doubled compared to the amorphous copolymer. As a result the T_g becomes very broad. In fact a single T_g transition is not present anymore. Instead, a transition range is observed. This is a result of the partial phase separation between PPE and PTMO₁₀₀₀, due to incompatibility of these two segments. Different phases with different PPE and PTMO contents and different T_g's are present. No single PPE/PTMO mixed phase as in the amorphous PPE-2T/PTMO₁₀₀₀ copolymer is present. The modulus already starts to drop above -50°C, which is the T_g of a PTMO rich phase. As a result of this phase separation the copolymers are not transparent.

Around 165°C a T_g transition of a PPE rich phase is visible. The copolymer shows a rubbery plateau above this T_g as a result of the crystallisation of T6T6T. A flow temperature of ~260°C is obtained and the rubber modulus is 1 MPa. So only a small amount of T6T6T (<10% relatively to T6T6T-PTMO/(DMT) copolymers^{2,10}) has crystallised compared to PPE-2T/C12/T6T6T². It can be concluded that PTMO₁₀₀₀ is not well suited as an extender between PPE and T6T6T to provide polymers with interesting properties.

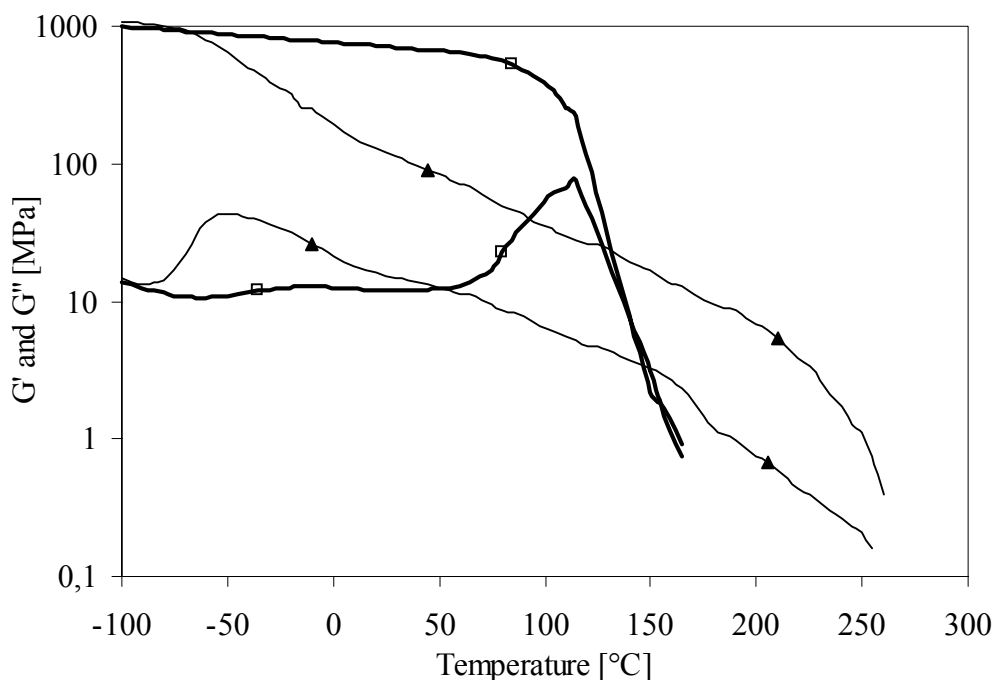


Figure 8.4: Storage and loss modulus for copolymers with $PTMO_{1000}$ as extender: (▲), PPE-2T/ $PTMO_{1000}$ /T6T6T (9 wt% T6T6T); (□), PPE-2T/ $PTMO_{1000}$ (0 wt% T6T6T).

Series 2: C36-diol

A series of copolymers with C36-diol (Figure 8.5) as extender between PPE-2T (~3100 g/mol) and T6T6T-dimethyl was made.

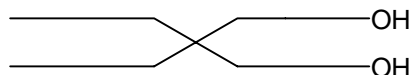


Figure 8.5: Structure of C36-diol dimerised fatty diol.

The T6T6T content was varied between 6 and 11 wt%. In the copolymer with 11 wt% T6T6T the PPE-2T and T6T6T-dimethyl endgroup concentrations are equal. As a result there will be some PPE units that are linked directly to other PPE units (-PPE-C36-PPE-) as well as T6T6T units that are coupled with C36-diol to form extended T6T6T units (-T6T6T-C36-T6T6T-). These diol-extended units are not expected to crystallise as such because chain folding is possible as with dodecanediol that is even shorter^{1,2}. The copolymers based on C36-diol all have high inherent viscosities of 0.53-0.65 dl/g. The test bars from this polymer series are not transparent. In Figure 8.6 the storage and loss modulus as measured by DMA are given for the copolymers with C36-diol as an extender. The results can also be found in Table 8.1.

With increasing T6T6T content the glass transition temperature decreases and the rubber modulus and flow temperature increase. The T_g and T_{flow} are not sharp. The modulus in the rubbery plateau decreases with increasing temperature. The crystallinity of T6T6T relatively to T6T6T-PTMO(/DMT) copolymers^{2,10} in these copolymers is around 20%. This is low compared to copolymers with C12 as extender (Table 8.1)^{1,2}.

With increasing T6T6T content the T_g decreases because the C36-diol content increases with increasing T6T6T content as well. Apparently a large part of T6T6T and C36-diol is mixed with the amorphous PPE phase (Figure 8.3, II and IV).

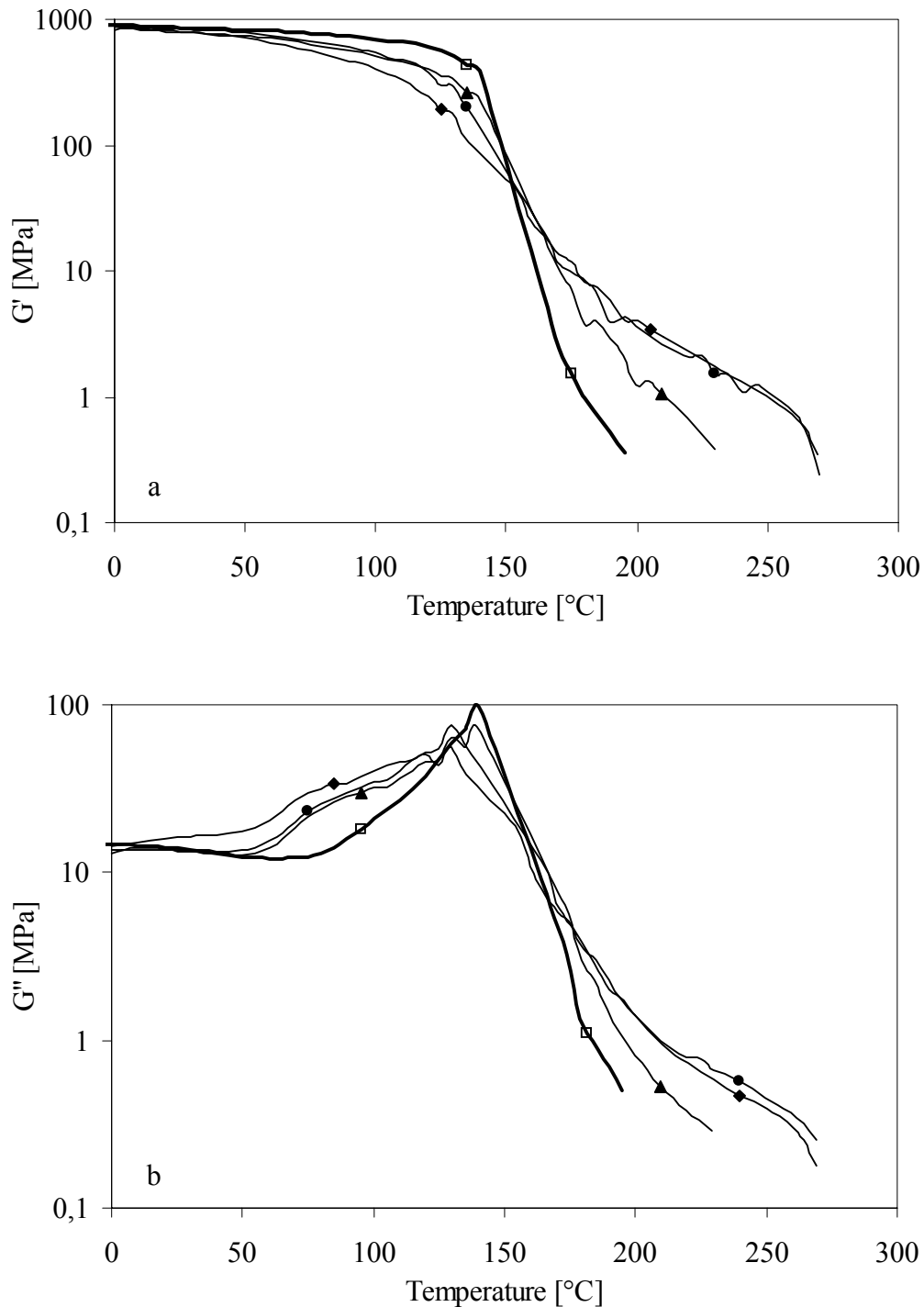


Figure 8.6: Storage (a) and loss (b) modulus for copolymers of PPE-2T and T6T6T-dimethyl with C36-diol as an extender: (□), 0 wt%; (▲), 6 wt%; (●), 8 wt%; (◆), 11 wt%.

The rubber modulus and flow temperature increase with increasing T6T6T content because the crystallinity increases. However the copolymers with 8-11 wt% T6T6T all have about the same modulus and thus the same degree of crystallinity. The percentage of T6T6T that crystallises is lower for the copolymer with 11 wt% T6T6T than that of the copolymer with 8 wt% T6T6T. Probably the fact that the inherent viscosity and thus the molecular weight is higher with 11 wt% T6T6T content is responsible for this behaviour. When the molecular weight increases, the melt viscosity rises and the rate of diffusion of T6T6T units decreases. As a result the maximum degree of crystallinity is lower when the molecular weight is higher. This was also observed for copolymers with dodecanediol as an extender as was described before^{1,2}. Another explanation for the comparable crystallinity of the copolymers with 8-11 wt% T6T6T is that the number of extended T6T6T units (-T6T6T-C36-T6T6T-) increases when the amount of T6T6T increases. These C36-extended T6T6T units are less miscible with PPE and will phase separate more easily into separate amorphous domains.

In the Figure 8.6b a small peak at $\sim 80^\circ\text{C}$ can be seen in the loss modulus. The presence of this peak can be attributed to a crystalline transition, to the presence of frozen-in ordered T6T6T nano-phases (Figure 8.3, III), or to the presence of phase separated spherical amorphous domains that contain predominately T6T6T and C36 units^{1,2}. As the position of the peak in the loss modulus is $\sim 20^\circ\text{C}$ lower with C36-diol than with dodecanediol as extender it can not be ascribed to a crystalline transition in the crystalline T6T6T ribbons, which confirms the earlier conclusion that a crystalline transition is not likely to occur^{1,2}. Such a crystalline transition will not be influenced by the diol length.

It was concluded before^{1,2} that phase separation of T6T6T and C12 into spherical domains was absent in PPE-2T/C12/T6T6T copolymers at a T6T6T content below 15 wt% because these materials were transparent. Phase separated domains scatter light and as a result transparency is lost. Therefore the thermal transition below the T_g of PPE was ascribed to the presence of frozen-in ordered T6T6T nano-phases. The thermal transition temperature of such an ordered T6T6T nano-phase in copolymers with C36-diol as extender is $\sim 20^\circ\text{C}$ lower than with dodecanediol^{1,2}. The diol at the interface between the T6T6T nano-ordered phase and the PPE amorphous phase influences this transition temperature.

The PPE-2T/C36/T6T6T copolymers are not transparent. Therefore it can also be that next to these ordered T6T6T nano-phases some small phase separated domains are present. A part of the T6T6T that does not crystallise can form separate amorphous domains with a high concentration of T6T6T and C36 next to the amorphous PPE phase and ordered T6T6T nano-phases. In particular C36-extended T6T6T units are thought to undergo such phase separation. Phase separation is more likely to occur with C36 as compared to C12 as extender because the miscibility decreases with increasing segment length. This phase separation probably already starts in the melt (melt phasing or liquid-liquid demixing). This is consistent with the fact that miscibility of PPE and C36 in amorphous copolymers without T6T6T is lower than that of PPE and C12⁸.

Another possible explanation for the fact that these copolymers are not transparent is a change in the crystalline morphology. When spherulitic structures are formed instead of ribbons or threads of T6T6T or at high concentration of T6T6T when the threads cannot be randomly

distributed light will be scattered and transparency is lost. However in the copolymers of series 2 the T6T6T content is low and phase separation is more likely to explain the absence of transparency.

Series 3: Dodecanediol

Copolymers of PPE-2T (~3100 g/mol) and uniform T6T6T-dimethyl with dodecanediol (C12) as an extender were described before^{1,2} (Table 8.1). These copolymers had a high T_g of 170-180°C and a well-developed rubbery plateau when more than 8 wt% T6T6T was incorporated. The rubbery plateau (4-13 MPa) and flow temperature (260-275°C) increased with increasing T6T6T content. The crystallinity of the uniform T6T6T relatively to T6T6T-PTMO/(DMT)¹⁰ in these copolymers was between 50 and 80%.

The PPE-2T/C12/T6T6T copolymers were transparent when the T6T6T content was below 15 wt%. Therefore it was concluded that the T6T6T units that were not crystallised were mixed with the amorphous PPE phase or formed frozen-in ordered T6T6T nano-phases. The peak in the loss modulus of PPE-2T/C12/T6T6T copolymers at 100°C was ascribed to a thermal transition in the frozen-in ordered T6T6T nano-phases in combination with a possible crystalline transition in the T6T6T ribbons. However, from the results in this chapter with C36-diol as an extender, it can be concluded that such a crystalline transition does not occur.

Series 4: Hexanediol

In this polymer series, copolymers of PPE-2T (~3100 g/mol) and T6T6T-dimethyl with hexanediol as an extender were synthesised. The T6T6T content was varied from 5-14 wt%. With 14 wt% T6T6T the PPE-2T and T6T6T-dimethyl endgroup concentrations are equal. So at this T6T6T content the highest concentration of C6-extended T6T6T units will be found.

The copolymers based on hexanediol all have low inherent viscosities of 0.30-0.37 dl/g. Both the low molecular weight of hexanediol as repeating unit and the problem of evaporation of hexanediol during the reaction are responsible for this. Higher molecular weights can probably be obtained after further optimisation of the reaction conditions. The molecular weights of these copolymers were high enough to make test bars by injection moulding. The test bars were transparent. The storage modulus as measured by DMA for the PPE-2T/C6/T6T6T polymers of series 4 is given in Figure 8.7. The results are also given in Table 8.1.

When hexanediol is used as an extender between PPE and T6T6T a rubbery plateau is obtained for copolymers with 11 and 14 wt% T6T6T. The T_g and the T_{flow} are sharp. The presence of a sharp flow temperature indicates that no C6-extended T6T6T units have crystallised. Hexanediol as extender is long enough to allow chain folding.

The T_g is not influenced by the T6T6T content, although the hexanediol content increases with increasing T6T6T content as well. Apparently the amount of T6T6T and diol-extended T6T6T (Figure 8.3, II and IV) that mixes with the amorphous PPE phase is constant. And the hexanediol interphase between PPE and crystallised T6T6T or ordered T6T6T nano-phases has probably hardly an effect on the T_g .

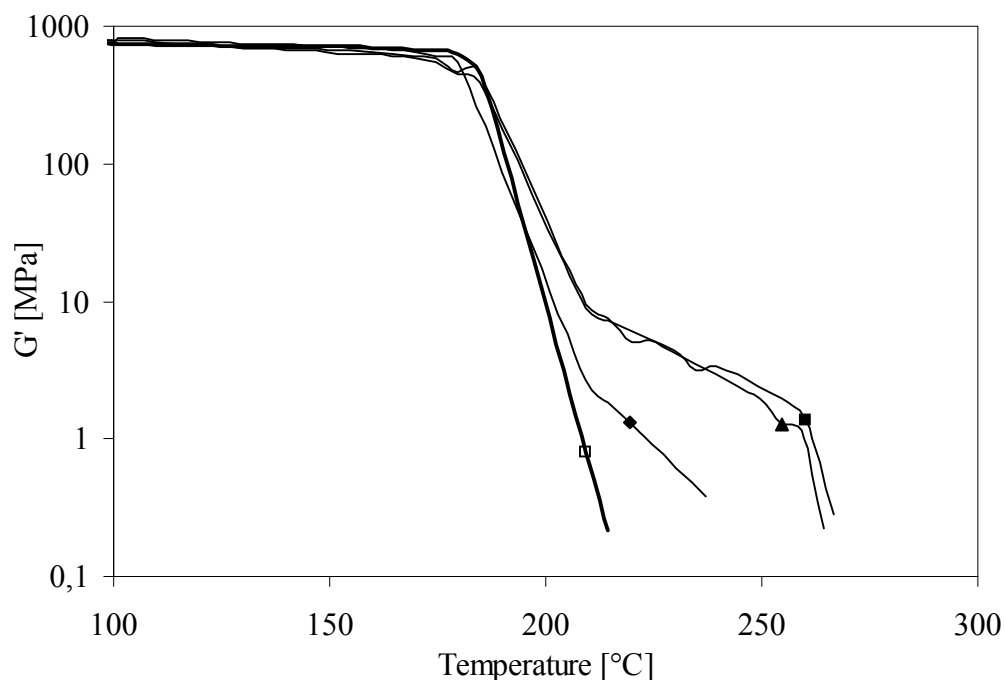


Figure 8.7: Storage modulus for PPE-2T/C6/T6T6T copolymers with different amounts of T6T6T: (□), 0 wt%; (◆), 9 wt%; (▲), 11 wt%; (■), 14 wt%.

In the loss modulus (not given) there is a peak around 100°C. As a result of this thermal transition the modulus decreases at this temperature. The origin of this peak was already discussed for copolymers with C36-diol and dodecanediol as extender. The PPE-2T/C6/T6T6T copolymers are transparent, as were the copolymers with C12 as an extender. Therefore this peak can solely be ascribed to the presence of frozen-in ordered T6T6T nano-phases. The peak in the loss modulus at ~100°C is larger for the copolymer with 14 wt% T6T6T. Probably more T6T6T units are in ordered instead of crystalline T6T6T nano-phases for this copolymer.

The rubber modulus and flow temperature increase with increasing T6T6T content. The rubber modulus and flow temperature are the same for the copolymers with 11 and 14 wt% T6T6T and thus the degree of crystallinity of these copolymers is comparable. The crystallinity of T6T6T relatively to T6T6T-PTMO/(DMT) copolymers¹⁰ in the PPE-2T/C6/T6T6T copolymer with 11 wt% T6T6T is 48% and with 14 wt% T6T6T 37%. These crystallinities are comparable with PPE-2T/C12/T6T6T copolymers². The molecular weight of the copolymer with 14 wt% T6T6T is a little higher, which could reduce the crystallisability of T6T6T. As a result more T6T6T units are in frozen-in ordered T6T6T nano-phases. Probably also the fact that the number of C6-extended T6T6T units (-T6T6T-C6-T6T6T-) is higher in this copolymer is responsible for this behaviour. These extended units crystallise less easily and will mix with the amorphous PPE phase instead.

Series 5: Ethanediol

In polymer series 5, copolymers of PPE-2T (~3100 g/mol) and T6T6T-dimethyl with ethanediol as an extender were synthesised. The T6T6T content was varied from 5-14 wt%.

With 14 wt% T6T6T the PPE-2T and T6T6T-dimethyl endgroup concentration are equal. The copolymers based on ethanediol all have low inherent viscosities of 0.29-0.36 dl/g. The low molecular weight of ethanediol as repeating unit and the problem of evaporation of ethanediol during the reaction account for this and further optimisation of the reaction conditions is necessary. All copolymers could be injection moulded into test bars. The test bars of this series were transparent. The storage modulus as measured by DMA for the PPE-2T/C2/T6T6T copolymers of series 5 is given in Figure 8.8. The results are also given in Table 8.1.

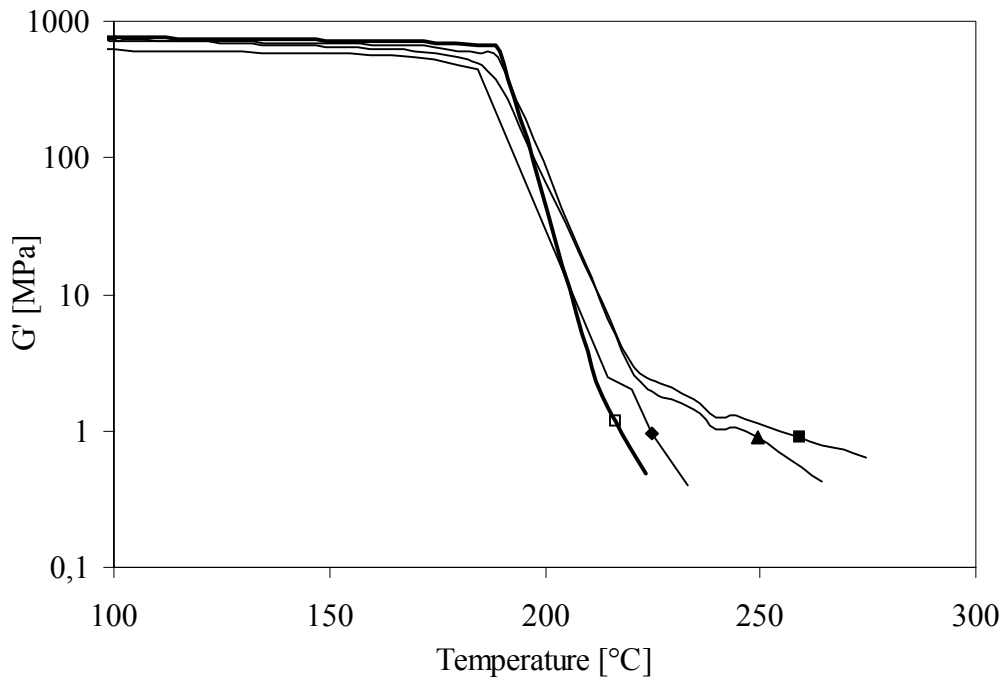


Figure 8.8: Storage modulus for PPE-2T/C2/T6T6T copolymers with different amounts of T6T6T: (□), 0 wt%; (◆), 9 wt%; (▲), 11 wt%; (■), 14 wt%.

When ethanediol is used as an extender the rubber modulus and flow temperature increase with increasing T6T6T content, while the T_g remains almost constant. This effect can be explained in the same way as with C12 or C6 as extender. The crystallinity of T6T6T in these copolymers is below 20% relatively to T6T6T-PTMO(DMT) copolymers^{2,10}. This is much lower than in copolymers with C12 or C6 as extender. Apparently the length and thus the flexibility of the diol that links the PPE-2T and T6T6T segment is important for the rate and extent of crystallisation of T6T6T.

The flow temperature is not sharp when ethanediol is used. The flow temperature was defined as the temperature where the storage modulus reaches 0.5 MPa. When the flow temperature is very broad it does not correspond well to the melting temperature. Apparently C2 is too short to chain fold and the extended T6T6T units (-T6T6T-C2-T6T6T-) with ethanediol are able to crystallise as extended chain segment. These crystallites have a higher lamellar thickness and thus a higher melting temperature¹¹. As a result the polymers show a melting trajectory with a broad flow temperature.

Series 6: PPE-2OH/T6T6T

In series 6 PPE/T6T6T copolymers based on PPE-2OH (~3500 g/mol) instead of PPE-2T were made. PPE-2OH can be coupled directly with T6T6T-diphenyl. In this reaction it is more difficult to obtain high molecular weights, because the phenolic endgroups of PPE-2OH have a lower reactivity than the methyl ester endgroups of PPE-2T and the number of functional groups per chain of PPE-2OH is lower. With long reaction times copolymers with an inherent viscosity of 0.31-0.38 dl/g were obtained.

The T6T6T content was varied between 7 and 11 wt%. The advantage of coupling PPE and T6T6T directly without an extender is that no extended T6T6T units with a higher melting temperature (as for the C2 series) can be formed. As a result the copolymer with 11 wt% T6T6T, which is the maximum amount of T6T6T for this PPE-2OH segment, is perfectly alternating. Also it is expected that there is no phase separation as was found for the longer diols (PTMO₁₀₀₀, C36-diol), because the T6T6T unit alone is probably too short to form a separate phase. When a copolymer with a lower T6T6T content is made, part of the T6T6T is replaced by diphenyl terephthalate (DPT). The copolymers of series 6 were transparent. In Figure 8.9 and Table 8.1 the DMA results for the copolymers of series 6 are given.

The results in Figure 8.9 show that it is possible to obtain crystallisation of T6T6T when PPE and T6T6T are coupled directly. So a flexible unit between PPE and T6T6T is not essential. With 9 wt% T6T6T or more a rubbery plateau is obtained. The modulus of the rubbery plateau is low and ~20% T6T6T relatively to T6T6T-PTMO/(DMT) copolymers^{2,10} has crystallised. In the other copolymers less than 10% of the T6T6T has crystallised. This is much lower than in copolymers with a diol such as C6 or C12 as extender.

The rubbery plateau and flow temperature do not increase gradually with increasing T6T6T content. So the crystallinity does not increase with increasing T6T6T content. The rubbery plateau is higher when the flow temperature is higher, because both are related to the crystallinity. The high crystallinity of the copolymer with 9 wt% T6T6T compared to the other copolymers cannot be ascribed to a difference in molecular weight, as the molecular weight of this copolymer is higher. Probably a difference in temperature of injection moulding accounts for the better crystallisation of the copolymer with 9 wt% T6T6T. It was found before^{1,2} that the processing conditions can influence the crystallinity of T6T6T.

The T_g of the copolymers with T6T6T is lower than that of the amorphous copolymer PPE-2OH/DPT, thus some T6T6T units are mixed with the amorphous PPE phase as well (Figure 8.3, II).

In the loss modulus the PPE-2OH/T6T6T copolymers show a peak at ~130°C. This further confirms the conclusion that this is not a crystalline transition because the transition temperature increases with decreasing diol length. The peak in the loss modulus can thus be attributed to the presence of ordered T6T6T nano-phases (Figure 8.3, III) or phase separated domains with high T6T6T and diol concentration. It is also not likely that the T6T6T units in PPE-2OH/T6T6T phase separate, because they are too short. Therefore the peak in the loss modulus for PPE-2OH/T6T6T copolymers can solely be ascribed to the presence of frozen-in ordered T6T6T nano-phases. The temperature at which this small peak in the loss modulus is

found is higher than for C12 and C6 (both at $\sim 100^\circ\text{C}$). Thus the diol at the interphase between PPE and ordered T6T6T nano-phase influences the transition temperature of the ordered T6T6T nano-phase. The peak at 130°C is larger in the copolymers with 10 and 11 wt% T6T6T than the copolymer with 9 wt% T6T6T. So the higher rubbery plateau for the copolymer with 9 wt% T6T6T is a result of more complete crystallisation of T6T6T.

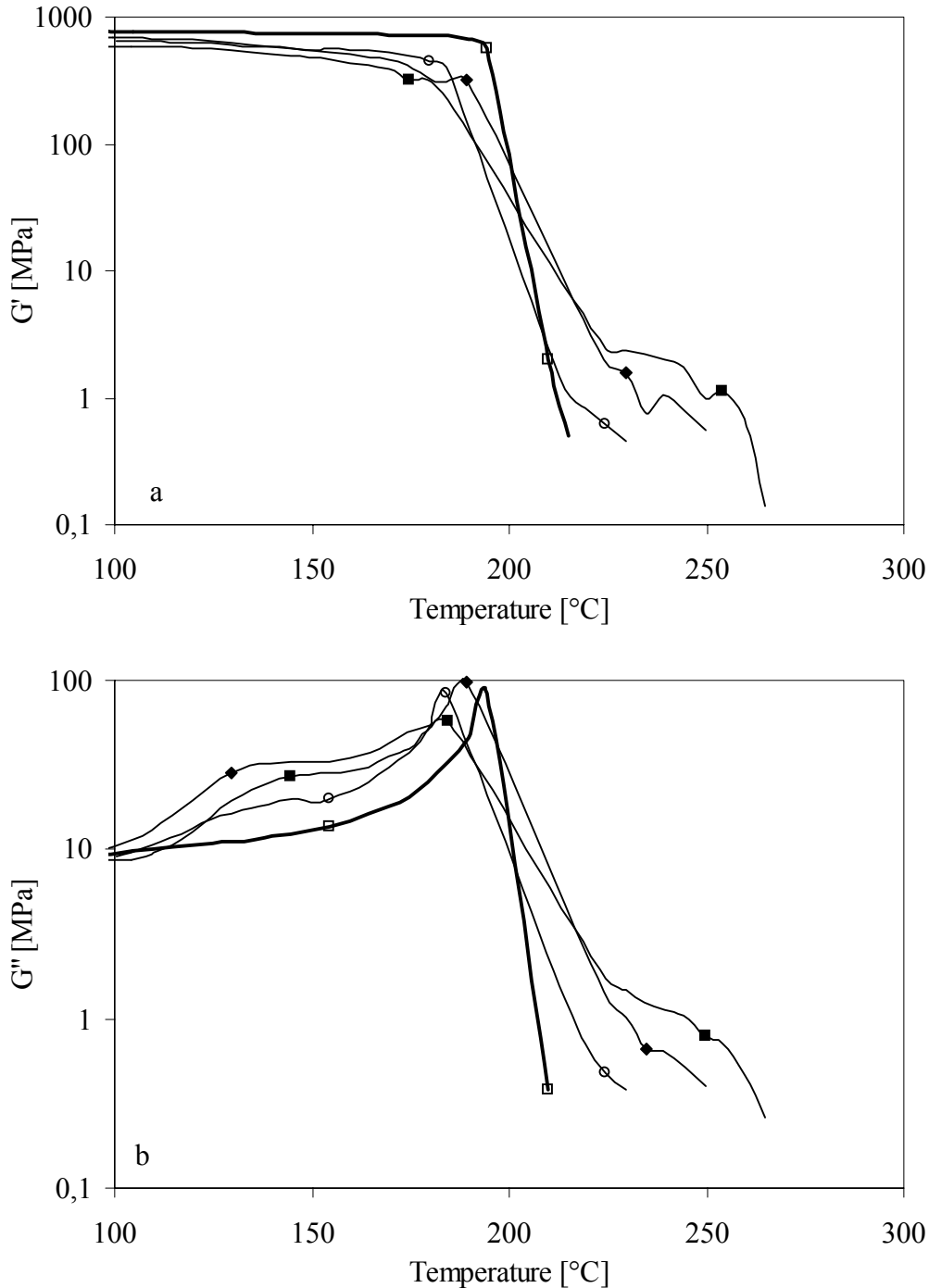


Figure 8.9: Storage (a) and loss (b) modulus of PPE-2OH/T6T6T copolymers with different amounts of T6T6T: (□), 0 wt%; (○), 7 wt%; (■), 9 wt%; (◆), 10 wt%.

Series 7: PPE-2OH/DPT/6T6

In series 7 copolymers based on PPE-2OH and T6T6T were made in which T6T6T was formed during the reaction from 6T6-diamine and diphenyl terephthalate (DPT). 6T6-Diamine is the precursor for T6T6T and has a melting temperature of 178°C⁷. Therefore this reaction can be performed in the melt in principle, however in this study NMP was used as a solvent like in series 1-6. A disadvantage of synthesis of T6T6T during the polymerisation reaction is probably that the uniformity of T6T6T in the copolymer will be much lower than when starting with uniform T6T6T. There will be a length distribution in the T(6T)_n units with n being 2, 4, 6 or higher. With 11 wt% of T6T6T the 6T6-diamine and PPE-2OH endgroup concentrations are equal. Due to the random reaction of DPT with 6T6-diamine and PPE-2OH some PPE units in this copolymer will be linked via DPT only, while others are linked via for example T6T6T6T6T. With 14 wt% of T6T6T a lot of T(6T)_n units with n≥4 will be present.

The molecular weight of the polymers of series 7 was higher than that of series 6. It was expected that the molecular weight would be comparable, because the reactivity and functionality of the PPE-2OH segments is the same. There is no explanation for this result. The copolymers of series 7 were transparent. In Figure 8.10 and Table 8.1 the DMA results for series 7 are given.

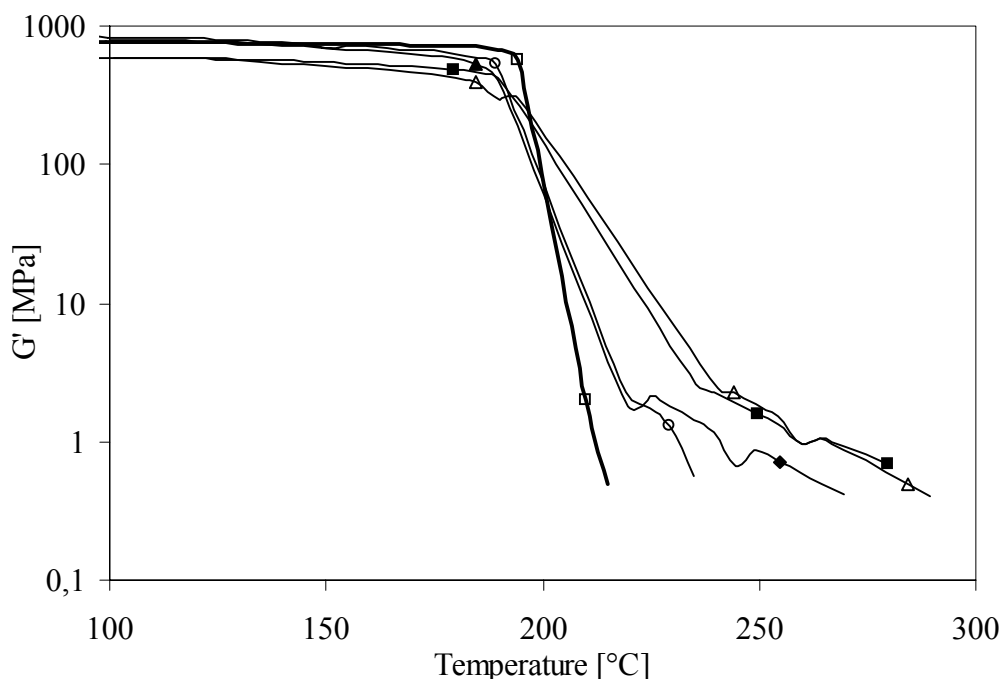


Figure 8.10: Storage modulus for PPE-2OH/DPT/6T6 copolymers with different amounts of T6T6T: (□), 0 wt%; (○), 7 wt%; (△), 9 wt%; (◆), 11 wt%; (■), 14 wt%.

When T6T6T is prepared from 6T6-diamine and DPT during the polymerisation reaction, a semi-crystalline material with a high glass transition temperature and a rubbery plateau is obtained, despite the high T_g/T_{flow} ratio of >0.8. However the flow temperature is broadened a lot, because the T6T6T units in the polymers of series 7 have a low uniformity. In fact a real

melting point, which is indicated by a sharp decrease in modulus, is not present. T(6T)_n units of different lengths form lamellae with different thickness and therefore different melting temperatures¹⁸.

The modulus of the rubbery plateau and the flow temperature ($G' = 0.5$ MPa) increase with increasing T6T6T content. The crystallinity is below 20% relatively to T6T6T-PTMO(/DMT)^{2,10} for all copolymers of this series. This is low compared to copolymers with C6 or C12 as extender. The polymer with 11 wt% T6T6T has a low modulus and melting temperature compared to the rest. This polymer does not have a much higher inherent viscosity, which could result in a lower crystallinity. Probably the test bars from this polymer were injection moulded at a lower temperature, which can result in a lower crystallinity because of decreased flow¹. The same effect probably explains the fact that the copolymers with 9 and 14 wt% T6T6T have a comparable rubber modulus and flow temperature.

In the loss modulus (not given) the polymers with 11 and 14 wt% T6T6T show a larger peak at ~130°C than the copolymer with 9 wt% T6T6T. Thus more T6T6T units are present in frozen-in ordered T6T6T nano-phases instead of crystalline ribbons. Also the copolymer with 11 wt% T6T6T shows a lower T_g , which indicates that the PPE phase is less pure and contains some T(6T)_n units.

Influence of extender flexibility

The influence of the type and length of the extender between PPE and T6T6T segment influences the T_g of the amorphous phase⁸. On the other hand the length and flexibility of this extender seems to have an effect on the crystallisability of the T6T6T in the copolymer as well. The storage moduli of different PPE-2T/diol/T6T6T copolymers with 11 wt% T6T6T (9 wt% for PTMO₁₀₀₀) of series 1-5 are compared Figure 8.11.

The rubber modulus increases with increasing diol length for C2-C12. The height of the rubber modulus as well as the flow temperature is indicative for the total crystallinity of the copolymer. The crystallinity is important as it is related to the solvent resistance of the material. The solvent resistance is important for many applications for this type of high T_g semi-crystalline materials, in particular the automotive industry. It is however not known how much crystallinity is needed for good solvent resistance.

With increasing diol length the T_g/T_{flow} ratio decreases a little because the T_g decreases. This can explain the increasing crystallinity with increasing diol length. Probably also the increasing flexibility of the diol that connects the PPE and T6T6T units enhances the crystallisability of the T6T6T units. This difference in crystallinity cannot be ascribed to a molecular weight effect, because for example the molecular weight of the copolymers with ethanediol as an extender is lower than with hexanediol or dodecanediol.

When the diol length is increased further to C36 or PTMO₁₀₀₀ the crystallinity does not seem to be enhanced compared to C12. With PTMO₁₀₀₀ the T_g is very broad and the modulus is not high above -50°C. The rubbery plateau is low (<10% T6T6T crystallised). With C36 as an extender the modulus is high up to 50°C. The rubbery plateau is lower than with C12 and the

crystallinity of T6T6T is below 10%. Apparently phase separation reduces the crystallisation of T6T6T. Despite the low rubbery plateau the copolymers with C36 or PTMO₁₀₀₀ as extender have a flow temperature that is comparable with that of the other diols. It was found before that the flow temperature is only little influenced by the degree of crystallinity as the solvent effect²⁵ of the amorphous PPE phase is small².

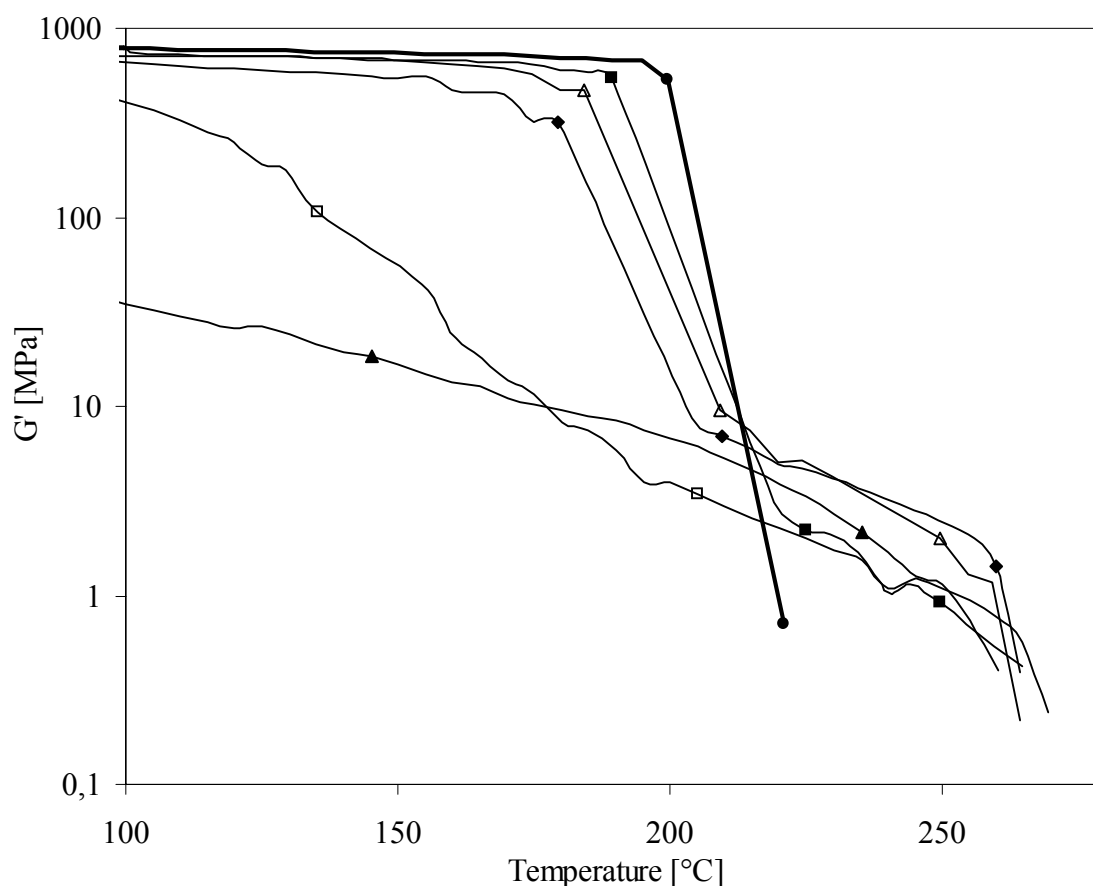


Figure 8.11: Storage modulus for PPE-2T/diol/T6T6T copolymers with different diols as flexible link between PPE and T6T6T and 11 wt% T6T6T (series 1-5): (\blacktriangle), PTMO₁₀₀₀ (9 wt% T6T6T); (\square), C36; (\blacklozenge), C12; (\triangle), C6; (\blacksquare), C2; (\bullet), PPO-803[®].

The rubber modulus of the copolymers of series 6 and 7 based on PPE-2OH is comparable with that of the copolymers based on PPE-2T with ethanediol as an extender. Apparently the flexibility of T-C2-T between PPE and T6T6T does not enhance the crystallisation as compared to the copolymers where PPE and T6T6T are coupled directly.

The T_g decreases with increasing length of the diol that is used as an extender between PPE and T6T6T. So in all copolymers a part of the diol units is present in the amorphous PPE phase. This is probably at least the diol that is at the interphase between T6T6T and PPE. The T_g becomes less sharp when the diol length increases. The same effects of diol length on T_g were found for amorphous copolymers of PPE-2T and different diols without T6T6T⁸.

The flow temperature is sharp with all diols except for PPE-2T/C2/T6T6T. With ethanediol probably double T6T6T units are able to crystallise, because of the low flexibility and length of the C2 unit that cannot chain fold. These double blocks have a higher lamellar thickness

and melt at a higher temperature¹⁸ and as a result the flow temperature becomes very broad. A broad flow temperature was also found for PPE-2OH/6T6/DPT copolymers of series 7 with no flexible extender between PPE and T6T6T (Figure 8.10). With 6T6/DPT longer T(6T)_n units are present. These T(6T)_n units have higher lamellar thickness and melt at a higher temperature as well¹⁸.

The optimum diol length for good crystallisation with a high rubber modulus and flow temperature lies between C6 and C12. Both diols are useful extenders for the PPE-2T/T6T6T system.

The loss moduli of different PPE/T6T6T copolymers of series 1-6 are compared in Figure 8.12.

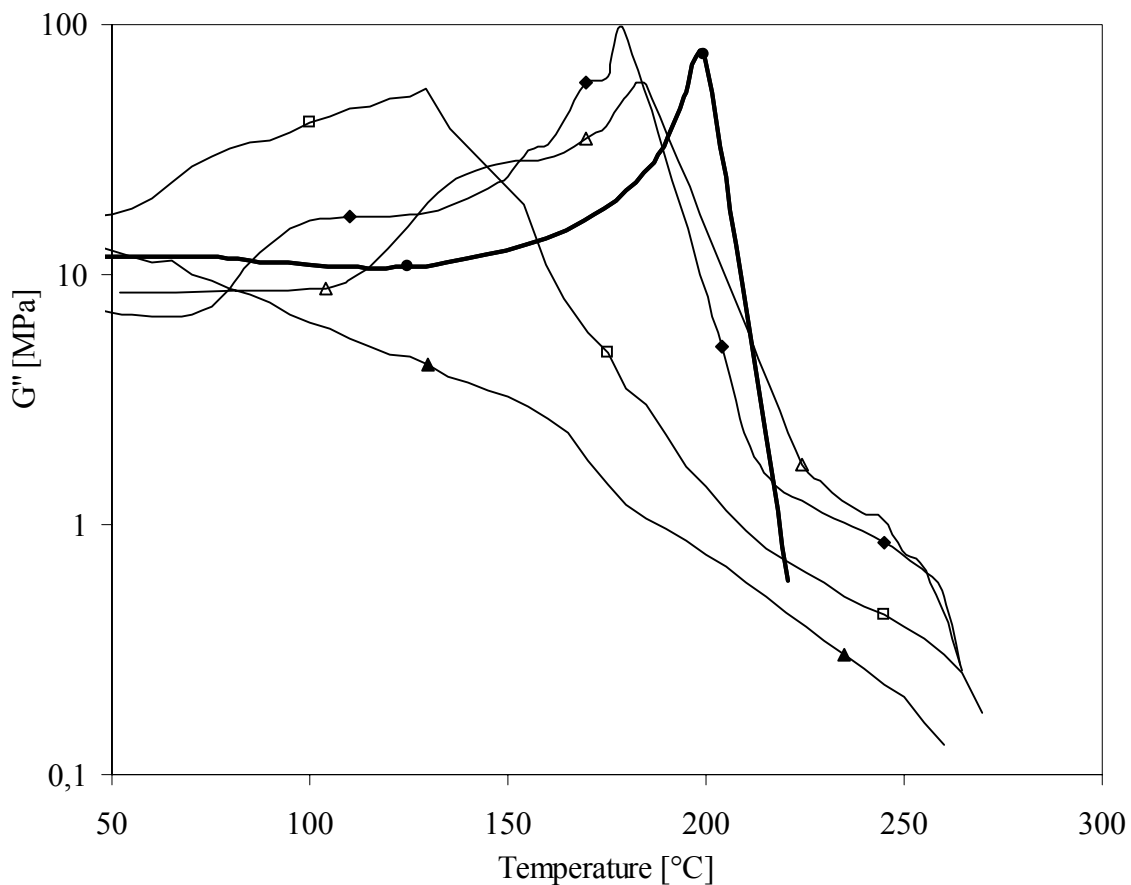


Figure 8.12: Loss modulus for different PPE/T6T6T copolymers: (▲), PPE-2T/PTMO₁₀₀₀/T6T6T (9 wt% T6T6T); (□), PPE-2T/C36/T6T6T (11 wt% T6T6T); (◆), PPE-2T/C12/T6T6T (11 wt% T6T6T); (△), PPE-2OH/T6T6T (9 wt% T6T6T); (●), PPO-803[®].

The different PPE/T6T6T copolymers all show a peak below the T_g of the amorphous PPE phase. As was discussed before this peak can be ascribed to a crystalline transition in the crystalline T6T6T ribbons, a thermal transition in a frozen-in ordered T6T6T nano-phase or a glass transition of amorphous T6T6T-rich domains^{1,2}.

A crystalline transition of the crystalline T6T6T ribbons is expected around 100°C, which is comparable with the crystalline transition of 6T6-diamine⁷ or some polyamides^{26,27}. However

the T6T6T-dimethyl segment did not show such a thermal transition⁷. Also such a transition temperature is thought to be independent of the extender length and flexibility. Therefore a crystalline transition in the T6T6T crystalline ribbons is probably not present for the PPE/T6T6T copolymers.

All copolymers are likely to consist of frozen-in ordered T6T6T nano-phases next to the crystalline T6T6T ribbons, because not all T6T6T that was already pre-ordered in the melt¹³⁻¹⁷ can crystallise upon cooling due to the high T_g/T_m ratio. This will occur especially at the surface of injection moulded test bars. The thermal transition of these frozen-in ordered T6T6T nano-phases is around 130°C when no extender is present, which is around the T_g of nylon-6,T (125°C)²⁸. The transition temperature decreases with increasing length and flexibility of the extender. The copolymers based on PPE-2T and T6T6T with a diol such as C2-C12 as extender show a peak in the loss modulus at ~100°C. When C36-diol is used as extender this peak is at ~80°C. With PTMO₁₀₀₀ as extender the copolymer has no distinct peak in the loss modulus. When the copolymer consists of amorphous PPE, crystalline T6T6T ribbons and frozen-in ordered T6T6T nano-phases it will be transparent.

Phase separation (melt phasing or liquid-liquid demixing) between segments due to incompatibility can only occur when the segments are long enough (>C12). And phase separation will increase with increasing segment length. Phase separated domains are spherical and scatter light as their dimensions are above 100 nm. Phase separation seems to occur when a lot of diol-extended T6T6T units are present, thus at high T6T6T contents. Also phase separation occurs more readily when long diols (such as C36 and PTMO₁₀₀₀) are used as an extender between PPE and T6T6T. The T_g of such a phase separated T6T6T/diol rich phase will depend on the diol length and flexibility.

At high T6T6T concentration the formation of spherulites of T6T6T instead of crystalline ribbons or stacking of ribbons can also account for a decrease in transparency.

DSC

With DSC the melting temperature and enthalpy and crystallisation temperature and enthalpy were measured for copolymers of series 2-6 with 11 wt% T6T6T. The results (after correction for the thermal lag^{23,24}) are given in Table 8.2.

Table 8.2: DSC results for copolymers of series 2-6 with 11 wt% T6T6T.

	T_m [°C]	ΔH_m [J/g]	ΔH_m [J/g T6T6T]	Cryst. ^b [%]	T_c [°C]	ΔH_c [J/g]	$T_m - T_c$ [°C]
PPE-2OH/T6T6T	261	1	9	<10	222	-1	39
PPE-2T/C2/T6T6T ^a	249	1	9	<10	239	-1	10
PPE-2T/C6/T6T6T	267	9	82	54	250	-7	17
PPE-2T/C12/T6T6T	267	10	91	60	249	-11	18
PPE-2T/C36/T6T6T	277	10	91	60	259	-9	18

(a), for ethanediol the melting and crystallisation peaks were very broad; (b), the crystallinity of T6T6T was calculated with the enthalpy of melting of T6T6T-dimethyl (152 J/g)⁷

The undercooling ($T_m - T_c$) is approximately constant at 18°C for the PPE/T6T6T copolymers with C6-C36 as an extender. However the melting and crystallisation temperatures are higher with C36. The melting and crystallisation peak with C2 (series 4) and in PPE-2OH/T6T6T (series 5) are very small and also broad for C2, which makes the results unreliable. The melting and crystallisation enthalpies are around 1 J/g, thus the crystallinity is very low for series 4 and 5. With C2 a low undercooling of only 10°C was found, but this is probably due to the large error in determining the peak temperature of the melting and crystallisation peak for this copolymer. The undercooling is higher for PPE-2OH/T6T6T (39°C) indicating slower crystallisation.

The crystallinity of T6T6T in these copolymers with 11 wt% T6T6T was calculated from their enthalpy of melting compared to the enthalpy of melting of T6T6T-dimethyl⁷. The crystallinity of T6T6T in PPE-2OH/T6T6T and PPE-2T/C2/T6T6T is very low (<10%). The crystallinity of T6T6T in the copolymers with C6-C36 as extender is between 54 and 60%. These values correspond quite well with the crystallinities that were calculated from the rubbery plateau moduli of these copolymers.

Conclusions

Copolymerisation of PPE with uniform, crystallisable tetra-amide units is a good method to obtain semi-crystalline material with a very high T_g/T_{flow} ratio. It is particular that the T6T6T units can actually crystallise in these copolymers despite the very high T_g/T_{flow} ratio above 0.8 and the low concentrations of T6T6T (<15 wt%).

Copolymers based on PPE-2T and T6T6T-dimethyl (10-15 wt%) with dodecanediol or hexanediol as an extender have the best combination of properties. With longer diols, the T_g is decreased and broadened a lot, while the modulus starts decreasing before the T_g . Also the modulus in the rubbery plateau is not as high as with C6 and C12. With shorter diols or by coupling PPE and T6T6T directly the T_g can be increased, which is desirable. However at the same time the crystallinity of the copolymer decreases. Both the increased T_g/T_{flow} ratio and the decreased flexibility of the units that link PPE and T6T6T are thought to be responsible for this behaviour.

Part of the T6T6T does not crystallise. At low T6T6T content (<15 wt%) and for short diols ($\leq C12$) the materials are transparent. The T6T6T that does not crystallise partially mixes with the amorphous PPE phase and partially forms frozen-in ordered T6T6T nano-phases. These ordered T6T6T nano-phases have a T_g of 80-130°C depending on the flexibility of the extender between PPE and T6T6T. At higher T6T6T concentration (>15 wt%) and with longer diols ($\geq C36$) phase separation can occur in the melt, resulting in the presence of small spherical domains and loss of transparency. Such domains have a T_g at 80-130°C as well. The crystalline T6T6T ribbons are not likely to undergo a thermal transition upon heating.

For all copolymers the crystallinity can probably be improved by optimising the molecular weight and the processing conditions.

Literature

1. Chapter 6 of this thesis.
2. Chapter 7 of this thesis.
3. D.W. van Krevelen, 'Properties of Polymers', Elsevier, Amsterdam, Ch. 19, 585 (1990).
4. J. Bicerano, *J. Macromol. Sci.*, C38, 391 (1998).
5. Chapter 2 of this thesis.
6. H.S.-I. Chao, J.M. Whalen, *React. Polym.* 15, 9 (1991).
7. Chapter 5 of this thesis.
8. Chapter 3 of this thesis.
9. M.C.E.J. Niesten, R.J. Gaymans, *Polymer*, 42, 6199 (2001).
10. Chapter 9 of this thesis.
11. L. Zhu, G. Wegner, *Makromol. Chem.*, 182, 3625 (1981).
12. B.B. Sauer, R.S. McLean, R.R. Thomas, *Polym. Int.*, 49, 449 (2000).
13. M.C.E.J. Niesten, S. Harkema, E. van der Heide, R.J. Gaymans, *Polymer*, 42, 1131 (2001).
14. D. Garcia, H. Starkweather, *J. Polym. Sci. Phys. Ed.*, 32, 537 (1985).
15. C. Ramesh, A. Keller, S.J.E.A. Eltink, *Polymer*, 35, 5293 (1994).
16. A.C.M. van Bennekom, R.J. Gaymans, *Polymer*, 38, 657 (1997).
17. P.F. van Hutten, R.M. Mangnus, R.J. Gaymans, *Polymer*, 35, 4193 (1993).
18. J.D. Hoffman, J.J. Weeks, *J. Res. Nat. Bur. Stand., Sect. A*, 66, 13 (1962).
19. M.C.E.J. Niesten, H. Bosch, R.J. Gaymans, *J. Appl. Polym. Sci.*, 81, 1605 (2001).
20. E. Sorta, G. della Fortuna, *Polymer*, 21, 728 (1980).
21. G. Perego, M. Cesari, G. della Fortuna, *J. Appl. Polym. Sci.*, 29, 1141 (1984).
22. L. Guang, R.J. Gaymans, *Polymer*, 38, 4891 (1997).
23. Y. Mubarak, E.M.A. Harkin-Jones, P.J. Martin, M. Ahmad, III Jordanian Chemical Engineering Conference, vol. I, 49 (1999).
24. Y. Mubarak, E.M.A. Harkin-Jones, P.J. Martin, M. Ahmad, *Polymer*, 42, 3171 (2001).
25. P.J. Flory, *Trans. Faraday Soc.*, 51, 848 (1955).
26. M. Todoki, T. Kawaguchi, *J. Polym. Sci. Phys. Ed.*, 15, 1067 (1977).
27. J. Hirschinger, H. Miura, K.H. Gardner, A.D. English, *Macromolecules*, 23, 2153 (1990).
28. P.W. Morgan, S.L. Kwolek, *Macromolecules*, 8, 104 (1975).

Chapter 9

Synthesis and properties of thermoplastic elastomers based on PTMO and tetra-amide units

Abstract

Segmented copolymers based on T6T6T-dimethyl (two-and-a-half repeating unit of nylon-6,T, 5-16 wt%) and PTMO or PTMO₁₀₀₀/DMT that are thermoplastic elastomers were made via a polycondensation reaction. The materials have a good solvent resistance, are melt-processable and transparent. With DMA experiments it was shown that the polymers all have a low glass transition temperature (-60 to -70°C). The rubbery plateau of all copolymers is wide and extremely flat and the melting temperature is sharp and high. The modulus of the rubbery plateau (3.3 to 14.5 MPa) and the flow temperature (183 to 220°C) increase with decreasing PTMO₁₀₀₀/DMT length (10000 to 3000 g/mol) or increasing T6T6T content (5 to 16 wt%) and thus with increasing crystallinity. The crystallinity of T6T6T in injection moulded test bars as calculated from their rubber modulus is between 70 and 100%. The undercooling, as measured by DSC, is 20-30°C. The compression set at room temperature is low (6-7%) and decreases slightly with decreasing T6T6T content. The uniformity of T6T6T, when it is at least 76%, does not have much influence on the polymer properties, except for the flow temperature that is broadened at decreasing uniformity. With AFM it was confirmed that the crystalline T6T6T units form long threads or ribbon like structures with a high aspect ratio in the amorphous PTMO matrix.

Introduction

Thermoplastic elastomers (TPE's)^{1,2} are polymers that show elastomeric behaviour at their service temperature and that can be melt-processed at elevated temperatures. A special kind of thermoplastic elastomers are segmented copolymers or multi-block copolymers that consist of alternating crystallisable hard segments and amorphous soft segments.

The hard segments can crystallise and have a high melting temperature. As a result the segmented copolymers have a two-phase structure. The crystalline hard segment domains act as physical crosslinks for the copolymer. The hard segments give the material dimensional stability, heat stability and solvent resistance. Crystallisable hard segments can be based on polyesters, polyamides, polyurethanes or polyureas. Polyamides are preferred for their combination of high melting temperature, fast crystallisation and thermal stability.

The soft segment has a glass transition temperature below room temperature and gives the material flexibility. The glass transition temperature (T_g) of the amorphous phase depends on the type and length of soft segment and on the amount of dissolved hard segment in this phase. The T_g increases when the amount of not crystallised hard segments in the amorphous phase increases.

Segmented copolymers that are crystallised from a homogeneous melt can form spherulitic structures³. However at fast cooling rates (high nucleation rates) and low concentration (<20 wt%) intermeshing bundles of lamellae with a high aspect ratio without a sharp spherulitic boundary are formed³⁻⁵. The lamellae have the form of long threads or ribbons. Based on these observations a model for the morphology (Figure 9.1) of segmented copolymers that form a crystalline structure of ribbons that have a high aspect ratio was proposed⁶. The crystalline ribbons (C) act as physical crosslinks and reinforcing filler for the amorphous phase (A). Some crystallisable segments cannot crystallise and are mixed with the amorphous phase (B). As a result the mobility of the amorphous phase decreases and the T_g increases.

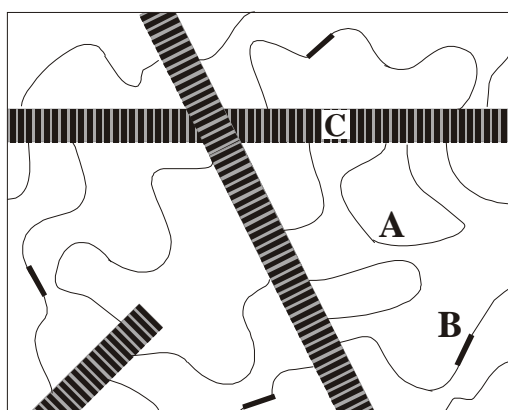


Figure 9.1: Schematic representation of the morphology of crystallised segmented copolymers with uniform crystallisable segments: A = amorphous PTMO phase; B = amorphous crystallisable segments; C = crystalline ribbons^{5,6}.

The crystallisation of the hard segment can be improved by using uniform crystallisable hard segments⁷⁻¹⁰. This is in the first place a result of the fact that uniform hard segments crystallise faster and more complete than non-uniform ones. Furthermore uniform hard segments will crystallise over their full length, giving sharp boundaries and therefore no transition zone between the amorphous and the crystalline phase. As a result the minimum segment length for crystallisation is lower. Another advantage is that the modulus of the rubbery plateau will be constant over a broad temperature range, as the crystalline lamellae that are formed from the uniform segments are stable and melt in a narrow temperature range.

Previous research on segmented copolymers having uniform crystallisable amide units focused on T6T-PTMO¹¹, T4T-PTMO¹², T2T-PTMO¹³ and TΦT-PTMO^{6,14-16} (Figure 9.2). The T6T, T4T, T2T and TΦT uniform crystallisable units are di-amide segments based on 1,6-hexanediamine (6), 1,4-butanediamine (4), 1,2-ethanediamine (2) or *p*-phenylenediamine (Φ) and dimethyl terephthalate (T). Poly(tetramethylene oxide) (PTMO) is used as amorphous segment.

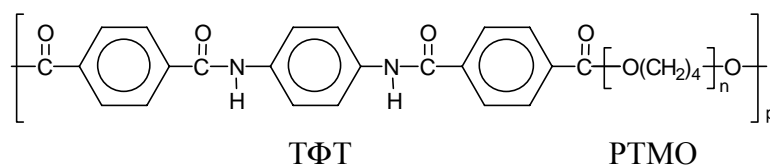


Figure 9.2: Structure of TΦT-PTMO segmented copolymer.

These segmented copolymers are also called copolyether-esteramides. The crystallisable segments are extremely short (~2 nm) and crystallise fast and almost complete, resulting in a two-phase structure with good properties. The melting temperatures of the copolymers consisting of T6T, T4T, T2T or TΦT and PTMO of 1000 g/mol are respectively 111, 153, 132 and 222°C. The melting temperature increases with increasing hard segment rigidity. The lamellar thickness is also important.¹⁷ The T2T unit is very short and has a lower melting temperature in the copolymer. With TΦT (one-and-a-half repeating unit of poly(*p*-phenylene terephthalamide)) as uniform crystallisable unit the crystallisation is even faster and more complete and the phase separation is better than with T4T and T6T. The fast crystallisation is possibly due to the fact that the di-amide units remain organised in the melt^{12,18-22} and probably form nano-ordered phases.

In these segmented copolymers the amide segment content has a large effect on the properties^{6,11-16}. With increasing hard segment concentration the melting temperature and modulus at room temperature increase. Furthermore the yield stress increases. The molecular weight of the copolymer is also important⁶. With increasing molecular weight of the polymer the tensile stress and strain increase due to an increased number of entanglements per chain. The length and type (regularity) of amorphous segment is important as it influences the strain-induced crystallisation. Regular PTMO segments longer than 2000 g/mol show strong strain hardening above 300% strain. It was found that the length of the amorphous segment in PTMO extended with dimethyl terephthalate (PTMO/DMT, Figure 9.3) seems to have little effect on the extent of strain hardening¹⁵.

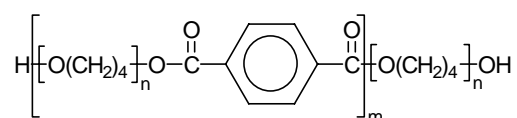


Figure 9.3: Structure of PTMO extended with DMT. The value of n determines the PTMO length, m determines the length of extended PTMO/DMT.

The properties of T Φ T-(PTMO₁₀₀₀/DMT) segmented copolymers, as function of the PTMO₁₀₀₀/DMT length and structure, have been studied thoroughly^{6,14-16}. The mechanical properties of these copolymers are very good. The copolymers show sharp transition temperatures (T_g , T_m) and a wide and constant rubbery plateau. The copolymers have good processability, good solvent resistance and are transparent. Also the elastic properties are good. Fibres that were spun from the melt can be stretched up to 2000% and after orientation still have a high fracture strain. The compression and tensile set are low compared to other melt-processable segmented copolymers. The best elasticity was obtained when the amorphous segment consists of PTMO of 1000 g/mol extended with DMT to 3000-7000 g/mol. However with such long PTMO₁₀₀₀/DMT segments the amide content is very low and as a result the melting temperature is low. For example T Φ T-(PTMO₁₀₀₀/DMT)₇₀₀₀ contains only 4 wt% of T Φ T and has a melting temperature of 119°C¹⁵. For the copolymers with the longer PTMO₁₀₀₀/DMT segments the elastic recovery after straining to 300% is comparable to that of commercial elastic materials such as Lycra[®]. The di-amides form thin lamellae, which can be deformed relatively easily. This is positive for high fracture strains, but not so good for the elastic properties. The question is if the elastic behaviour can be improved and if the melting temperature can be increased when longer crystallisable segments than di-amides are used that form ribbons with increased lamellar thickness.

Di-amide units with a higher melting temperature than the fully aromatic T Φ T are not known. The melting temperature can be increased by using di-amide segments that are extended via a diol^{11,23-25}, because the lamellar thickness of such extended segments is higher¹⁷. Copolymers with diol-extended di-amides have a higher melting temperature, but the melting temperature is broadened and also melt phasing occurs. This is caused by the length distribution in the diol-extended di-amides.

In this study segmented copolymers based on a new uniform crystallisable amide segment and PTMO were made. In these copolymers a tetra-amide crystallisable unit T6T6T based on two-and-a-half repeating units of nylon-6,T was used²⁶. The structure of the bisester tetra-amide T6T6T-dimethyl, having methyl ester endgroups, is given in Figure 9.4.

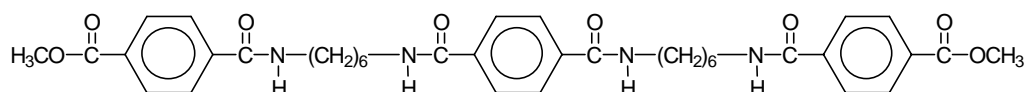


Figure 9.4: Structure of the crystallisable segment T6T6T-dimethyl.

The T6T6T tetra-amide segment can form four hydrogen bonds as compared to the T6T segment and other di-amide segments that can only form two hydrogen bonds. As a result the lamellar thickness will be higher and the melting temperature is expected to be higher than with di-amide units¹⁷. The expectation is that copolymers of PTMO with tetra-amide units show better elasticity than copolymers with di-amide units because it is more difficult to shear the thicker T6T6T crystallites.

The uniformity of the tetra-amide segment is defined as the percentage of T6T6T-dimethyl in the starting material. When the uniformity is below 100%, part of the product consists of side products such as T6T6T6T-dimethyl or T6T6T6T6T-dimethyl²⁶.

Aim

In this chapter the synthesis and structure-property relationships of segmented copolymers based on poly(tetramethylene oxide) as an amorphous segment and T6T6T-dimethyl as crystallisable segment will be discussed. As amorphous segment PTMO and extended PTMO₁₀₀₀/DMT of different lengths were used. As crystallisable segment T6T6T-dimethyl of high and low uniformity were used. The polymers were injection moulded into test bars and the mechanical and elastic properties of the polymers were studied. The morphology of the polymers was studied using AFM and WAXD. The crystallisation was studied with DSC.

Experimental

Materials. Dimethyl terephthalate (DMT) and N-methyl-2-pyrrolidone (NMP) were purchased from Merck and used as received. Tetra-isopropyl orthotitanate (Ti(i-OC₃H₇)₄), purchased from Merck, was diluted in anhydrous *m*-xylene (to 0.05M), obtained from Fluka. Poly(tetramethylene oxide) (PTMO, 1000, 2000 and 2900 g/mol) was provided by DuPont. Irganox 1330 was obtained from CIBA. T6T6T-dimethyl was synthesised from DMT, MPT (methyl phenyl terephthalate) and 1,6-hexamethylenediamine (HMDA) as described in Chapter 5²⁶.

Synthesis of T6T6T-PTMO. The T6T6T-PTMO copolymers were synthesised by a polycondensation reaction¹⁴ using PTMO of different lengths and T6T6T-dimethyl. The preparation of T6T6T-PTMO₂₀₀₀ is given as an example.

The reaction was carried out in a 250 ml stainless steel reactor with a nitrogen inlet and mechanical stirrer. The vessel was loaded with T6T6T-dimethyl (6.86 g, 10 mmol), PTMO₂₀₀₀ (20.0 g, 20 mmol), Irganox 1330 (0.2 g), 100 ml NMP and catalyst solution (2 ml of 0.05M Ti(i-OC₃H₇)₄ in *m*-xylene). This mixture was first heated in an oil bath to 180°C under nitrogen flow. After 30 minutes reaction time, the temperature was raised to 220°C and after another 30 minutes to 250°C and maintained for two hours. The pressure was then carefully reduced (P<20 mbar) to distil off the NMP during 30 minutes and then further reduced (P<1 mbar) for 60 minutes. During this last hour, the temperature was first raised to 280°C for 15 minutes and reduced to 250°C for the final 45 minutes. Finally, the vessel was allowed to

slowly cool to room temperature whilst maintaining the low pressure. Then the polymer was cooled with liquid nitrogen, cut out of the reactor and crushed.

Synthesis of T6T6T-(PTMO₁₀₀₀/DMT). The T6T6T-(PTMO₁₀₀₀/DMT) copolymers were synthesised by a polycondensation reaction¹⁴ using PTMO (1000 g/mol) extended with DMT and T6T6T-dimethyl. The preparation of T6T6T-(PTMO₁₀₀₀/DMT)₃₀₀₀ (PTMO of 1000 g/mol extended to 3000 g/mol with DMT) is given as an example.

The reaction was carried out in a 250 ml stainless steel reactor with a nitrogen inlet and mechanical stirrer. The vessel was loaded with T6T6T-dimethyl (6.86 g, 10.0 mmol), PTMO₁₀₀₀ (27.7 g, 27.7 mmol), DMT (3.44 g, 17.7 mmol), Irganox 1330 (0.3 g), 100 ml NMP and catalyst solution (3 ml of 0.05M Ti(i-OC₃H₇)₄ in *m*-xylene). This mixture was first heated in an oil bath to 180°C under nitrogen flow. After 30 minutes reaction time, the temperature was raised to 220°C and after another 30 minutes to 250°C and maintained for two hours. The pressure was then carefully reduced (P<20 mbar) to distil off the NMP and then further reduced (P<1 mbar) for 60 minutes. Finally, the vessel was allowed to slowly cool to room temperature whilst maintaining the low pressure. Then the polymer was cooled with liquid nitrogen, cut out of the reactor and crushed.

Viscometry. The inherent viscosity of the polymers was determined with a capillary Ubbelohde type 1B at 25°C, using a polymer solution with a concentration of 0.1 g/dl in phenol/1,1,2,2-tetrachloroethane (50/50, mol/mol).

DMA. Samples for the DMA test (70x9x2mm³) were prepared on an Arburg-H manual injection moulding machine. Before use, the samples were dried in a vacuum oven at 70°C overnight. The torsion behaviour (G' and G'' versus temperature) was studied at a frequency of 1 Hz, a strain of 0.1% and a heating rate of 1°C/min using a Myrenne ATM3 torsion pendulum. The glass transition temperature (T_g) was expressed as the temperature where the loss modulus G'' has a maximum. The flow temperature (T_{flow}) was defined as the temperature where the storage modulus G' reached 1 MPa. The storage modulus of the rubbery plateau is determined at room temperature ($G'(25^\circ\text{C})$).

Compression set. A piece of an injection moulded test bar (~2.15 mm thickness), was placed between two steel plates and compressed to 1 mm (~55% compression) or 1.6 mm (~25% compression). After 24 hours at 20 or 70°C the compression was released. One hour later the thickness of the sample was measured. The compression set (CS) was defined as:

$$\text{Compression set} = \frac{d_0 - d_2}{d_0 - d_1} \times 100\% \quad [\%] \quad \text{Equation 9.1}$$

with: d_0 = thickness before compression [mm]
 d_1 = thickness during compression [mm]
 d_2 = thickness one hour after release of compression [mm]

DSC. DSC spectra were recorded on a Perkin Elmer DSC7 apparatus, equipped with a PE7700 computer and TAS-7 software. Dried samples of 5-10 mg polymer were measured with a heating and cooling rate of 20°C/min. The samples were heated to 300°C, kept at that temperature for 2 minutes, cooled to 50°C and reheated to 300°C. The (peak) melting temperature and enthalpy were taken from the second heating scan. The crystallisation temperature was taken as the maximum of the peak in the cooling scan.

WAXD. X-ray diffraction data of melt-pressed samples were collected with a Philips PW3710 based X'Pert-1 diffractometer in Bragg-Brentano geometry, using a Θ compensating divergence slit (12.5 mm length). Diffraction data collection was performed at room temperature, using a low-background spinning (1 r/s) specimen holder. $\text{CuK}\alpha_1$ radiation of 1.54056 Å was obtained with a curved graphite monochromator. The data were collected in a range of $2\Theta = 4\text{-}60^\circ$.

Melt-pressed samples of 10x15x1 mm were prepared from an injection-moulded test bar in a mould at 280°C for 5 minutes with a pressure of 10 bar, after which the samples were slowly cooled with 5°C/min.

AFM. AFM measurements were performed on a Nanoscope III A (Veeco/Digital Instruments) AFM in tapping mode. The AFM was equipped with a D-scanner with a maximum scan size of 15 μm^2 . Commercially available Si-cantilevers (Nanosensors) were used to obtain the height and phase images.

Solution cast samples of ~1 μm thickness on glass were prepared from a 1 wt% solution in NMP (100°C) and dried at 100°C during one night. Bulk samples (solidified from the melt) were taken from the wall of the reaction vessel after cooling slowly to room temperature and used as such.

Results and Discussion

Copolymers based on T6T6T-dimethyl and PTMO or PTMO extended with DMT were synthesised via a polycondensation reaction. The first part of the polymerisation reaction was carried out in NMP solution, because of the high melting temperature of T6T6T-dimethyl (303°C)²⁶. After two hours at 250°C, the reaction had progressed enough to allow the final part of the reaction to be performed in the melt. A vacuum of <1 mbar was applied during the last hour to strip off any methanol formed and to obtain polymers with high molecular weights. For high T6T6T content (PTMO length <3000 g/mol) the temperature was raised to 280°C for 15 minutes during the last stage of the reaction to get a homogeneous, clear melt.

Three series of segmented copolymers based on T6T6T-dimethyl and PTMO were made:

1. Uniform T6T6T-dimethyl with PTMO of different lengths (2000 and 2900 g/mol).
2. Uniform T6T6T-dimethyl with extended PTMO of 1000 g/mol with a $\text{PTMO}_{1000}/\text{DMT}$ length of 3000-10000 g/mol.
3. T6T6T-dimethyl with a uniformity of ~76% (76 mol% T6T6T-dimethyl and 24 mol% $\text{T}(6\text{T})_n$ with $n>2$) with $\text{PTMO}_{1000}/\text{DMT}$ of 3000-6000 g/mol.

The copolymers could be easily obtained with high molecular weights (inherent viscosity > 1 dl/g, ~15.000 g/mol), but it was more difficult to obtain high molecular weight (> 2 dl/g, ~30.000 g/mol) with non-uniform T6T6T. With NMR it was shown that the uniformity of the tetra-amide segments is preserved in the copolymer. The solvent resistance of the materials is very good, as they are only soluble at low concentration and after long time in solvents such as a 50/50 mixture of phenol/1,1,2,2-tetrachloroethane, trifluoro acetic acid or NMP (above 100°C). Furthermore the materials are transparent, which indicates that the crystallite sizes are very small (no spherulites) and that no liquid-liquid demixing or melt phasing has occurred¹⁴. The materials have a faint yellow colour. The intensity of the colour decreases with increasing soft segment length. The mechanical properties of the polymers will be discussed first, followed by the data obtained by DSC experiments, compression set, WAXD and AFM.

Thermal-mechanical properties

The polymers were injection moulded into bars and dried in a vacuum oven at 70°C. The thermal-mechanical properties were measured by DMA. The results are given in Table 9.1. The T6T6T content was calculated, assuming that the ester carbonyl does not crystallise and belongs to the amorphous phase¹⁸. The results of the three different series will be discussed successively.

Series 1: T6T6T-PTMO

T6T6T-PTMO copolymers based on uniform T6T6T and PTMO of 2000 and 2900 g/mol were made. The thermal-mechanical properties as studied by DMA are given in Table 9.1 and Figure 9.5.

The hard segment content decreases with increasing soft segment length, due to the uniform length of the hard segments. Both copolymers show a rather broad glass and melting transition of the PTMO phase, a sharp flow temperature of the T6T6T phase and a wide and temperature-independent rubbery plateau. The modulus of the rubbery plateau, the loss modulus and the flow temperature increase with increasing T6T6T content, due to increased crystallinity.

The glass transition temperature is determined as the maximum of the loss modulus G'' . The T_g of the copolymers with PTMO of 2000 and 2900 g/mol is -70°C , which is close to the T_g of pure PTMO (-86°C)²⁷. The low and constant glass transition temperature of PTMO in the copolymer suggests that little amorphous T6T6T is being mixed with PTMO¹⁴ and thus that crystallisation of T6T6T is almost complete. The shoulder in the modulus after the glass transition at $-50 - 0^\circ\text{C}$ is a result of the presence of a PTMO crystalline phase that melts at this temperature. Especially longer PTMO segments above 1400 g/mol are able to crystallise^{14,15}.

The DMA data do not show the presence of a second T_g which can be ascribed to the presence of a separate amorphous T6T6T phase (T_g nylon-6, $T = 125^\circ\text{C}$ ²⁸). Thus all T6T6T that is pre-ordered in the melt crystallises and the part of the T6T6T units that does not crystallise mixes with the amorphous PTMO phase.

Table 9.1: Thermal-mechanical properties as measured by DMA of the T6T6T-PTMO copolymers with uniform T6T6T (series 1), T6T6T-(PTMO₁₀₀₀/DMT) with uniform T6T6T (series 2) and T6T6T-(PTMO₁₀₀₀/DMT) with T6T6T with a uniformity of 76% (series 3).

	T6T6T content [wt%]	η_{inh} [dl/g]	T_g [°C]	$G'(25^\circ\text{C})$ [MPa]	T_{flow} [°C]
Series 1: uniform					
T6T6T-PTMO ₂₀₀₀	22	2.2	-70	34	226
T6T6T-PTMO ₂₉₀₀	16	2.7	-70	17	216
Series 2: uniform					
T6T6T-(PTMO ₁₀₀₀ /DMT) ₃₀₀₀	15.7	3.1	-61	14.5	220
T6T6T-(PTMO ₁₀₀₀ /DMT) ₄₀₀₀	12.3	2.3	-60	8.5	208
T6T6T-(PTMO ₁₀₀₀ /DMT) ₆₀₀₀	8.6	2.6	-61	6.8	200
T6T6T-(PTMO ₁₀₀₀ /DMT) ₈₀₀₀	6.6	2.2	-63	5.1	190
T6T6T-(PTMO ₁₀₀₀ /DMT) ₁₀₀₀₀	5.4	2.5	-63	3.3	183
Series 3: non-uniform					
T6T6T-(PTMO ₁₀₀₀ /DMT) ₃₀₀₀	15.7	1.4	-60	23.5	242
T6T6T-(PTMO ₁₀₀₀ /DMT) ₄₀₀₀	12.3	1.5	-61	14.3	240
T6T6T-(PTMO ₁₀₀₀ /DMT) ₆₀₀₀	8.6	1.9	-61	6.9	210

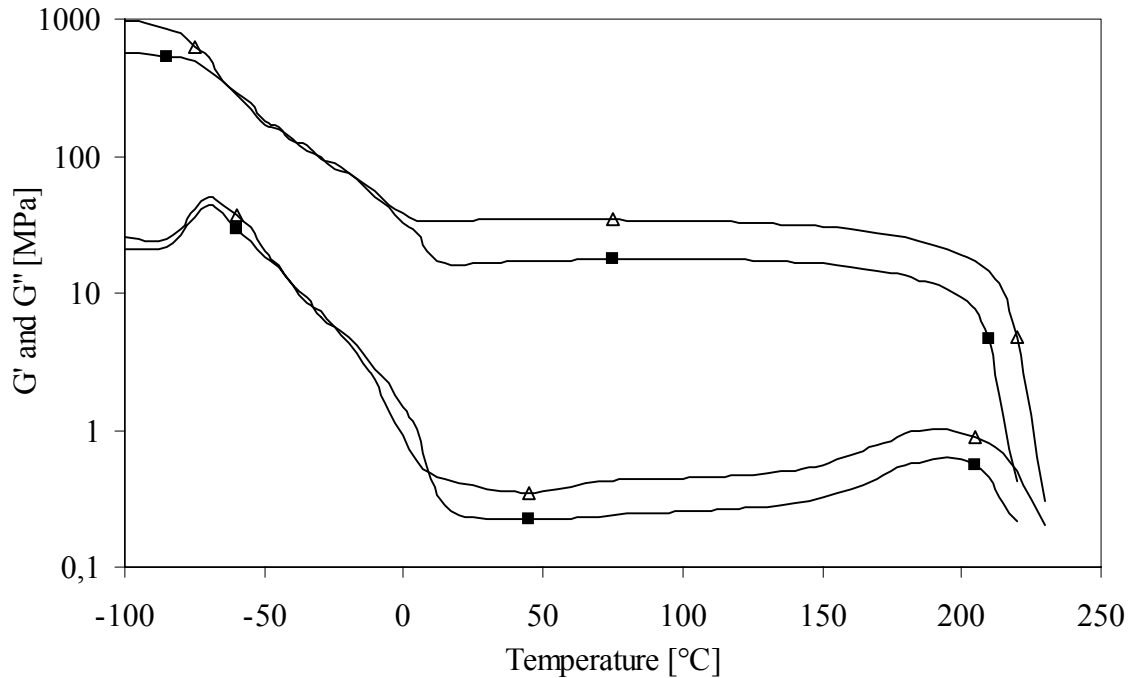


Figure 9.5: Storage and loss modulus of T6T6T-PTMO copolymers with different soft segment lengths and uniform T6T6T (series 1): (\square), 2000 g/mol; (\blacksquare), 2900 g/mol.

The flow temperature is defined as the temperature where the storage modulus G' reaches 1 MPa. The flow temperature is 0 - 10°C lower than the melting temperature. The flow temperature is more close to the melting temperature when the flow temperature is sharp. The copolymers of series 1 show a sharp flow temperature. This can be explained by the formation of perfect, uniform lamellae from uniform T6T6T. Lamellae of uniform thickness melt in a narrow temperature range. The T_{flow} decreases with decreasing T6T6T content. This result is in agreement with what has been observed in other systems¹¹⁻¹⁵. This effect has been explained by the solvent effect theory of Flory²⁹. The degree of crystallinity increases when the T6T6T content increases or when the PTMO length decreases. The flow temperature of the T6T6T segmented copolymers is considerably higher than the T_{flow} of the T6T-PTMO¹¹ copolymers and other di-amide copolymers¹²⁻¹⁵. Copolymers based on tetra-amide crystallisable segments have higher melting temperatures in the copolymer compared to di-amide segments.

The modulus of the rubbery plateau is constant over a wide temperature range. This is also a result of the formation of perfect crystalline lamellae with T6T6T. When some of the crystallites would melt at a lower temperature, a decrease in modulus with temperature would be expected.

Series 2: T6T6T-(PTMO₁₀₀₀/DMT) (uniform T6T6T)

A polymer series of T6T6T-(PTMO₁₀₀₀/DMT) with uniform T6T6T and PTMO₁₀₀₀/DMT of 3000-10000 g/mol was made. The thermal-mechanical properties as studied by DMA are given in Table 9.1 and Figure 9.6.

All polymers of series 2 show a sharp glass transition of the PTMO₁₀₀₀/DMT phase, a sharp flow temperature of the T6T6T phase and a wide and temperature-independent rubbery plateau. The glass transition temperature of PTMO₁₀₀₀/DMT is independent of the T6T6T content, which suggests that little T6T6T is dissolved in this phase and that this amount is independent of the T6T6T content.

With increasing T6T6T content the rubber modulus and flow temperature increase due to increased crystallinity as was explained for series 1. The influence of T6T6T content on T_g , rubber modulus and T_{flow} will be discussed in more detail later.

The loss modulus is very low for all copolymers of series 2, except for T6T6T-(PTMO/₁₀₀₀DMT)₃₀₀₀ that shows a somewhat higher G'' . This indicates that the elasticity decreases with increasing T6T6T content.

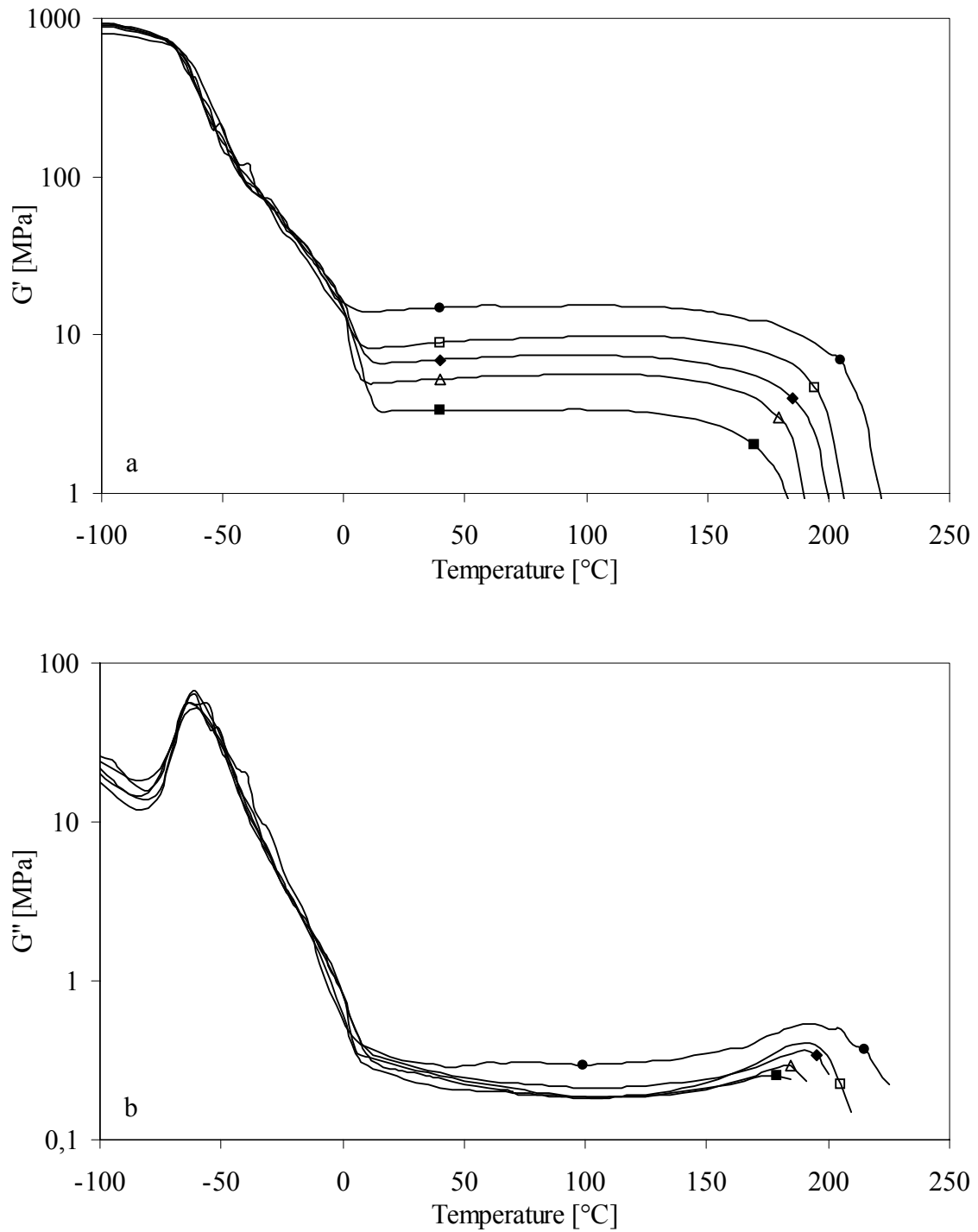


Figure 9.6: Storage (a) and loss (b) modulus of T6T6T-(PTMO₁₀₀₀/DMT) copolymers with different soft segment lengths and uniform T6T6T (series 2): (●), 3000 g/mol; (□), 4000 g/mol; (◆), 6000 g/mol; (△), 8000 g/mol; (■), 10000 g/mol.

In Figure 9.7 the storage and loss modulus of T6T6T-(PTMO/1000DMT)₃₀₀₀ are compared with those of T6T6T-PTMO₂₉₀₀. Both have about the same T6T6T content. The T_g is in general a little higher (5-10°C) for extended PTMO₁₀₀₀ than for copolymers of series 1 with regular PTMO. This is caused by the incorporation of the terephthalic unit in the PTMO amorphous phase, which makes this phase a little less flexible. When the segmental mobility decreases, the T_g increases. The same difference between regular and extended PTMO was found for copolymers with aromatic di-amides as crystallisable unit^{14,15}.

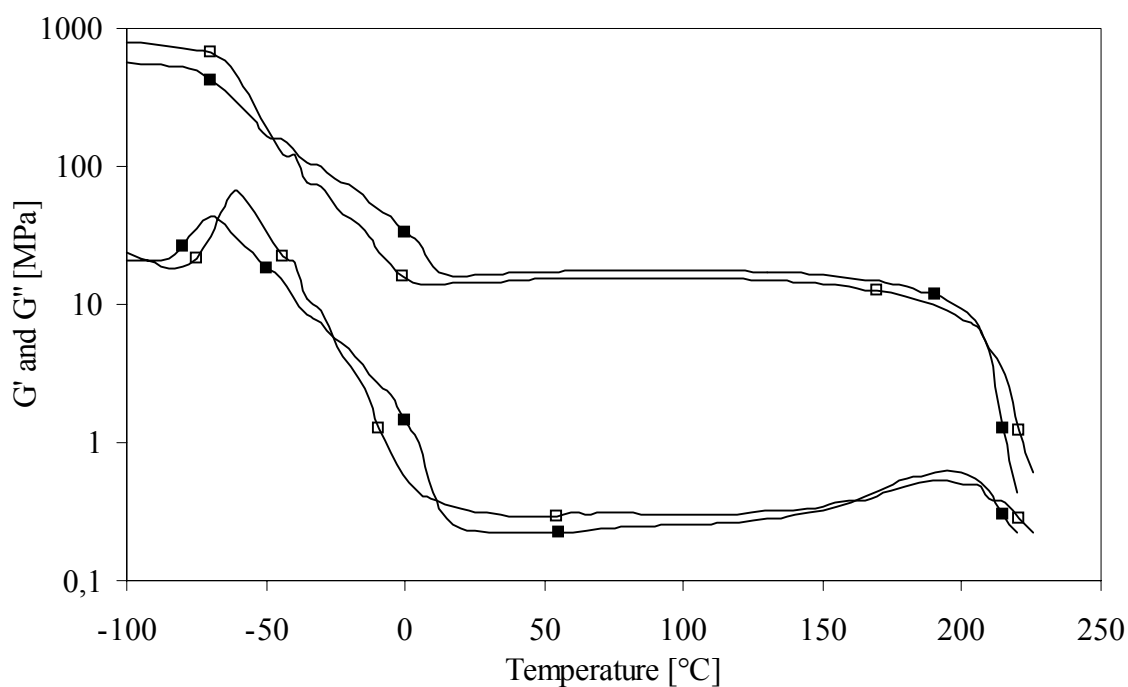


Figure 9.7: Storage and loss modulus of copolymers of series 1 and 2 with soft segment length around 3000 g/mol and uniform T6T6T: (■), T6T6T-PTMO₂₉₀₀ (series 1); (□), T6T6T-(PTMO₁₀₀₀/DMT)₃₀₀₀ (series 2).

Both copolymers based on regular PTMO₂₉₀₀ or extended PTMO₁₀₀₀/DMT of 3000 g/mol show a shoulder in the modulus after the glass transition at -50 - 0°C as a result of the presence of a PTMO crystalline phase. The shoulder is smaller for extended PTMO than regular PTMO of the same length. PTMO₁₀₀₀/DMT is less easy to crystallise¹⁵.

The modulus in the rubbery plateau and the flow temperature of T6T6T-PTMO₂₉₀₀ and T6T6T-(PTMO₁₀₀₀/DMT)₃₀₀₀ are comparable, which indicates that the degree of crystallinity and crystalline morphology of both copolymers are equal.

In Figure 9.8 the modulus is given as function of temperature for T6T6T-(PTMO₁₀₀₀/DMT)₃₀₀₀, compared to two other copolymers based on extended PTMO₁₀₀₀/DMT and the di-amide segment TΦT as crystallisable segment¹⁵. TΦT is based on one-and-a-half repeating unit of poly-(*p*-phenylene terephthalamide). In TΦT-(PTMO₁₀₀₀/DMT)₁₅₀₀ the content of crystallisable units (16 wt%) is the same as in T6T6T-(PTMO₁₀₀₀/DMT)₃₀₀₀. In TΦT-(PTMO₁₀₀₀/DMT)₃₀₀₀ (9 wt% TΦT) the soft segment length between two crystallisable

units (3000 g/mol) is the same as in T6T6T-(PTMO₁₀₀₀/DMT)₃₀₀₀ (16 wt% T6T6T) and as a result the hard segment content with TΦT is lower. The T6T6T and TΦT polymers with an amorphous segment length of 3000 g/mol have the same molar content of amide units and thus at constant molecular weight the same number of physical crosslinks per chain (network density).

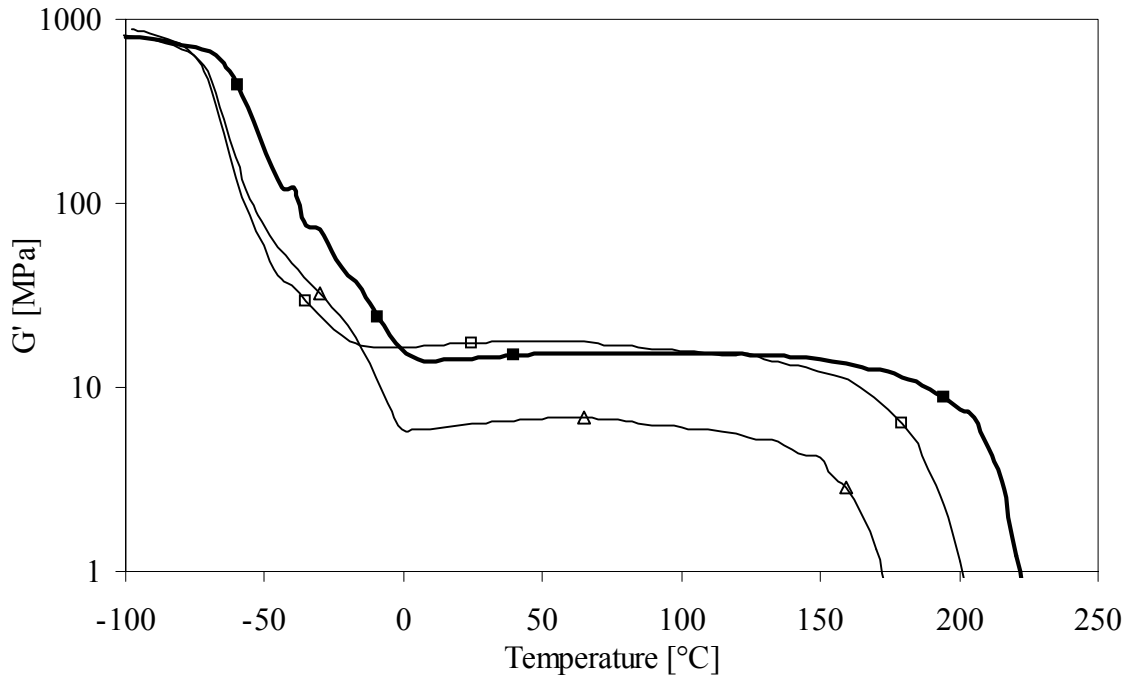


Figure 9.8: Storage modulus of copolymers with PTMO₁₀₀₀/DMT soft segment and T6T6T compared to TΦT as crystallisable segment: (■), T6T6T-(PTMO₁₀₀₀/DMT)₃₀₀₀; (△), TΦT-(PTMO₁₀₀₀/DMT)₃₀₀₀ (same molar content amide)¹⁵; (□) TΦT-(PTMO₁₀₀₀/DMT)₁₅₀₀ (same weight content amide)¹⁵.

Figure 9.8 shows that the glass transition temperature is 5°C lower with TΦT as compared to T6T6T in PTMO₁₀₀₀/DMT. This indicates that more T6T6T than TΦT can dissolve in the amorphous PTMO phase. Probably T6T6T has more interaction with the PTMO₁₀₀₀/DMT phase than TΦT. As a result the phase separation is a little less complete and part of the T6T6T is present in the amorphous phase.

As a result of the increased T_g with T6T6T the rubbery plateau for T6T6T-(PTMO₁₀₀₀/DMT)₃₀₀₀ starts at a higher temperature than with TΦT. For some applications it is important that the material has constant properties down to very low temperatures.

The modulus of the rubbery plateau is influenced by the crystallinity (reinforcement by fibres or crystalline ribbons) and the network density. A polymer with 16 wt% T6T6T (PTMO₁₀₀₀/DMT of 3000 g/mol) has the same modulus as a polymer with 16 wt% TΦT (PTMO₁₀₀₀/DMT of 1500 g/mol). The modulus of the TΦT-(PTMO₁₀₀₀/DMT)₃₀₀₀ (9 wt% TΦT) copolymer is much lower than that of T6T6T-(PTMO₁₀₀₀/DMT)₃₀₀₀ (16 wt% T6T6T). The modulus of the rubbery plateau is thus determined predominately by the weight content of amide units. The crystallinity of the amide units in both copolymers with 16 wt% amide units is expected to be about the same, since the rubber moduli are the same. It was however

expected that the crystallinity of T6T6T-(PTMO₁₀₀₀/DMT)₃₀₀₀ would be a little lower, because the T_g of this polymer was higher as a result of more mixing with amorphous T6T6T. Therefore, probably only a small percentage of the 16 wt% of T6T6T is dissolved in the amorphous PTMO₁₀₀₀/DMT phase.

With 16 wt% T6T6T the flow temperature is about 20°C higher than with 16 wt% T Φ T. The melting temperature of T Φ T-dimethyl is 371°C¹⁴ and that of T6T6T-dimethyl is 303°C²⁶. Apparently the solvent effect of PTMO is lower for T6T6T than for T Φ T. This is due to the higher lamellar thickness of crystalline ribbons of T6T6T. The more the segment length approaches that of the homopolymer of the crystalline segment, the smaller the solvent effect of the amorphous phase²⁹.

Series 3: T6T6T-(PTMO₁₀₀₀/DMT) (T6T6T with a uniformity of 76%)

In Figure 9.9 and Table 9.1 an overview of the thermal-mechanical properties as measured by DMA of the T6T6T-(PTMO₁₀₀₀/DMT) copolymers with T6T6T-dimethyl of low uniformity (76%) is given. This T6T6T-dimethyl consists for 76 mol% of T6T6T-dimethyl and 24 mol% of T(6T)_n with $n > 2$. It is more difficult to obtain high molecular weight polymers when non-uniform T6T6T is used because it is not possible to calculate the amount of reactants in stoichiometry.

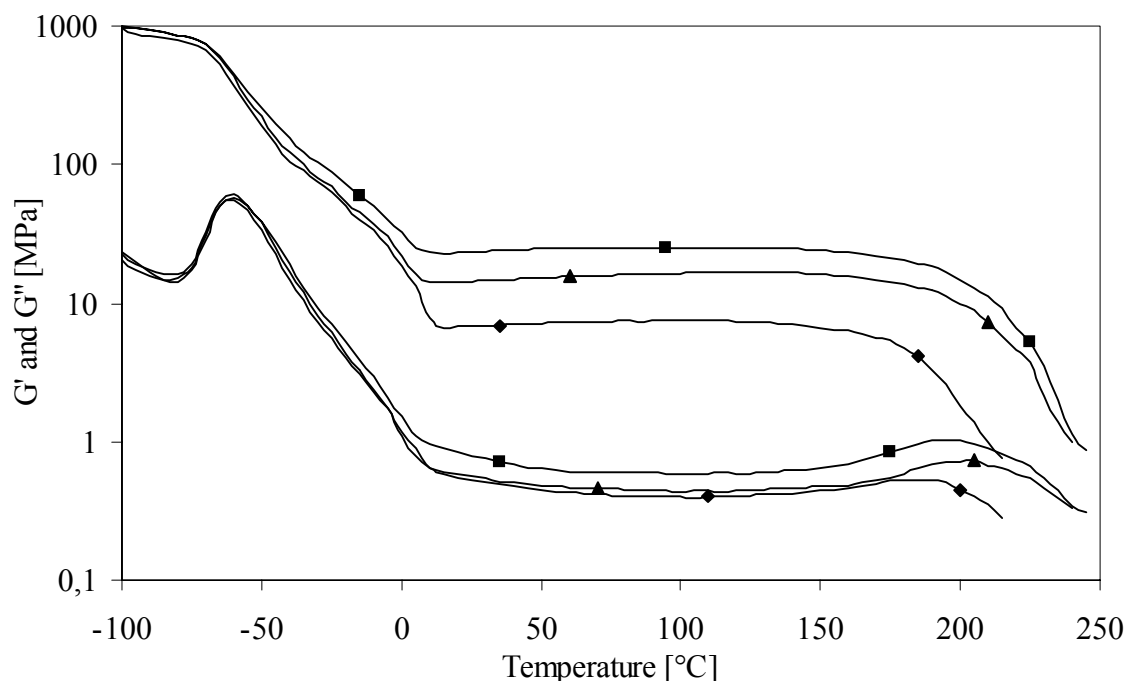


Figure 9.9: Storage and loss modulus of T6T6T-(PTMO₁₀₀₀/DMT) copolymers with different soft segment lengths and T6T6T with a uniformity of 76% (series 3): (■), T6T6T-(PTMO/1000DMT)₃₀₀₀; (▲), T6T6T-(PTMO/1000DMT)₄₀₀₀; (◆), T6T6T-(PTMO/1000DMT)₆₀₀₀.

The effect of T6T6T content on T_g , rubbery plateau and T_{flow} in polymers based on non-uniform T6T6T and PTMO₁₀₀₀/DMT is comparable with that using uniform T6T6T (series 2). The T_g is constant and the rubbery plateau and flow temperature increase with increasing

T6T6T content. Also the loss modulus increases with increasing T6T6T content, especially for the higher T6T6T content. The only difference with series 2 is that the flow temperature with non-uniform T6T6T is shows a trajet. The influence of T6T6T content on T_g , rubber modulus and T_{flow} will be discussed in more detail later.

It is difficult to compare the results of the polymers with uniform and non-uniform T6T6T at the same PTMO₁₀₀₀/DMT length, because there is a large difference in molecular weight. When the inherent viscosity is lower than 2.0 the properties seem to change. The crystallinity seems to increase while the polymers become less elastic. Also the crystallinity of PTMO seems to be enhanced when the molecular weight of a copolymer decreases. As a result the polymers with low molecular weight are less transparent. The influence of molecular weight will be studied in more detail in the near future.

The inherent viscosity of T6T6T-(PTMO₁₀₀₀/DMT)₆₀₀₀ (1.9 dl/g) with non-uniform T6T6T (series 3) is high enough to allow comparison of the DMA data with that of series 2. In Figure 9.10 the storage moduli of T6T6T-(PTMO₁₀₀₀/DMT)₆₀₀₀ with uniform and non-uniform T6T6T are compared.

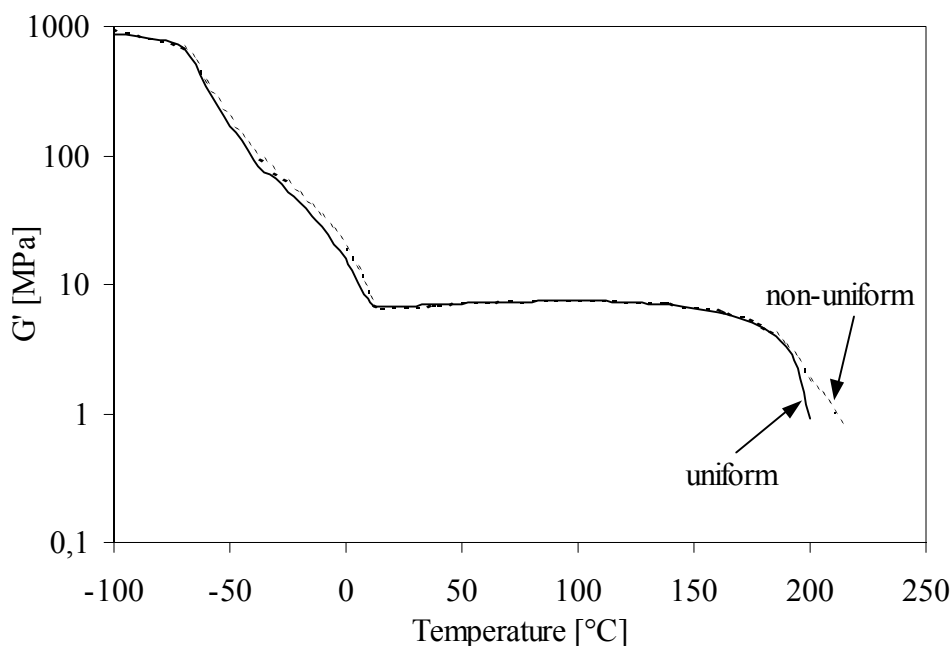


Figure 9.10: Storage modulus of T6T6T-(PTMO₁₀₀₀/DMT)₆₀₀₀: (—), series 2 (uniform T6T6T, 2.0 dl/g); (- - -), series 3 (non-uniform T6T6T, 1.9 dl/g).

From Figure 9.10 it can be concluded that using non-uniform T6T6T has no effect on the glass transition temperature or rubbery plateau. Therefore the phase separation and the crystallinity of T6T6T are the same. The rubbery plateau remains flat because there are only T(6T)_n units with a higher melting temperature ($n > 2$) present and not for example T6T units that melt at a lower temperature. Therefore the only difference can be seen at the flow temperature. The flow temperature is sharper and therefore lower with uniform T6T6T as

compared to non-uniform T6T6T. This is due to the presence of longer $T(6T)_n$ segments (such as T6T6T6T) in the non-uniform T6T6T. These longer segments will form thicker crystalline lamellae with a higher melting temperature¹⁷. A disadvantage of this higher and broader flow temperature is that the processing temperature for the polymer with non-uniform T6T6T is higher. As a result there is more chance for thermal degradation.

Glass transition temperature

In Figure 9.11 the glass transition temperature of the PTMO(/DMT) phase is given as function of the hard segment content for T6T6T-PTMO(/DMT) (series 1-3) and T Φ T-PTMO(/DMT) copolymers.

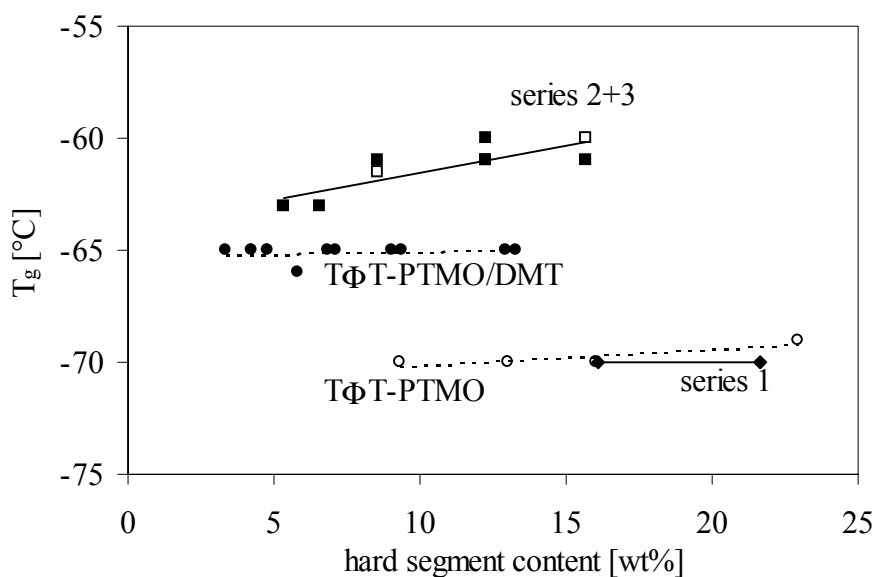


Figure 9.11: Glass transition temperature of PTMO(/DMT) as function of hard segment content: (♦), T6T6T-PTMO, series 1; (■), T6T6T-(PTMO₁₀₀₀/DMT), series 2; (□), T6T6T-(PTMO₁₀₀₀/DMT), series 3, non-uniform; (○), T Φ T-PTMO¹⁴; (●), T Φ T-PTMO₁₀₀₀/DMT¹⁵.

The glass transition temperature is near the T_g of pure PTMO (-86°C)²⁶ for copolymers of PTMO and T6T6T (series 1) or T Φ T¹⁴. With extended PTMO₁₀₀₀/DMT and T Φ T the T_g is increased to -65°C and with T6T6T to -63 to -60°C . Apparently PTMO₁₀₀₀/DMT has a little higher T_g than PTMO because the flexibility decreases by incorporation of a terephthalic unit. The explanation is consistent with the observation that the T_g is almost independent of the hard segment content.

The somewhat higher T_g of PTMO₁₀₀₀/DMT in the copolymers with T6T6T compared to T Φ T might be caused by less complete crystallisation of T6T6T. As a result more T6T6T units are mixed with the amorphous PTMO₁₀₀₀/DMT phase which decreases the mobility. It could also be that more hydrogen bonding between T6T6T and terephthalic units in PTMO₁₀₀₀/DMT is possible than with T Φ T, which increases the stiffness of this phase as well.

Rubber modulus

In Figure 9.12 the rubber modulus for T6T6T-PTMO(/DMT) with T6T6T (series 1-3) is given as a function of the hard segment content. The modulus of the rubbery plateau at 25°C with T6T6T is compared with that of polymers with TΦT as a hard segment.

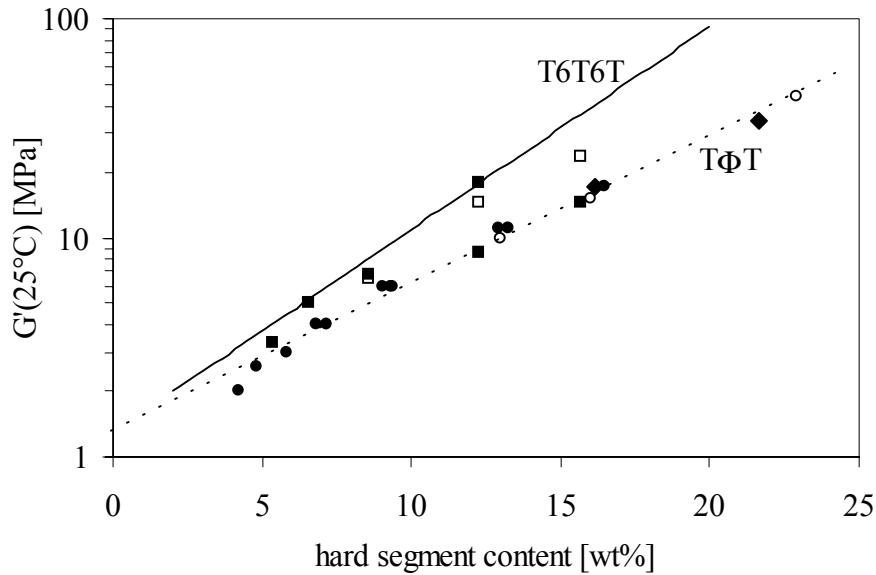


Figure 9.12: Modulus at room temperature as function of hard segment content: (◆), T6T6T-PTMO, series 1; (■), T6T6T-(PTMO₁₀₀₀/DMT), series 2; (□), T6T6T-(PTMO₁₀₀₀/DMT), series 3, non-uniform; (○), TΦT-PTMO¹⁴; (●), TΦT-PTMO₁₀₀₀/DMT¹⁵.

Figure 9.12 shows that the logarithm of the modulus at room temperature ($G'(25^\circ\text{C})$) increases with the T6T6T and TΦT content. With TΦT a linear increase of rubber modulus with TΦT content was found. According to Wegner³⁰, the logarithm of the modulus in the rubbery plateau of a segmented copolymer follows a linear relationship with the crystallinity. Equation 9.2 describes this relationship where E is the modulus, E_c is the modulus of the crystalline fraction, E_a is the modulus of the amorphous fraction and x_c is the crystallinity.

$$\log E = \log E_a + x_c \log \frac{E_c}{E_a} \quad \text{Equation 9.2}$$

The effect of increasing hard segment content on the modulus is strong. The strong increase in modulus with T6T6T and TΦT content is probably due to the formation of threads or ribbons of crystalline units that act as reinforcing fillers for the amorphous matrix⁶. The copolymers with T6T6T as crystallisable units with high inherent viscosity (> 2 dl/g) follow the line for TΦT. With T6T6T the copolymers with an inherent viscosity of ~ 1.5 dl/g have a higher rubber modulus. This suggests that the crystallisation is better and more complete or more effective when the molecular weight is not too high (around 1.4-1.6 dl/g).

A linear relationship between rubber modulus and T6T6T content is drawn for T6T6T using the points with maximum crystallinity and the intercept for TΦT-PTMO(/DMT) copolymers

(1.3 MPa). When it is assumed that the crystallinity is 100% in these copolymers the following relation between rubber modulus and crystallinity can be set:

$$G'(25^{\circ}\text{C}) = 1.3 * \exp(0.21 * x_c) \quad [\text{MPa}] \quad \text{Equation 9.3}$$

With Equation 9.3 the crystallinity (x_c ; wt% crystalline T6T6T) and crystallinity of T6T6T (crystalline T6T6T content x_c /T6T6T content) in the copolymers of series 1-3 can be calculated. The results can be found in Table 9.2.

Table 9.2: Degree of crystallinity as calculated with Equation 9.3 and crystallinity of T6T6T in T6T6T-PTMO(/DMT) copolymers of series 1-3.

	η_{inh} [dl/g]	$G'(25^{\circ}\text{C})$ [MPa]	T6T6T content [wt%]	Crystalline content [wt%]	Crystallinity T6T6T [%]
Series 1: uniform					
T6T6T-PTMO ₂₀₀₀	2.2	34	21.7	16	72
T6T6T-PTMO ₂₉₀₀	2.7	17	16.1	12	76
Series 2: uniform					
T6T6T-(PTMO ₁₀₀₀ /DMT) ₃₀₀₀	3.1	14.5	15.7	11	73
T6T6T-(PTMO ₁₀₀₀ /DMT) ₄₀₀₀	1.4	18	12.3	12	100
T6T6T-(PTMO ₁₀₀₀ /DMT) ₄₀₀₀	2.3	8.5	12.3	8	73
T6T6T-(PTMO ₁₀₀₀ /DMT) ₆₀₀₀	2.6	6.8	8.6	7	92
T6T6T-(PTMO ₁₀₀₀ /DMT) ₈₀₀₀	2.2	5.1	6.6	5	99
T6T6T-(PTMO ₁₀₀₀ /DMT) ₁₀₀₀₀	2.5	3.3	5.4	3	83
Series 3: non-uniform					
T6T6T-(PTMO ₁₀₀₀ /DMT) ₃₀₀₀	1.4	23.5	15.7	14	88
T6T6T-(PTMO ₁₀₀₀ /DMT) ₄₀₀₀	1.5	14.3	12.3	11	93
T6T6T-(PTMO ₁₀₀₀ /DMT) ₆₀₀₀	1.9	6.9	8.6	7	93

The crystallinity of T6T6T in the copolymers is between 72 and 100%, provided that the T6T6T in the copolymers that were assumed to have 100% crystallinity has indeed crystallised completely. When the crystallinity of T6T6T in these reference polymers is somewhat lower than 100%, then the calculated, relative crystallinity of the other copolymers decreases correspondingly.

The effect of the inherent viscosity (molecular weight) on the crystallisation of T6T6T is as yet unclear. It seems that the crystallinity of T6T6T is higher when the inherent viscosity is below 2 dl/g.

Flow temperature

In Figure 9.13 the flow temperature for T6T6T-PTMO(/DMT) with uniform T6T6T (series 1 and 2) is given as function of the hard segment content. The copolymers with non-uniform T6T6T have a higher flow temperature due to the presence of thicker crystalline lamellae¹⁷.

These results are not incorporated in Figure 9.13. The flow temperature with T6T6T is compared with that of copolymers with TΦT as crystallisable segment.

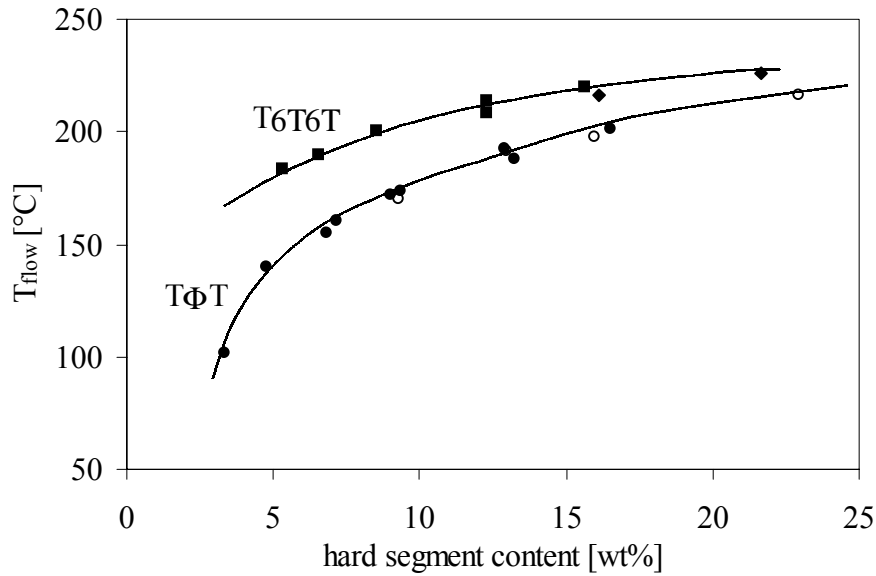


Figure 9.13: Flow temperature ($G' = 1$ MPa) as function of hard segment content: (♦), T6T6T-PTMO, series 1; (■), T6T6T-(PTMO₁₀₀₀/DMT), series 2; (○), TΦT-PTMO¹⁴; (●), TΦT-PTMO₁₀₀₀/DMT¹⁵.

The flow temperature decreases with decreasing hard segment content. This phenomenon has been explained by the solvent effect theory of Flory^{14,29} (Equation 9.4). According to this theory a decrease in the melting temperature can mainly be ascribed to differences in the molar fraction of crystalline units. With decreasing T6T6T content the molar fraction decreases and thus the melting temperature and flow temperature decrease.

$$\frac{1}{T_m} - \frac{1}{T_m^0} = \frac{R}{\Delta H_m^0} \times \frac{V_p}{V_s} \times (v_1 - \chi v_1^2) \quad [\text{MPa}] \quad \text{Equation 9.4}$$

- with: T_m = observed melting temperature of the copolymer
 T_m^0 = theoretical melting temperature of the homopolymer of the crystallisable unit
 R = gas constant
 ΔH_m^0 = theoretical heat of fusion
 V_p = molar volume of the crystalline segment
 V_s = molar volume of the solvent (amorphous segment)
 χ = Flory interaction parameter
 v_1 = volume fraction of diluent (amorphous segment).

The flow temperature of the copolymer is higher for T6T6T than for TΦT as a crystalline segment at the same hard segment content, although the melting temperature of TΦT-dimethyl (371°C)¹⁴ is higher than that of T6T6T-dimethyl (303°C)²⁶. The solvent effect of the

amorphous PTMO phase is less for T6T6T than for T Φ T. This is due to the lower molar volume and higher lamellar thickness of crystalline ribbons of T6T6T. The more the segment length approaches that of the homopolymer of the crystalline segment, the smaller the solvent effect of the amorphous phase. Another effect could be the higher interaction of PTMO and T6T6T compared to PTMO and T Φ T.

DSC

With DSC the melting and crystallisation temperatures of several T6T6T-PTMO(/DMT) copolymers of series 1 and 2 were determined. The melting enthalpy of T6T6T-dimethyl was 152 J/g. The melting enthalpy of T6T6T in the copolymers can be calculated from the T6T6T content and with these values the crystallinity can roughly be calculated. The results are given in Table 9.3. Figure 9.14 shows the second heating and cooling scan of T6T6T-(PTMO₁₀₀₀/DMT)₄₀₀₀ (series 2).

Table 9.3: DSC results for several polymers of series 1 and 2 with uniform T6T6T segments at a heating and cooling rate of 20°C/min.

	T6T6T content [wt%]	T _{flow} [°C]	T _m [°C]	ΔH_m [J/g]	ΔH_m [J/g T6T6T]	Cryst. ^a [%]	T _c ^b [°C]	ΔH_c ^b [J/g]	T _m - T _c [°C]
Series 1: uniform									
T6T6T-PTMO ₂₀₀₀	22	226	227	20	91	60	186; 142	8; 2	40
T6T6T-PTMO ₂₉₀₀	16	217	220	16	100	66	187; 141	5; 2	33
Series 2: uniform									
T6T6T-(PTMO ₁₀₀₀ /DMT) ₃₀₀₀	16	220	222	16	102	67	198; 133	10; 2	24
T6T6T-(PTMO ₁₀₀₀ /DMT) ₄₀₀₀	12	208	213	12	98	65	190; 126	6; 1	23

(a), the crystallinity of T6T6T was calculated with the melting enthalpy of T6T6T-dimethyl (152 J/g); (b), first the peak crystallisation temperature and enthalpy of the main crystallisation peak are given, secondly the corresponding data for the second peak at lower temperature are given

The melting temperature as measured by DSC is a little higher than the flow temperature as determined by DMA. At the flow temperature the polymer is not yet completely molten. The melting peak is quite broad and seems to show a shoulder at the high temperature side.

The crystallisation curve shows two peaks, one around 190°C and one around 135°C. The second peak can probably be attributed to a crystalline transition. Such a crystalline transition was also found for 6T6-diamine²⁶, and is quite common for polyamides^{31,32}. However T6T6T-dimethyl did not show such a crystalline transition in DSC²⁶.

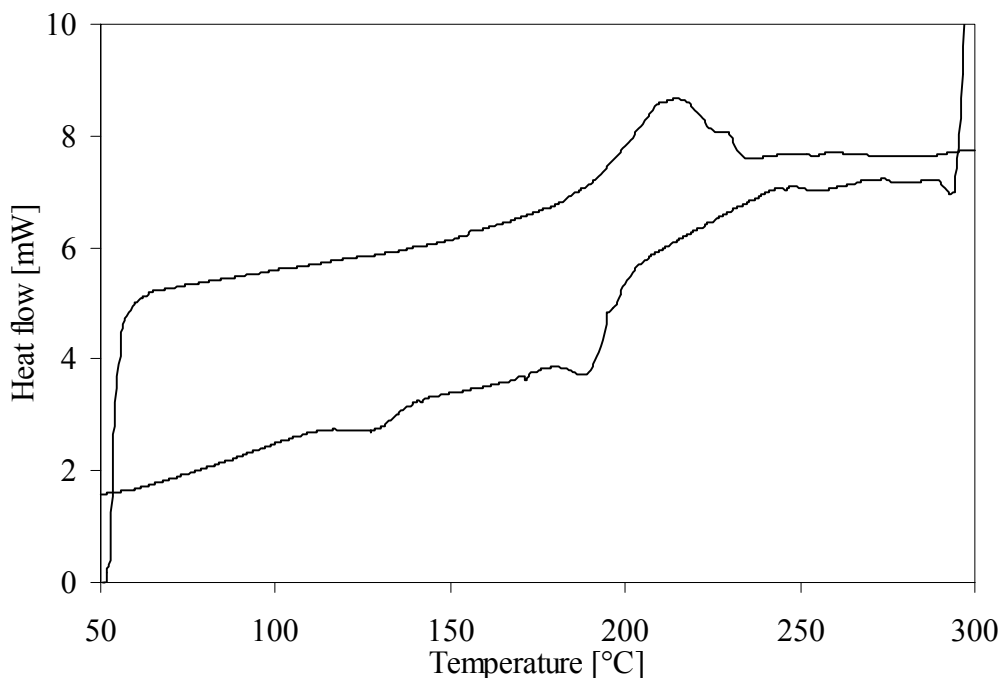


Figure 9.14: DSC second heating scan and first cooling scan for T6T6T-(PTMO₁₀₀₀/DMT)₄₀₀₀ (series 2) at 20°C/min.

The undercooling ($T_m - T_c$) is only 23-24°C for the copolymers with extended PTMO₁₀₀₀/DMT. This indicates that the crystallisation of T6T6T in these polymers is very fast. It seems that with increasing T6T6T content and with regular PTMO, the rate of crystallisation decreases somewhat.

The crystallinities as calculated from the enthalpy of melting of T6T6T in the copolymer compared to the starting material T6T6T-dimethyl are somewhat lower (about 10%) than the crystallinities that were calculated from the modulus in the rubbery plateau (Table 9.2). This could be due to the fact that the T6T6T unit has a different enthalpy of melting than T6T6T-dimethyl.

Compression set

The compression set (CS) at 20 and 70°C was measured with polymer pieces, cut from the injection moulded bars. The samples were compressed for 24 hours to 25 or 55%. The CS for T6T6T-PTMO(/DMT) polymers with uniform and non-uniform T6T6T segments (series 1-3) are given in Table 9.4.

The compression set at 25% is almost independent of the hard segment content. The compression set as function of the rubber modulus for 55% compression at 20 and 70°C is given in Figure 9.15. In these figures the compression set data of T6T6T-PTMO(/DMT) of series 1-3 are compared with that of TΦT-PTMO(/DMT).

Table 9.4: Compression set for T6T6T-PTMO (series 1), T6T6T-(PTMO₁₀₀₀/DMT) with uniform (series 2) and non-uniform T6T6T (series 3).

	T6T6T content [wt%]	η_{inh} [dl/g]	$G'(25^\circ\text{C})$ [MPa]	CS _{25%} (20°C) [%]	CS _{55%} (20°C) [%]	CS _{25%} (70°C) [%]	CS _{55%} (70°C) [%]
Series 1: uniform							
T6T6T-PTMO ₂₀₀₀	21.7	2.2	34	-	14	-	36
T6T6T-PTMO ₂₉₀₀	16.1	2.7	17	-	9	-	29
Series 2: uniform							
T6T6T-(PTMO ₁₀₀₀ /DMT) ₃₀₀₀	15.7	3.1	14.5	7	10	32	32
T6T6T-(PTMO ₁₀₀₀ /DMT) ₄₀₀₀	12.3	2.3	18	7	8	24	34
T6T6T-(PTMO ₁₀₀₀ /DMT) ₄₀₀₀	12.3	1.4	8.5	11	18	39	45
T6T6T-(PTMO ₁₀₀₀ /DMT) ₆₀₀₀	8.6	2.6	6.8	7	9	21	29
T6T6T-(PTMO ₁₀₀₀ /DMT) ₈₀₀₀	6.6	2.2	5.1	6	7	22	34
T6T6T-(PTMO ₁₀₀₀ /DMT) ₁₀₀₀₀	5.4	2.5	3.3	6	6	24	33
Series 3: non-uniform							
T6T6T-(PTMO ₁₀₀₀ /DMT) ₃₀₀₀	15.7	1.4	23.5	10	12	23	24
T6T6T-(PTMO ₁₀₀₀ /DMT) ₄₀₀₀	12.3	1.5	14.3	-	8	-	21
T6T6T-(PTMO ₁₀₀₀ /DMT) ₆₀₀₀	8.6	1.9	6.9	6	7	18	20

The compression set of T6T6T-PTMO(/DMT) copolymers at 20°C is very low. Copolymers with T6T6T instead of T Φ T show better elastic properties over the whole hard segment content range. Also the copolymers based on T6T6T as a hard segment can be applied over a larger hard segment content range with good elasticity because the compression set is less dependent on the hard segment content. A compression set of only 6-7% at 20°C is very favourable for several kinds of applications.

The compression set at 20°C decreases slightly with decreasing rubber modulus and thus with decreasing crystallinity (series 1-3). When the crystallinity is lower, there is less plastic deformation during compression, and therefore less permanent damage. The data at 20°C suggest that the compression set would decrease even further with lower T6T6T content. For T Φ T-PTMO(/DMT)⁶ a minimum in the compression set at 10-12 wt% hard segment content is observed, and this was explained by the fact that at very low hard segment concentrations the physical crosslink density is too low to prevent plastic flow in this compression test. Such a minimum is not observed for T6T6T-PTMO(/DMT) for concentrations down to 5 wt%.

The compression set at 70°C is higher than at 20°C for copolymers with T6T6T or T Φ T as crystallisable segment, but still low. For these copolymers the melting temperature is at 70°C not reached by far, and thus plastic flow is still suppressed. At 70°C there is some difference between the three series based on T6T6T. For series 1 and 2 the compression set seems almost independent of hard segment content, although there is some spread in the data points. It is remarkable that the polymers of series 3 with non-uniform T6T6T show a lower compression set at 70°C than the polymers with uniform T6T6T. At room temperature there is no difference. This is possibly caused by the lower molecular weight of the copolymers of

series 3, but more research is necessary to investigate this. It could also be a result of the presence of thicker crystallites based on longer T6T6T6T or T6T6T6T6T.

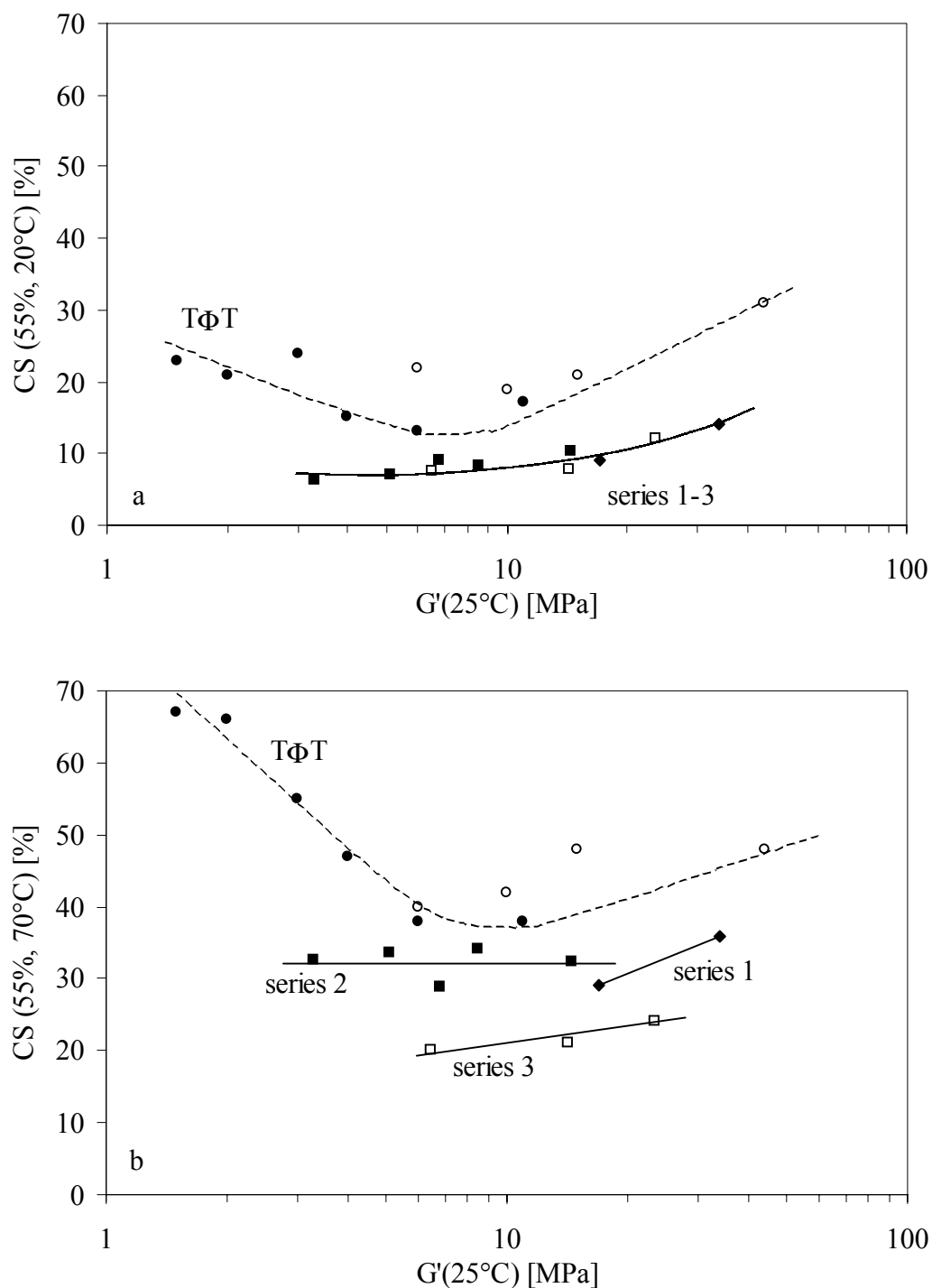


Figure 9.15: Compression set (55% compression) at (a) 20°C and (b) 70°C as function of the rubber modulus: (\blacklozenge), T6T6T-PTMO, series 1; (\blacksquare), T6T6T-(PTMO₁₀₀₀/DMT), series 2; (\square), T6T6T-(PTMO₁₀₀₀/DMT), series 3, non-uniform; (\circ), T Φ T-PTMO⁶; (\bullet), T Φ T-PTMO₁₀₀₀/DMT⁶.

The better elasticity in copolymers with T6T6T instead of TΦT over the whole hard segment content range can have several causes. It can be a result of the larger thickness of the T6T6T lamellae as compared to the TΦT lamellae. As a result it will be more difficult to shear the T6T6T lamellae. It could also be a result of the larger PTMO length at a certain hard segment content for T6T6T. The deformation should then mainly take place in the PTMO phase.

The compression set (55% compression) at 20°C is given as a function of 1000/PTMO (in which PTMO is the PTMO/(DMT) length) in Figure 9.16. The figure shows that the compression set of T6T6T-PTMO/(DMT) copolymers decreases with decreasing 1000/PTMO or with increasing PTMO/(DMT) length. The decrease becomes less steep below PTMO/(DMT) values of 0.4 (PTMO/(DMT) length above 2500 g/mol).

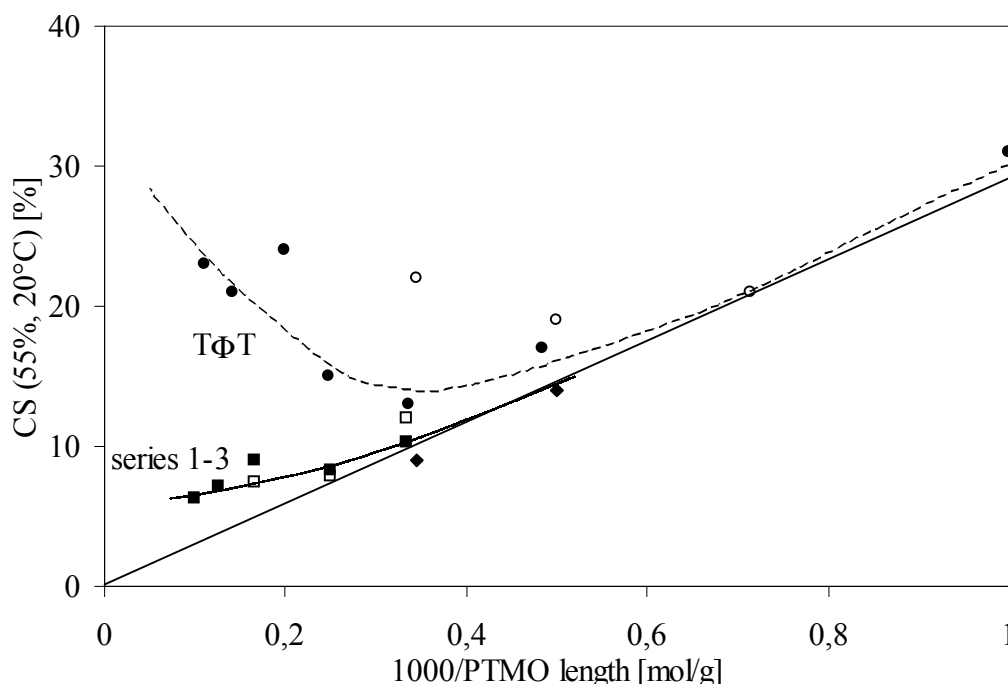


Figure 9.16: Compression set (55% compression) at 20°C as function of 1000/PTMO (the PTMO/(DMT) length): (◆), T6T6T-PTMO, series 1; (■), T6T6T-(PTMO₁₀₀₀/DMT), series 2; (□), T6T6T-(PTMO₁₀₀₀/DMT), series 3, non-uniform; (○), TΦT-PTMO⁶; (●), TΦT-PTMO₁₀₀₀/DMT⁶.

Above a 1000/PTMO value of 0.4 the compression set values of T6T6T-PTMO/(DMT) copolymers seem to be comparable with that of TΦT-PTMO/(DMT) copolymers. These data follow a line that crosses the origin. This suggests that the length of the amorphous segment and not the hard segment type and content determines the compression set below a PTMO/(DMT) length of ~3000 g/mol. Apparently the deformation takes place mainly in the PTMO phase.

Below a 1000/PTMO value of 0.4 (PTMO/(DMT) length above 2500 g/mol) the compression set values of T6T6T-PTMO/(DMT) copolymers are lower than that of TΦT-PTMO/(DMT) copolymers. For TΦT systems⁶ at low TΦT content the compression set was thought to increase because the crystalline content is too low to prevent plastic flow. Apparently the thicker T6T6T ribbons are more effective or less deformed in compression than the thin TΦT

crystalline ribbons. This figure also suggests that even lower compression set values could be obtained, probably by increasing the lamellar thickness of the crystalline ribbons. At higher lamellar thickness the PTMO length between two crystalline ribbons at constant hard segment content is higher.

The low uniformity of T6T6T in series 3 does not seem to have a negative effect on the properties. With a uniformity of 76% the crystallinity is still high (Table 9.2) and the properties of T6T6T-(PTMO₁₀₀₀/DMT) copolymers are comparable with that using uniform T6T6T. It was expected that the properties would be better in the copolymers based on uniform T6T6T⁷⁻¹⁰. Apparently the uniformity of T6T6T is not important as long as it is above a certain value (at least 76%).

AFM

The morphology of several T6T6T-(PTMO₁₀₀₀/DMT) copolymers based on uniform T6T6T (series 2) was studied by AFM. In Figure 9.17 the morphology of T6T6T-(PTMO₁₀₀₀/DMT)₆₀₀₀ (sample cooled down from the melt) and in Figure 9.18 of T6T6T-(PTMO₁₀₀₀/DMT)₃₀₀₀ (solution cast sample from NMP) is given. Each figure shows a height and phase image. The phase image corresponds to a picture of the hardness of the sample over the measured area. The crystallinity in the picture seems higher because of measurement is not only on the surface.

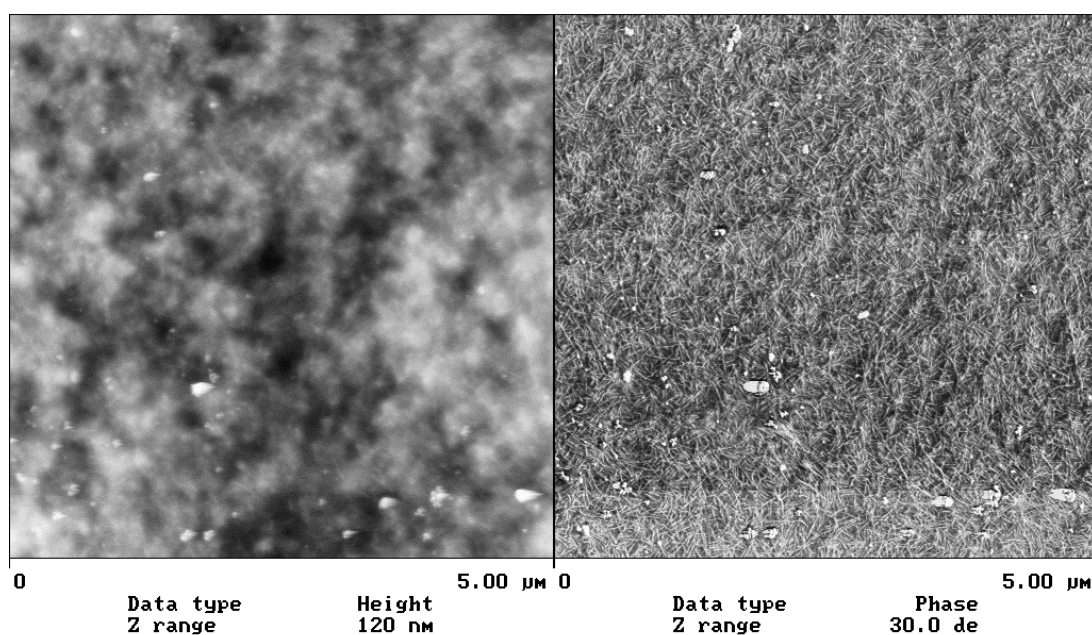


Figure 9.17: Morphology as measured by AFM at 5x5 μm for a melt sample of T6T6T-(PTMO₁₀₀₀/DMT)₆₀₀₀ (series 2, 9 wt% T6T6T) taken from the reactor side; (left, height image; right, phase angle image)

The AFM pictures (phase images) show a well-defined morphology of hard threads or ribbon-like structures of T6T6T in a soft amorphous matrix. The threads are not very long for the melt sample of T6T6T-(PTMO₁₀₀₀/DMT)₆₀₀₀. The solution cast sample of T6T6T-

(PTMO₁₀₀₀/DMT)₃₀₀₀ shows threads that are very long (up to 0.5 μm) and also some spherulitic structures. This is probably due to the high T6T6T content in these copolymers. In the height images the individual threads are visible as well, especially at the 1x1 μm picture. It seems that the samples contain clusters of T6T6T threads, so the threads are not randomly distributed. The clusters are larger for the solution cast sample of T6T6T-(PTMO₁₀₀₀/DMT)₃₀₀₀ than for the melt sample of T6T6T-(PTMO₁₀₀₀/DMT)₆₀₀₀. Both the higher concentration of T6T6T and the method of sample preparation are probably responsible for this.

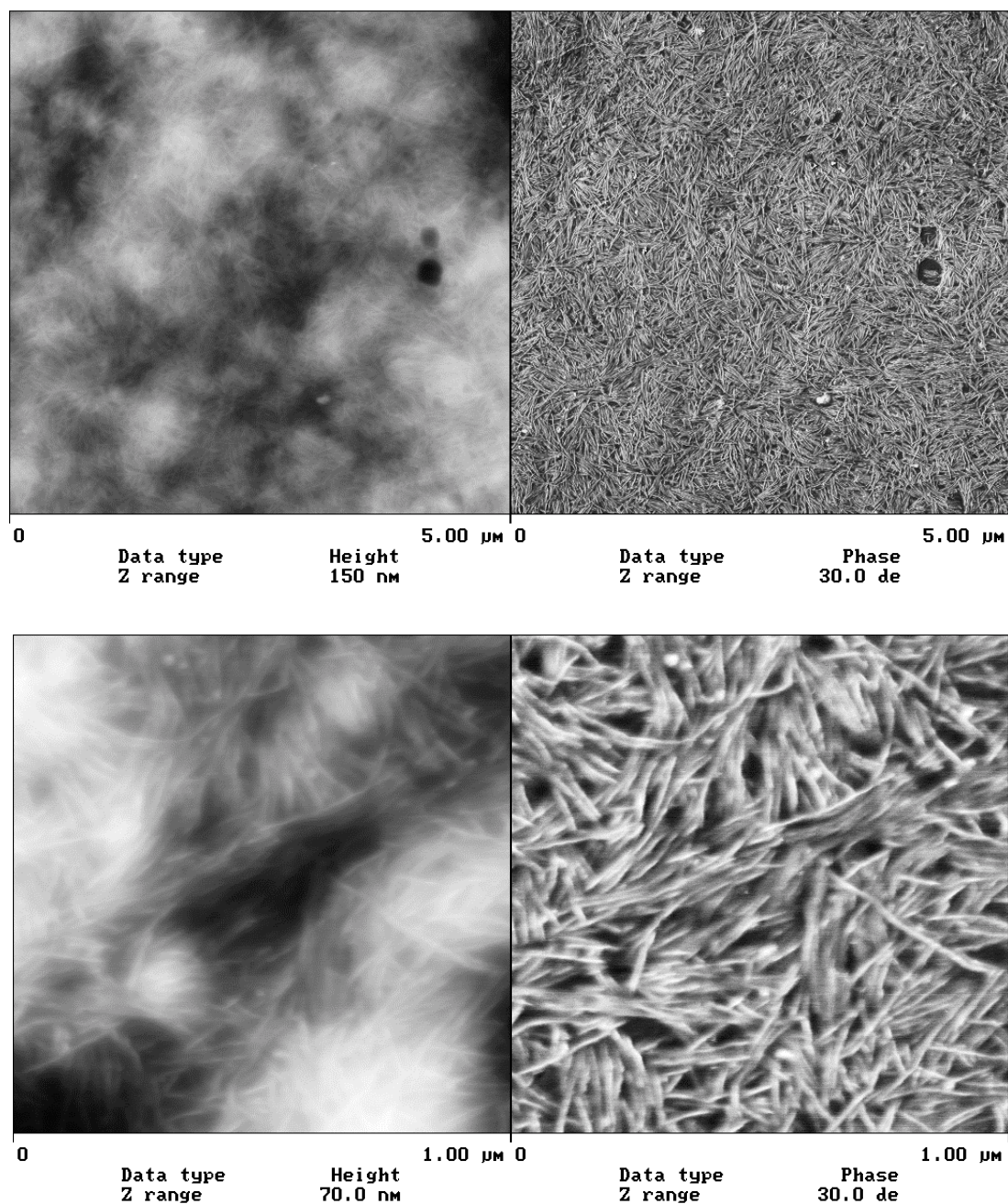


Figure 9.18: Morphology as measured by AFM at 5x5 μm and 1x1 μm for a solution cast sample of T6T6T-(PTMO₁₀₀₀/DMT)₃₀₀₀ (series 2, 16 wt% T6T6T); (left, height image; right, phase angle image).

WAXD

With wide angle X-ray diffraction (WAXD) the morphology of the crystalline phase of a melt-pressed strip of 1 mm thickness of T6T6T-(PTMO₁₀₀₀/DMT)₃₀₀₀ was measured. The WAXD diagram of the copolymer is compared with that of T6T6T-dimethyl²⁶ in Figure 9.19.

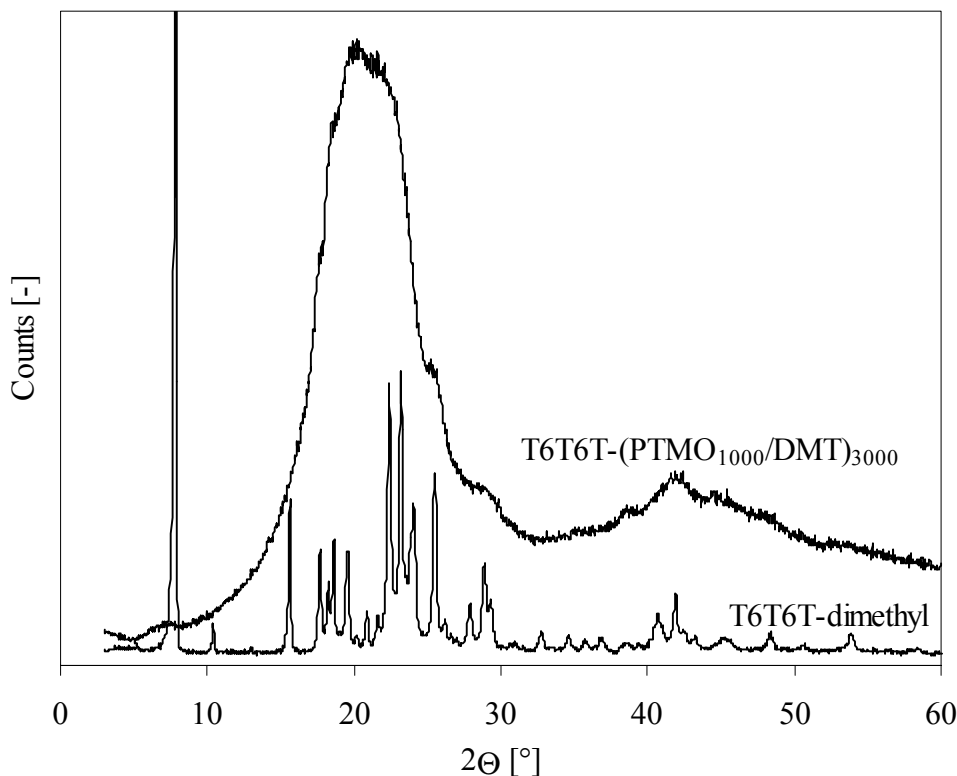


Figure 9.19: WAXD data of T6T6T-(PTMO₁₀₀₀/DMT)₃₀₀₀ (series 2) compared to T6T6T-dimethyl²⁶.

The amorphous PTMO phase in T6T6T-(PTMO₁₀₀₀/DMT)₃₀₀₀ gives a broad peak in the area where the main crystallisation peak of T6T6T is expected (around 23°). Other small peaks in T6T6T-(PTMO₁₀₀₀/DMT)₃₀₀₀ at $2\Theta = 8, 26, 29$ and 42° correspond nicely with peaks of T6T6T-dimethyl.

Comparison with other systems

The T6T6T and TΦT based segmented copolymers are copolyether-esteramides, a special type of the thermoplastic copolyether-amides (TPE-A). These materials are new compared to the commercial materials that are described here, as they consist of uniform hard, crystallisable segments.

The commercial material Arnitel[®] is a segmented copolyether-ester (TPE-E) based on a PBT-PTMO copolymer. Desmopan[®] is a commercial thermoplastic polyurethane (TPE-U), based on polyether soft segments. In both materials the hard segments are not of uniform length. The properties of a hard and a soft grade of these commercial materials were evaluated³³.

The T6T6T-PTMO(/DMT) copolymers that are described in this article are compared with the T Φ T-PTMO(/DMT) copolymers from previous research^{6,14-16} and several commercial thermoplastic elastomers³³ in Table 9.5.

Table 9.5: Comparison of T6T6T-PTMO(/DMT) segmented copolymers with other systems.

	Hard segment [wt%]	G'(25°C) [MPa]	T _{flow} [°C]	T _g [°C]	CS _{55%} (20°C) [%]	CS _{55%} (70°C) [%]
T6T6T-PTMO(/DMT) (series 1 and 2)						
T6T6T-PTMO ₂₀₀₀	22	34	226	-70	14	36
T6T6T-(PTMO ₁₀₀₀ /DMT) ₃₀₀₀	16	14.5	225	-61	10	32
T6T6T-(PTMO ₁₀₀₀ /DMT) ₄₀₀₀	12	8.5	208	-60	8	34
TΦT-PTMO(/DMT)^{6,14-16}						
T Φ T-PTMO ₂₀₀₀	13	10	191	-65	19	42
T Φ T-(PTMO ₁₀₀₀ /DMT) ₃₀₀₀	9	6	172	-65	15	47
T Φ T-(PTMO ₁₀₀₀ /DMT) ₄₀₀₀	7	4	155	-65	24	55
Commercial polymers³³						
Arnitel [®] EM400	-	18	182	-70	15	36
Arnitel [®] EL550	-	67	205	-50	30	58
Desmopan [®] KU-8672	-	11	150	-45	13	41
Desmopan [®] 955u	-	91	176	-31	23	60

With T6T6T and extended PTMO₁₀₀₀/DMT, a TPE with very good properties such as sharp transition temperatures and a very wide and constant rubbery plateau can be obtained, comparable to the copolymers with T Φ T as crystallisable segment, but with a higher melting temperature and lower compression set. Another advantage of copolymerisation with T6T6T instead of T Φ T is that the products are less coloured, due to the absence of aromatic amines. Therefore the use of T6T6T is preferred over the use of T Φ T in segmented copolymers. The materials also have good melt processability and can be recycled. Therefore, the new T6T6T-(PTMO₁₀₀₀/DMT) materials are very interesting for TPE applications similar to Arnitel[®] and Desmopan[®]. T6T6T-(PTMO₁₀₀₀/DMT) is a TPE with a constant modulus over a wider temperature range and lower compression set. The properties of this polymer can be easily tuned as desired by changing the PTMO(/DMT) length.

It is expected that the properties of T6T6T-PTMO(/DMT) copolymers can probably be changed and optimised in several ways: the choice of the soft segment type and length, the polymerisation reaction conditions, the processing conditions and by using additives. The synthesis would become more economically feasible when it can be performed in the melt, so when the T6T6T segment is formed in situ, for example by starting from 6T6-diamine or even by starting from 1,6-hexamethylenediamine. This is however at the cost of uniformity of the T6T6T in the copolymer, but it was shown that a uniformity of 76% is sufficient for good properties. Another interesting modification would be to use other tetra-amides as crystallisable segment instead of T6T6T, for example T4T4T²⁶. The melting temperature of nylon-4,T is 60°C higher than that of nylon-6,T²⁸ and therefore the melting temperature of a

copolymer with T4T4T instead of T6T6T is expected to be maximal 60°C higher. So with this segment it is possible to increase the melting temperature of the polymer and to make the rubbery plateau even wider while keeping a low modulus and good elasticity. Also optimisation of the processing of the polymer, for example by injection moulding, can lead to better properties.

Conclusions

Segmented copolymers based on T6T6T-dimethyl and PTMO₁₀₀₀/DMT that are thermoplastic elastomers can be made via a polycondensation reaction. Copolymers with different soft segment types and lengths and with uniform and non-uniform T6T6T were studied. With DMA experiments it was shown that the polymers all have a low glass transition temperature (-60 to -70°C). The glass transition temperature of PTMO is lower for regular PTMO than for DMT extended PTMO₁₀₀₀. With regular PTMO of >2000 g/mol crystallisation of PTMO occurs. The rubbery plateau of all copolymers is wide and extremely flat and the melting temperature is sharp and high when uniform T6T6T is used. With non-uniform T6T6T the flow temperature is somewhat broadened. The modulus of the rubbery plateau and the flow temperature increase with increasing T6T6T content and thus with increasing crystallinity. The modulus of T6T6T-(PTMO₁₀₀₀/DMT) increases from 3.3 to 14.5 MPa and the flow temperature from 183 to 220°C when the PTMO₁₀₀₀/DMT length is decreased from 10000 to 3000 g/mol (5-16 wt% T6T6T). The modulus is not dependent on the PTMO length or network density but on the crystallinity. The content of reinforcing crystalline ribbons in the amorphous matrix determines the modulus. The crystallinity of T6T6T in injection moulded test bars as calculated from their rubber modulus is between 70 and 100%.

The undercooling, as measured by DSC, is 20-30°C, which is low compared to other semi-crystalline polymers. The crystallinity of T6T6T as calculated from the melting enthalpy of the polymers is about 10% lower than that calculated from the rubber modulus. The compression set at room temperature is low (6-7%) and decreases slightly with decreasing T6T6T content. The uniformity of T6T6T, when it is at least 76%, does not have much influence on the polymer properties, except for the flow temperature. With AFM it was confirmed that the crystalline T6T6T units form long threads or ribbon like structures with a high aspect ratio in the amorphous PTMO matrix.

This type of thermoplastic elastomers is very interesting for application as TPE. The segmented copolymers show a good combination of properties as they have a good elasticity, are melt-processable (and can be recycled), have a high modulus, have a good solvent resistance, are transparent and are dimensional stable up to high temperatures.

Literature

1. G. Holden, N.R. Legge, R. Quirk, H.E. Schroeder, 'Thermoplastic Elastomers', Second Ed., Hanser Publishers, Munich (1996).
2. B.P. Grady, S.L. Cooper, in 'Science and Technology of Rubber', J.E. Mark, B. Erman, F.R. Eirich Eds., Academic Press, San Diego, Chapter 13 (1978).
3. L. Zhu, G. Wegner, Makromol. Chem., 182, 3625 (1981).
4. B.B. Sauer, R.S. McLean, R.R. Thomas, Polym. Int., 49, 449 (2000).
5. R.J. Cella, J. Polym. Sci.: Symp., 42, 727 (1973).
6. M.C.E.J. Niesten, R.J. Gaymans, Polymer, 42, 6199 (2001).
7. L.L. Harrell, Macromolecules, 2, 607 (1969).
8. H.N. Ng, A.E. Allegrazza, R.W. Seymour, S.L. Cooper, Polymer, 14, 255 (1973).
9. C.D. Eisenbach, M. Baumgartner, G. Gunter, in 'Advances in Elastomer and Rubber Elasticity, proc. Symposium', J. Lal, J.E. Mark Eds., Plenum Press, New York, 51 (1985).
10. J.A. Miller, B.L. Shaow, K.K.S. Hwang, K.S. Wu, P.E. Gibson, S.L. Cooper, Macromolecules, 18, 32 (1985).
11. E. Sorta, G. della Fortuna, Polymer, 21, 728 (1980).
12. R.J. Gaymans, J.L. de Haan, Polymer, 34, 4360 (1993).
13. K. Bouma, G.A. Wester, R.J. Gaymans, J. Appl. Polym. Sci., 80, 1173 (2001).
14. M.C.E.J. Niesten, J. Feijen, R.J. Gaymans, Polymer, 41, 8487 (2000).
15. M.C.E.J. Niesten, J.W. ten Brinke, R.J. Gaymans, Polymer, 42, 1461 (2001).
16. M.C.E.J. Niesten, J. Krijgsman, R.J. Gaymans, J. Appl. Polym. Sci., 82, 2194 (2001).
17. J.D. Hoffman, J.J. Weeks, J. Res. Nat. Bur. Stand., Sect. A, 66, 13 (1962).
18. M.C.E.J. Niesten, S. Harkema, E. van der Heide, R.J. Gaymans, Polymer, 42, 1131 (2001).
19. D. Garcia, H. Starkweather, J. Polym. Sci. Phys. Ed., 32, 537 (1985).
20. C. Ramesh, A. Keller, S.J.E.A. Eltink, Polymer, 35, 5293 (1994).
21. A.C.M. van Bennekom, R.J. Gaymans, Polymer, 38, 657 (1997).
22. P.F. van Hutten, R.M. Mangnus, R.J. Gaymans, Polymer, 35, 4193 (1993).
23. M.C.E.J. Niesten, H. Bosch, R.J. Gaymans, J. Appl. Polym. Sci., 81, 1605 (2001).
24. G. Perego, M. Cesart, G. della Fortuna, J. Appl. Polym. Sci., 29, 1141 (1984).
25. L. Guang, R.J. Gaymans, Polymer, 38, 4891 (1997).
26. Chapter 5 of this thesis.
27. P. Dreyfuss in 'Encyclopedia. Of Polymer Science and Engineering', H.F. Mark, N.M. Bikales, C.G. Overberger, G. Menges, John Wiley & Sons, New York, 654 (1989).
28. P.W. Morgan, S.L. Kwolek, Macromolecules, 8, 104 (1975).
29. P.J. Flory, Trans. Faraday Soc., 51, 848 (1955).
30. G. Wegner, Chapter 12 in: 'Thermoplastic Elastomers', N.R. Legge, G. Holden, H.E. Schroeder, First Ed., Carl Hanser Verlag, Munich (1987).
31. M. Todoki, T. Kawaguchi, J. Polym. Sci. Phys. Ed., 15, 1067 (1977).
32. J. Hirsinger, H. Miura, K.H. Gardner, A.D. English, Macromolecules, 23, 2153 (1990).
33. M.C.E.J. Niesten, R.J. Gaymans, J. Appl. Polym. Sci., 81, 1372 (2001).

Chapter 10

Tensile and elastic properties of thermoplastic elastomers based on PTMO and tetra-amide units

Abstract

The tensile and elastic properties of melt spun threads of segmented copolymers based on T6T6T-dimethyl (two-and-a-half repeating unit of nylon-6,T; 5-16 wt%) and PTMO₁₀₀₀/DMT of different lengths (3000-10000 g/mol) are very good. Stress-strain measurements show that extruded threads of these polymers have high fracture strains (>1000%) and little strain hardening. The modulus and yield stress increase with increasing T6T6T content. The modulus decreases with increasing drawing-strain as a result of the breaking up of the crystalline network (strain softening). The compression set (6-10%) and tensile set (5-20%) increase with increasing T6T6T content (5-16 wt%) and are low. The uniformity of T6T6T has little influence on the properties when it is at least 76%. At a soft segment length of 6000 g/mol a fibre with a tensile set of 5% after spinning at high speed, flow temperature of 200°C and rubber modulus of 7 MPa is feasible. The advantage of such a high modulus is that the granulate will not be sticky.

Introduction

Thermoplastic elastomers (TPE's)^{1,2} are polymers that show elastomeric behaviour at their service temperature and that can be melt-processed at elevated temperatures. A special kind of thermoplastic elastomers are segmented copolymers or multi-block copolymers that consist of alternating crystallisable hard segments and amorphous soft segments. Especially segmented copolymers with crystallisable units of uniform length were found to crystallise fast and complete³⁻⁶. Such segmented copolymers may possess good elastic properties.

Segmented copolymers based on T6T6T-dimethyl⁷ crystallisable segments and PTMO or PTMO₁₀₀₀/DMT (PTMO of 1000 g/mol extended with dimethyl terephthalate) soft segments (Figure 10.1) were found to have very interesting thermal-mechanical and elastic properties⁸. The polymers all have a low glass transition temperature (-60 to -70°C), a wide and extremely flat rubbery plateau and a sharp melting temperature. The modulus of the rubbery plateau and the flow temperature increase with decreasing PTMO length or increasing T6T6T content as the degree of crystallinity increases. The modulus of T6T6T-(PTMO₁₀₀₀/DMT) increases from 3.3 to 14.5 MPa and the flow temperature from 183 to 220°C when the PTMO₁₀₀₀/DMT length is decreased from 10.000 to 3000 g/mol (5-16 wt% T6T6T). The properties of copolymers with T6T6T of lower uniformity of 76% (76% T6T6T and 24% T(6T)_n with n>2) are comparable except for the flow temperature, which is broadened. The crystallinity of T6T6T in copolymers after injection moulding is probably between 70 and 100%. The compression set at room temperature is only 6-7% after 55% compression and decreases slightly with decreasing T6T6T content. The injection moulded test bars of these copolymers had a light yellow to brown colour and were transparent.

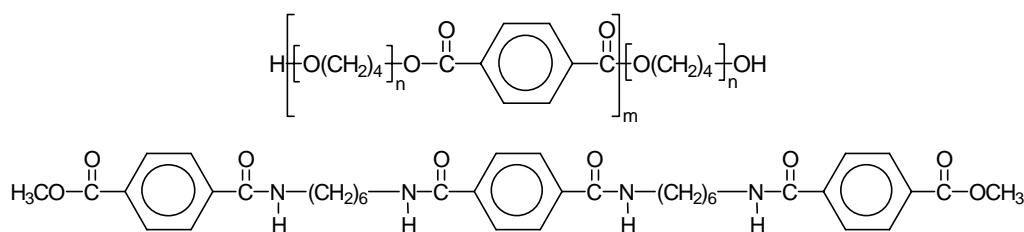


Figure 10.1: Structure of PTMO/DMT amorphous segment and T6T6T-dimethyl crystallisable segment.

The possible morphology of the T6T6T-(PTMO₁₀₀₀/DMT) segmented copolymers is schematically drawn in Figure 10.2. The crystallisable T6T6T units form threads or ribbons with a high aspect ratio in the amorphous matrix⁸⁻¹². The crystalline lamellae (C) act as physical crosslinks and reinforcing filler for the amorphous phase (A). Some crystallisable segments cannot crystallise and are mixed with the amorphous phase (B). As a result the mobility of the amorphous phase decreases and the T_g increases.

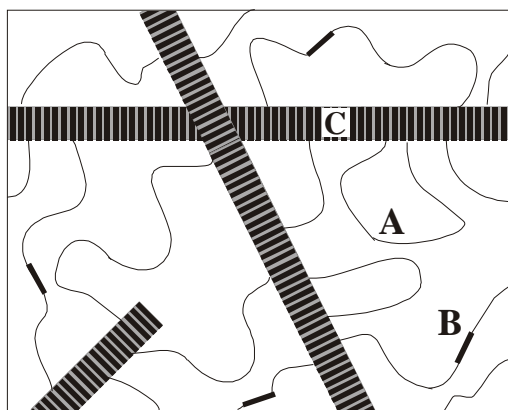


Figure 10.2: Schematic representation of the morphology of crystallised segmented copolymers with uniform crystallisable segments: A = amorphous PTMO phase; B = amorphous crystallisable segments; C = crystalline ribbons⁸⁻¹².

Thus far only the thermal-mechanical and elastic properties of test bars of ~2 mm thickness were studied⁸. Melt-spun T6T6T-(PTMO₁₀₀₀/DMT) fibres are expected to have desirable properties such as high tensile stress and strain and low tensile set. The properties will be compared with that of TΦT-(PTMO₁₀₀₀/DMT) copolymers¹³ and commercial elastic materials such as Lycra[®]. The TΦT segment is a di-amide segment that corresponds to one-and-a-half repeating unit of poly(*p*-phenylene terephthalamide).

The properties of TΦT-(PTMO₁₀₀₀/DMT) segmented copolymers, as function of the PTMO/(DMT) length and structure, have been studied thoroughly¹²⁻¹⁵. The mechanical properties of these copolymers are very good. The copolymers show sharp transition temperatures (T_g , T_m) and a wide and constant rubbery plateau. Also the fibre properties are good. Fibres that are spun from the melt can be stretched up to 2000% and after orientation still have a high fracture strain. The compression and tensile set are very low compared to other melt-processable segmented copolymers. The best elasticity was obtained when the amorphous segment consists of PTMO of 1000 g/mol extended with DMT to 2000-7000 g/mol. For the copolymers with the longer PTMO₁₀₀₀/DMT soft segments, the elastic recovery after drawing to 300% or after spinning at high winding speed is comparable to that of commercial elastic materials such as Lycra[®] (~5%). However, the elasticity is only good at low TΦT content (<5 wt%) and thus at low modulus and melting temperature. The combination of a high melting temperature and high modulus at room temperature (“non-sticky” material) with a very low tensile set is not observed for TΦT-(PTMO₁₀₀₀/DMT) copolymers.

A major disadvantage of Lycra[®], a segmented polyether-urethane, is that it is spun from solution (dimethyl formamide or dimethyl acetamide). This spinning process is expensive and environmentally unfriendly. Another disadvantage is the low thermal stability of the polyether-urethane, which makes it difficult to dye, a process that is usually performed at elevated temperatures. It would be interesting to have a segmented copolymer that is processable from the melt with a modulus above 5 MPa at room temperature, a melting temperature above 200°C and a very low tensile set below 10% that can compete with Lycra[®].

Aim

In this chapter the structure-property relationships of extruded threads of T6T6T-(PTMO₁₀₀₀/DMT) will be discussed. Extended PTMO₁₀₀₀/DMT of different lengths was used as amorphous segment. T6T6T-dimethyl of high and low uniformity was applied as crystallisable segment. The polymers were melt spun into threads and the tensile and elastic properties of these threads were studied. Also the effect of pre-drawing on the tensile and elastic properties was studied.

Experimental

Materials. The T6T6T-(PTMO₁₀₀₀/DMT) copolymers were synthesised by a polycondensation reaction using PTMO (1000 g/mol) extended with DMT and T6T6T-dimethyl⁷ as was described in Chapter 9⁸.

Viscometry. The inherent viscosity of the polymers was determined with a capillary Ubbelohde type 1B at 25°C, using a polymer solution with a concentration of 0.1 g/dl in phenol/1,1,2,2-tetrachloroethane (50/50, mol/mol).

Sample preparation. Samples for the tensile tests were prepared by melt extruding the polymers into threads on a 4cc DSM res RD11H-1009025-4 corotating twin screw mini extruder. The extruder temperature was approximately 60°C above the flow temperature, and the screw speed was 30 rpm. The threads were wound at a speed of 20-40 m/min. The titer of the threads (expressed in tex = 10⁻⁶ kg/m) was measured by weighing 1 meter of thread. The density of the polymers was approximately 1.0 g/cm³.

For some experiments the threads were pre-drawn with a Zwick Z020 universal tensile machine with a speed of 250 mm/min up to the desired strain. Then the strain was released with the same speed. The pre-drawn threads were used for further experiments after 1 hour relaxation.

Tensile tests. Tensile tests on threads and pre-drawn threads were carried out on a Zwick Z020 universal tensile machine equipped with a 10 N load cell. The strain was measured with the clamp displacement. Stress-strain curves were obtained at a strain rate of 250 mm/min with a starting clamp distance of 25 mm. Above 500% strain, necking occurred also within the clamps. Therefore the strain at break was corrected. The amount of necking within the clamps was determined with optical markers on the thread. By this method it can roughly be concluded that at the measured strain is 10% too high at ~1300% and 20% too high at ~1700%.

Tensile set. The tensile set of threads and pre-drawn threads was measured on a Zwick Z020 universal tensile machine equipped with a 10 N load cell. The strain was measured with the clamp displacement. The strain rate was 200 mm/min with a starting clamp distance of 50

mm. The tensile set was measured in a cyclic test to 300% strain. The residual strain (strain where the force becomes positive again) in the second cycle was determined. $TS_{300\%}$ was defined as:

$$TS_{300\%} = \frac{\text{residual strain}}{300} \times 100\% \quad [\%] \quad \text{Equation 10.1}$$

Cyclic tensile tests. Cyclic tensile tests on threads were carried out on a Zwick Z020 universal tensile machine equipped with a 10 N load cell. The strain was measured with the clamp displacement. The strain rate was 200 mm/min with a starting clamp distance of 50 mm. Until 100% strain, the strain was increased by 20% each cycle, followed by a strain increase of 100% for each cycle until the sample broke. There was no dwell time between the steps. The E-modulus was redetermined after each load cycle. The E-modulus in each cycle was corrected for the change in area of the thread by multiplying with the corresponding straining factor ($=1+(\epsilon/100)$).

Results and Discussion

The copolymers of T6T6T-dimethyl and PTMO of 1000 g/mol extended with DMT that were described in Chapter 9⁸ were extruded into threads. The threads were transparent and had a faint yellow colour. The tensile and elastic properties of two series of T6T6T-(PTMO₁₀₀₀/DMT) were studied. In the first series uniform T6T6T-dimethyl was used with a PTMO₁₀₀₀/DMT length of 3000-10000 g/mol. In the second series T6T6T-dimethyl with a lower uniformity of ~76% (76% T6T6T and 24% T(6T)_n with n>2) was used with a PTMO₁₀₀₀/DMT length of 3000-6000 g/mol. This non-uniform T6T6T-dimethyl contains some further reacted units such as T6T6T6T-dimethyl and T6T6T6T6T-dimethyl⁷. These units will form thicker lamellae upon crystallisation and melt at a higher temperature¹⁶.

Stress-strain behaviour

The T6T6T-(PTMO₁₀₀₀/DMT) copolymers with different PTMO lengths and uniform and non-uniform T6T6T were extruded into threads with a titer of 10-50 tex (mg/m). An inherent viscosity of at least 1.4 dl/g is necessary for melt spinning. When the inherent viscosity is lower the melt strength of the material is not sufficient for spinning. Stress-strain curves were determined using extruded threads and are given in Figure 10.3 for uniform T6T6T. The E-modulus, yield stress and fracture stress and strain are given in Table 10.1.

Table 10.1: Tensile testing properties of the T6T6T-(PTMO₁₀₀₀/DMT) copolymers with uniform T6T6T (series 1) and non-uniform T6T6T (series 2).

PTMO ₁₀₀₀ /DMT length [g/mol]	T6T6T content [wt%]	η_{inh} [dl/g]	$G'(25^\circ\text{C})$ [MPa]	E [MPa]	σ_y^a [MPa]	σ_b [MPa]	ϵ_b^b [%]	$\sigma_b(\text{true})^c$ [MPa]
Series 1: uniform								
3000	15.7	3.1	14.5	21	5.2	42	1100	500
4000	12.3	2.3	8.5	18	4.0	20	1150	250
4000	12.3	1.4	18	100	4.1	8	750	70
6000	8.6	2.6	6.8	14	3.4	25	1450	390
8000	6.6	2.2	5.1	12	2.7	20	1400	300
10000	5.4	2.5	3.3	10	2.0	31	1400	470
Series 2: non-uniform								
3000	15.7	1.4	23.5	95	5.3	24	1100	290
4000	12.3	1.5/1.8 ^d	14.3	60	4.4	23	1200	300
6000	8.6	1.9/2.1 ^d	6.9	35	3.3	34	1300	480

(a), determined by Considère's method¹⁷; (b), after correction for necking in the clamps; (c), $\sigma_b(\text{true})$ was obtained multiplying σ_b and the straining factor ($=1+(\epsilon_b/100)$); (d), the first number is the inherent viscosity for the $G'(25^\circ\text{C})$ data; the second number is the inherent viscosity of the polymer that was used for extruding into threads (tensile test data)

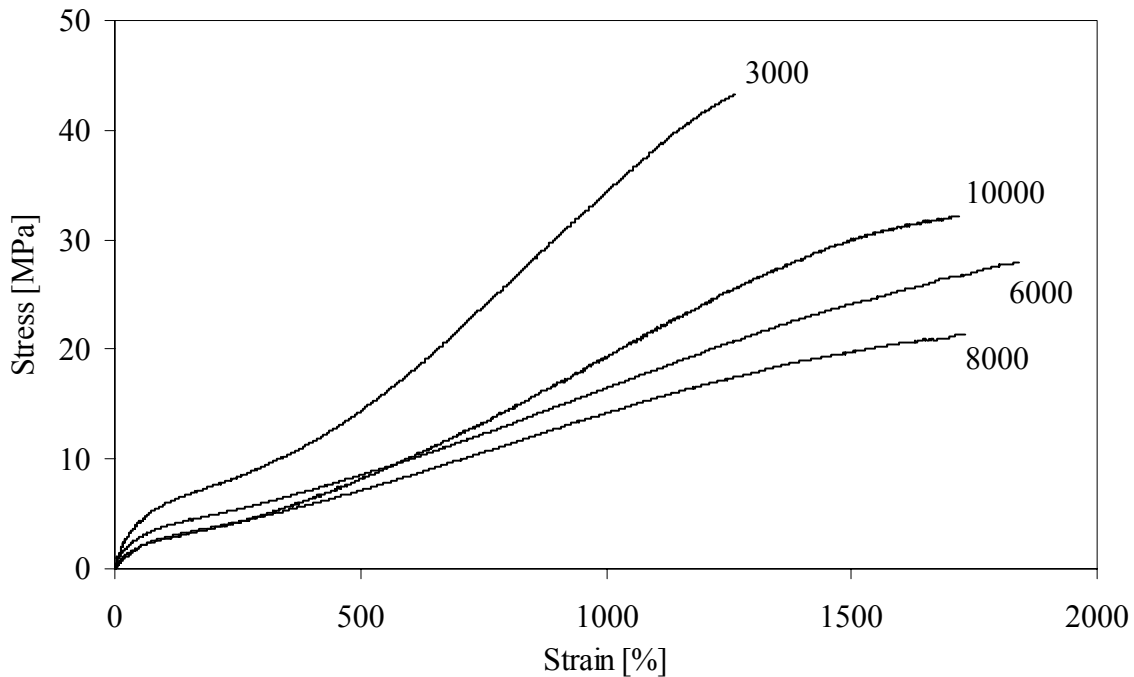


Figure 10.3: Stress-strain curves of different T6T6T-(PTMO₁₀₀₀/DMT) with uniform T6T6T and different PTMO₁₀₀₀/DMT lengths as indicated in the figure (series 1).

The shear modulus (G') and the tensile modulus (E) both decrease strongly with decreasing T6T6T concentration. For a rubber, with a Poisson ratio of 0.5 the E -modulus is three times as high as the G' -modulus¹⁸. In the values obtained for the E and G' this is not the case. A possible reason for this discrepancy is an error in the thickness of the threads and the determination of E . Also the spread in E -modulus for different tensile tests on these threads is large.

The fracture strain and stress are high for all copolymers. The fracture stress of T6T6T-(PTMO₁₀₀₀/DMT)₃₀₀₀ is higher than for PTMO₁₀₀₀/DMT lengths of 6000-10000 g/mol. Above 300%, strain hardening – strain-induced crystallisation of PTMO – takes place, which results in a high fracture stress. There is no relationship between the soft segment length or crystalline segment concentration and the fracture stress and strain. Previous research⁶ on T Φ T-(PTMO₁₀₀₀/DMT) copolymers showed that with PTMO₁₀₀₀/DMT as amorphous segment the fracture stress and strain are mainly dependent on the molecular weight of the copolymer. This can be explained by the fact that longer chains can be oriented further. The high fracture stress and strain of T6T6T-(PTMO₁₀₀₀/DMT)₃₀₀₀ might thus be due to a molecular weight effect.

In Figure 10.4 the stress-strain curves of T6T6T-(PTMO₁₀₀₀/DMT)₄₀₀₀ with high (2.3 dl/g) and low (1.4 dl/g) inherent viscosity are compared. The molecular weight has a strong effect on the stress-strain behaviour. The fracture stress and strain and the true fracture stress are much lower at low molecular weight. The yield stresses are comparable, although the yield stress is more pronounced when the molecular weight is lower. The E -modulus is higher at lower inherent viscosity (Table 10.1). As was described in Chapter 9⁸, the crystallinity of T6T6T in injection moulded test bars was probably somewhat higher for the copolymer with an inherent viscosity of 1.4 dl/g.

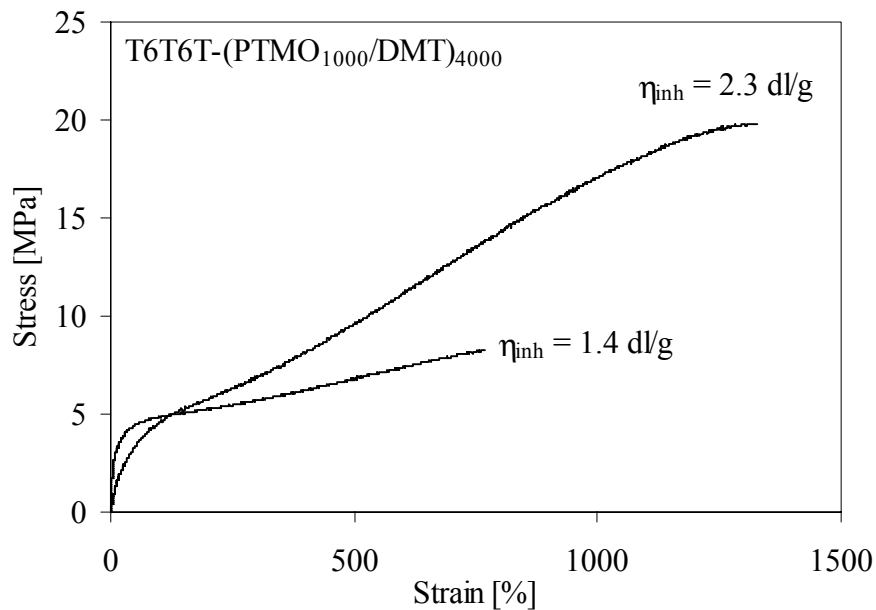


Figure 10.4: Stress-strain curves of T6T6T-(PTMO₁₀₀₀/DMT)₄₀₀₀ with uniform T6T6T and different inherent viscosities.

In Figure 10.5 the true fracture stress of the T6T6T-(PTMO₁₀₀₀/DMT) copolymers of series 1 and 2 compared to TΦT-(PTMO₁₀₀₀/DMT)¹² copolymers is given as function of the inherent viscosity (molecular weight). The true fracture stress increases linearly with increasing inherent viscosity for copolymers based on extended PTMO₁₀₀₀/DMT and TΦT or uniform T6T6T. The fracture strength in these materials is thus highly dependent on the molecular weight of these polymers and not on the length of the amorphous segment. The maximum attainable true fracture stresses are high considering that these are very soft materials.

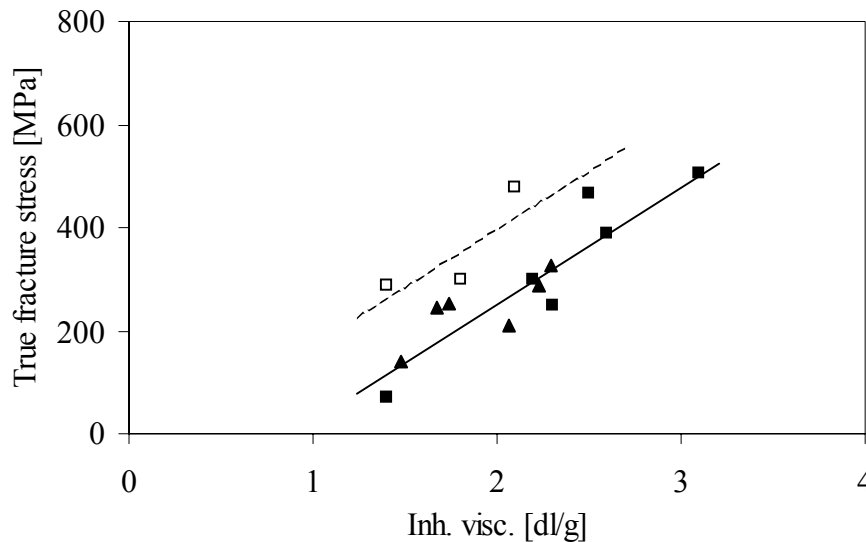


Figure 10.5: True fracture stress as function of the inherent viscosity: (■), T6T6T-(PTMO₁₀₀₀/DMT), series 1; (□), T6T6T-(PTMO₁₀₀₀/DMT), series 2, non-uniform T6T6T; (▲), TΦT-(PTMO₁₀₀₀/DMT)¹².

With non-uniform T6T6T the true fracture stress is higher. TΦT-PTMO copolymers based on regular PTMO of 2000 g/mol and higher were found to have higher true fracture stresses as well¹². This is due to the occurrence of more strain hardening of regular PTMO. Apparently the copolymers based on non-uniform T6T6T and extended PTMO₁₀₀₀/DMT strain harden more than those based on uniform T6T6T and extended PTMO₁₀₀₀/DMT.

In Figure 10.6 T6T6T-(PTMO₁₀₀₀/DMT)₆₀₀₀ with uniform (series 1) and non-uniform (series 2) T6T6T are compared. Both have an inherent viscosity above 2 dl/g. The yield stresses of T6T6T-(PTMO₁₀₀₀/DMT)₆₀₀₀ with uniform and non-uniform T6T6T are comparable. The true fracture stress of the material based on non-uniform T6T6T is higher, although the inherent viscosity (molecular weight) is lower. It seems that the T6T6T-(PTMO₁₀₀₀/DMT)₆₀₀₀ copolymer based on non-uniform T6T6T shows more strain hardening of PTMO. The other copolymers based on non-uniform T6T6T show the same behaviour and have a higher true fracture stress as well (Figure 10.5).

The E-modulus of extruded threads of T6T6T-(PTMO₁₀₀₀/DMT)₆₀₀₀ with non-uniform T6T6T is higher (Table 10.1). This difference is however not visible in the stress-strain curves in Figure 10.6. Apparently the error in determining the E-modulus is large for these thin threads. The rubber moduli ($G'(25^\circ\text{C})$) of injection moulded test bars of these two copolymers are comparable (Table 10.1). Both the E- and G-modulus are dependent on the crystallinity.

Usually the E-modulus is 3 times as high as the G-modulus at most for a rubber¹⁸. It is strange that the E- and G-modulus of the copolymers with non-uniform T6T6T (series 2) differ by a factor 5. The same relationship between E- and G-modulus was found for the T6T6T-(PTMO₁₀₀₀/DMT)₄₀₀₀ copolymer with a low inherent viscosity of 1.4 dl/g. Next to the effect of an error in the determination of the E-modulus there may be an effect of molecular weight. Also the effect of non-uniformity on stress-strain properties is as yet unexplained. More research is necessary to fully understand these effects.

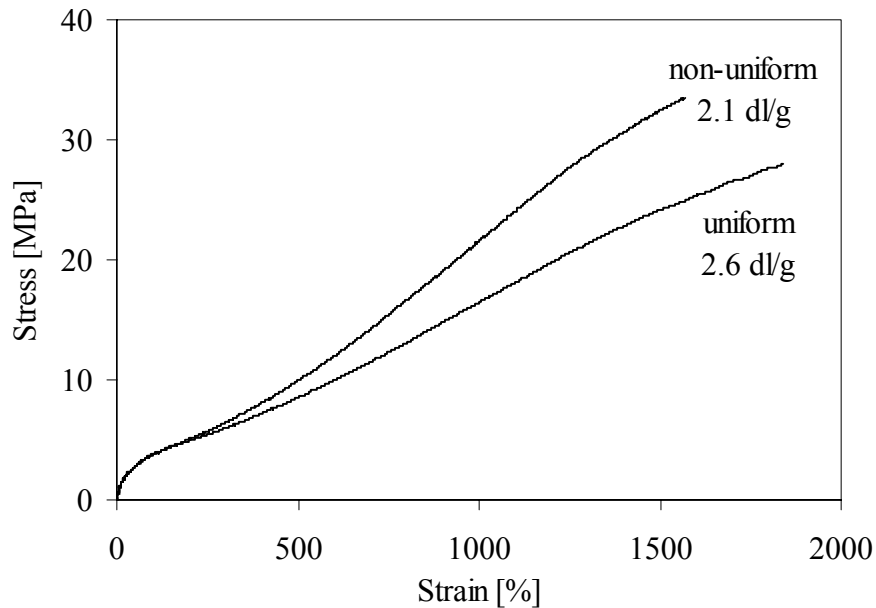


Figure 10.6: Stress-strain curves of T6T6T-(PTMO₁₀₀₀/DMT)₆₀₀₀ with uniform (series 1) and non-uniform (series 2) T6T6T having comparable inherent viscosities.

The stress-strain curves in Figure 10.3, 10.4 and 10.6 show a yield point, which is indicative for the breaking up of the crystalline structure^{2,9}. The yield stress decreases and becomes less pronounced with decreasing hard segment content, because the degree of crystallinity decreases in this direction. In Figure 10.7 the yield stress is given as function of the hard segment content for the copolymers of series 1 and 2 compared to TΦT-(PTMO₁₀₀₀/DMT)¹² copolymers.

The yield stress of copolymers based on T6T6T (uniform and non-uniform) and extended PTMO₁₀₀₀/DMT increases linearly with the hard segment content. The yield stress of the copolymers based on TΦT and extended PTMO₁₀₀₀/DMT show such a linear increase as well¹². The yield stresses of threads based on T6T6T or TΦT at a certain hard segment content are comparable.

The height of the yield stress in polyethylene is said to dependent on both the crystallinity and the lamellar thickness¹⁹⁻²¹. The lamellar thickness within a series of copolymers based on T6T6T or TΦT¹² as crystallisable unit is constant. However the lamellar thickness of T6T6T is higher than that of TΦT, while the yield stresses are comparable. In these systems the yield stress seem only dependent on the hard segment content (degree of crystallinity). This can be explained by the fact that at a certain hard segment content the number of crystalline TΦT

ribbons is higher, because the thickness of the T Φ T crystalline ribbons is lower. Therefore the cross section of the sheared T Φ T crystalline ribbons is comparable to that of the T6T6T ribbons at a certain hard segment content.

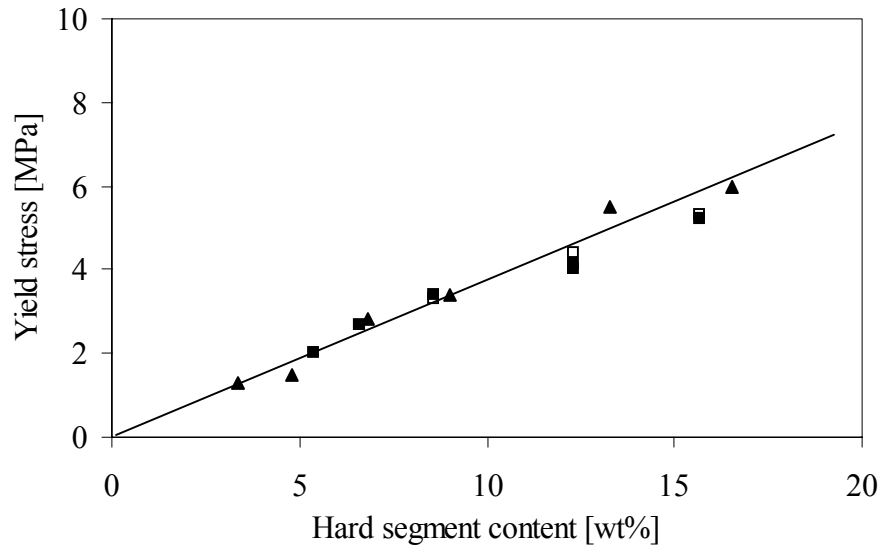


Figure 10.7: Yield stress as function of the hard segment content: (■), T6T6T-(PTMO₁₀₀₀/DMT), series 1; (□), T6T6T-(PTMO₁₀₀₀/DMT), series 2, non-uniform T6T6T; (▲), T Φ T-(PTMO₁₀₀₀/DMT)¹².

Orientation

By drawing, the crystalline ribbons in the copolymers are broken up and oriented in the straining direction. During breaking up of the crystalline structure the aspect ratio of the crystalline ribbons decreases¹². During drawing the PTMO phase is oriented, but on releasing the strain the orientation of the PTMO phase is lost for PTMO₁₀₀₀/DMT¹³. The modulus is thus only dependent on the structure and orientation of the crystalline phase. As the crystallites become smaller on orientation they also become more difficult to deform plastically. When a highly drawn thread is stretched a second time, the PTMO phase can more easily be oriented, which results in a higher fracture stress and lower fracture strain with a similar true fracture stress.

The effect of drawing-strain on the tensile and elastic behaviour for T6T6T-(PTMO₁₀₀₀/DMT)₆₀₀₀ copolymers was studied. In Figure 10.8 the stress-strain curves of threads of T6T6T-(PTMO₁₀₀₀/DMT)₆₀₀₀ based on non-uniform T6T6T (series 2) after different drawing-strains are given.

When the drawing-strain increases, the modulus decreases, the fracture stress increases and the fracture strain decreases. The true fracture stress however, is comparable for all samples. After drawing, fibres with a low modulus, a high fracture stress and still a high strain at break can be obtained. As the modulus decreases after drawing, shearing of the T6T6T ribbons upon straining is an irreversible process. This type of oriented fibres with stress-strain curves as given in Figure 10.8 (500-750% drawing-strain) could also be obtained directly in a commercial fibre spinning process at high spinning speeds in one step¹³.

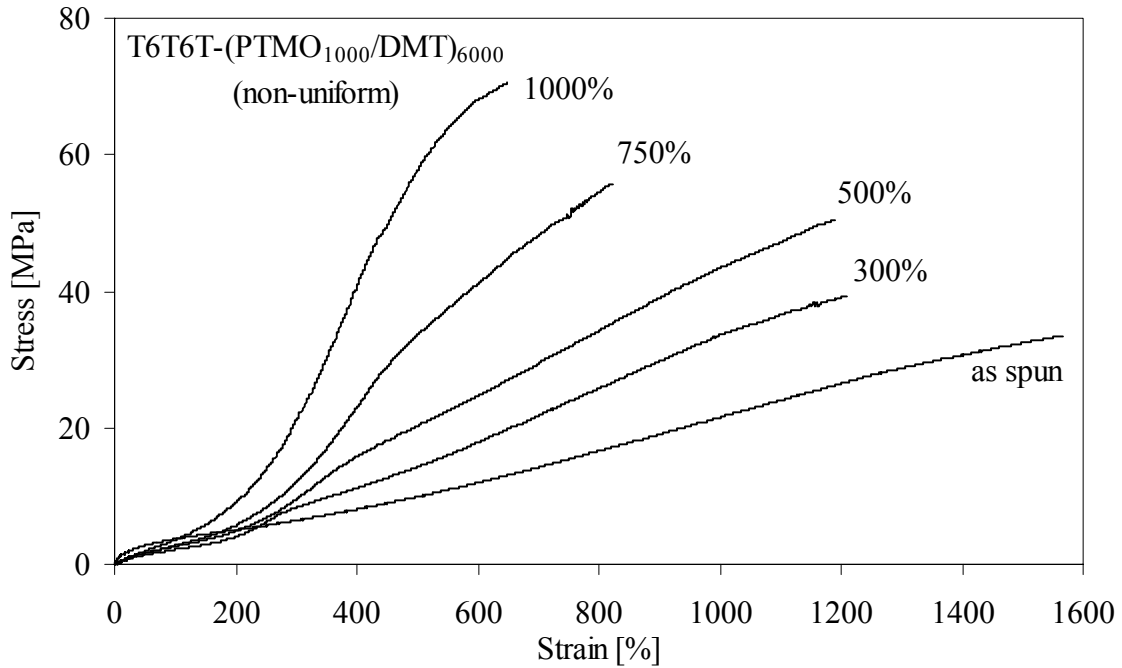


Figure 10.8: Stress-strain curves of T6T6T-(PTMO₁₀₀₀/DMT)₆₀₀₀ (non-uniform T6T6T) after drawing; the amount of drawing-strain is given for each line in the figure.

Strain softening

As was shown in Figure 10.8 the modulus decreases after drawing. Upon drawing the crystalline ribbons are broken up and their aspect ratio decreases. As a result their reinforcing effect decreases and the modulus of the copolymers will decrease. On the other hand, upon drawing, orientation of the crystalline ribbons will occur, which results in an increase in modulus. At higher drawing-strains (>500%) strain-induced crystallisation of PTMO can also occur which increases the modulus when it is not able to relax upon strain release^{12,13}.

The influence of drawing-strain on the E-modulus for T6T6T-(PTMO₁₀₀₀/DMT) copolymers was determined in cyclic tests with a step growth of 20% up to 100%, followed by a step growth of 100% up to break. There was no dwell time between the steps. The E-modulus as function of the percentage drawing-strain is given in Figure 10.9 for copolymers of series 1. The E-modulus in each cycle was corrected for the change in area of the thread by multiplying with the corresponding straining factor.

At low drawing-strains (<40%) there is only a small decrease of the E-modulus. At higher drawing-strains (>60%) the decrease is strong and has a linear relationship in a log-log plot. In the first 200% strain (just above the yield point), the modulus decreases by a factor 3-4 for all five copolymers. The PTMO length or T6T6T content seems to have little effect on this, thus the degree of crystallinity has little effect either. Between 100 and 300% or 300 and 900% strain, the decrease in modulus is comparable, about a factor 2. Only for the copolymers with a soft segment length of 3000 and 4000 g/mol the drop in modulus is somewhat lower above 500% strain.

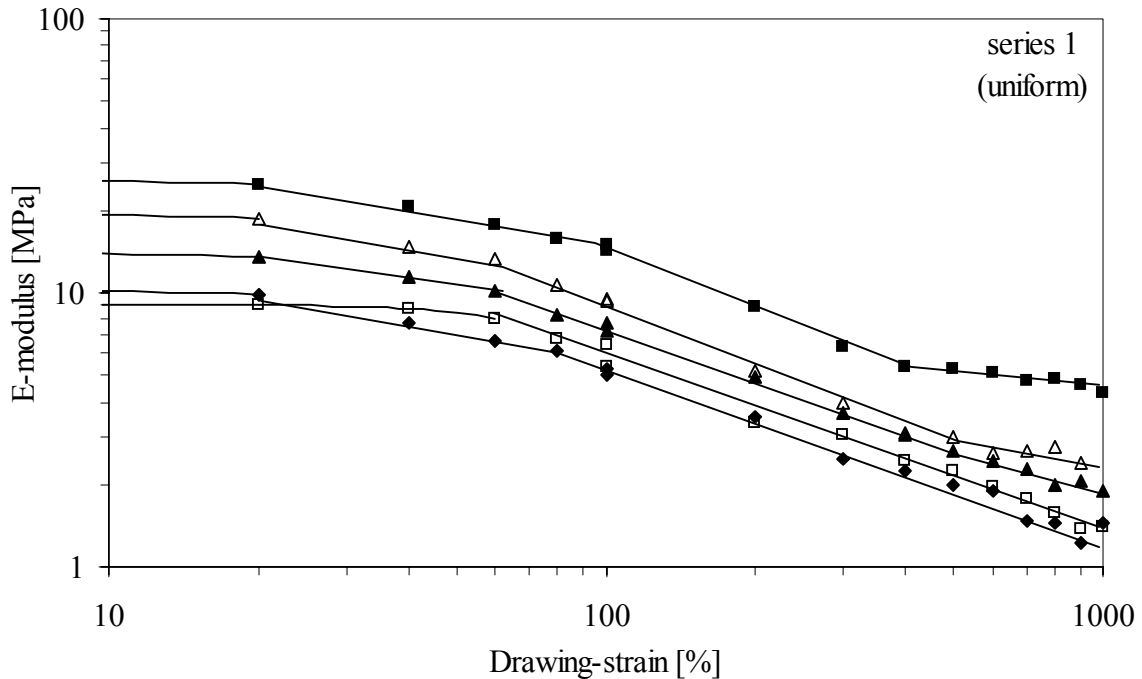


Figure 10.9: E-modulus as function of the drawing-strain in a cyclic test for T6T6T-(PTMO₁₀₀₀/DMT) with uniform T6T6T (series 1) and different soft segment lengths: (■), 3000 g/mol; (△), 4000 g/mol; (▲), 6000 g/mol; (□), 8000 g/mol; (◆), 10000 g/mol.

The decrease in modulus or strain softening that is observed is caused by disruption of the crystalline ribbon structure upon drawing²¹⁻²³. The modulus decreases because the crystalline structure is broken up and the aspect ratio of the crystallites decreases. When a material is strained a second time the modulus is lower and less stress is needed due to this strain softening².

At low strains (<30%) the strain is mainly elastic. No plastic deformation occurs and the modulus is hardly lowered. At higher strains plastic deformation takes place and the modulus decreases as the PTMO phase is broken up. At strains above 500%, the T6T6T phase is further broken up and also strain hardening of the PTMO phase can occur. As a result of strain hardening the modulus will increase¹². Only for T6T6T-(PTMO₁₀₀₀/DMT)₃₀₀₀ the modulus does not decrease much with increasing strain above 500% strain. This is probably due to the occurrence of some (irreversible) strain hardening of the PTMO phase that partially counteracts the effect of decreasing aspect ratio of the T6T6T crystallites. The stress-strain test on the T6T6T-(PTMO₁₀₀₀/DMT)₃₀₀₀ thread (Figure 10.3) also shows more strain hardening than that of threads of the other copolymers. However the effect of strain hardening is much smaller than for regular PTMO with a length above 2000 g/mol in TΦT-PTMO copolymers that show an increase of the modulus above 500% drawing-strain¹². Probably most of the strain-induced crystallisation of extended PTMO₁₀₀₀/DMT is reversible¹³.

Even at very high strains (>1000% up to break) the modulus decreases further, indicating that the process of breaking up of the crystalline ribbons continues up to high strains. It is thought that the crystalline ribbons are broken up further until they reach a square shape (aspect ratio of 1)¹². Apparently the crystallites still have an aspect ratio above 1 at break.

In Figure 10.6 it was shown that the stress-strain curves of T6T6T-(PTMO₁₀₀₀/DMT)₆₀₀₀ with uniform and non-uniform T6T6T are somewhat different. The copolymer based on non-uniform T6T6T has a higher E-modulus and shows more strain hardening. It was not possible to explain these differences because the high values for the E-modulus are unreliable.

In Figure 10.10 the E-moduli as a function of the percentage of drawing-strain are given for T6T6T-(PTMO₁₀₀₀/DMT)₆₀₀₀ with uniform (series 1) and non-uniform (series 2) T6T6T. The data of these two copolymers are compared with that of TΦT-(PTMO₁₀₀₀/DMT)₃₀₀₀¹² that has the same hard segment content (~9 wt%).

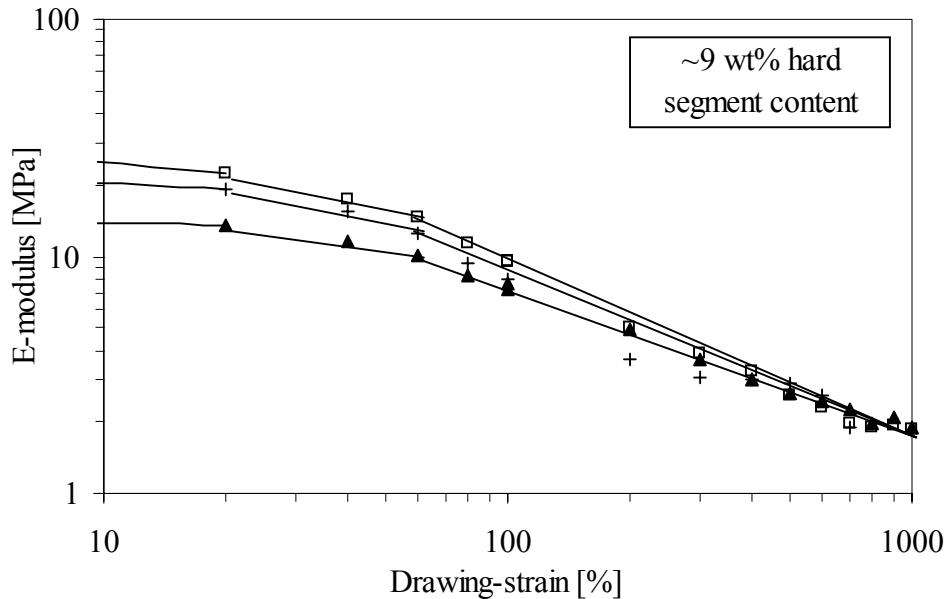


Figure 10.10: E-modulus as function of the drawing-strain in a cyclic test up to break for copolymers with ~9 wt% hard segment: (▲), T6T6T-(PTMO₁₀₀₀/DMT)₆₀₀₀, uniform T6T6T (series 1); (□), T6T6T-(PTMO₁₀₀₀/DMT)₆₀₀₀, non-uniform T6T6T (series 2); (+), TΦT-(PTMO₁₀₀₀/DMT)₃₀₀₀¹².

Above 200% drawing-strain the E-moduli of T6T6T-(PTMO₁₀₀₀/DMT)₆₀₀₀ with uniform (series 1) and non-uniform (series 2) T6T6T are comparable, so the aspect ratio and orientation of the T6T6T ribbons are the same. The higher strain hardening of the copolymer with non-uniform T6T6T (Figure 10.6) does not result in a higher modulus at high strains, which is indicative of the occurrence of strain hardening. This suggests that the strain-induced crystallisation of PTMO in these copolymers has little effect on the modulus, probably because the strain-induced crystallisation of PTMO₁₀₀₀/DMT is reversible on releasing the strain.

The E-modulus of TΦT-(PTMO₁₀₀₀/DMT)₃₀₀₀¹² that contains 9 wt% of crystallisable units as well is comparable with that of T6T6T-(PTMO₁₀₀₀/DMT)₆₀₀₀ of series 1 and 2. The E-modulus and strain softening are thus determined by the hard segment content, and not by the number of crystalline ribbons in the material or the lamellar thickness.

Elasticity

The compression set (CS) at 20 and 70°C was measured using polymer pieces, cut from the injection moulded bars. These data were already discussed in Chapter 9⁸. The tensile set (TS_{300%}) was measured in a cyclic tensile test up to 300% strain with extruded threads. The TS_{300%} is the strain in the second cycle at which a force is required to strain the thread. The CS and TS_{300%} of T6T6T-(PTMO₁₀₀₀/DMT) copolymers with uniform and non-uniform T6T6T segments are given in Table 10.2.

Table 10.2: Compression set⁸ and tensile set of T6T6T-(PTMO₁₀₀₀/DMT) copolymers with uniform (series 1) and non-uniform T6T6T (series 2).

PTMO ₁₀₀₀ /DMT length [g/mol]	T6T6T content [wt%]	η_{inh} [dl/g]	G'(25°C) [MPa]	CS _{55%} ⁸ (20°C) [%]	CS _{55%} ⁸ (70°C) [%]	TS _{300%} [%]
Series 1: uniform						
3000	15.7	3.1	14.5	10	32	19
4000	12.3	2.3	8.5	8	34	13
4000	12.3	1.4	18	18	45	26
6000	8.6	2.6	6.8	9	29	7.5
8000	6.6	2.2	5.1	7	34	5.7
10000	5.4	2.5	3.3	6	33	5.1
Series 2: non-uniform						
3000	15.7	1.4	23.5	12	24	20
4000	12.3	1.5/1.8 ^a	14.3	8	21	11
6000	8.6	1.9/2.1 ^a	6.9	8	20	7.0

(a), the first number is the inherent viscosity for the G'(25°C) and compression set data; the second number is the inherent viscosity of the polymer that was used for extruding into threads (tensile set data)

The compression set⁸ at 20 and 70°C decreases with decreasing T6T6T content, thus with increasing diol length. For T Φ T-(PTMO₁₀₀₀/DMT)¹² a minimum was observed in the compression set at ~9 wt% hard segment content. This behaviour was thought to be due to the fact that at very low hard segment concentrations the physical crosslink density is too low to prevent plastic flow in this compression test. In the copolymers based on T6T6T such a minimum is not (yet) observed when the T6T6T content is decreased⁸. The compression set (55%, 20°C) is low for all T6T6T contents and decreases slightly from 10 to 6% when the T6T6T content is decreased from 15.7 to 5.4 wt%. With non-uniform T6T6T the compression set values at 20°C are comparable. The compression set seems to decrease linearly with decreasing 1000/PTMO (increasing PTMO length) for 1000/PTMO > 0.4 (mol/g). The reciprocal value of the soft segment length corresponds to the network density, the number of physical crosslinks per chain.

The compression set at 70°C of T6T6T-(PTMO₁₀₀₀/DMT) copolymers, is still relatively low. For these copolymers the melting temperature is not reached by far at 70°C, and thus plastic flow is still suppressed.

For fibre applications the tensile set value is an important property. In Figure 10.11 the tensile set is given as a function of the rubber modulus (a) and the reciprocal value of the PTMO₁₀₀₀/DMT length (b) for T6T6T-(PTMO₁₀₀₀/DMT) with uniform (series 1) and non-uniform T6T6T (series 2) and for TΦT-(PTMO₁₀₀₀/DMT)¹³.

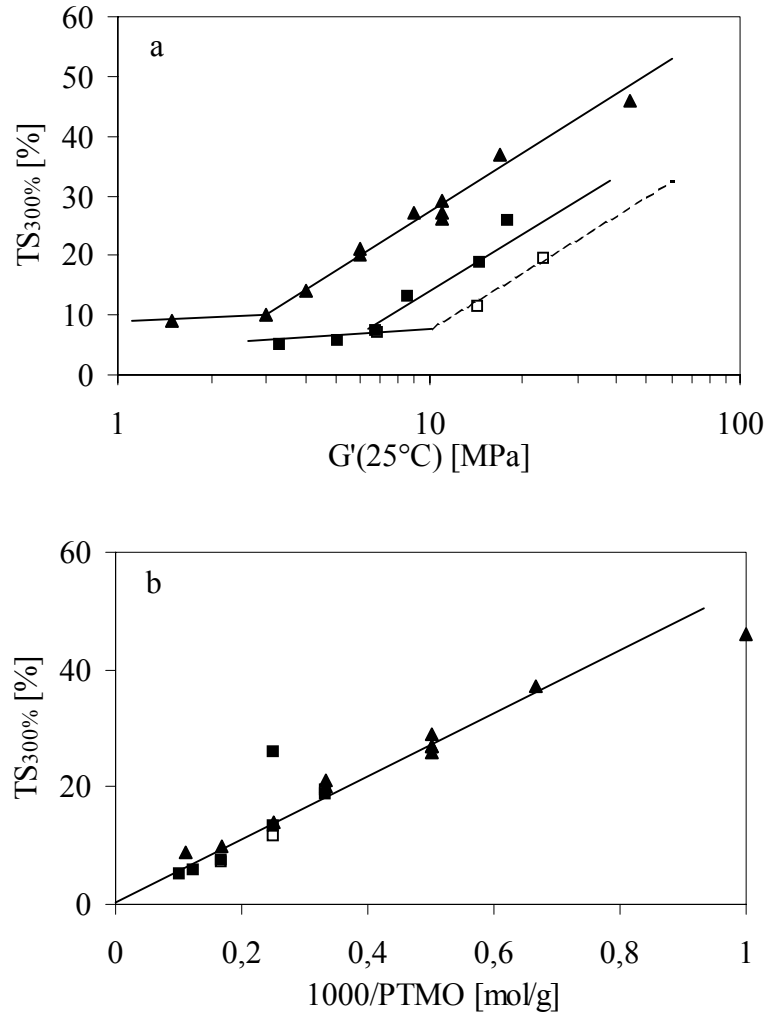


Figure 10.11: Tensile set after 300% strain of copolymers with different crystallisable segments as function of (a) the rubber modulus G' at 25°C and (b) $1000/\text{PTMO}$: (■), T6T6T-(PTMO₁₀₀₀/DMT), series 1; (□), T6T6T-(PTMO₁₀₀₀/DMT), series 2, non-uniform T6T6T; (▲), TΦT-(PTMO₁₀₀₀/DMT)¹³.

For all copolymer series the tensile set decreases with decreasing rubber modulus. When the rubber modulus decreases, the degree of crystallinity decreases. At a lower rubber modulus the hard segment content is lower. A larger part of the strain is taking place in the PTMO phase and there is less plastic deformation possible and therefore the tensile set decreases. The tensile set values for the T6T6T copolymers are low and even lower than for the TΦT system. This is surprisingly as the yield stresses and strain softening behaviour are comparable (Figure 10.7 and 10.9).

With TΦT¹³ as crystallisable segment a minimum tensile set of 9-10% after 300% strain can be obtained at a rubber modulus below 4 MPa. The tensile set increases linearly with

increasing T6T6T content above 4 MPa. The tensile set of all T6T6T-(PTMO₁₀₀₀/DMT) copolymers is lower than that of TΦT-(PTMO₁₀₀₀/DMT) at a certain rubber modulus. With T6T6T as crystallisable segment a very low tensile set of only 5-8% after 300% strain can be obtained when the rubber modulus is below 10 MPa. The rubber modulus has only little effect on the tensile set when it is below 10 MPa. When the rubber modulus is above 10 MPa the tensile set increases linearly with increasing rubber modulus. The slope of this line is comparable with that of copolymers based on TΦT as crystallisable unit.

The tensile set as a function of rubber modulus seems a little lower for non-uniform T6T6T (series 2) than for uniform T6T6T (series 1) at a rubber modulus above 10 MPa. This could be explained by fact that the copolymers with non-uniform T6T6T have a higher rubber modulus at a constant soft segment length, probably because the crystallinity is higher⁸.

In Figure 10.11b the tensile set is given as a function of the reciprocal value of the PTMO₁₀₀₀/DMT length for the T6T6T-(PTMO₁₀₀₀/DMT) copolymers. The reciprocal value of the soft segment length corresponds to the network density, the number of physical crosslinks per chain. The tensile set follows a linear relationship with increasing 1000/PTMO for copolymers with uniform and non-uniform T6T6T. The tensile set values are compared with those of the TΦT-(PTMO₁₀₀₀/DMT) copolymers¹³. The tensile set values of copolymers based on T6T6T or TΦT as function of 1000/PTMO are the same. The compression set was shown to deviate from such a linear relationship for 1000/PTMO values below 0.4⁸. Apparently the elasticity under tension is better than under compression at large soft segments lengths.

From Figure 10.11b it can be concluded that for the tensile set not the crystallinity, but the distance between two crystalline ribbons is important in these copolymers. When the distance between the crystalline ribbons increases, the elasticity increases. This can be explained by the fact that when more PTMO is present between crosslinks more deformation is taking place in this PTMO phase.

When a thread with a certain PTMO length for both T6T6T and TΦT is stretched to 300% the fraction of ribbons that is broken up to reach this strain is probably comparable. Also the strain softening factor is independent of the hard segment content (Figure 10.9) and type (Figure 10.10). The fact that the modulus and yield stress at a particular PTMO length are larger for T6T6T than for TΦT does not seem to influence the elasticity. Apparently the deformation of the crystalline phase has no effect on the elasticity.

Therefore it can probably be concluded that the elasticity is mainly dependent on the length of PTMO between two crystalline ribbons and not on the type of crystallisable units for this type of segmented copolymers.

Orientation

For the copolymers of series 2 with non-uniform T6T6T the tensile set was also measured as a function of the amount of drawing-strain. A thread that is drawn to 500-750% corresponds to a fibre that is obtained in a commercial process directly after spinning¹³. The results are given in Table 10.3 and Figure 10.12.

Table 10.3: Tensile set for T6T6T-(PTMO₁₀₀₀/DMT) copolymers with non-uniform T6T6T (series 2), measured in a cyclic tensile test up to 300% strain after spinning (as spun) and different drawing-strains of 300-1000%.

PTMO ₁₀₀₀ /DMT length [g/mol]	T6T6T content [wt%]	η_{inh} [dl/g]	TS _{300%} [%]				
			as spun	300%	500%	750%	1000%
3000	15.7	1.4	19.5	16.5	17.2	18.8	-
4000	12.3	1.8	11.5	9.0	8.7	11.1	12.0
6000	8.6	2.2	7.0	5.0	4.8	5.1	5.8

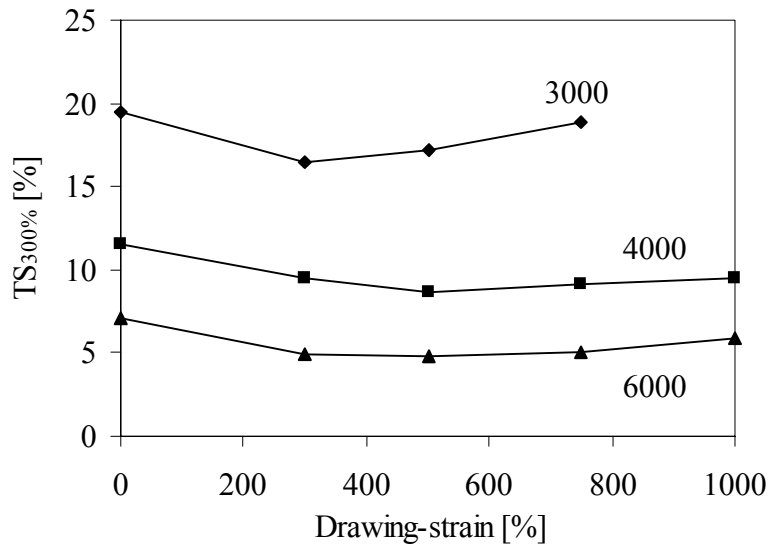


Figure 10.12: TS_{300%} as a function of the drawing-strain for T6T6T-(PTMO₁₀₀₀/DMT) copolymers with non-uniform T6T6T (series 2) and PTMO₁₀₀₀/DMT length as indicated in the figure.

After drawing to 300%, the tensile set is somewhat lower than that of an as spun thread. A minimum in tensile set with the drawing-strain is observed for all three polymers. The minimum with T6T6T-(PTMO₁₀₀₀/DMT)₃₀₀₀ is reached after 300% drawing-strain. With T6T6T-(PTMO₁₀₀₀/DMT)₄₀₀₀ and T6T6T-(PTMO₁₀₀₀/DMT)₆₀₀₀ the minimum is at 500% drawing-strain.

Upon drawing, strain softening occurs (Figure 10.9) and the modulus drops as the crystalline network is broken up. The crystalline ribbons are broken up into smaller pieces and oriented in the straining direction. This process continues up to high strains. Apparently the aspect ratio has only little effect on the tensile set, as it does not change a lot after pre-drawing to 500, 750 or 1000%. It could also be that part of the crystalline ribbons that are broken up

upon drawing can recover after stress release, however the modulus was found to stay low after stress release.

Above 500% strain, strain induced crystallisation of the PTMO phase can take place, as has been observed before¹³. However with strain induced crystallisation a large increase of the tensile set with increasing drawing-strain is expected as for T Φ T-PTMO with PTMO lengths above 2000 g/mol. Therefore strain induced crystallisation of extended PTMO₁₀₀₀/DMT is probably reversible¹³.

In Figure 10.13 the TS_{300%} for as spun extruded threads and 500% drawn threads is given versus the E-modulus of these threads (non-uniform T6T6T, series 2). By drawing the modulus is decreased by a factor 10 for these copolymers, while the TS_{300%} is decreased only slightly.

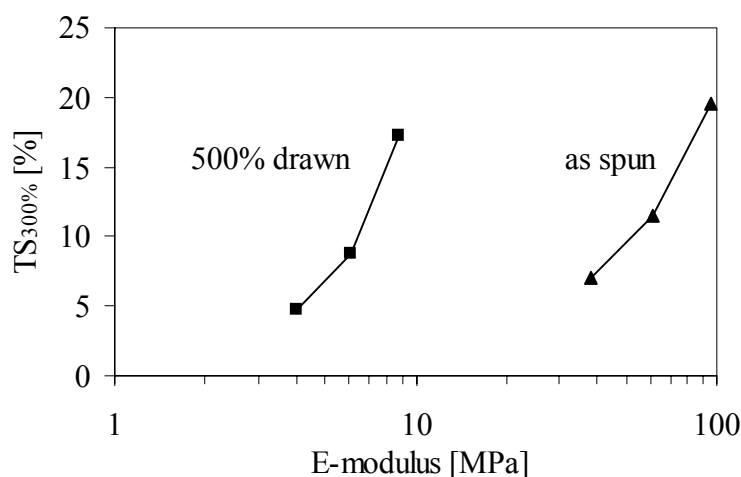


Figure 10.13: TS_{300%} versus E-modulus of T6T6T-(PTMO₁₀₀₀/DMT) copolymers with non-uniform T6T6T (series 2): (▲), as spun threads; (■), 500% pre-stained threads.

The modulus of the extruded thread is high and therefore the granulate of the T6T6T-(PTMO₁₀₀₀/DMT) copolymers will not be sticky. For processing this result is important, as it is very inconvenient to have a sticky granulate. After spinning from the melt at high speed, fibres that are comparable with extruded threads at a drawing-strain of 500% can be obtained. These are fibres with a low modulus, high tensile strength and strain and very low tensile set.

The low uniformity of T6T6T in series 2 does not seem to have a negative effect on the properties. With a uniformity of 76% the tensile and elastic properties of T6T6T-(PTMO₁₀₀₀/DMT) are comparable with that using uniform T6T6T. It was expected that the properties would be better in the copolymers based on uniform T6T6T³⁻⁶. Apparently excellent uniformity of T6T6T is not very important. A uniformity of 76% seems sufficient for good properties. As yet the effect of uniformity of T6T6T is not fully understood.

Comparison with other systems

The T6T6T and T Φ T based segmented copolymers are copolyether-esteramides, a special type of the thermoplastic copolyether-amides (TPE-A). These materials are new compared to the commercial materials that are described here, as they contain crystallisable segments that are uniform in length.

The commercial material Arnitel[®] is a segmented copolyether-ester (TPE-E) based on a PBT-PTMO copolymer. Desmopan[®] is a commercial thermoplastic polyurethane (TPE-U), based on polyether soft segments. In both materials the hard segment are not of uniform length. Lycra[®] is a segmented polyurethane fibre that was spun by solution spinning. The properties of a hard and a soft grade of these commercial materials were evaluated²⁴.

The T6T6T-(PTMO₁₀₀₀/DMT) copolymers that are described in this article are compared with the T Φ T-(PTMO₁₀₀₀/DMT) copolymers from previous research^{12,13} and several commercial materials²⁴ in Table 10.4. In Figure 10.14 the tensile set is given as a function of the flow temperature and rubber modulus for the T6T6T-(PTMO₁₀₀₀/DMT) copolymers compared to other systems.

Table 10.4: Comparison of T6T6T-(PTMO₁₀₀₀/DMT) segmented copolymers with other systems^{12,13,24} (Desm. = Desmopan).

	Hard segment [wt%]	G' (25°C) [MPa]	T _{flow} [°C]	T _g [°C]	σ_b [MPa]	ϵ_b^a [%]	TS _{300%} (0%) [%]	TS _{300%} (500%) [%]	CS _{55%} (20°C) [%]	CS _{55%} (70°C) [%]
T6T6T-(PTMO₁₀₀₀/DMT) with PTMO/DMT length:										
6000	8.6	6.8	200	-61	25	1450	7.5	5	9	29
10000	5.4	3.3	183	-63	31	1400	5.1	4	6	33
TΦT-(PTMO₁₀₀₀/DMT)^{12,13} with PTMO/DMT length:										
4000	7	4	155	-65	21	1250	14	-	24	55
9000	3	1.5	102	-65	15	1600	9	7	23	67
Commercial polymers²⁴										
Arnitel [®] EM400	-	18	182	-7	61	860	41	-	15	36
Arnitel [®] EL550	-	67	205	-50	106	470	76	-	30	58
Desm. [®] KU-8672	-	11	150	-45	79	950	18	-	13	41
Desm. [®] 955u	-	91	176	-31	86	830	30	-	23	60
Lycra [®] 269B	-	2.5	290	-	-	-	-	4 ^b	-	-
Lycra [®] 136C	-	2	210	-	-	-	-	7.5 ^b	-	-

(a), after correction for necking in the clamps above 500% strain; (b), oriented fibre used as received

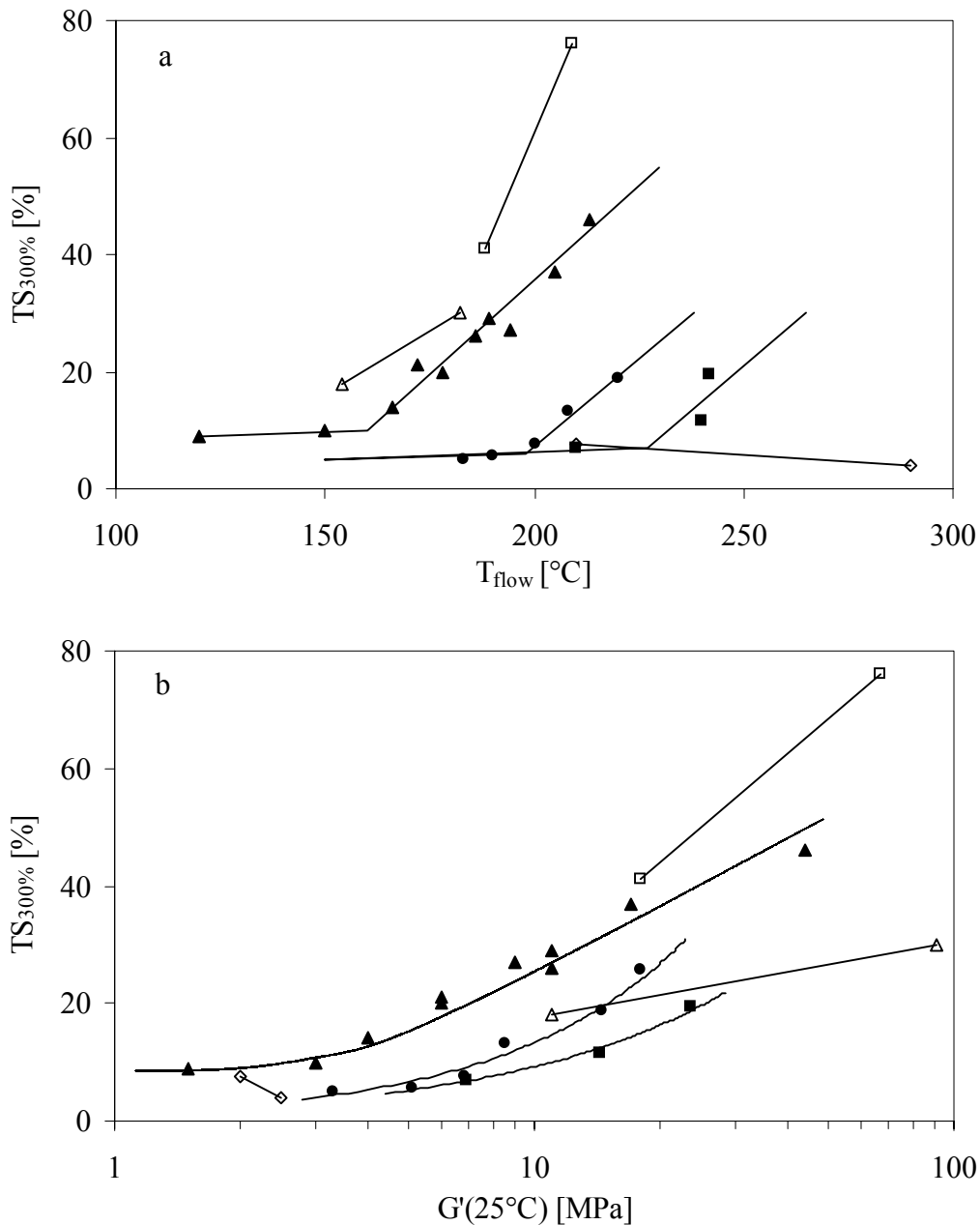


Figure 10.14: Tensile set after 300% strain as a function of (a) the flow temperature and (b) the rubber modulus for different copolymers with T6T6T or TΦT as crystallisable segment compared to commercial materials: (●), T6T6T-(PTMO₁₀₀₀/DMT), series 1; (■), T6T6T-(PTMO₁₀₀₀/DMT), series 2, non-uniform; (▲), TΦT-(PTMO₁₀₀₀/DMT)¹³; (□), Arnitel^{®24}; (△), Desmopan^{®24}; (◇), Lycra^{®24}.

The fracture stress and strain of extruded threads of T6T6T-(PTMO₁₀₀₀/DMT) copolymers are comparable with that of similar materials, in particular TΦT-(PTMO₁₀₀₀/DMT). The flow temperature of polymers with T6T6T is higher compared to TΦT, while the compression and tensile set are lower. Another advantage of copolymerisation with T6T6T instead of TΦT is that the products are less coloured. Therefore the use of T6T6T is preferred over the use TΦT in segmented copolymers.

T6T6T-(PTMO₁₀₀₀/DMT)₆₀₀₀ has a tensile set of only 5% after straining to 500%, in combination with a flow temperature of 200°C and a rubber modulus of 6.8 MPa. A high flow temperature is important for dyeing of the fibre, a high rubber modulus is important for processing of pellets. Another advantage of the T6T6T-(PTMO₁₀₀₀/DMT) copolymers is that they can be recycled. Lycra[®]-269B shows a tensile set of 4% at a flow temperature of 290°C. Lycra[®], however, does not really melt and cannot be melt spun or recycled. Furthermore Lycra[®] has a very low modulus, which makes the material sticky. The new T6T6T-(PTMO₁₀₀₀/DMT) materials are very interesting as elastic fibres.

Arnitel and Desmopan are not well suitable for application as elastic fibre due to the high tensile set values and low flow temperatures. These commercial materials are mainly used for other applications for thermoplastic elastomers where a high modulus in combination with a good compression set and good processability are most important. The T6T6T-(PTMO₁₀₀₀/DMT) copolymers are very interesting for such applications as well, as was discussed in Chapter 9⁸.

It is expected that the properties of T6T6T-(PTMO₁₀₀₀/DMT) copolymers can probably be changed and optimised in several ways: the choice of the soft segment type and length, the melt polymerisation conditions, the processing conditions and by using additives. The elastic properties of the material can for example be improved further by using DMI instead of DMT as PTMO extender¹⁵. The synthesis would become more economically feasible when it can be performed in the melt, so when the T6T6T segment is formed in situ, for example by starting from 6T6-diamine or even by starting from 1,6-hexamethylenediamine. Of course this is at the cost of uniformity of the T6T6T in the copolymer, but it was shown that a uniformity of at least 76% is sufficient for good properties. Another interesting modification would be to use other tetra-amides as crystallisable segment instead of T6T6T, for example T4T4T. The melting temperature of nylon-4,T is 60°C higher than that of nylon-6,T²⁵ and therefore the melting temperature of a copolymer with T4T4T instead of T6T6T is expected to be about 60°C higher. It is expected that the elasticity will be the same with T4T4T. Furthermore fibres that are processed by a commercial meltspinning process, where processing conditions are optimised will have better properties.

Conclusions

The tensile and elastic properties of segmented copolymers based on T6T6T-dimethyl (uniform and 76% uniform) and (PTMO₁₀₀₀/DMT) of different lengths (3000-10000 g/mol) are good. Stress-strain measurements show that extruded threads of these polymers have high fracture strains (>1000%) and little strain hardening. The modulus and yield stress increase with increasing T6T6T content. The modulus decreases with increasing drawing-strain as a result of the breaking up of the crystalline network (strain softening).

The compression and tensile set decrease with decreasing T6T6T content and are very low. The tensile set correlates well with other systems when it is given as function of soft segment

length. The lower the hard segment content and the longer the length between the crosslink points, the higher is the elasticity. The tensile set ($TS_{300\%}$) decreases after drawing of the extruded threads, goes to a minimum at 300-500% drawing-strain and then increases a little. The length between crosslink points is not expected to change much upon drawing and at high drawing-strains strain induced crystallisation of the PTMO phase might take place. The influence of the uniformity of T6T6T is as yet not fully understood.

With T6T6T-(PTMO₁₀₀₀/DMT) with soft segment lengths of 6000 to 10000 g/mol a tensile set lower than 5% is feasible. At a soft segment length of 6000 g/mol such a fibre has a flow temperature of 200°C and the rubber modulus is 6.8 MPa, which means that the granulate will not be sticky.

This type of thermoplastic elastomers is very interesting for application as elastic fibres. The segmented copolymers show a good combination of properties as they have a very good elasticity, are melt-processable (and can be recycled), have a high modulus, are transparent and are dimensionally stable up to high temperatures.

Literature

1. G. Holden, N.R. Legge, R. Quirk, H.E. Schroeder, 'Thermoplastic Elastomers', Second Ed., Hanser Publishers, Munich (1996).
2. B.P. Grady, S.L. Cooper, in 'Science and Technology of Rubber', J.E. Mark, B. Erman, F.R. Eirich Eds., Academic Press, San Diego, Chapter 13 (1978).
3. L.L. Harrell, *Macromolecules*, 2, 607 (1969).
4. H.N. Ng, A.E. Allegrazza, R.W. Seymour, S.L. Cooper, *Polymer*, 14, 255 (1973).
5. C.D. Eisenbach, M. Baumgartner, G. Gunter, in 'Advances in Elastomer and Rubber Elasticity, proc. Symposium', J. Lal, J.E. Mark Eds., Plenum Press, New York, 51 (1985).
6. J.A. Miller, B.L. Shaow, K.K.S. Hwang, K.S. Wu, P.E. Gibson, S.L. Cooper, *Macromolecules*, 18, 32 (1985).
7. Chapter 5 of this thesis.
8. Chapter 9 of this thesis.
9. R.J. Cella, *J. Polym. Sci.: Symp.*, 42, 727 (1973).
10. L. Zhu, G. Wegner, *Makromol. Chem.*, 182, 3625 (1981).
11. B.B. Sauer, R.S. McLean, R.R. Thomas, *Polym. Int.*, 49, 449 (2000).
12. M.C.E.J. Niesten, R.J. Gaymans, *Polymer*, 42, 6199 (2001).
13. M.C.E.J. Niesten, J. Krijgsman, R.J. Gaymans, *J. Appl. Polym. Sci.*, 82, 2194 (2001).
14. M.C.E.J. Niesten, J. Feijen, R.J. Gaymans, *Polymer*, 41, 8487 (2000).
15. M.C.E.J. Niesten, J.W. ten Brinke, R.J. Gaymans, *Polymer*, 42, 1461 (2001).
16. J.D. Hoffman, J.J. Weeks, *J. Res. Nat. Bur. Stand., Sect. A*, 66, 13 (1962).
17. N.G. McCrum, C.P. Buckley, C.B. Bucknall, "Principles of Polymer Engineering", First Ed., Oxford University Press, Oxford, Chapter 5 (1988)
18. L.H. Sperling, "Introduction to physical polymer science", Second Ed., John Wiley & Sons, New York, Chapter 8 (1992).
19. BASF, Lupolen series, Datasheet (1979).
20. N. Brown, in 'Failure of plastics', W. Browstow, R.D. Corneliussen Eds., Hanser Publishers, Munich, Chapter 6 (1979).
21. R.J. Young, *Mater. Forum*, 11, 210 (1988).
22. M.C.E.J. Niesten, S. Harkema, E. van der Heide, R.J. Gaymans, *Polymer*, 42, 1131 (2001).

23. R.S. McLean, B.B. Sauer, J. Polym. Sci.: Part B: Polym. Phys., 37, 859 (1999).
24. M.C.E.J. Niesten, R.J. Gaymans, J. Appl. Polym. Sci., 81, 1372 (2001).
25. P.W. Morgan, S.L. Kwolek, Macromolecules, 8, 104 (1975).

Summary

The importance of polymer materials as construction materials is continually growing. Polymers are a cheap and light alternative to conventional materials used for construction. In the automotive industry there is a specific need for materials with a high modulus up to a high glass transition temperature (T_g) ($\sim 200^\circ\text{C}$), good processability and excellent chemical resistance. Therefore the material should be semi-crystalline and crystallise fast upon cooling from the melt. Polymer systems with a high T_g , a not too high melting temperature (T_m) and thus a high T_g/T_m ratio are thought to fulfil these requirements. Noryl-GTX[®], a blend of poly(2,6-dimethyl-1,4-phenylene ether) and polyamide-6,6 approaches the required properties. However a high polyamide content (40%) is necessary in order to obtain enough crystallinity. The PPE and polyamide phase separate and the polyamide phase is semi-crystalline with a T_g at 70°C .

The **aim** of the work described in this thesis is to study the synthesis and structure-property relationships of semi-crystalline segmented copolymers with a high T_g ($>150^\circ\text{C}$), high T_m ($250\text{-}300^\circ\text{C}$) and high T_g/T_m ratio (around 0.8). These segmented copolymers will be based on poly(2,6-dimethyl-1,4-phenylene ether) (PPE) as amorphous segment and uniform tetra-amide units as crystallisable segment. It is expected that this novel high T_g polymer crystallises fast from the melt, has a good solvent resistance and is transparent. Such a material may serve as an alternative to known engineering polymers systems e.g. for use as or in construction materials in high temperature applications.

The synthesis of telechelic PPE segments is described in **Chapter 2**. A good method to make partly bifunctional PPE (PPE-2OH) is by redistribution or depolymerisation of high molecular weight commercial PPE with tetramethyl bisphenol A. The product has a bimodal molecular weight distribution (MWD) because only $\sim 70\text{-}80\%$ of the high molecular weight starting material is depolymerised. The phenolic endgroups can be modified by a fast and complete reaction with methyl chlorocarbonyl benzoate. The product after endgroup modification is called PPE-2T and has terephthalic methyl ester endgroups, a molecular weight of $2000\text{-}4000$ g/mol and a functionality of ~ 1.8 . The bimodal PPE-2OH and PPE-2T products can be separated in a high and low molecular weight fraction by selective precipitation of the reaction product. The low molecular weight fraction has a narrow MWD with a polydispersity between 1.2 and 1.5.

Amorphous copolymers based on PPE-2T (3700 g/mol, bimodal MWD) and different diols are described in **Chapter 3**. The copolymers were made via a polycondensation reaction. The terephthalic endgroups of PPE-2T are stable during this reaction. The T_g of these polyether-ester copolymers decreases with increasing diol length and flexibility. The T_g can be set between 100 and 200°C by changing the type of diol. However at increasing diol length the T_g becomes broader and the test bars are less transparent because the extent of phase separation increases. Only polymers with a diol length up to C12 are homogeneous. Phase separation is probably enhanced by the bimodal MWD of PPE-2T. Phase separation can be

suppressed by using shorter PPE-2T segments, shorter diols or fractionated PPE-2T. Copolymerisation of PPE with a flexible diol is much more effective in decreasing the T_g of PPE than blending with polystyrene. It is expected that the processability of these copolymers is much better than that of pure PPE.

Amorphous copolymers of PPE-2T (3500 g/mol, bimodal MWD) and poly(dodecane terephthalate) (PDDT) of different lengths are discussed in **Chapter 4**. The T_g of the PPE/PDDT copolymers decreases with increasing PDDT length. However at high PDDT length (>1000 g/mol, PDDT content >20 wt%) phase separation occurs as in PPE-2T/diol copolymers.

A polyester-ether copolymer of PDDT with some PPE (27 wt%) has a modulus in the rubbery plateau that is increased by a factor 3 compared to pure PDDT. The material has a phase separated morphology. The amorphous PDDT phase is the continuous phase and is almost pure. PPE probably forms rigid domains that act as reinforcing filler for the polyester. Polyester/PPE copolymers seem interesting as an alternative for glass-filled polyesters.

In **Chapter 5** the (two-step) synthesis of bisester tetra-amide segments (TxTxT-dimethyl) with T a terephthalic unit and $x = n$ in $(CH_2)_n$ ($n = 2-8$) is discussed. These segments are based on two-and-a-half repeating units of nylon-x,T. The first step is the synthesis of xTx-diamine in the melt, followed by recrystallisation. TxTxT-dimethyl can then be prepared in a reaction of xTx-diamine with methyl phenyl terephthalate in solution. The structure and purity of the products was confirmed by NMR. The melting temperature increases with decreasing length of x. For odd x the melting temperature is lower.

Semi-crystalline copolymers based on telechelic PPE and T6T6T are discussed in Chapter 6-8. Copolymers of PPE-2T (3500 g/mol, bimodal MWD), 13 wt% uniform T6T6T-dimethyl and dodecanediol (C12) as an extender are discussed in **Chapter 6**. The copolymers were made via a polycondensation reaction with a maximum reaction temperature of 280°C. The PPE-2T/C12/T6T6T copolymers are semi-crystalline materials with a sharp T_g around 170°C and a sharp T_m of 264-270°C. The modulus is high up to the T_g and the modulus in the rubbery plateau after injection moulding is 7-12 MPa. It is particular that the T6T6T units can actually crystallise in these copolymers despite the very high T_g/T_m ratio (>0.8). The materials are slightly transparent and have good solvent resistance, low water absorption and good processability. The T6T6T units probably form long threads or ribbon like structures in the amorphous matrix. The crystallinity of T6T6T in the copolymers is between 60 and 75%. The part of the T6T6T units that does not crystallise mixes with the amorphous PPE matrix or forms sort of frozen-in ordered T6T6T nano-phases with a T_g around 100°C. The crystallinity of T6T6T in a test bar can be improved by a heat treatment step. The crystallinity decreases with increasing molecular weight and is sensitive to processing conditions. The undercooling (T_m-T_c) as measured by DSC is 18°C at a cooling rate of 20°C/min. With WAXD it was shown that the copolymer contains ordered T6T6T above the melting temperature (at 300°C) and thus the tetra-amide units remain organised in the melt.

In **Chapter 7** the influence of the T6T6T content (8-20 wt%), type of PPE-2T and uniformity of T6T6T in PPE-2T/C12/T6T6T copolymers were studied. The modulus of the rubbery

plateau increases with increasing crystalline T6T6T content (3-15 MPa) and can be tuned by changing the amount of T6T6T in the copolymer or by improving the crystallinity of T6T6T. With increasing amount of crystalline T6T6T the flow temperature increases slightly as well (260-275°C). The materials are transparent when the T6T6T content is below 15 wt%. In copolymers based on fractionated, monomodal PPE-2T segments the crystallinity of T6T6T is very low (<30%). The uniformity of the T6T6T units seems to have little effect on the properties of the copolymer, as long as it is above 70%. At very low uniformity (<50%) the flow temperature is considerably broadened.

In **Chapter 8** the influence of the diol length (C2-C36, PTMO) that is used as extender in PPE-2T/diol/T6T6T was studied. A series of copolymers in which PPE with phenolic endgroups (PPE-2OH) and T6T6T-diphenyl were coupled directly was studied as well. Copolymers based on PPE-2T and T6T6T-dimethyl (10-15 wt%) with dodecanediol or hexanediol as an extender have the best combination of properties. With longer diols, the T_g is decreased and broadened and the modulus decreases before the T_g . Also the modulus in the rubbery plateau is not as high as with C6 and C12. With shorter diols (C2) or by coupling PPE and T6T6T directly the T_g can be increased, which is desirable. However at the same time the crystallinity of the copolymer decreases. Both the increased T_g/T_m ratio and the decreased flexibility of the units that link PPE and T6T6T are thought to be responsible for this behaviour. The PPE/diol/T6T6T copolymers are transparent when the diol length is C12 or lower.

Thermoplastic elastomers based on T6T6T-dimethyl (5-16 wt%) as crystallisable segment and aliphatic polyether amorphous segments (PTMO or PTMO₁₀₀₀/DMT) were studied as well. The synthesis and thermal mechanical properties are discussed in **Chapter 9**. The materials have a good solvent resistance, are melt-processable and transparent. With DMA it was shown that the polymers all have a low T_g (-60 to -70°C), a wide and extremely flat rubbery plateau and a sharp and high T_{flow} . The modulus of the rubbery plateau (3.3 to 14.5 MPa) and the T_{flow} (183 to 220°C) increase with decreasing PTMO₁₀₀₀/DMT length (10000 to 3000 g/mol) or increasing T6T6T content (5 to 16 wt%). The crystallinity of T6T6T in injection moulded test bars is between 70 and 100%. The undercooling, as measured by DSC (20°C/min), is 20-30°C. The uniformity of T6T6T, when it is at least 76%, does not have much influence on the polymer properties, except for the T_{flow} that is broadened at decreasing uniformity. With AFM it was confirmed that the crystalline T6T6T units form long threads or ribbon like structures with a high aspect ratio in the amorphous PTMO matrix.

The tensile and elastic properties of melt spun threads of T6T6T- PTMO₁₀₀₀/DMT segmented copolymers are discussed in **Chapter 10**. Stress-strain measurements show that extruded threads of these polymers have high fracture strains (>1000%) and little strain hardening. The modulus and yield stress increase with increasing T6T6T content. The modulus decreases with increasing drawing-strain as a result of the breaking up of the crystalline network (strain softening). The compression set (6-10%) and tensile set (5-20%) increase with increasing T6T6T content (5-16 wt%) and are low. The combination of good elasticity with high melting temperature and rubber modulus is very favourable. Further improvement is expected after spinning at high speed in a commercial process.

Levensloop

Josien Krijgsman werd op 18 mei 1975 geboren in Den Helder. Het middelbaar onderwijs (VWO) volgde zij op het Copernicus SG in Hoorn, waar zij in 1993 eindexamen deed. Na haar eindexamen besloot zij om Chemische Technologie te gaan studeren aan de Universiteit Twente. Tijdens haar stage bij het ATO-DLO deed zij onderzoek naar de chemische modificatie van zetmeel. Haar afstudeeropdracht voerde zij uit bij de vakgroep Synthese en Technologie van Engineering Plastics van Dr. Gaymans. Het onderzoek was gericht op de synthese van gesegmenteerde copolyether-estramides op basis van amorfe PTMO en kristalliseerbare di-amide segmenten op grote schaal. De materialen werden vervolgens gesponnen tot elastische vezels waarvan de eigenschappen bepaald werden. In september 1998 studeerde zij af en besloot om haar verblijf in Twente met nog eens vier jaar te verlengen als AIO binnen dezelfde groep. Haar promotor was Prof. Feijen. Het promotieonderzoek was gericht op de ontwikkeling van semi-kristallijne gesegmenteerde copolymeren met een hoge glasovergangstemperatuur en een hoge T_g/T_m verhouding. Dit werd gerealiseerd door poly(2,6-dimethyl-1,4-phenylene ether) segmenten te copolymeriseren met kristalliseerbare tetra-amide eenheden. Deze methode bleek succesvol en heeft mede geleid tot de aanvraag van drie patenten. Het resultaat van dit werk staat beschreven in het proefschrift dat nu voor u ligt.

